**US Army Corps
of Engineers**
Waterways Experiment
Station

Wave Response of Kahului Harbor, Maui, Hawaii

by Edward F. Thompson, Lori L. Hadley, Willie Ann Brandon,
David D. McGehee, Jon M. Hubertz

DTIC QUALITY INSPECTED 4

Approved For Public Release; Distribution Is Unlimited

19970416 015

Prepared for U.S. Army Engineer Division, Pacific Ocean

The contents of this report are not to be used for advertising,
publication, or promotional purposes. Citation of trade names
does not constitute an official endorsement or approval of the use
of such commercial products.

Wave Response of Kahului Harbor, Maui, Hawaii

by Edward F. Thompson, Lori L. Hadley, Willie Ann Brandon,
David D. McGehee, Jon M. Hubertz

U.S. Army Corps of Engineers
Waterways Experiment Station
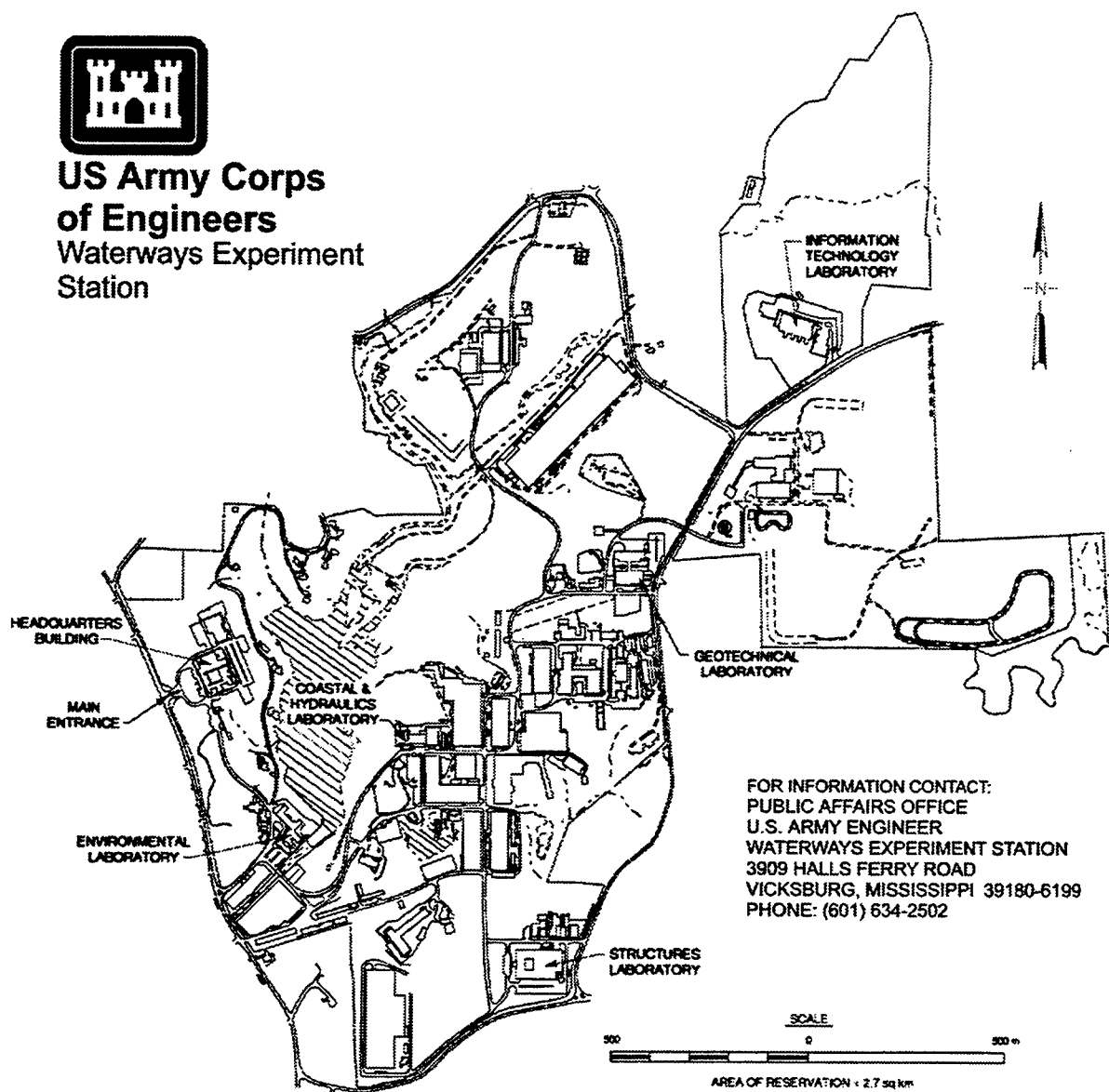3909 Halls Ferry Road
Vicksburg, MS 39180-6199

Final report

**US Army Corps
of Engineers**
Waterways Experiment
Station

INFORMATION
TECHNOLOGY
LABORATORY

-N-

HEADQUARTERS
BUILDING

COASTAL &
HYDRAULICS
LABORATORY

MAIN
ENTRANCE

GEOTECHNICAL
LABORATORY

ENVIRONMENTAL
LABORATORY

FOR INFORMATION CONTACT:
PUBLIC AFFAIRS OFFICE
U.S. ARMY ENGINEER
WATERWAYS EXPERIMENT STATION
3909 HALLS FERRY ROAD
VICKSBURG, MISSISSIPPI 39180-6199
PHONE: (601) 634-2502

STRUCTURES
LABORATORY

SCALE

500   0   500 m

AREA OF RESERVATION < 2.7 sq km

Contents

List of Figures

List of Tables

Preface

A request for field measurement and model investigations of Kahului Harbor, Maui, HI, was initiated by the U.S. Army Engineer Division, Pacific Ocean (POD), in coordination with the Harbors Division, Department of Transportation, State of Hawaii (HDOT). Authorization for the U.S. Army Engineer Waterways Experiment Station (WES), Coastal Engineering Research Center (CERC), to perform the study was subsequently granted by Headquarters, U.S. Army Corps of Engineers. Field measurements were collected during the period September 1993 through March 1995 and numerical model tests were conducted at WES from September 1994 to April 1996. The physical modeling component of the investigation, which is generally used to determine the final recommended design of harbor modifications, was postponed because of budget limitations.

Messrs. Stanley Boc, POD, and Fred Nunes, HDOT, oversaw progress of the study. Meetings at WES at critical points in the study were the mid-study model review conference on 11-12 July 1995 and the wrap-up conference on 28-29 February 1996.

Mr. Dennis G. Markle, Chief, Wave Processes Branch, Wave Dynamics Division, was the principal WES point of contact for the study. Mr. David D. McGehee, Prototype Measurement and Analysis Branch, Engineering Development Division, was responsible for the field measurement program. Ms. Willie Ann Brandon and Dr. Jon M. Hubertz, both of the Coastal Oceanography Branch (COB), Research Division (RD), CERC, conducted the wave climate analysis portion of the study. Dr. Edward F. Thompson and Ms. Lori L. Hadley, both of COB, performed some additional analysis of the field data, conducted the numerical harbor modeling, and assembled this report. Ms. Rebecca L. Russell, COB, assisted with data processing and analysis. Direct supervision was provided by Mr. Markle and Dr. Martin C. Miller, Chief, COB. General supervision was provided by Mr. H. Lee Butler, Chief, RD; Mr. Charles C. Calhoun, Jr., Assistant Director, CERC; and Dr. James R. Houston, Director, CERC.

Special appreciation is extended to Ms. Juliana Thomas and Messrs. David Castel and Joseph Keefe, Center for Coastal Studies, Scripps Institution of Oceanography, for not only providing field wave parameters and spectra but also modifying the methodology for calculating peak wave period to provide more accurate swell estimates. Drs. Mark A. Merrifield and Michele S. Okihiro,

Conversion Factors, Non-SI to SI Units of Measurement

Non-SI units of measurement can be converted to SI (metric) units as follows:

Multiply	By	To Obtain
degrees (angle)	0.01745329	radians
feet	0.3048	meters
miles (U.S. nautical)	1.852	kilometers
tons (2,000 pounds, mass)	907.1847	kilograms

Summary

Introduction

Because of present and projected commercial activities in Kahului Harbor, the needs and concerns of community, private business, and government have been reviewed under the state of Hawaii planning process. New berths for barge and passenger ship operations are an expected future requirement. Space for related land-based facilities is needed. Deepening of main harbor areas from 35 ft to 38 ft is also anticipated.

The new facilities would require expansion of harbor operations into areas not presently used, particularly the western part of the harbor. Field wave measurements and numerical (computer) model studies to evaluate the technical feasibility of alternative modifications were conducted from September 1993 to May 1996 by the U.S. Army Corps of Engineers at the U.S. Army Engineer Waterways Experiment Station, Coastal Engineering Research Center, Vicksburg, MS. Eleven alternative harbor plans were studied along with the existing harbor (see table that follows).

Study Results

Harbor basin

Wind waves and swell in the harbor are affected by distance from the entrance, directional exposure, and bottom depths. Wave approach directions at the entrance are consistently aimed at the southwest part of the harbor. Facilities in the western harbor and located closer to the entrance (as the extension of Pier 1) are prone to increased wind wave and swell conditions. A stub added to the west breakwater tip in some plans shelters the western harbor from wind waves and swell. Changes in the western harbor have no significant impact on wind waves and swell at existing facilities in the eastern harbor.

Summary of Kahului Harbor Plans and Wave Response

Harbor Plan	Distinctive Features	Wind Waves and Swell	Surge Oscillations	Remarks	See Figure
1	Slip cut in coral stockpile; Concept C for barge pier	2	3	Large oscillations at passenger pier	3
2	Slip cut in coral stockpile; Concept 12 for barge pier	2	3	Large oscillations at passenger pier	4
3a	Notch cut in coral stockpile; No breakwater stub	2	2		5
3b	Notch cut in coral stockpile; 600-ft breakwater stub	1	1		5
3c	Notch cut in coral stockpile; 1,000-ft breakwater stub	1	1		5
4a	Adjacent to coral stockpile; No breakwater stub	3	1	High wind waves and swell	6
4b	Adjacent to coral stockpile; 600-ft breakwater stub	2	1		6
4c	Adjacent to coral stockpile; 1,000-ft breakwater stub	1	1		6
5	Fill area in SW harbor	2	2	Large oscillations at barge and passenger piers	7
6	Same as 4b but with 38-ft depth	2	1		8
7	Fully utilized harbor (combination of 4b and 5)	2	2	Large oscillations at barge and passenger piers	9

[1] General indicator of plan performance: 1 = equal or better than existing facilities
2 = somewhat worse than existing facilities
3 = much worse than existing facilities

All of the proposed harbor plans have comparable or increased surge (or oscillation) activity relative to the existing harbor. The dredged access areas, straight piers, and corners added in the alternative plans tend to increase surge motions. Changes in the western harbor can potentially worsen surge conditions at the existing commercial piers.

Ship surge response

Kahului Harbor experiences natural resonance modes, which cause standing waves in the harbor. These waves are commonly present in the harbor, but their height varies considerably according to incident wave conditions. High standing waves can cause operational difficulties such as excessive ship motion and high mooring line forces. Areas of greatest horizontal motion (nodal areas) are most likely to experience problems. Possible actions to remedy effects of the surge include proper ballasting as ships are offloaded, adjustment to mooring line tensions, and modifications to mooring line configuration.

Piers 1-3

Wind wave and swell activity at existing Piers 1-3 is not appreciably changed in any of the alternative plans. The proposed Pier 1 extension will experience an increase in wave heights with closer proximity to the entrance. Surge level is increased in some plans. A nodal area between the seaward end of Pier 2 and the middle of Pier 1 is visible in all plans, including the existing harbor. The Pier 1 extension will likely be in the nodal area for the 176- to 178-sec resonant oscillation.

Barge facility

Wind waves and swell at the recommended Concept 12 configuration along the southwest side of Pier 2 are similar to the more seaward parts of existing Piers 1 and 2. Surge activity is substantially lower than at existing facilities except in plans which include a landfill in the southwest harbor.

Passenger ship pier

Wind wave and swell protection varies greatly between plans, ranging from better than any existing facilities to much worse. Surge activity is similar to or higher than the present Pier 1.

Boat ramp

Most plans have the added benefit of helping to shelter the boat ramp from wind waves and swell. Overall surge levels are generally similar to the existing harbor except in Plan 5.

Model performance

The final numerical model behaved realistically when compared to field observations at Kahului Harbor. There is a high level of confidence in the predictions made by the model, especially those involving comparisons between harbor alternatives.

Limitations

No instances of operational problems *inside* the harbor were reported during the measurement studies, although they are known to have occurred in the past. (One episode of hazardous waves at the *entrance*, resulting in harbor closing, was recorded.) Such events would have been very helpful in identifying more clearly the processes and threshold wave heights which deter specific operations in the harbor. They would also have aided the evaluation of alternative plans. There are inherent limits on the numerical model representations of the harbor response. Wave climate information used to evaluate each plan was based mainly on 11 months of field data. Ship and mooring system responses, the ultimate operational concern, were not explicitly studied.

Recommendations

Recommended modifications to Kahului Harbor include a 200-ft extension to Pier 1, dredging and a new T-pier for fuel barges between Piers 1 and 3, a new barge facility along the south side of Pier 2, and a new passenger ship pier located in the western harbor. Variations to the alternative plans studied may include design changes for improved performance. For example, the passenger ship facility in Plans 5 and 7 could be pile-supported rather than solid to reduce resonances.

Results of this study should be combined with operational experience at existing facilities to define a most-promising general plan. A final optimized plan should be determined with the aid of a physical model. The numerical model should be validated against the physical model studies to ensure that the final plan is free of problem surge response in existing pier areas and new facilities. Effects of future modifications to the harbor should be evaluated using the validated numerical model.

1 Introduction

Background

Kahului Harbor is the only deep-draft harbor on the Island of Maui and the busiest port in Hawaii outside of the Island of Oahu. The harbor is approximately 94 miles[1] southeast of Honolulu and is conveniently located on Maui's north shore (Figure 1).

The harbor is exposed to wind and waves from the north and northeast. The northwest end of Maui shelters the harbor from waves arriving from the northwest. The harbor is protected by two large breakwaters. High energy waves generated by intense winter storms in the north Pacific Ocean routinely attack the breakwaters. Hurricanes can also create large waves incident to the harbor. The breakwaters have a long history of construction and repair (Markle and Boc 1994; Sargent, Markle, and Grace 1988). Breakwaters are armored with molded concrete units of up to 35 tons on the trunk and 50 tons on the head. The harbor entrance is a 660-ft opening between the breakwaters.

Commercial piers are located in the southeast part of the harbor. Piers are used by a variety of vessels including barges, container ships, passenger cruise ships, and fishing vessels. Pier 1 accommodates the larger overseas vessels and barges. Water depth in the Federal entrance channel, harbor basin, and commercial pier areas is 35 ft.

Two canoe clubs are located along the shore immediately southwest of Pier 2. A large coral stockpile has been placed inside the harbor, adjacent to the west breakwater. This area, under the jurisdiction of the County of Maui, is being considered for park development. A public boat ramp is located near the landward end of the stockpile (Figure 2). The southern shore of the harbor, between the boat ramp and canoe clubs, includes a revetment along Kahului Beach Road and several rock groins further east.

Because of Kahului Harbor's size and importance (both recreational and commercial), the Harbors Division, Department of Transportation, State of

---

[1] A table of factors for converting non-SI units of measurement to SI units is presented on page xi.
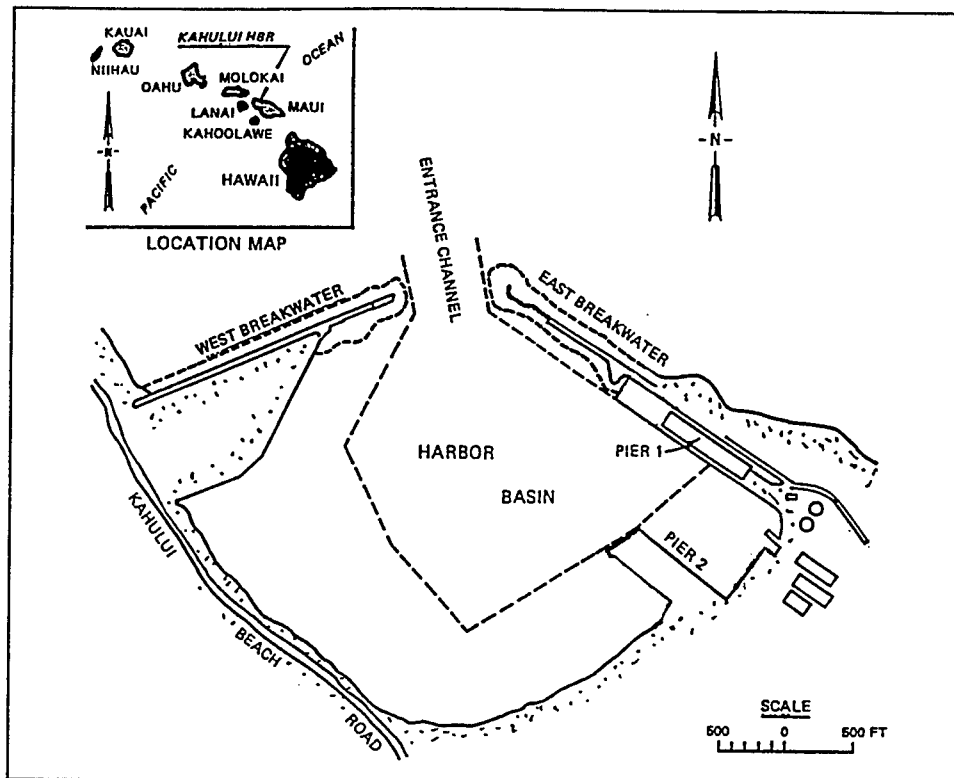
Figure 1. Study location
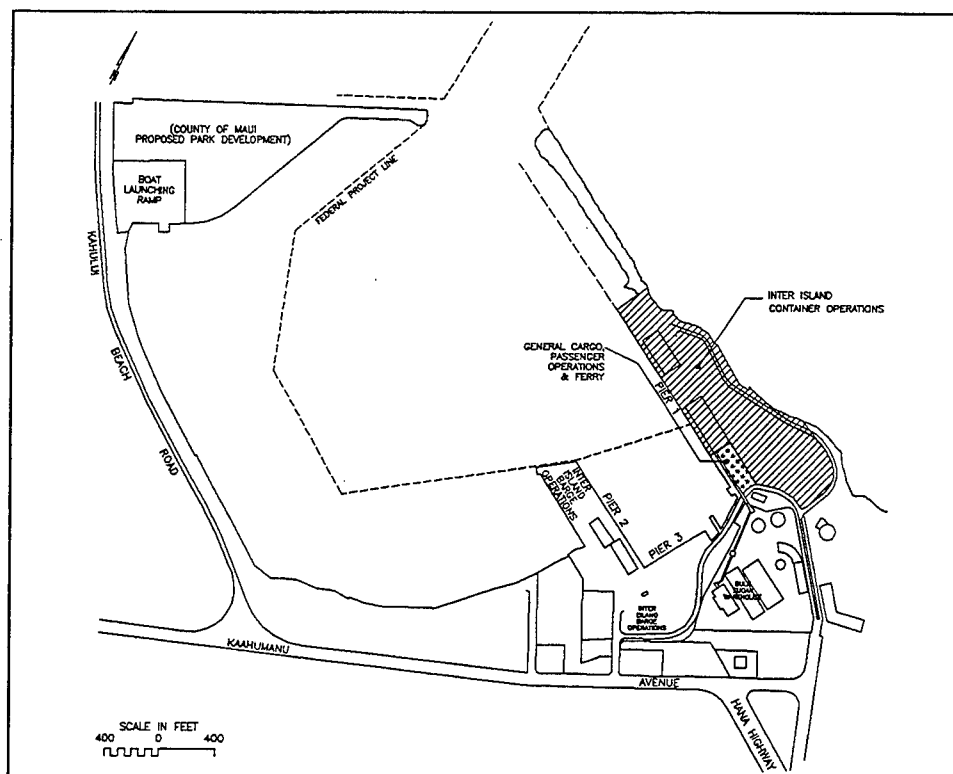
Figure 2. Kahului Harbor, existing plan

Hawaii (HDOT), has devoted special care to long-range planning. Plans and concerns are described in the 2010 Master Plan for Kahului Harbor produced by the State of Hawaii in 1994. A key concern is the possibility for expansion of the harbor in concert with projected increases in population and economic activity. Wave activity at the existing piers during heavy northerly swells is also a concern.

Study Approach

The study described in this report was performed by the U.S. Army Engineer Waterways Experiment Station (WES), Coastal Engineering Research Center (CERC), in support of the 2010 Master Plan for Kahului Harbor. The approach consisted of the following components:

a. Collect and analyze field wave data.

b. Relate field data to long-term wave climate.

c. Use field data to calibrate and validate a numerical wave model.

d. Use the numerical model to investigate alternative harbor modification plans.

Field wave gages were installed outside the harbor and at four locations inside the harbor. Locations for the harbor gages were selected with the aid of a preliminary numerical model study of harbor oscillations (Okihiro et al. 1994). Two events of special interest occurred during the measurement program. Intense wave activity causing closure of the harbor occurred on 14-15 March 1994. A sizeable (but not damaging) tsunami event due to an earthquake off the coast of Japan occurred on 4 October 1994. The field wave measurement portion of the study is described in Chapter 2.

Long-term wind wave and swell climate was investigated primarily with numerical hindcast information covering a period of 20 years. Statistics from the gage outside the harbor were evaluated relative to the long-term climate. The wave climate study is presented in Chapter 3.

A numerical wave model was set up to cover the entire harbor and the area outside the harbor extending to the wave gage. The model was tested, calibrated, and validated, mainly using the field data. Nine alternative harbor plans were defined as part of the mid-study model review conference, with provisions for two additional plans to be specified after evaluating the initial plans. Thus the study included a total of eleven plans and the existing harbor. All plans included the following features:

a. A 200-ft extension of Pier 1 toward the harbor entrance.

b. A dredged area between Piers 1 and 3 to 35-ft depth to accommodate fuel barges.

Each plan includes provisions for a new passenger vessel area on the west side of the harbor and a new barge facility on the south side of Pier 2. Appropriate dredging is incorporated into the plans to provide 35-ft depth for passenger vessels and 25-ft depth for barges. Special features of each plan are:

a. *Plan 1 (Figure 3).* Slip cut into coral stockpile to accommodate passenger ships; fill south of Pier 2 to provide barge pier oriented nearly north/south (referred to as *Concept C* in HDOT planning documents).

b. *Plan 2 (Figure 4).* Slip cut into coral stockpile to accommodate passenger ships; fill south of Pier 2 to provide barge pier parallel to Pier 2 (referred to as *Concept 12* in HDOT planning documents).

c. *Plans 3a, 3b, and 3c (Figure 5).* Notch cut into coral stockpile to accommodate passenger ships; protective stub aligned with entrance channel added to end of west breakwater in Plans 3b and 3c with length of 600 ft (Plan 3b), and 1,000 ft (Plan 3c); fill south of Pier 2 to provide barge pier parallel to Pier 2.

d. *Plans 4a, 4b, and 4c (Figure 6).* Passenger ship pier located adjacent to existing coral stockpile; protective stub added to end of west breakwater in Plans 4b and 4c with length of 600 ft (Plan 4b), and 1,000 ft (Plan 4c); fill south of Pier 2 to provide barge pier parallel to Pier 2.

e. *Plan 5 (Figure 7).* 800-ft by 800-ft fill area added in southwest area of harbor to accommodate passenger ships; fill south of Pier 2 to provide barge pier parallel to Pier 2.

f. *Plan 6 (Figure 8).* Identical to Plan 4b except 35-ft project depths dredged to 38 ft.

g. *Plan 7 (Figure 9).* Combination of Plans 4b and 5 with 35-ft project depth areas dredged to 38 ft and realignment of passenger ship pier along southeast side of fill area. This plan represents a fully utilized harbor.

Development of the numerical model and test procedures is described in Chapter 4.

Response of the existing harbor to waves was studied using field data and numerical model results. Response of the alternative harbor plans was investigated with only numerical model results. Harbor response to wind waves and swell (*short waves*) is presented in Chapter 5. Harbor oscillation characteristics (response to *long waves*) are presented in Chapter 6. For both short and long waves, the harbor response is related to wave climate and to relevant operational criteria at commercial piers.

Conclusions and recommendations are given in Chapter 7. This chapter is followed by references and appendices with detailed information supporting the main report and notation definitions.

4
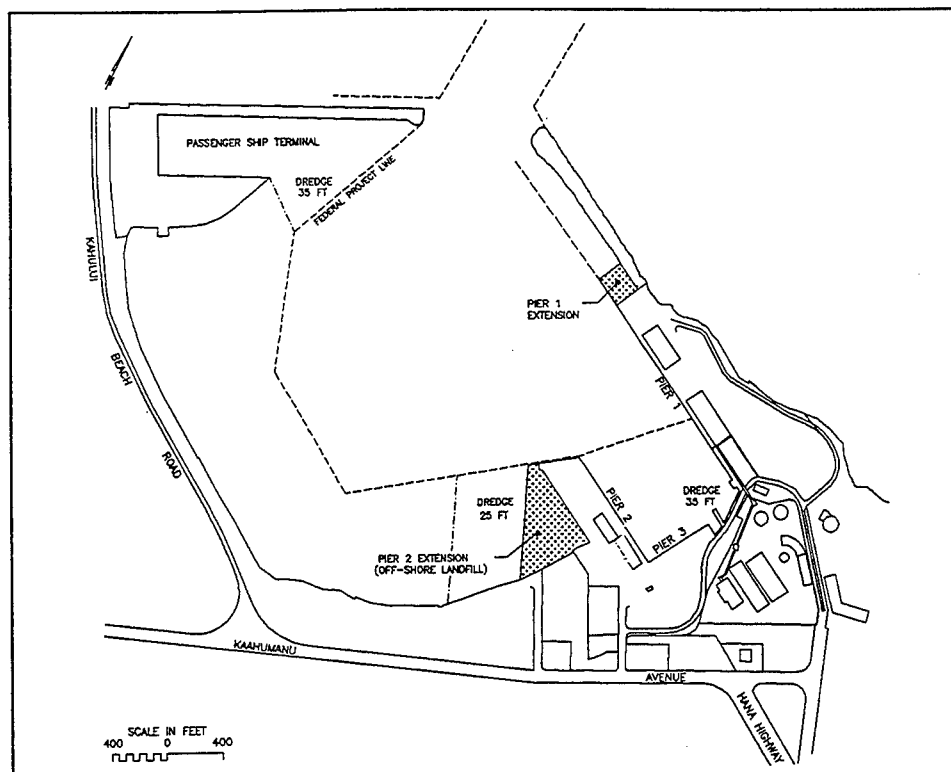
Figure 3. Plan 1
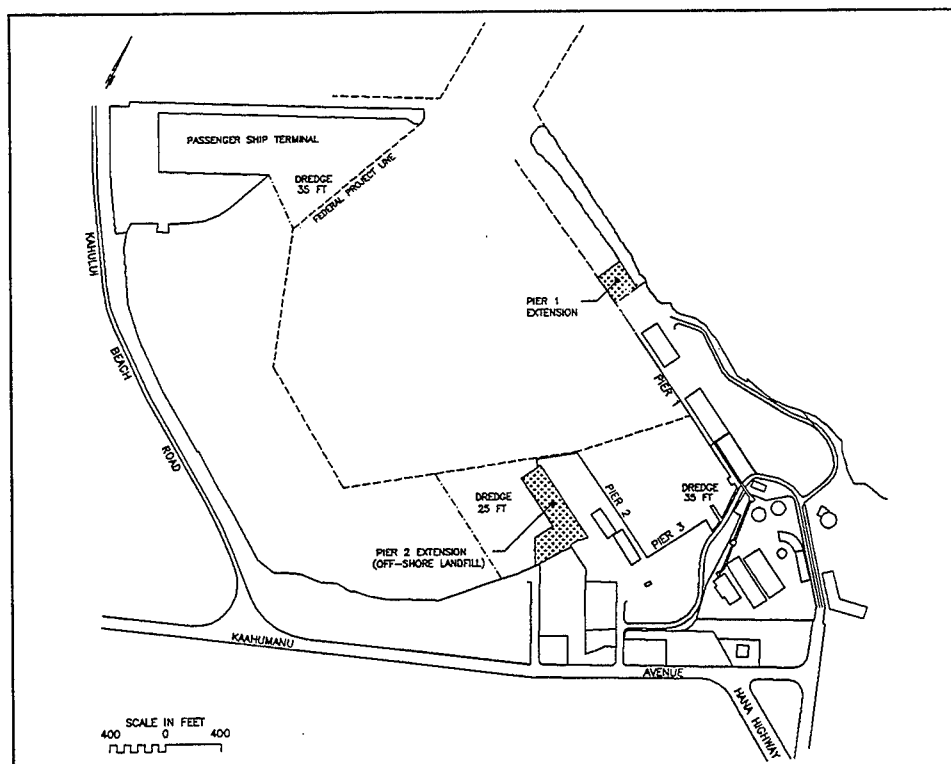
Figure 4. Plan 2
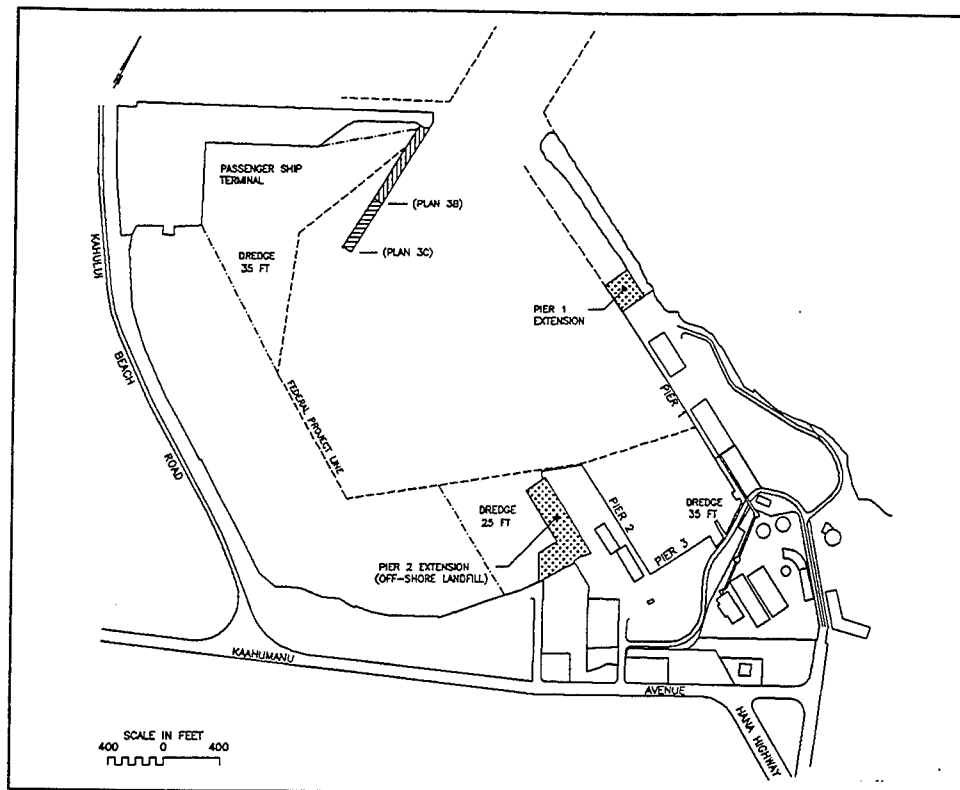
Figure 5. Plan 3
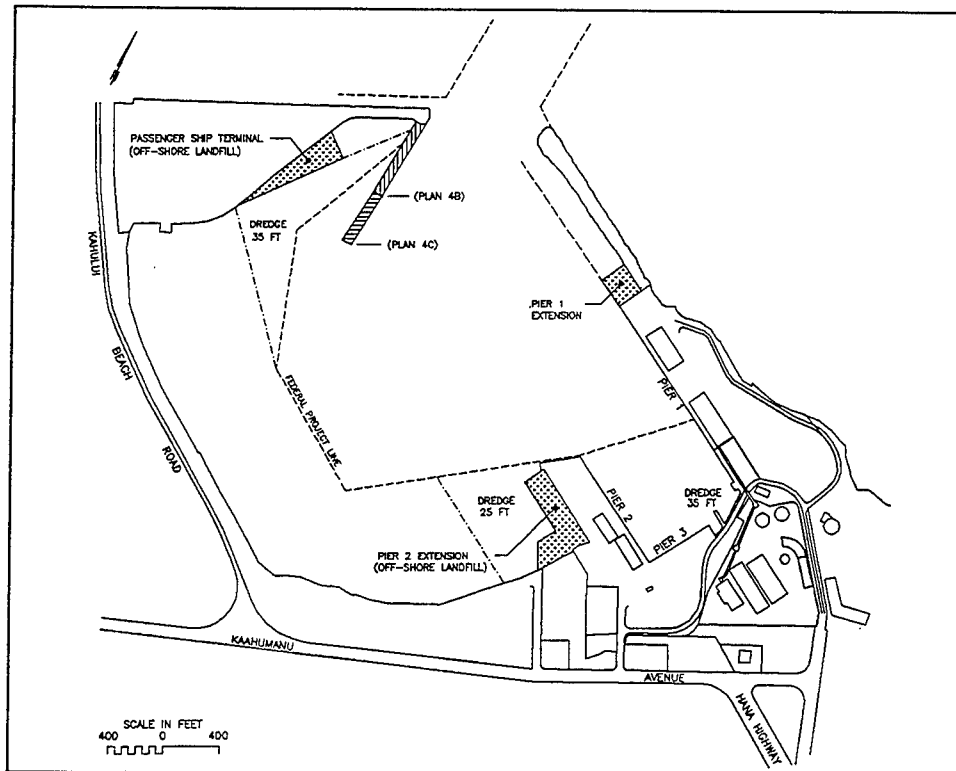
Figure 6. Plan 4
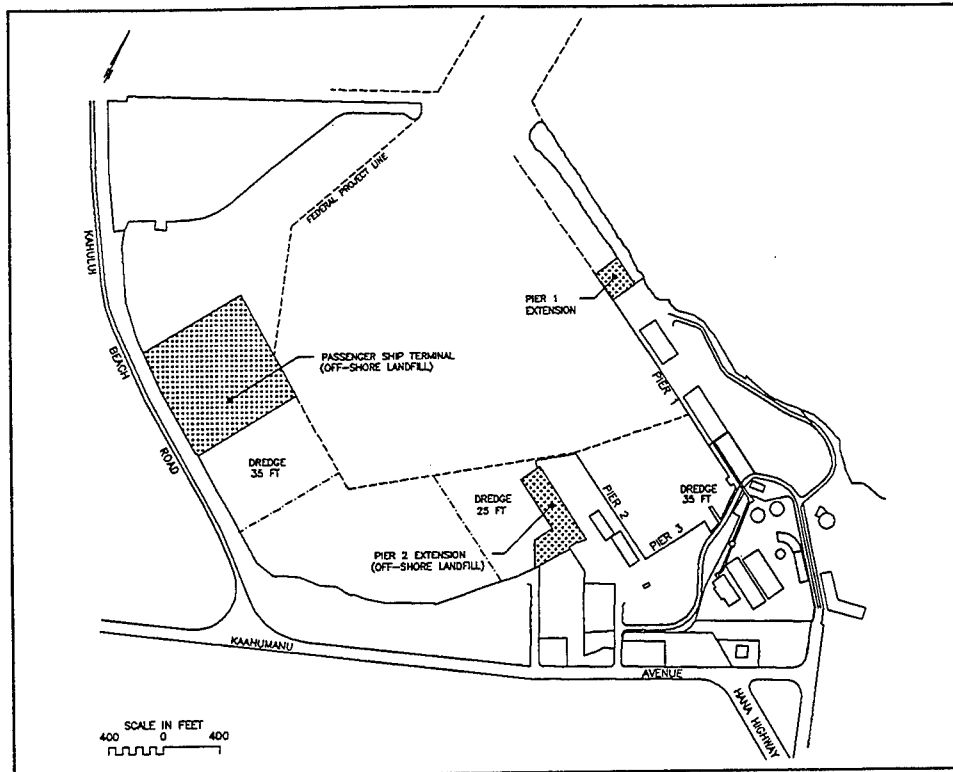
Figure 7. Plan 5
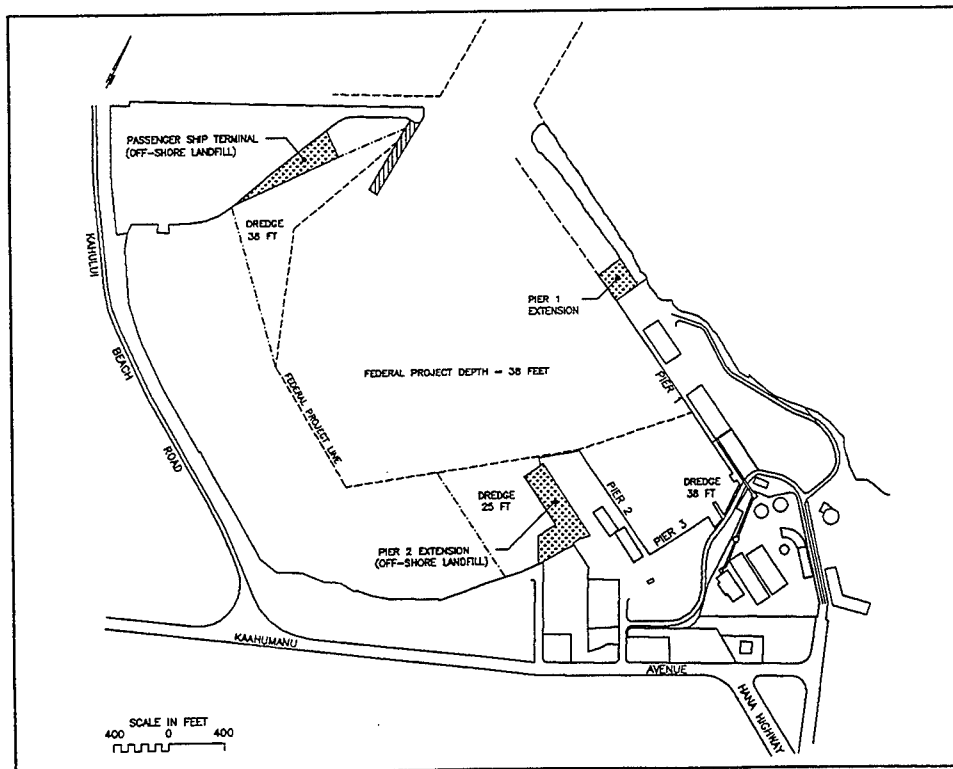
Figure 8. Plan 6
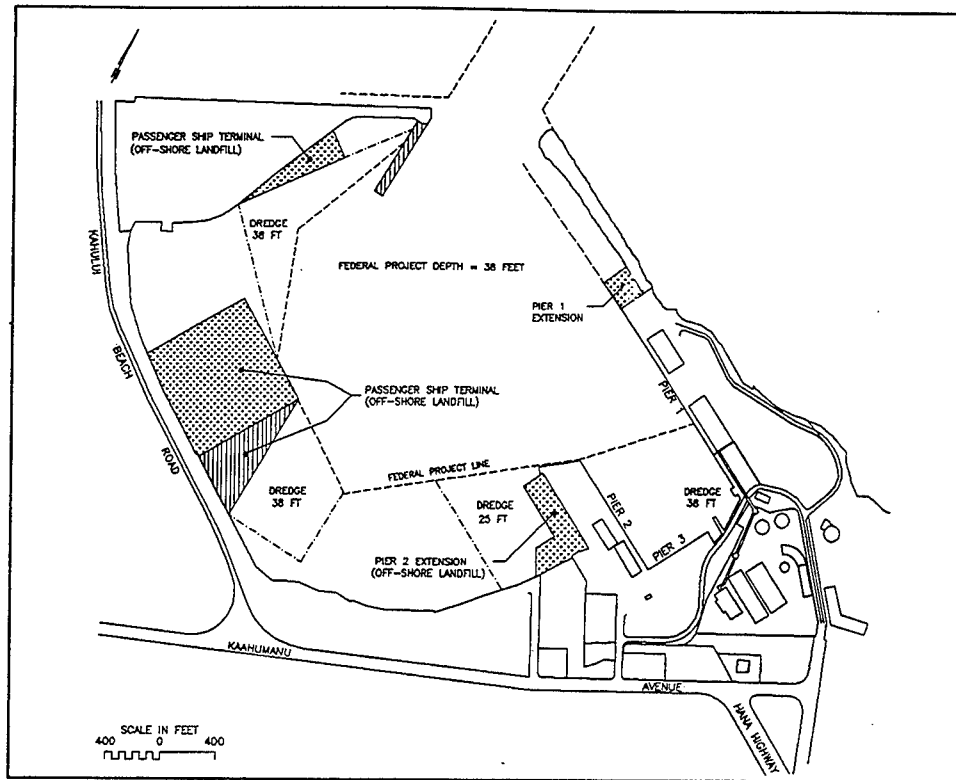
Figure 9. Plan 7

2 Field Wave Measurements

Planning

Wave data were required at Kahului Harbor to document present conditions and provide data to validate numerical and physical models of harbor response to incident wind waves and long waves, also called seiche, or infragravity waves (typically, waves with frequencies lower than 0.03 Hz or wave periods longer than 33 sec). Tidal response was not included. The numerical model calculates the amplitude of the response at each grid point to an incident wave of a particular height, frequency, and approach angle. For each frequency and direction, validation involves driving the model with measured data of known energy and comparing the model's output to the measured energy at one or more sites within the harbor.

Planning the measurement program requires specifying the location, duration, and type of data collected. Ideally, incident measurements coincide with the outer boundary of the model, and there are sufficient interior measurements to define spatial variability within the harbor. Finally, the types of data (wave energy, wave direction, currents, etc.) and the range of frequencies measured should equal or exceed the requirements of the model. Fiscal, logistic, and schedule limits always constrain the ideal measurement plan.

Due to the random nature of waves, it is always difficult to schedule the duration of a wave study in advance based solely on engineering considerations. It is desirable to continue measurements long enough to obtain a broad range of incident conditions - up to or exceeding design conditions - but study schedules and budgets usually override this issue. The plan for Kahului was an initial deployment of one year. A decision to continue measurements would be based on the amount and type of measurements obtained by the end of that year.

Instrument Type and Site Selection

Incident waves in deep water are used to define the wave field before it is affected by local shallow water. For ocean swell with a period of 25 sec, deep water is considered greater than about 500 m. Surface-following buoys are typically used to measure waves in deep water, but the accelerometer-based

sensors have a low frequency cutoff near 0.05 Hz (20 sec), or about at the infragravity band, so only wind waves are measured. In January 1993, a 3-m discus buoy, station number 51026, was installed at latitude 21.37° N, longitude 156.96° W - about 20 n. m. north of Molokai in 7,618 ft (2,322 m) of water. While not directly offshore of the study site, the difference in the deep-ocean conditions over distances less than 100 n. m. was considered small. The wave climate portion of this study (Chapter 3) helped confirm this judgement. The buoy, which measures directional wave energy and meteorological data, is operated by the National Weather Service (NWS) National Data Buoy Center (NDBC). The station was installed prior to, and maintained after, the Kahului Harbor study by the Corps of Engineers' Field Wave Gaging Program. During the scheduled Kahului field data collection period, the station was funded by HDOT.

The range of frequencies of interest for wave energy inside the harbor extends from approximately 0.001 Hz to 0.2 Hz. Experience has shown bottom-mounted pressure sensors provide the desired frequency response, flexibility of placement, reliability, and survivability in the coastal environment. Due to the attenuation of wave-induced pressure fluctuations with depth, measurement of the higher frequency wind waves limits the allowable water depth of the bottom-mounted sensors to around 10 m. (This constraint indirectly affected the offshore extent of the numerical model grid boundary.) Directional information was needed for incident energy at the model boundary. Three or more pressure sensors in an array provide a two-dimensional (energy and direction) spectrum. Only non-directional wave energy, provided by a single pressure sensor at each site, is required inside the model domain. Design, installation, and operation of the shallow water gaging system was provided by the Coastal Data Information Program (CDIP), a joint effort of the Corps and the California Department of Boating and Waterways. The CDIP is a network of wave gages operated by the Scripps Institution of Oceanography (SIO). Gages in the network are linked by radio and/or telephone to a central computing facility in La Jolla, CA, where data are collected, analyzed, qualified, and stored.

Given the size and complexity of the harbor, a minimum of three interior sites, in addition to the incident, or boundary site, were planned. Usually, these sites are selected based on engineering judgement and logistics (Basco and McGehee 1990). For this study, the numerical model itself was used to optimize the measurement sites (Okihiro et al. 1994). Four interior sites were used in this study. Gage locations are summarized in Figure 10 and Table 1.

Data Acquisition

The NDBC buoy measures directional energy with a pitch-roll-heave sensor and magnetometer. The superstructure supports dual anemometers and baro-meters for wind velocity and atmospheric pressure. Thermistors measure near-surface sea and air temperature. Signals from the sensors are time averaged or spectrally analyzed with on-board computers. Reduced parameters are

Table 1
Field Wave Gages

| Name | No. | Type | Coordinates | | Depth MSL (ft) | Sampling Freq. (Hz) | Record Length (sec) |
			N. Lat.	W. Long.			
N. Molokai	51026	NDBC buoy	21°22.2′	156°57.6′	7,618	1.7	1,200
Array	77	CDIP array	20°54.2′	156°28.2′	47.6	1	8,192
Pier 2	79-1	CDIP single pt.	20°53.7′	156°28.0′	45.3	1	8,192
Canoe Club	79-2	CDIP single pt.	20°53.7′	156°28.1′	9.5	2	8,192
Back Basin	79-3	CDIP single pt.	20°53.6′	156°28.3′	12.1	1	8,192
Channel Entrance	79-4	CDIP single pt.	20°53.9′	156°28.5′	30.5	1	8,192
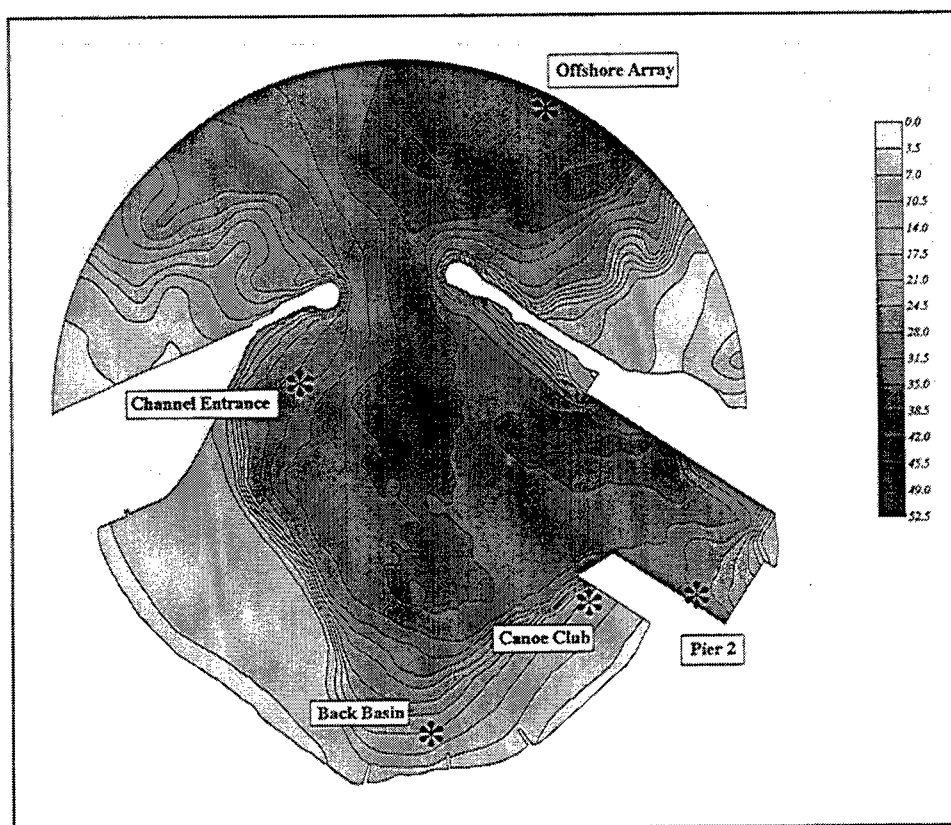
Figure 10. Field gage locations and bathymetry, in feet

transmitted hourly to the NWS gateway via Geostationary Operational Environmental Satellite (GOES) for additional analysis, qualification, and distribution. Edited data are provided monthly to CERC. Details of the measurement, transmission, and analysis process can be found in Steele and Mettlach (1993).

The CDIP system was operated as a "hardwired" system. Signals from the pressure sensors are sampled at 1-2 Hz (Table 1) via submarine cables from an onshore field data logging station. The field station was designed to operate independently, under locally resident program control, as a software-driven, autonomous, data acquisition system. Its primary function is to locally acquire, log, and, in response to a call from a host computer, upload the stored data. The data are received through a phase lock loop, electronically conditioned and optimally compacted, according to the header block instructions, and stored locally in 16 K-bytes of RAM. Storage is based on the "first in, first out" principle, with the oldest word overwritten by the latest word as the storage buffer is filled. Two-way communication between the field station and the central station in La Jolla is accomplished via modem connections, through normal phone service. In response to a phone query from the central station, typically every 3 hr, the field station uploads the latest data buffer. Since each record is over 2 hr long, this allows for nearly continuous sampling (gaps of several minutes occur during downloading). The central station data collection computer, a Sun workstation, superficially examines the incoming data for obvious defects, such as incomplete transmissions and failed phone connections. A detected fault will trigger a retry call to the field station. After additional quality control, final data are transferred monthly to CERC via Internet. Additional details of the CDIP operation are given by Seymour et al. (1993).

Data collection commenced for the NDBC buoy in January 1993, was interrupted briefly in May 1993, and continued through May 1994. Repairs were effected in September 1994, and the buoy continued operation through 1995. Table 2 provides summary statistics for the deployment with 20-year hindcast statistics for comparison (Corson et al. 1986).[1] Figure 11 is a rose plot of the mean significant wave height and occurrence by direction (convention is direction waves are coming from, with respect to true north).

The CDIP system was installed in October 1994 and operated without interruption through the duration of the study. As planned, the adequacy of the measurements was assessed after the first year of operation (McGehee 1995). The principal issues were the *range* of different types of incident conditions measured by the buoy, and the *level* of infragravity energy measured by the harbor gages.

While a reasonable variety of incident wave directions and frequencies was captured, it was not a particularly energetic year. One event sufficient to affect harbor operations occurred, on 14-15 March 1994, reportedly due to wind wave conditions in the entrance. Figure 12 expresses the total measured infragravity energy for each record (high-energy cases only) at each site as an equivalent wave height during the first 8 months of record. Infragravity wave heights experienced in mid-March were exceeded in other months without reported problems. It is not clear whether the lack of reported impacts on operations in

---

[1] For convenience, mathematical symbols used in Table 2 and throughout this report are listed in the notation (Appendix I).

Table 2
Summary Statistics, NDBC Buoy 51026, N. Molokai

Statistical Parameter	NDBC Buoy 51026[1]	WIS Station 31
Mean H_s (ft)	8.5	8.2
Standard deviation of H_s (ft)	2.6	3.0
Mean T_p (sec)	10.7	9.3
Standard deviation of T_p (sec)	2.9	2.6
Most frequent direction (deg coming from)	90	45
Maximum H_s (ft)	23.9	23.3
Associated T_p (sec)	16.7	10.0
Associated direction (deg coming from)	344	196
Percent occurrence, period>18.2 sec	1.2	0.0
Percent occurrence, period>15.4 sec	7.7	0.4

[1] Data from Jan 93 through Feb 96
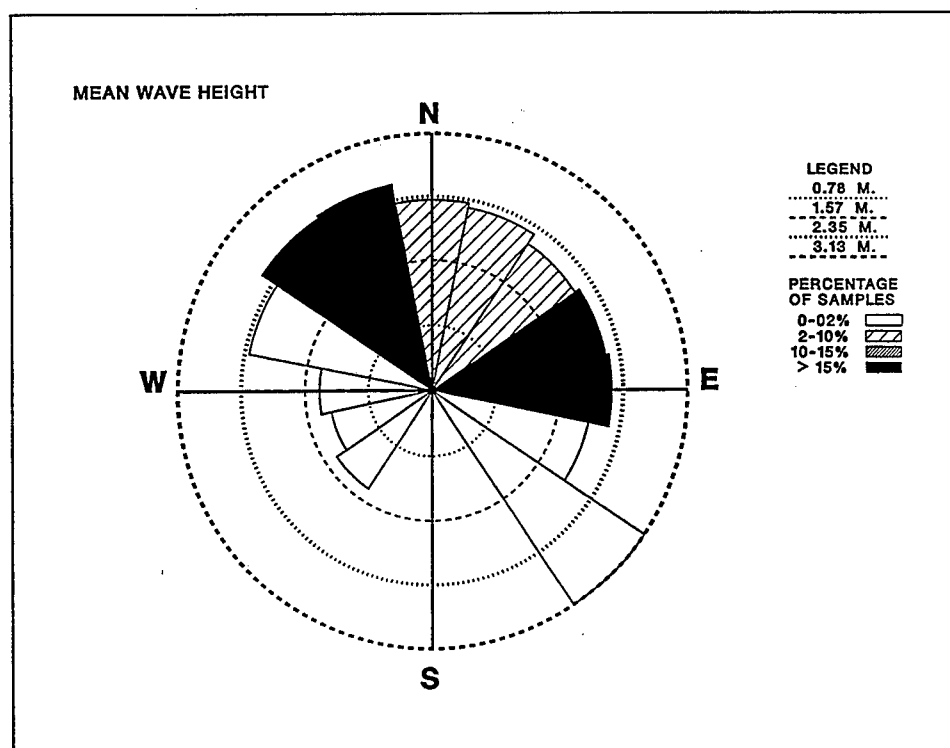
Figure 11. Wave rose, NDBC buoy 51026, N. Molokai

the harbor at those other times results from lack of problems, or failure of problems to be observed/documented. Thus, a simple, quantifiable threshold for allowable infragravity energy was not determined. Additional measurements

were recommended to attempt the capture of a high infragravity event concurrently with noticeable impacts on harbor operations.
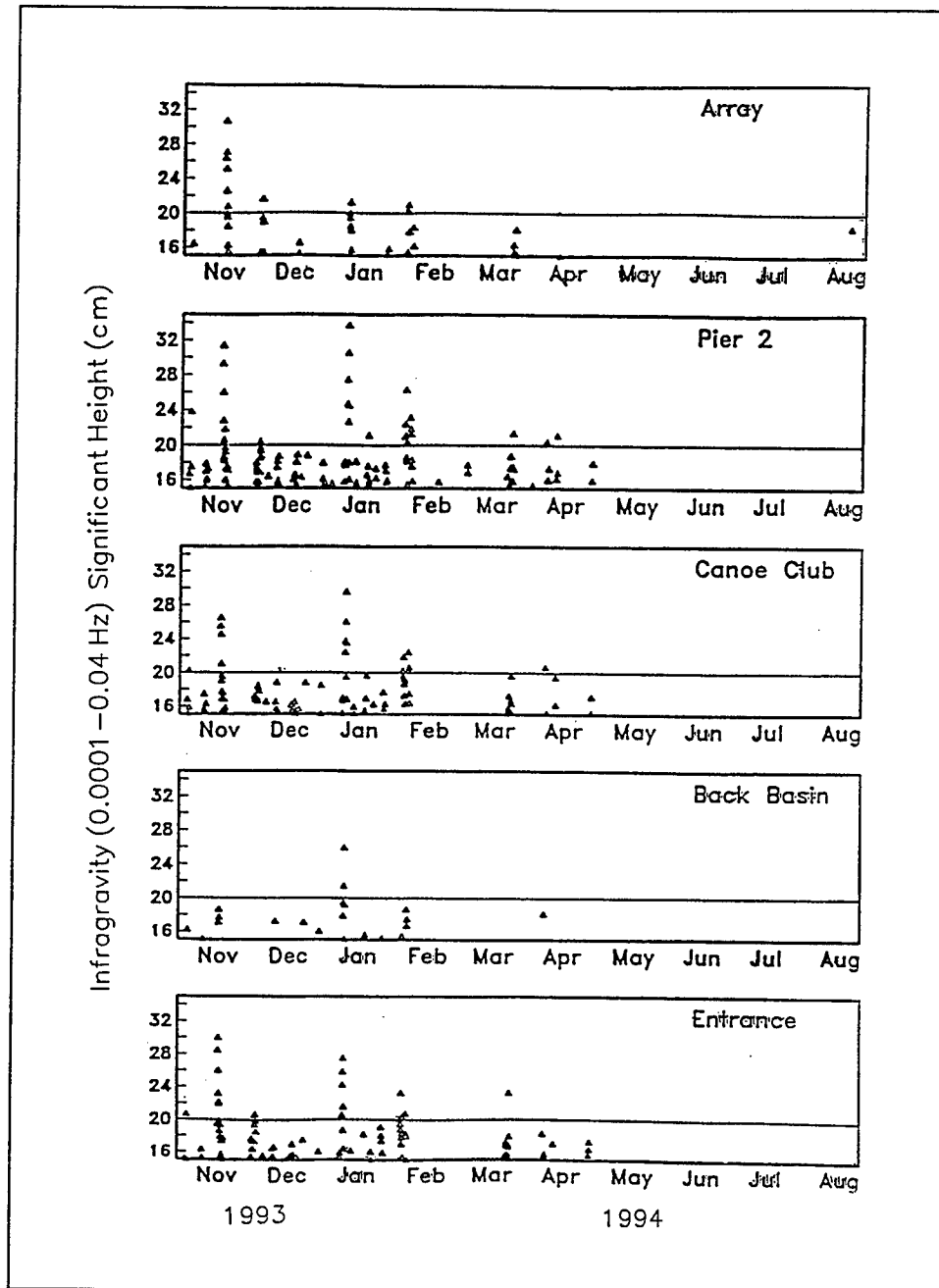
Figure 12. Overview of extreme infragravity wave events; only events with $H_{s,long} \geq 15$ cm are shown (from McGehee (1995))

The memorandum (McGehee 1995) also supported a statistical correlation study to test the ability to predict the amplitude of observed infragravity energy in shallow water with the characteristic wind wave parameters measured offshore. Preliminary analysis showed weak correlation. A longer data set was recommended for statistical reliability of the correlation study. The recommen-

14

dation was followed, and the gages were funded for an additional winter season, through March 1995.

Analysis Methods

The CDIP nearshore wave gage data were processed to give two types of output for each record: spectra and parameters. These outputs, which were customized to meet needs of the Kahului Harbor study, are briefly described here. NDBC buoy data were analyzed with standard NDBC procedures.

SIO provided customized spectra and parameters covering the time period Nov 93 - Sep 94. Subsequent wave climate studies indicated that this data set gives a reasonable representation of the wind wave and swell climate. Wind wave and swell data from the winter of 1994-5 are comparable to the winter of 1993-4. Fewer extreme infragravity (long) wave events occurred in the winter of 1994-5 than in the winter of 1993-4. There were eight events with significant wave heights for long (infragravity) waves $H_{s,long} > 15$ cm in 1993-4 and only three such events in 1994-5 (Merrifield and Okihiro 1996). Also there were no reported operational problems in the harbor during the winter of 1994-5. Because of these considerations, harbor data from Nov 93 - Sep 94 were considered sufficiently representative of the full measurement period for validation of the numerical model and for relating numerical model results to operational concerns.

Spectra

Time series from the CDIP gages were subjected to SIO's standard spectral analysis for long records. The 8,192-sec records gave a spectral resolution of 0.000122 Hz. Spectral output files were created with energy values for the first 286 spectral frequencies, or spectral *lines* (up to a frequency of 0.0349 Hz, corresponding to a wave period of 28.6 sec), followed by energy values for higher frequencies (shorter wave periods) grouped into bands of width 0.01 Hz. A total of 32 frequency bands were included, with central frequencies ranging from 0.04 Hz (25 sec) to 0.35 Hz (2.9 sec). Thus the analysis system produced a high-resolution spectrum for infragravity waves and a conventional resolution spectrum for wind waves and swell. The wind wave and swell spectrum is estimated with an unusually high level of confidence (high number of *degrees of freedom*) because of the exceptionally long records.

Parameters

Spectral results were also condensed into a small number of parameters for output (Table 3). Significant wave height and peak spectral period for long waves were computed from the infragravity portion of the spectrum using the same procedures traditionally used for wind waves and swell (short waves). The Back Basin gage, used for water depth measurement, had a higher quality pressure transducer than the other gages, and was more stable over long time periods.

The last three parameters in the table were added at CERC to the basic parameter files provided by SIO. The number of major peaks in the short wave spectrum was computed by a procedure similar to that of Thompson (1980). Peaks were considered major if their energy density differed from that of the intervening low point by at least 3 percent of the total energy. Amplification factors for long and short waves were defined as

$$A_{amp,l} = \frac{(H_{s,long})_{harbor\ gage}}{(H_{s,long})_{array}} \quad ; \quad A_{amp,s} = \frac{(H_s)_{harbor\ gage}}{(H_s)_{array}} \quad (1)$$

Table 3 Field Wave Parameters	
Description	Symbol
Year, month, day, hour, minute	
Significant wave height, long waves	$H_{s,long}$
Peak wave period, long waves (greater than 29 sec)	$T_{p,long}$
Significant wave height, short waves	H_s
Peak wave period, short waves (3-25 sec)	T_p
Incident wave direction, short waves	θ_m
Long-term average depth at Back Basin	
Mean depth over record length at Back Basin	$\bar{\eta}$
Number of major peaks in short wave spectrum	N_p
Amplification factor, long waves	$A_{amp,l}$
Amplification factor, short waves	$A_{amp,s}$

Estimation of T_p

The traditional procedure for estimating T_p for wind waves and swell was modified in this study to obtain better resolution in the swell periods. Peak period is normally calculated as the reciprocal of the frequency at the midpoint of the highest energy spectral band. This is a standard, widely accepted procedure. The resolution with standard 0.01-Hz spectral bands is sufficient to give a good estimate of peak period over most of the possible frequency range, but it is rather coarse for the longer swell periods. The standard procedure imposes some limitations on the Kahului Harbor study for the following two reasons:

a. Much of the wave energy at Kahului Harbor, including cases of greatest interest, is long period, low frequency swell.

16

b. The range of possible wave period variation within a single low-frequency band translates into significantly different harbor responses in the numerical model and, presumably, the field.

The most straightforward change is to use a finer spectral bandwidth, though finer bands have the undesirable consequence of lower confidence levels. SIO provided CERC with one month (January 1994) of detailed line spectral coefficients to explore alternatives (Thompson 1995). The effect of bandwidth on the T_p estimate is illustrated in Figure 13 using data from the array (line spectra from all four sensors averaged together). This record was selected because there was an exceptional level of long wave energy in the harbor. Bandwidth is expressed in the figure in terms of the number of spectral lines. The standard SIO procedure for the Kahului Harbor gages gives 82 lines per band. Peak period estimates are quite variable. For this particular case, T_p estimated by the standard procedure is 14.29 sec while the "true" peak period (middle of the scatter) appears to be around 15 sec. The sawtooth shape of the plotted data arises because the main energy concentration slowly marches toward shorter period as bandwidth increases. Eventually, the band preceding the main energy extends far enough to encompass that energy, and peak period abruptly shifts to the center of that band.

The artificial variability induced by bandwidth can be reduced by using overlapping bands to identify a T_p. The approach is to select a bandwidth and identify T_p. Then the bands (keeping the same bandwidth) are shifted a fixed number of lines toward higher frequency (shorter period) and T_p is again estimated. The bands are shifted repeatedly and the final estimate of T_p is based on whichever band gives the very highest energy. The whole process can be repeated with different choices of bandwidth to examine this effect as well. Results with a two-line shift show a significantly reduced scatter relative to the nonoverlapping approach (Figure 14). Thus the overlapping bands allow a more refined estimate of T_p.

Two other cases in January 1994 corresponding to high levels of long wave energy in the harbor were examined using the same overlapping band approach. Peak period for 20 Jan 94 (1314) appears to be well-estimated by both the overlapping approach and the standard approach (Table 4). However, this case has a relatively short T_p and broad energy spectrum. The T_p for 31 Jan 94 (0719) is around 18 sec by the overlapping approach and 20 sec by the standard approach. The standard analysis is not sufficiently discriminating for this case.
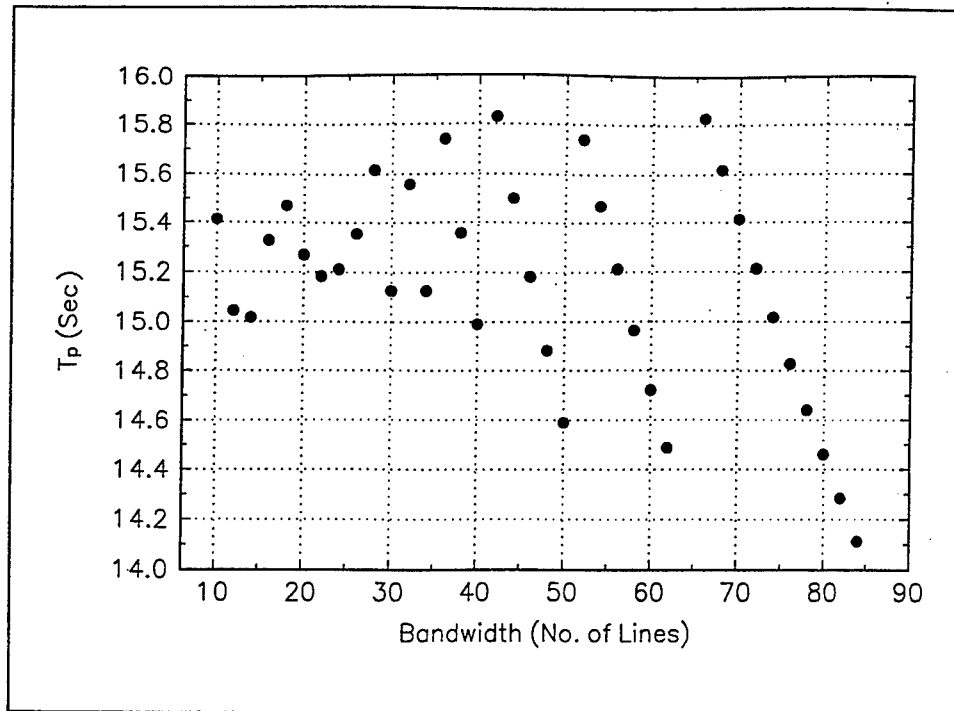
Figure 13. Influence of spectral bandwidth on T_p , non-overlapping bands; array,
3 Jan 94 (1311)
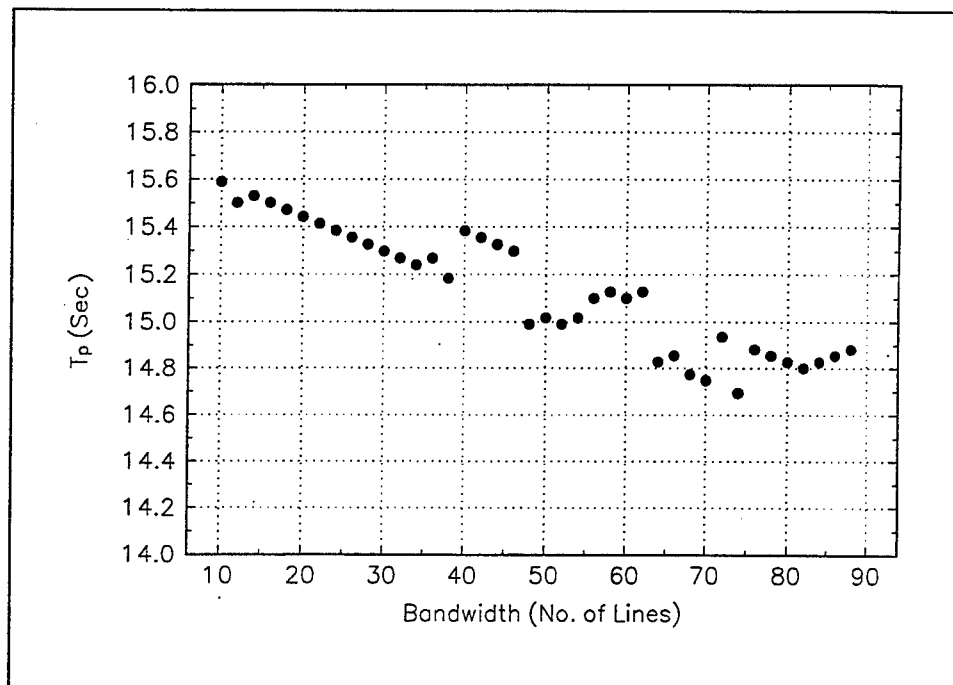
Figure 14. Influence of spectral bandwidth on T_p , overlapping bands (two-line
offset); array, 3 Jan 94 (1311)

Table 4 Effect of Overlapping Bands on T_p Estimates, Array		
	T_p (sec)	
Date	Standard Analysis	Overlapping Bands, Two-Line Offset
1311 03 Jan 94	14.3	14.8
1314 20 Jan 94	10.0	10.1
0719 31 Jan 94	20.0	18.0

Because of these considerations, the SIO procedure for estimating T_p values for wind waves and swell in this study was modified to an overlapping approach with a one-line overlap. Thus the reported T_p corresponds to the midpoint of the 82 consecutive spectral lines which collectively have the highest energy in the spectrum.

Results

Parameters and spectra from the CDIP array and harbor gages were studied and evaluated in various ways to better understand harbor behavior and to prepare results in a form useful for validating the numerical model. Summaries are included in Appendix A of this report and in monthly compendia (e.g., Coastal Engineering Research Center (1996)). Complementary studies by Okihiro and Guza (1996) have also contributed to understanding of the harbor.

Parameters

Parameter time-histories were plotted by month, as illustrated in Figures 15-17. The plots are useful for reviewing the variety of conditions recorded and for identifying relationships between parameters. As an example, Figure 16 shows a strong tendency for high values of H_s and $H_{s,long}$ to occur together. Correlation coefficient statistics were computed between selected parameters, as illustrated in Table 5 for Pier 2. The correlation coefficient for H_s and $H_{s,long}$ is fairly high, 0.81 at Pier 2. That correlation was also high at other gages (not shown): 0.74 at the array and between 0.61 and 0.72 at the other harbor gages. Other parameters showed lower correlations, but evidence of some other tendencies, such as a weak correlation between $H_{s,long}$ in the harbor and $(H_s)_{array}$.

The variation of $A_{amp,s}$ and $A_{amp,l}$ with various long and short wave parameters is an important concern. These parameters are actually quite consistent at any given location. For example at Pier 2, $A_{amp,s}$ is around 0.1 and $A_{amp,l}$ is generally between 1.2 and 1.8. Peaks in $A_{amp,s}$ tend to coincide with long period swell events (high values of T_p). The smallest values of $A_{amp,l}$ generally occur with high energy events (high values of H_s and $H_{s,long}$).

Parameter summaries are especially useful for numerical modeling of short waves. The range and distribution of measured T_p and θ_m values at the array help determine wave conditions to be modeled (Figures 18 and 19). Since the numerical model produces amplification factors as a function of incident short wave period and direction, similar results from the field data are needed for validation. Values of $A_{amp,s}$ from field gage records were grouped according to 1-sec bins of T_p and 10-deg bins of θ_m. A mean and standard deviation were computed from values of $A_{amp,s}$ in each bin (Appendix B).

The parameter N_p (number of spectral peaks) at the array was found to be one in almost every case. Thus short wave conditions at Kahului Harbor are generally well-represented by T_p. More than one major wave event (e.g. sea and swell) occurring simultaneously is unusual.
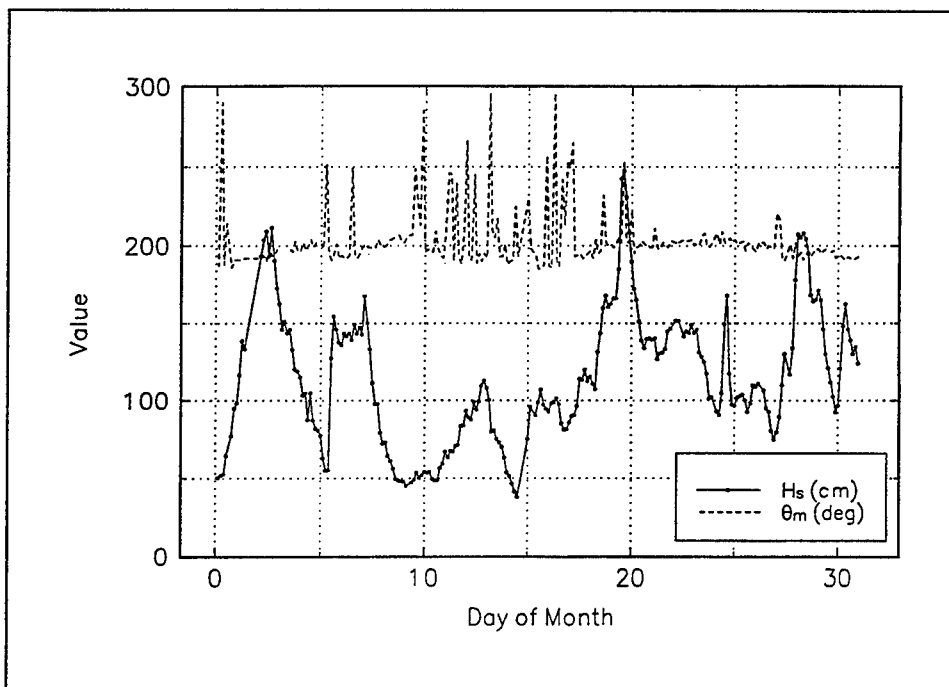
Figure 15. Time-history of H_s and θ_m (deg, going toward); array, Jan 94

Table 5
Field Wave Gage Parameter Correlation Coefficients, Pier 2, Jan 94

Para-meter	Parameter								
	$T_{p,long}$	H_s	T_p	θ_m	$\bar{\eta}$	$A_{amp,s}$	$A_{amp,l}$	$(H_s)_{array}$	$(T_p)_{array}$
$H_{s,long}$	0.49	0.81	0.42	0.03	0.06		0.10	0.47	0.12
H_s		1.00	0.33	0.03	0.10	0.44			0.24
T_p			1.00	0.05		0.54			
θ_m				1.00	0.01	0.10			
$A_{amp,s}$						1.00			0.66
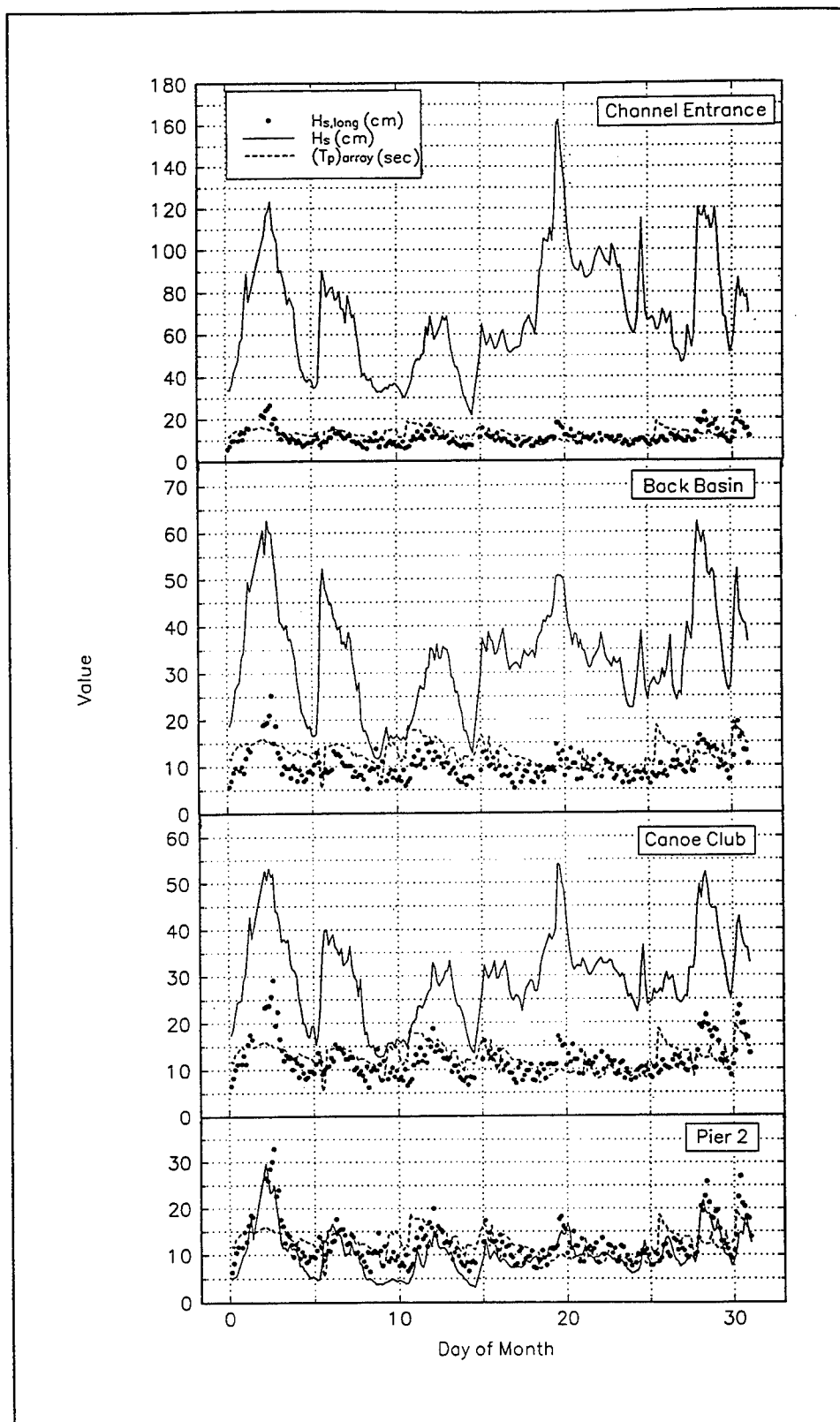
Figure 16. Time-history of $H_{s,long}$, H_s, and $(T_p)_{array}$; harbor gages, Jan 94
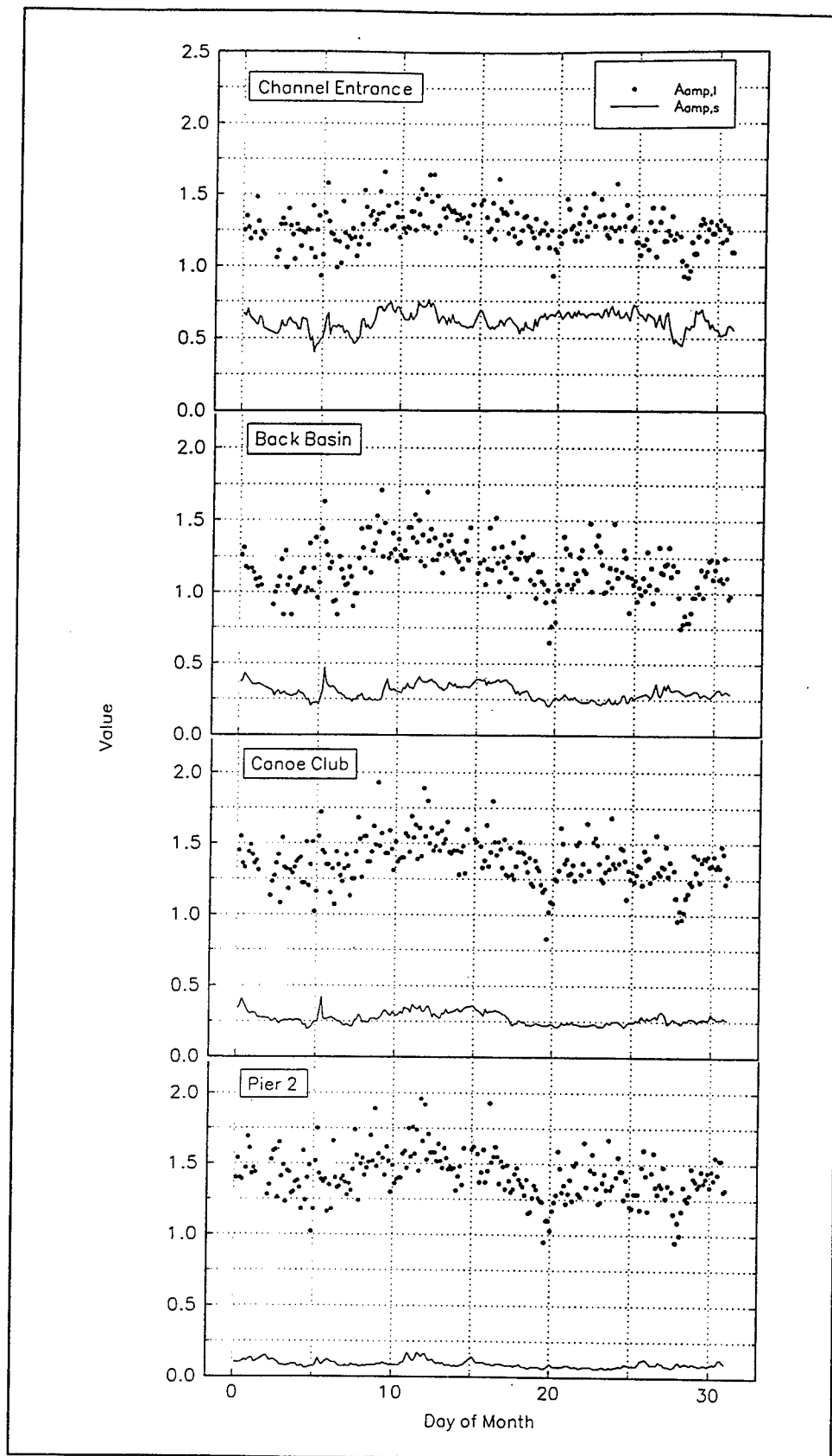
Figure 17. Time-history of $A_{amp,s}$ and $A_{amp,l}$; harbor gages, Jan 94
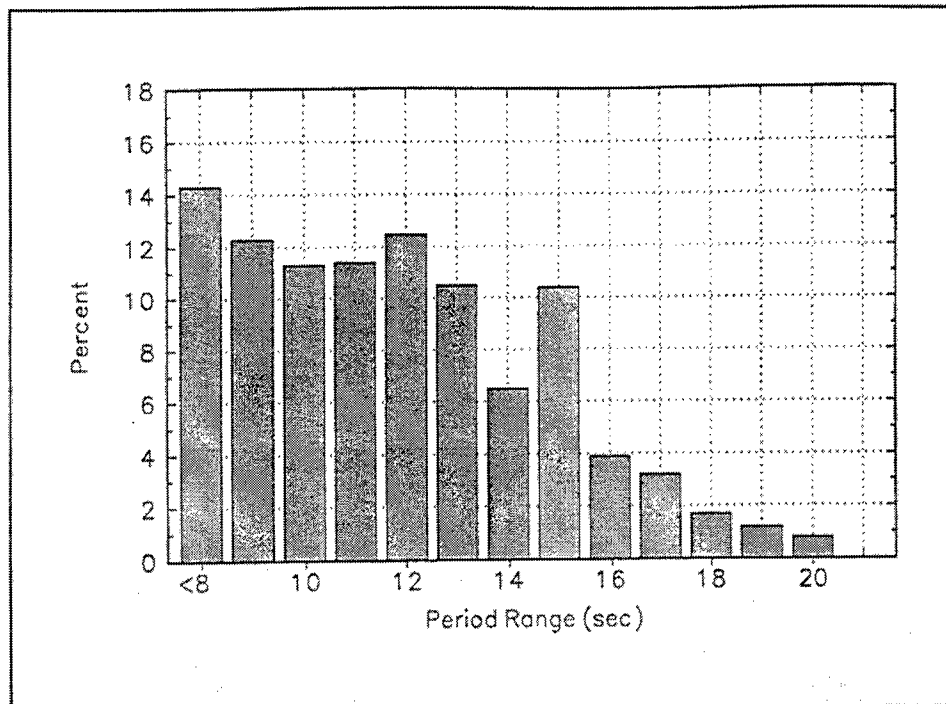
Figure 18. Probability distribution of $(T_p)_{array}$; Nov 93-Sep 94, 1,785 observations
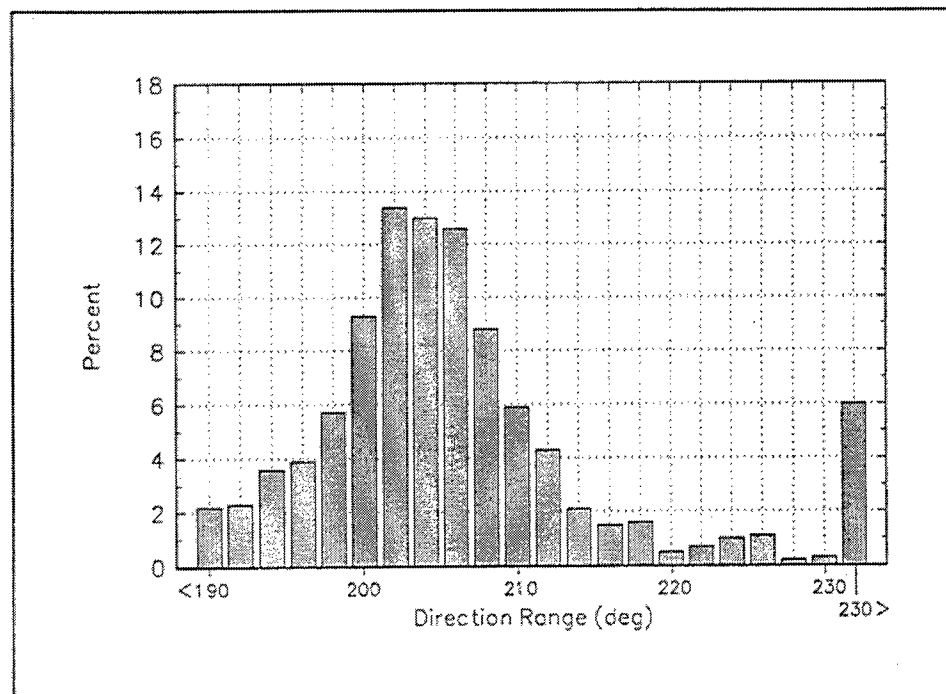
Figure 19. Probability distribution of $(\theta_m)_{array}$; Nov 93-Sep 94, 1,785 observations

Spectra

Short wave spectra were required to compute N_p. It is also helpful to examine spectra for specific events of interest to identify any presence of multiple wave systems or to confirm that H_s and T_p adequately characterize the sea state.

Spectra are especially useful in relation to long waves. Average long wave spectra were computed by month for each gage to reveal general structure in the long wave response of the harbor. A maximum energy density value (over all records during the month) at each spectral frequency was also identified. The results for January 1994 are typical (Figure 20). Average spectra are surprisingly similar from month to month. Maxima are typically an order of magnitude higher than the average, but they define a shape very similar to the average spectra. The maxima clearly show more statistical variability than the averages, as would be expected.

Long wave spectra were examined in more detail to better understand harbor response during high energy long wave events. Spectra for one such event are shown in Figure 21. Averages of the event spectra are also shown. Individual spectral values fluctuate over a very wide range. Averages follow the characteristic shape of monthly averages, suggesting that each area of the harbor tends toward a signature response curve which varies in energy level according to incident wave variations but not in shape. The energy level across all frequencies of the extreme event average spectra is considerably higher than that of the monthly average spectra (Figure 20). Mean water level variations during the event had no clear impact on energy level of the spectral peaks at Pier 2, but they did appear to cause very small shifts in the frequency at which the peaks occurred.

To explore whether high energy long wave events consistently excite the main resonant peaks of the signature response curve, the time-history of energy level at specific resonant frequencies was plotted. Figure 22 shows results for a dominant resonant frequency at Pier 2. Two adjacent frequencies are shown because varying conditions, such as tidal water level, caused the peak frequency to vary over this very small range. By comparing with Figure 16, it is clear that high values of $H_{s,long}$ are accompanied by high energy in this resonant peak. Other resonant peaks show similar correspondence, indicating that when $H_{s,long}$ is high, all of the characteristic resonant frequencies have high energy levels.

Correlations for predicting incident infragravity wave energy

A special study was conducted to relate incident infragravity (long) wave energy to offshore wave conditions, for which long-term information is available. The purpose of the correlation study was to determine the ability to predict infragravity energy levels incident to the harbor from deepwater, wind wave parameters (Merrifield and Okihiro 1996). Correlations and linear regressions were calculated between observed infragravity energy (converted to an $H_{s,long}$) in the frequency range 0.002-0.040 Hz (500 to 25 sec) at the array just outside of the harbor and reduced parameters (H_s, T_p, and θ_m) measured at the offshore

24

NDBC buoy. The distribution of $H_{s,long}$ at the array and θ_m at the buoy over the two-winter analysis period is shown in Figures 23 and 24.

In general, the correlations were weak. A correction for the reduction in wind wave energy at the array based on the direction of the deepwater waves provided some improvement, but predictions of infragravity energy levels based on offshore wind wave height still vary by a factor of five or more (Figure 25). The study concluded that detailed inspection of the deepwater spectra, perhaps in combination with a refraction-diffraction transformation model, would be needed to significantly improve the predictions.

Special events, harbor closing

The only reported operational problem during the period of harbor wave measurement was a closing of the harbor on 14-15 Mar 94. Figures 26-28 summarize CDIP array and NDBC buoy wave and meteorological measurements during the event. Figure 29 helps put the event in perspective relative to the full winter of 1993-4. The steepness parameter in the figure is the ratio of $(H_s)_{buoy}$ to deepwater wavelength based on $(T_p)_{buoy}$. Although $(H_s)_{array}$, $(H_{s,long})_{array}$, and $(H_s)_{buoy}$ are all high during the closure, they are not sufficiently high to distinguish the event as more extreme than other recorded events. The exceptional condition during closure appears to be a combination of high winds, high wave steepness, and long duration. Thus the harbor was apparently closed by a hazardous short wave condition (steep, energetic waves with likely wind-induced breaking).

Special events, tsunami

While tsunamis were not considered in the design of this study, the continuance of the gages beyond the first year resulted in a fortuitous measurement of the Shikotan tsunami on 4 October 1994 (McGehee and McKinney 1996). The measurement represents one of the few large (approximately 1-m wave height) tsunami time series sampled continuously at high frequency (1 Hz). The tsunami wave period was approximately 30-35 min, or about 0.0005 Hz. Aside from the scientific value, this data set provided an opportunity to examine the response of the harbor to one instance of large-amplitude infragravity energy.

Special events, extreme event parameters

A more detailed documentation of extreme events recorded by the CDIP gages is given in Appendix C. Included are tabular summaries of parameters for observations with $(H_s)_{array} \geq 200$ cm for short wave extremes and $H_{s,long} \geq 20$ cm at the array or Pier 2 for long wave extremes.
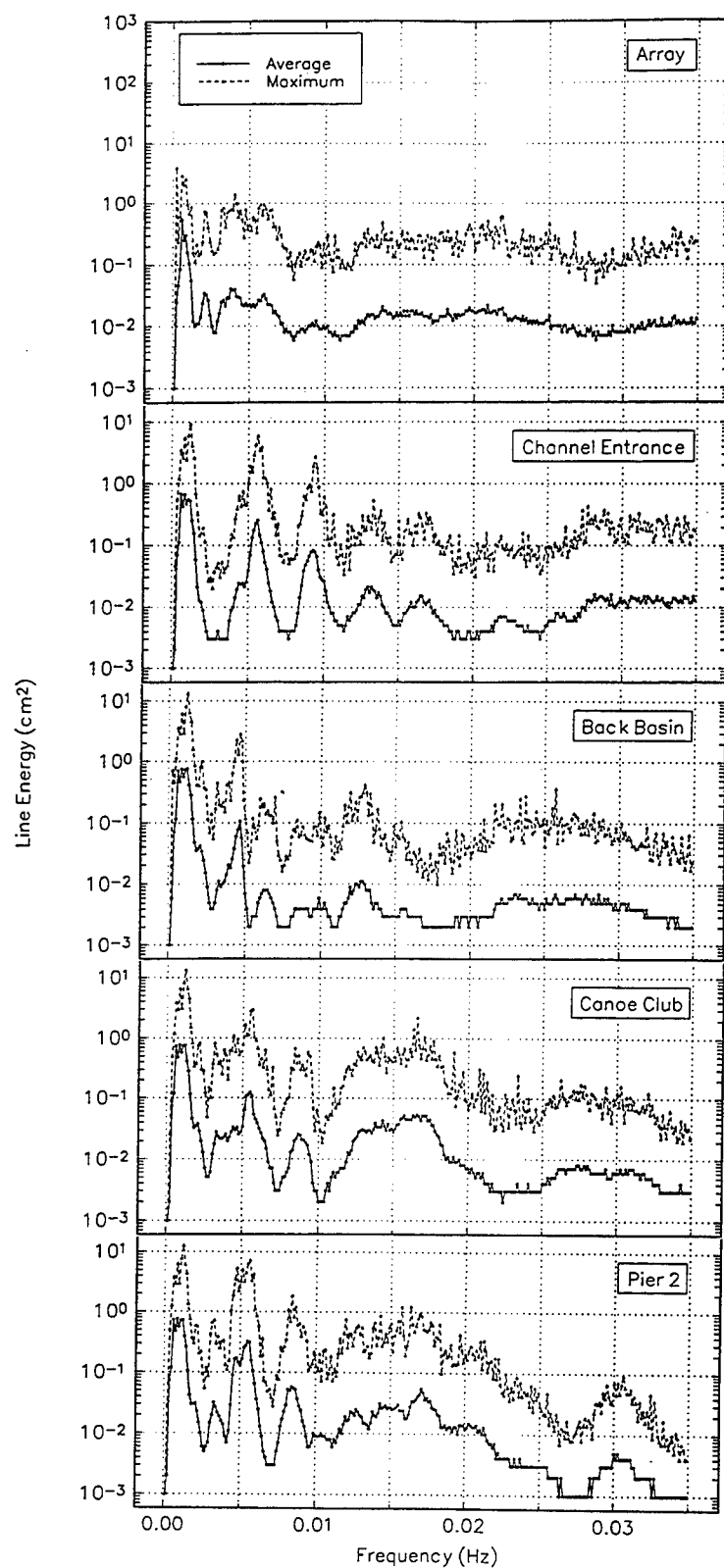
Figure 20. Average and maximum long wave spectra, Jan 94
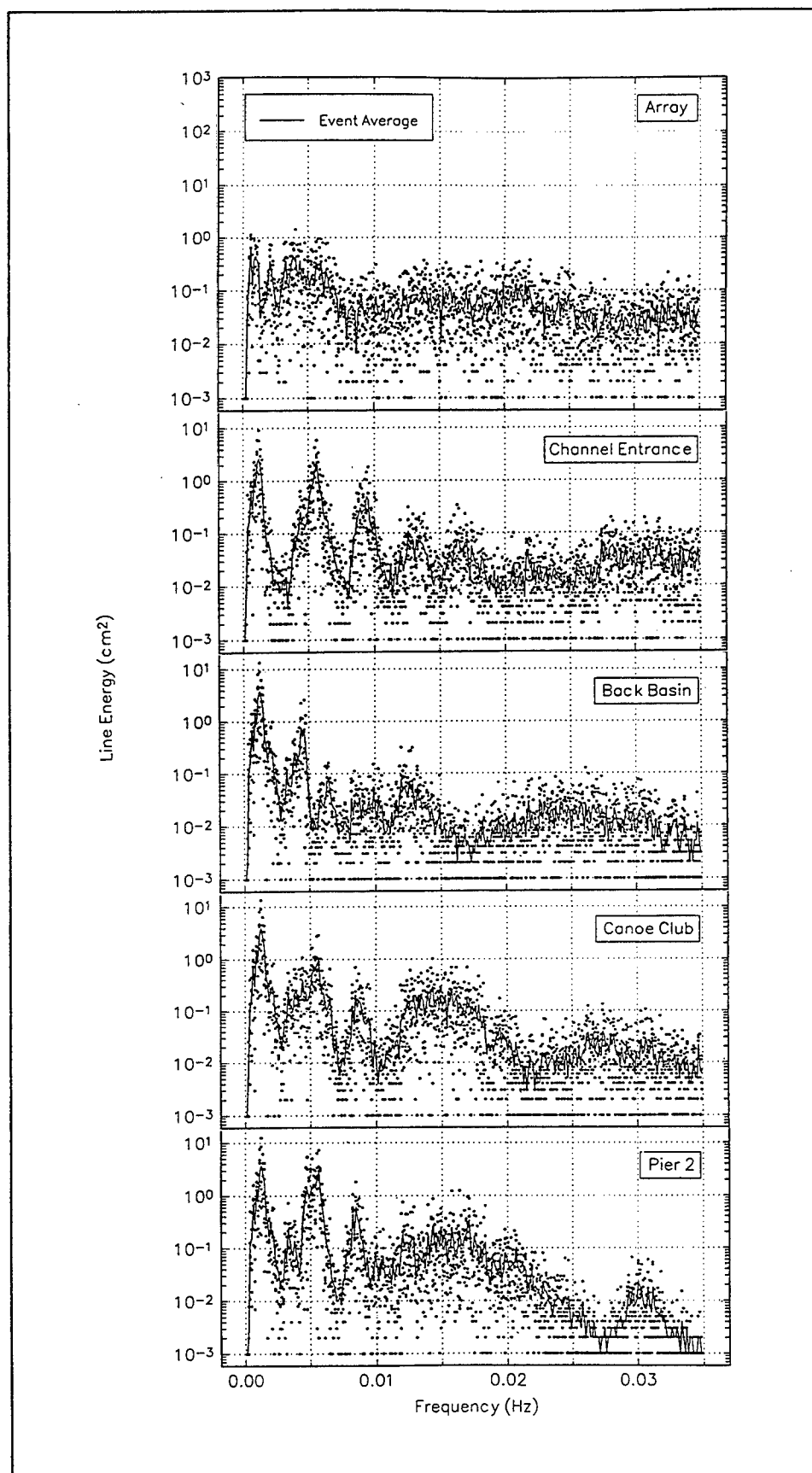
Figure 21. Long wave spectra for event on 2 Jan 94 (2355) to 3 Jan 94 (1900)
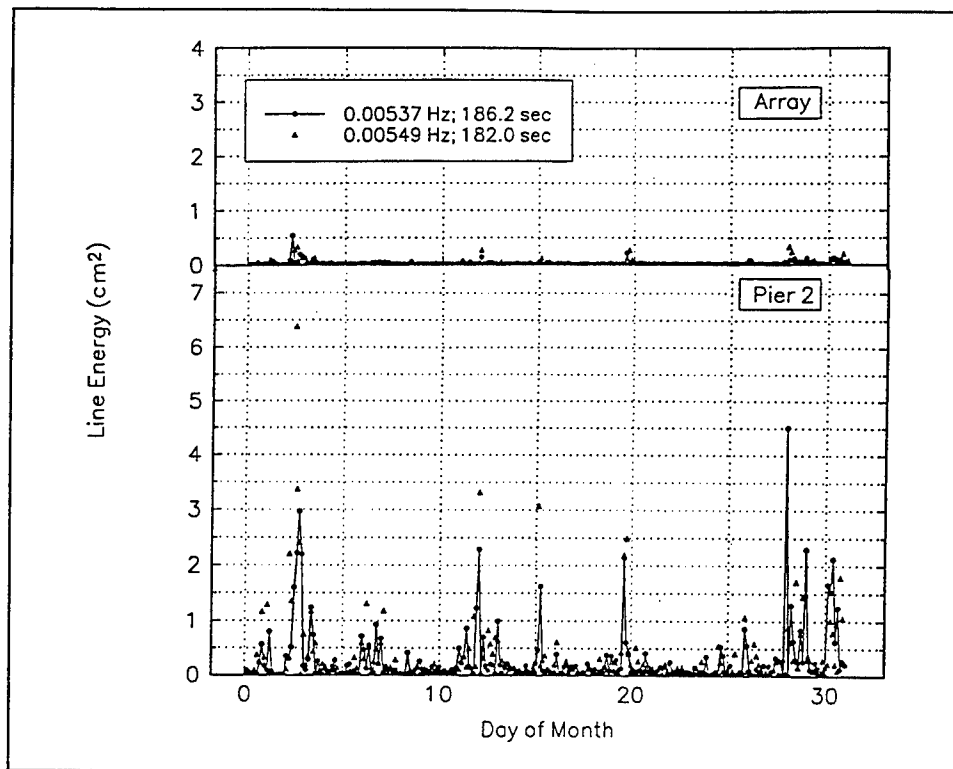
Figure 22. Time-history of amplification of specific resonant peak frequencies,
Jan 94
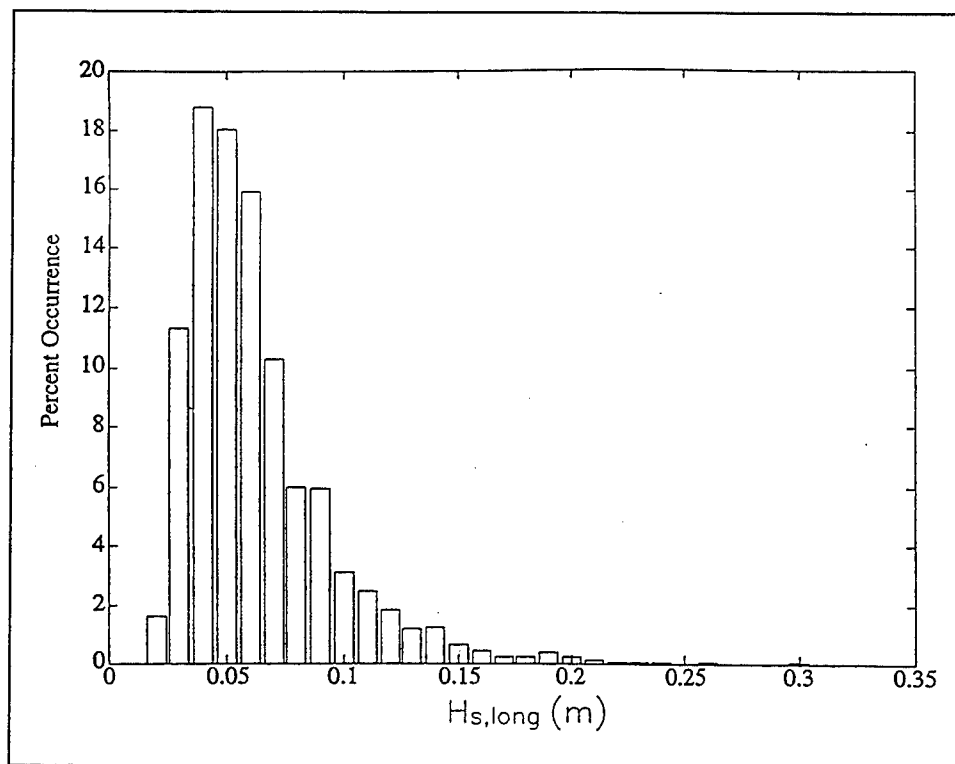
Figure 23. Probability distribution of $(H_{s,long})_{array}$, Oct 93-Mar 95 (from Merrifield
and Okihiro (1996))
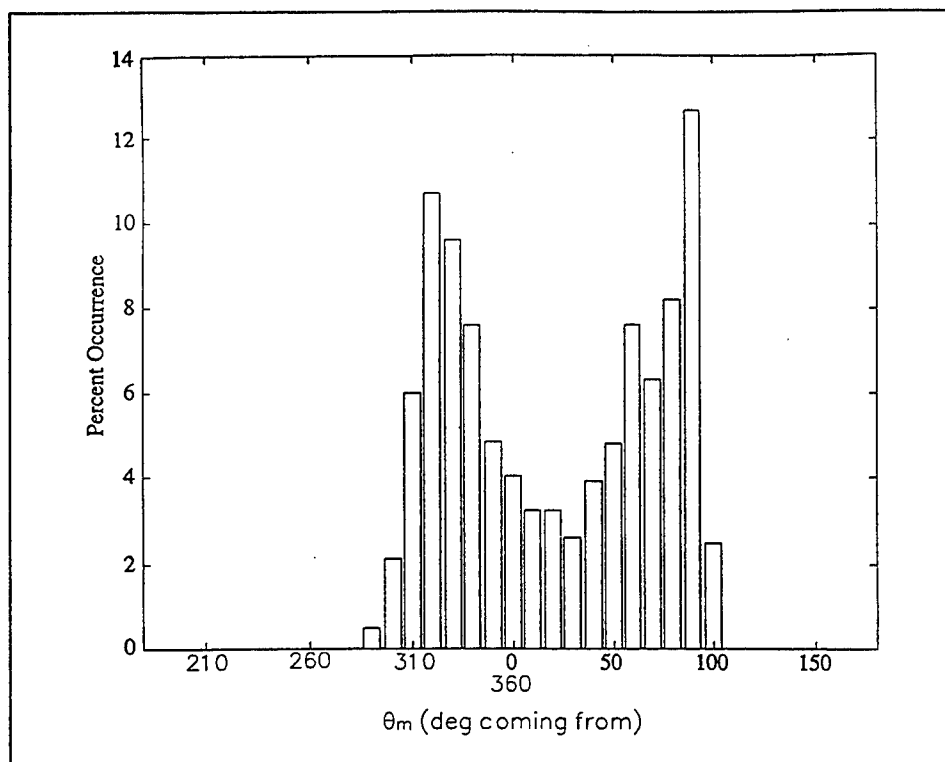
Figure 24. Probability distribution of (θ_m)$_{buoy}$, from NDBC buoy 51026, N. Molokai, Oct 93-Mar 95 (from Merrifield and Okihiro (1996))
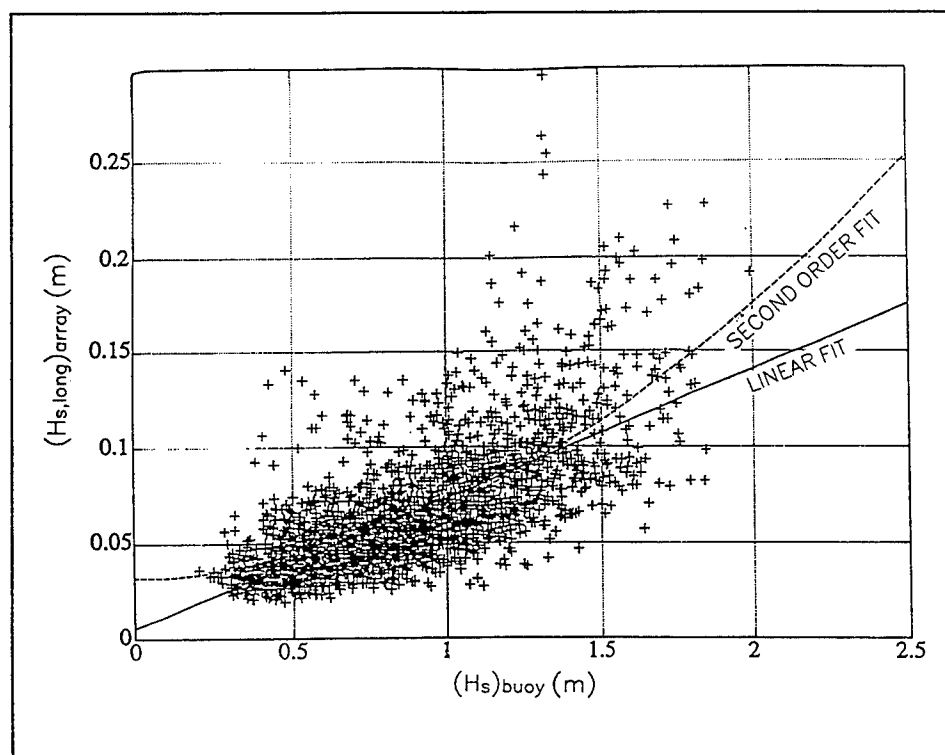
Figure 25. Scatter plot of ($H_{s,long}$)$_{array}$ versus (H_s)$_{buoy}$ (from Merrifield and Okihiro 1996)
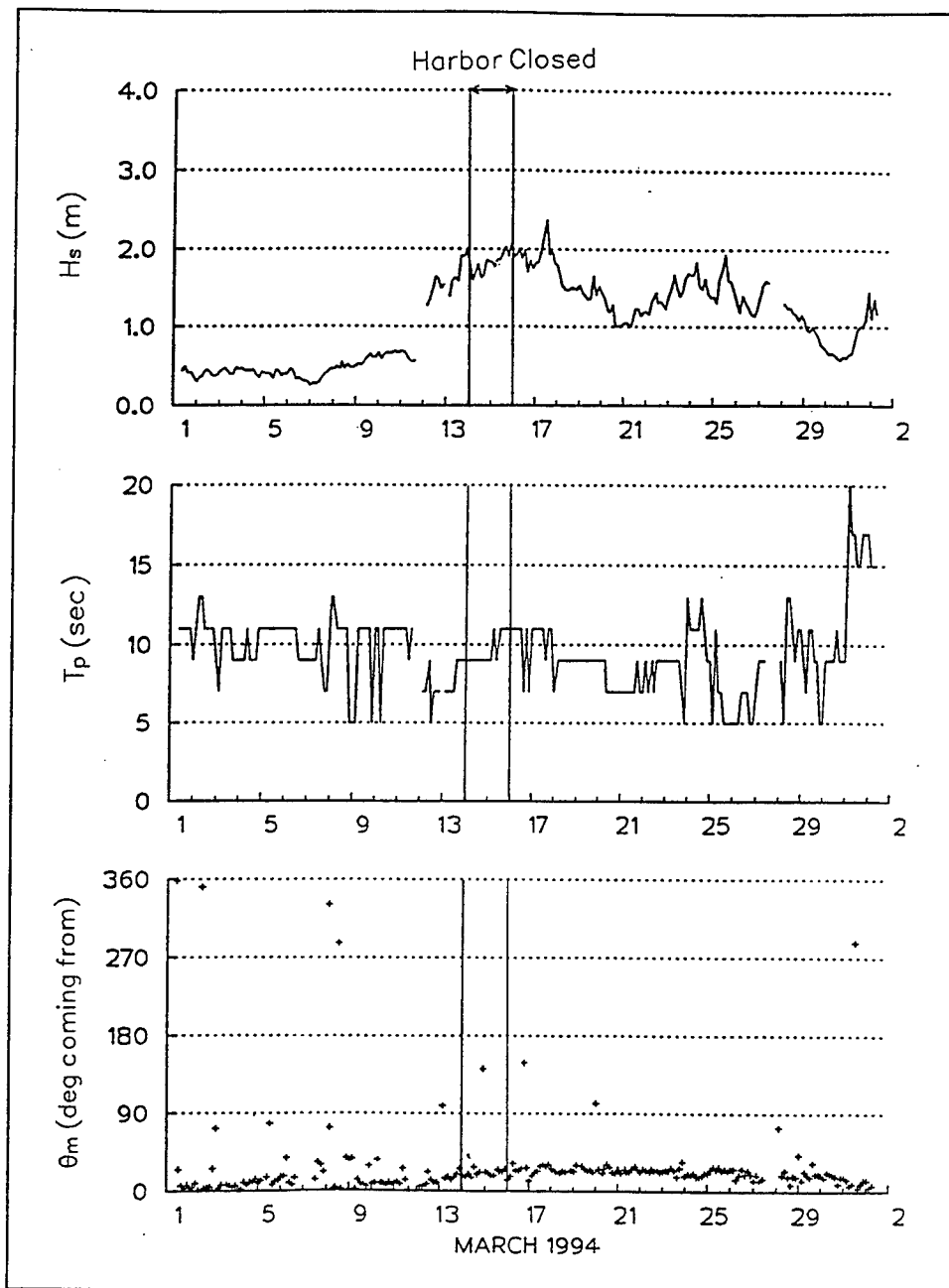
Figure 26. Harbor closing event; array parameters
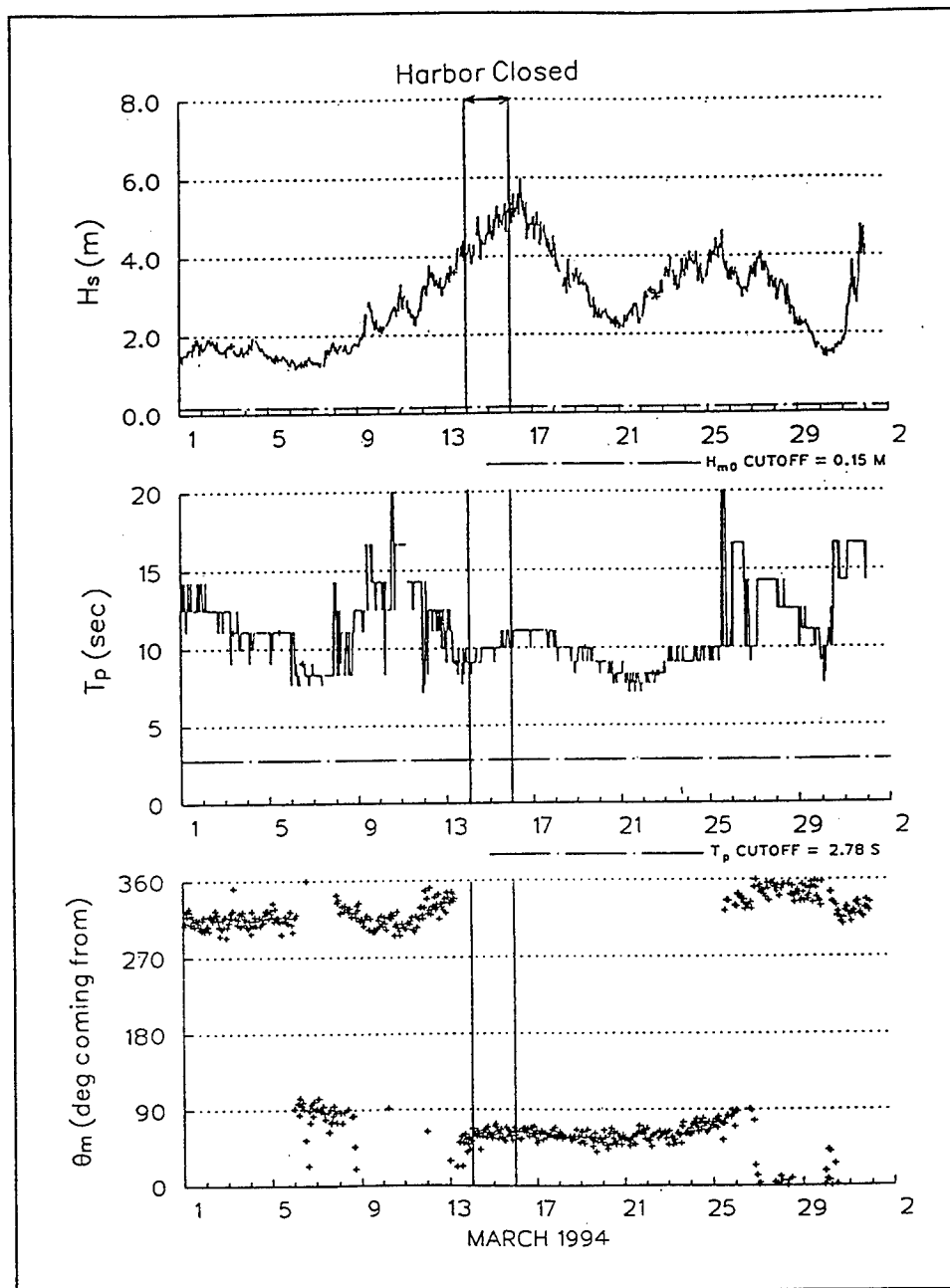
Figure 27. Harbor closing event; NDBC buoy wave parameters
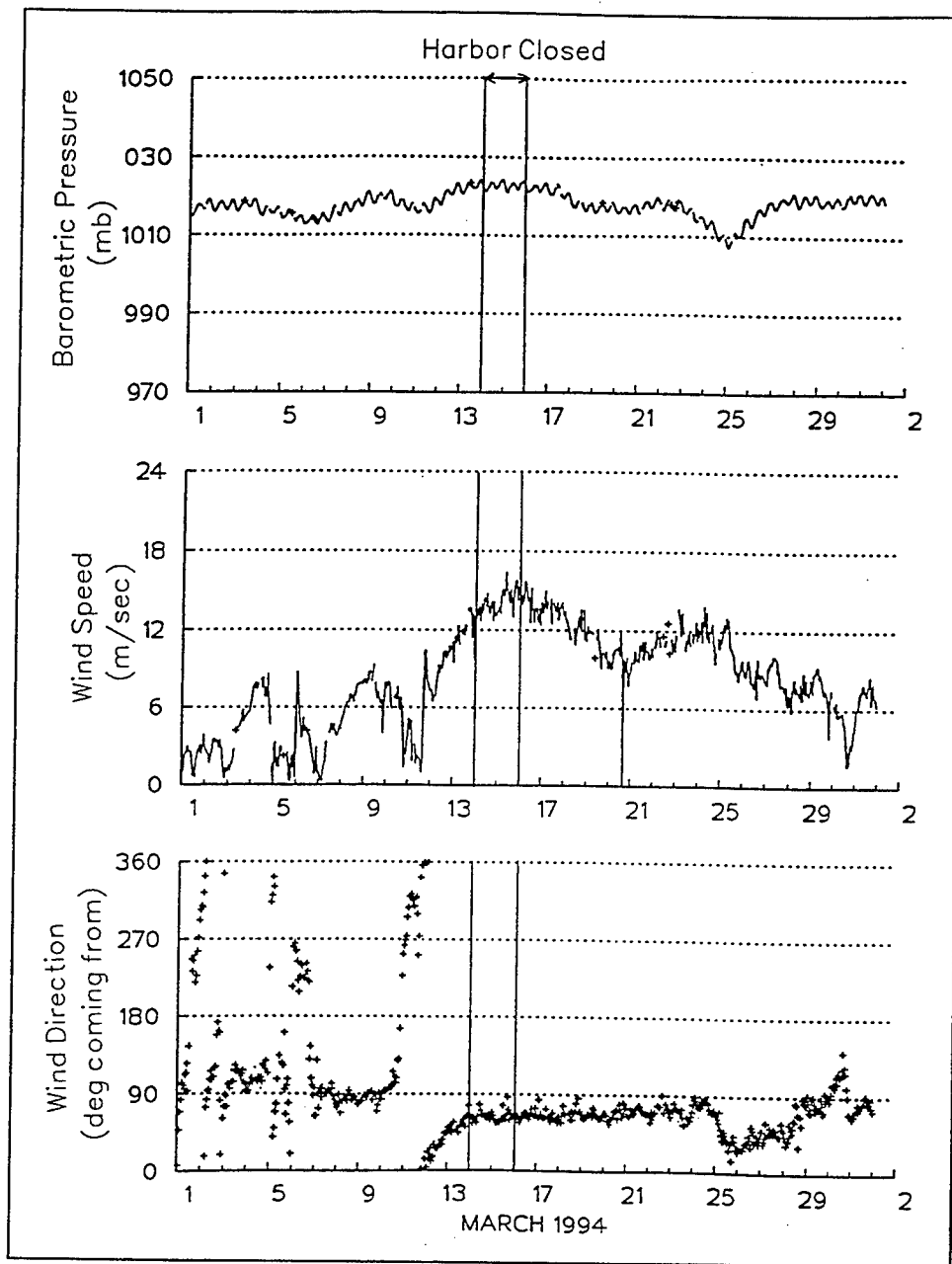
Figure 28. Harbor closing event; NDBC buoy meteorological parameters
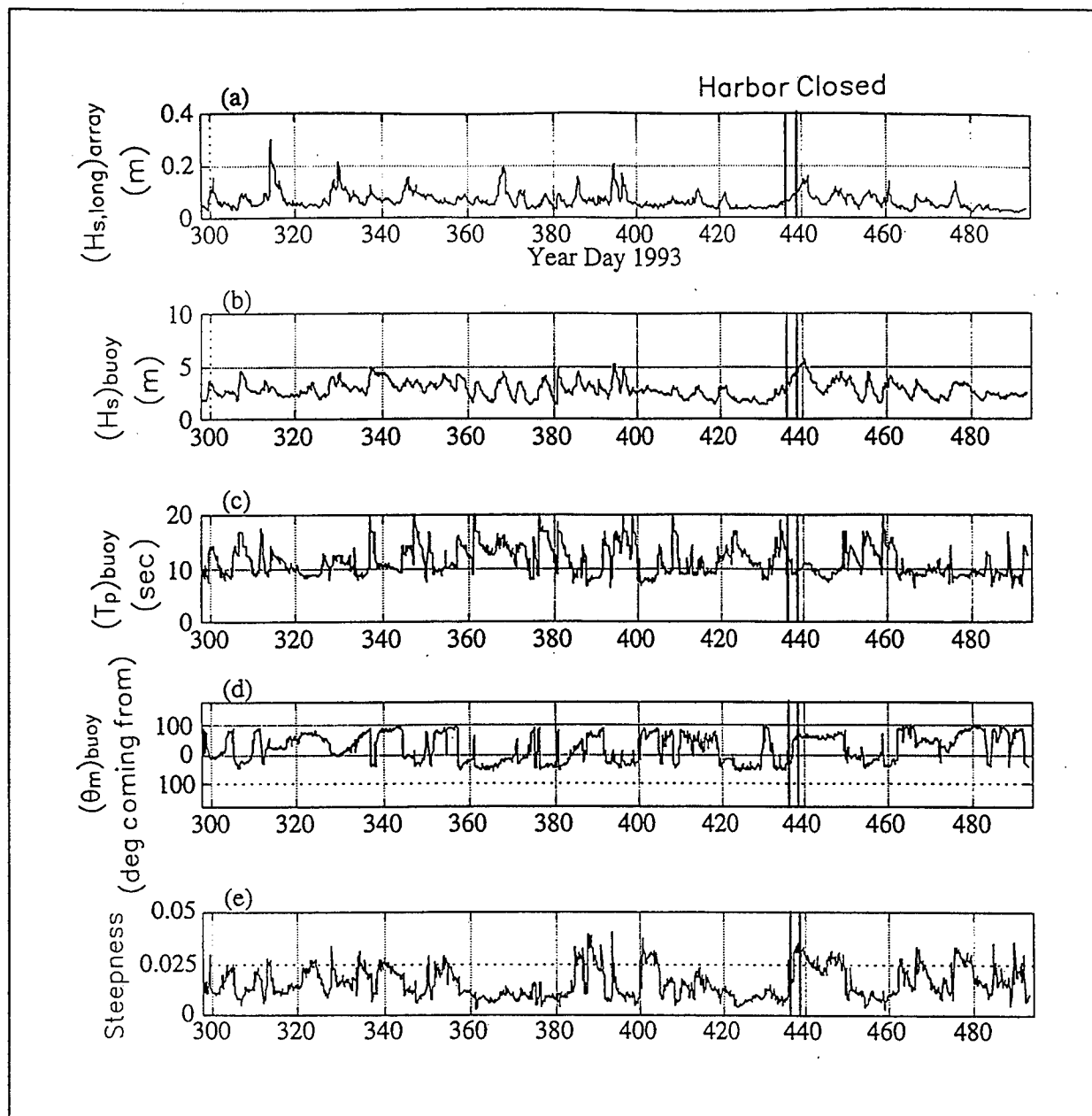
Figure 29. Time-history of selected wave parameters, array and NDBC buoy, winter of 1993-4 (from Merrifield and Okihiro (1996))

3 Wind Wave and Swell Climate

Sources

Three sources of wind wave and swell information were available to develop wave climate outside the harbor entrance (Table 6 and Figure 30). The first was the directional array gage in the 47.6-ft (14.5-m) depth just outside the harbor entrance (CDIP gage 77). Data from November 1993 through December 1994 were used. The second was the directional buoy north of Molokai (NDBC buoy 51026) with data from October 1993 through May 1994 and September through December 1994. These gages are discussed in Chapter 2. The time intervals used were intended to be reasonably representative of the seasons of the year so that the gage data could be compared to long-term climate. Inclusion of the additional three months of available array data (Jan-Mar 95) would have distorted the distribution toward winter conditions (high wave heights).

The third source was the Wave Information Studies (WIS). WIS has hindcast waves over the North Pacific Ocean and saved information at selected deepwater stations around the Hawaiian Islands (Corson et al. 1986). Station 31, north of Maui, from the main 20-year hindcast, was considered in this study. The study also included two stations from a specially prepared 1-year WIS update coincident with the measurement time period. Stations of interest in the special update, which used a different grid, are shown in Figure 30 (Stations 3 and 5). Results from Station 5 were compared to data from the NDBC buoy to validate the special hindcast. Sample validation plots and wave summaries are given in Appendix D.

Deepwater Wave Climate

Although an NDBC buoy and three WIS stations are available in deep water offshore from Kahului Harbor, only WIS Station 31 provides long-term climate information. It is important to evaluate whether the locations and time period of measurement and special hindcast are representative of the long-term

Table 6
Sources of Wave Climate Information

Source	Years	Latitude (deg N)	Longitude (deg W)
CDIP Gage 77 (Kahului array)	1993-94	20.90	156.47
NDBC Buoy 51026 (N. Molokai)	1993-94	21.37	156.96
WIS Station 31	1956-75	21.94	155.69
WIS Station 3	1994	22.20	155.63
WIS Station 5	1994	21.26	156.56
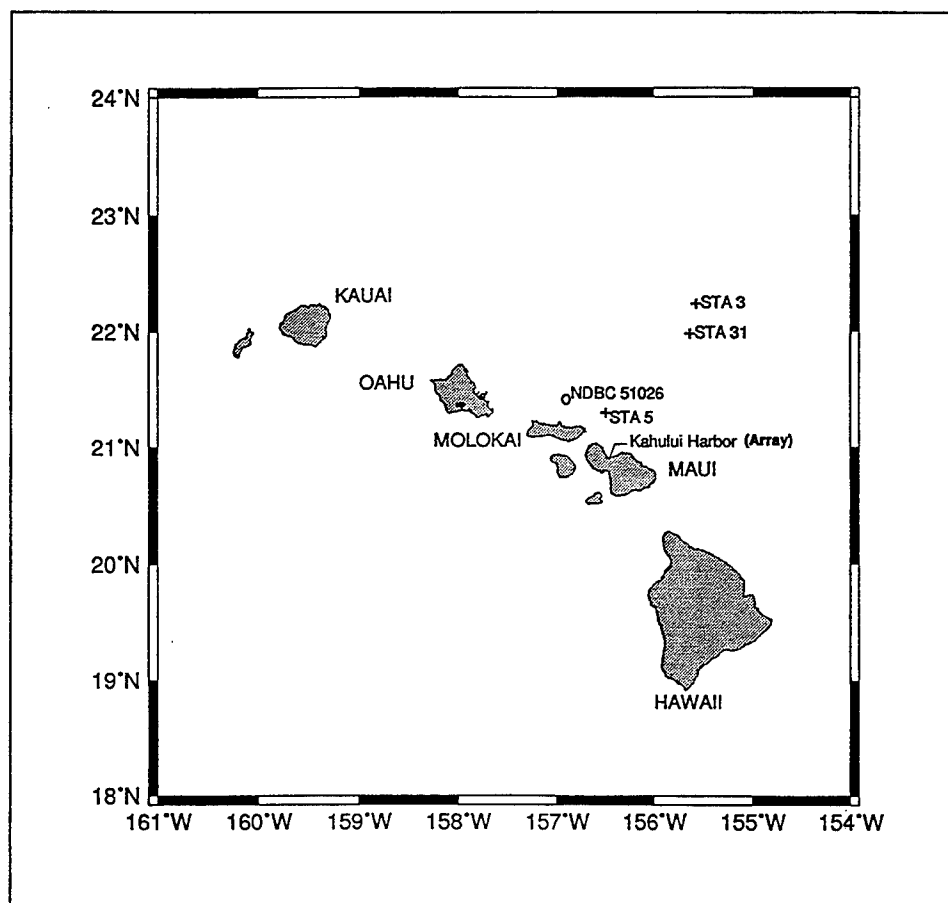
Figure 30. Location map for wave climate study

climate incident to the north coast of Maui. Wave parameter summaries for the deepwater sources are compared in Figures 31-33.

Peak wave direction was not available for the 20-year hindcast, only the mean wave direction. Wave components for sea (component 1) and swell (component 2) were available for this data set and consisted of height, period, and direction for each component. To get a representation of peak directions for comparison, a direction was chosen from either the sea or swell. If the overall
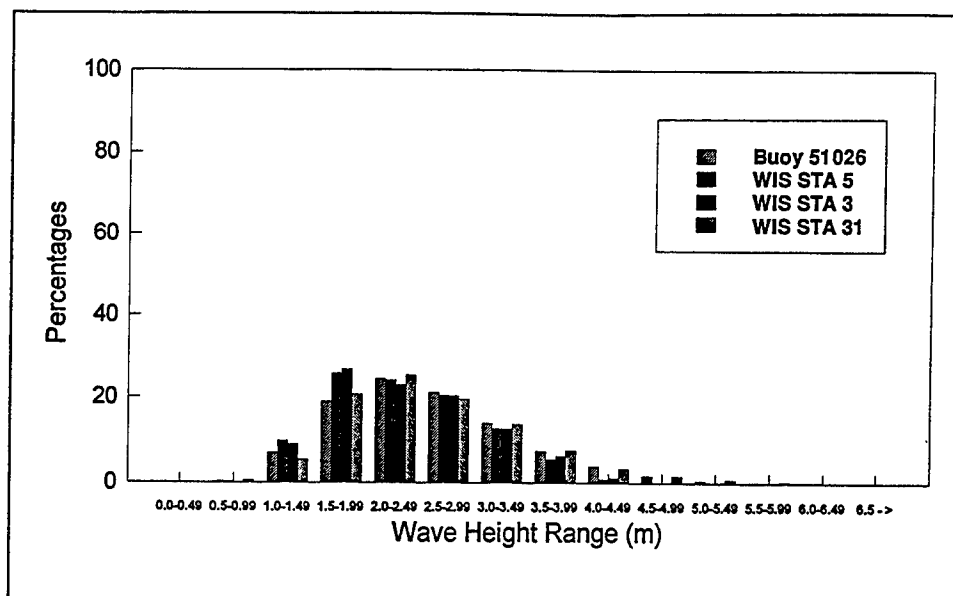
Figure 31. Deepwater wave climate comparison, H_s
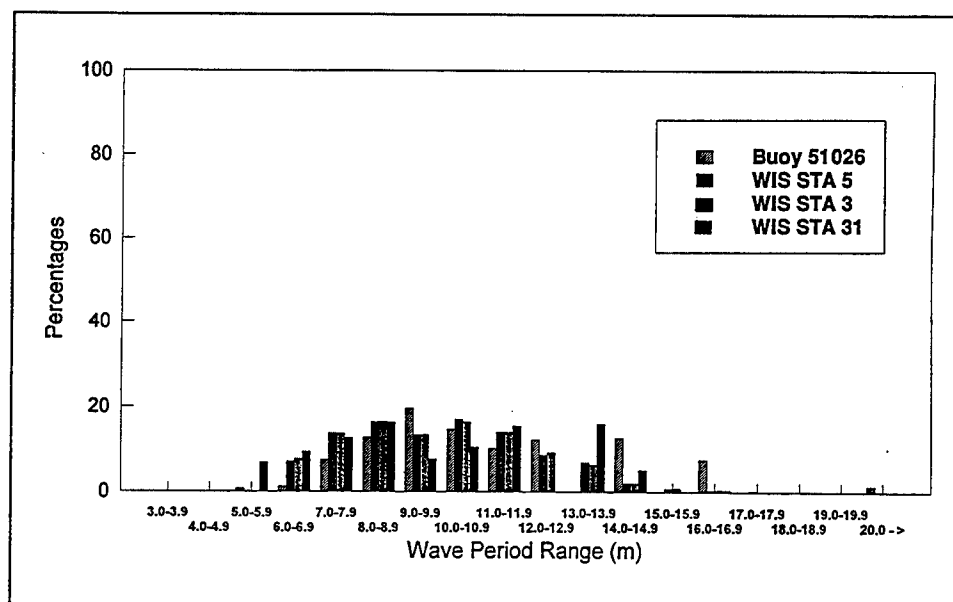
Figure 32. Deepwater wave climate comparison, T_p

peak period was close to the sea period, the direction associated with the sea was chosen as the peak direction. If the peak period was close to the swell peak, the direction associated with the swell was used.

Summaries shown in the figures are generally similar. Wave height and period distributions indicate virtually the same climate from all sources, although the buoy shows a tendency for a greater occurrence of swell periods above 14 sec. Wave direction distributions for the buoy and Station 31 both show
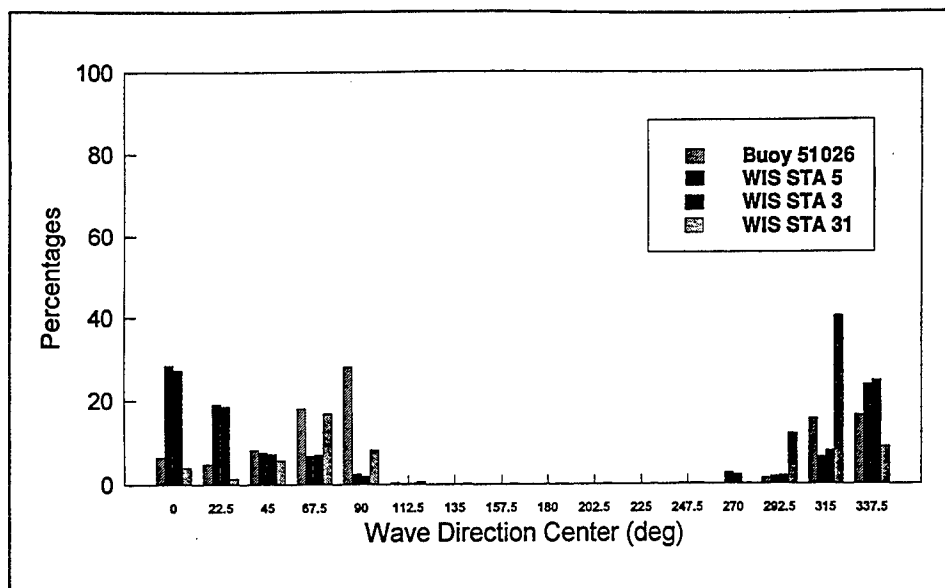
Figure 33. Deepwater wave climate comparison, θ_m (deg, coming from)

preferences for waves from the east, east-northeast, and northwest. Stations 3 and 5 also show a concentration of waves from northerly directions but the main concentration is centered on north. Despite these differences, it is concluded that the deepwater wave climate offshore from Maui's north coast is adequately represented by the available buoy measurements and long-term WIS station.

Wave Climate at Kahului Harbor

The deepwater wave climate analysis suggests that data from the array, which covers a time period comparable to the NDBC buoy and special hindcast sources, would reasonably characterize the wave climate immediately incident to Kahului Harbor. The array measurements incorporate local effects of sheltering and bathymetry.

To further validate the use of array data as the incident wave climate, an approximate procedure was used to relate the 20-year WIS hindcast to Kahului Harbor entrance. The procedure was to develop an empirical transformation between NDBC buoy and array measurement sites and then apply the transformation to the 20-year deepwater climate.

Wave heights and peak periods in the NDBC buoy and array data sets were segregated by direction bands, based on direction measured at the buoy. Linear regression equations were calculated for bands with more than 100 cases (Table 7). The regression equations were applied to the 20 years of WIS Station 31 information to estimate long-term climate at the Kahului gage. The transformed Station 31 (WIS 31T) and array gage summaries are very similar, especially considering the approximations involved in the transformation (Figures 34-36).

Table 7
Empirical Relationships Between Deepwater and Kahului Harbor Entrance

Parameter	NDBC Buoy Direction (deg. coming from)	Empirical Transformation[1]	Correlation
Significant Wave Height (m)	0-45	$H_s = -0.21 + 0.64\ H_{so}$	0.77
	45-90	$H_s = 0.06 + 0.34\ H_{so}$	0.77
	90-135	$H_s = 0.06 + 0.27\ H_{so}$	0.71
	270-315	$H_s = 0.18 + 0.21\ H_{so}$	0.71
	315-360	$H_s = 0.05 + 0.36\ H_{so}$	0.71
	0-360	$H_s = 0.07 + 0.35\ H_{so}$	0.71
Peak Wave Period (s)	0-45	$T_p = -2.5 + 0.77\ T_{po}$	0.62
	45-90	$T_p = 8.1 + 0.23\ T_{po}$	0.10
	90-135	$T_p = 5.9 + 0.53\ T_{po}$	0.17
	270-315	$T_p = 3.4 + 0.65\ T_{po}$	0.42
	315-360	$T_p = 4.1 + 0.65\ T_{po}$	0.58
	0-360	$T_p = 5.0 + 0.58\ T_{po}$	0.55
Wave Direction (deg, coming from)	0-45	$\theta_p = 22 + 0.20\ \theta_{po}$	0.14
	45-90	$\theta_p = 33 - 0.05\ \theta_{po}$	-0.04
	90-135	$\theta_p = 45 - 0.17\ \theta_{po}$	-0.06
	270-315	$\theta_p = -153 + 0.60\ \theta_{po}$	0.10
	315-360	$\theta_p = 95 - 0.19\ \theta_{po}$	-0.08
	0-360	$\theta_p = 29 + 0.01\ \theta_{po}$	0.10

[1] H_s, T_p, θ_p represent CDIP 77 array gage outside Kahului Harbor; H_{so}, T_{po}, θ_{po} represent NDBC buoy 51026.

In conclusion, the time period of available measurements at the array gage appears to give a good representation of the overall wind wave and swell climate immediately incident to Kahului Harbor. It is recommended that the array data be used as the primary source of wave information for driving numerical and physical models of the harbor.
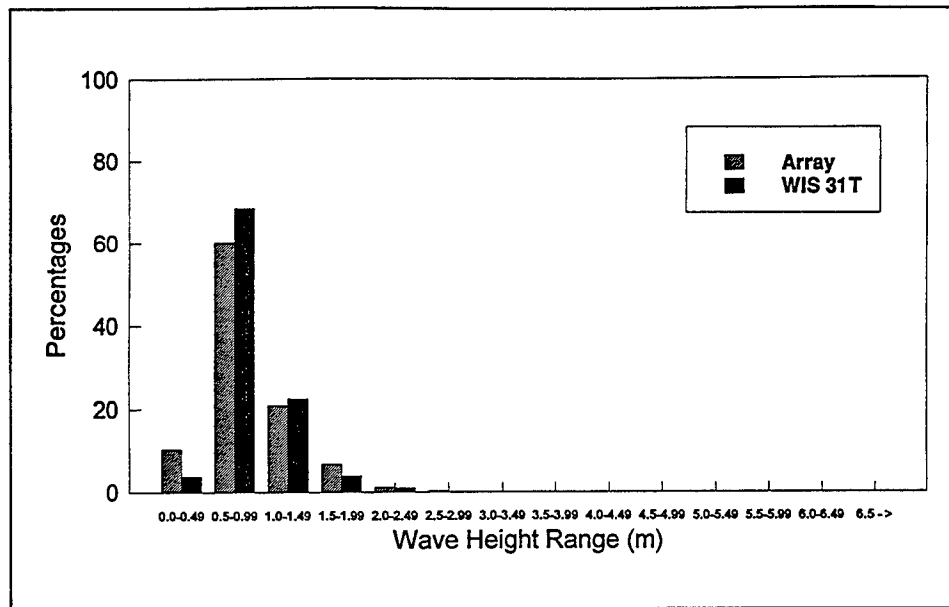
Figure 34. Harbor entrance wave climate comparison, H_s
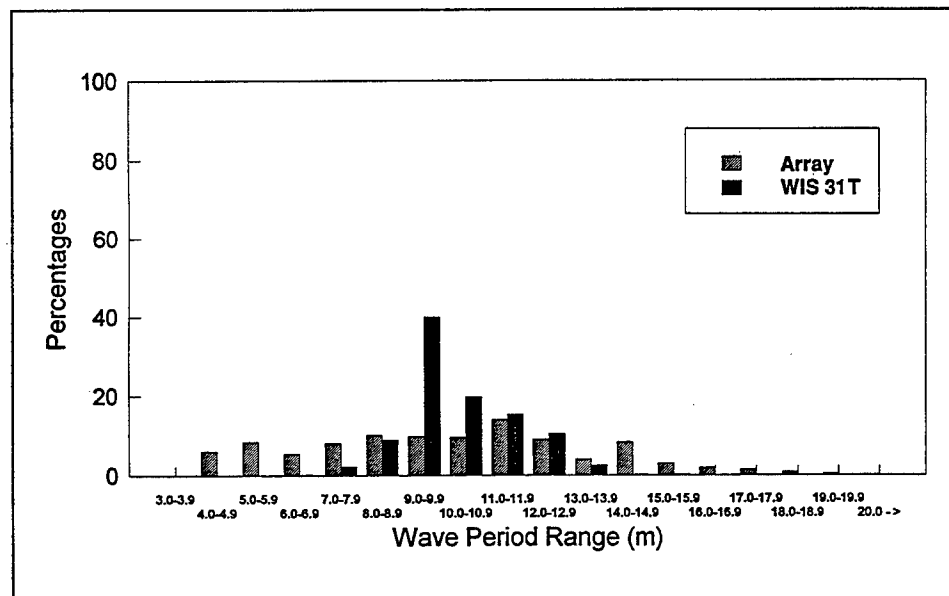
Figure 35. Harbor entrance wave climate comparison, T_p
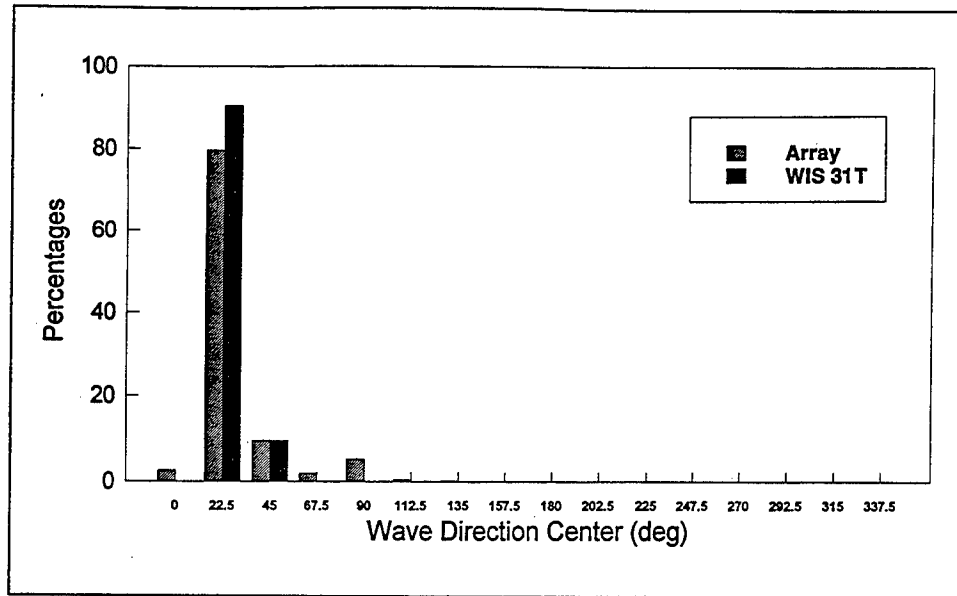
Figure 36. Harbor entrance wave climate comparison, θ_m (deg, coming from)

4 Numerical Model

Objectives and Approach

The numerical model studies have three main objectives:

a. Calibrate and validate the numerical model with field data.

b. Advance understanding of the existing harbor wave response.

c. Evaluate the effect of proposed harbor modifications on harbor wave response.

The numerical model used for the studies, HARBD, is the standard WES tool for numerical harbor wave investigations. The model includes the following assumptions:

a. No wave transmission through the breakwaters.

b. No wave overtopping of structures.

c. Structure crest elevations above the water surface cannot be tested or optimized.

d. Currents in the channel cannot be evaluated.

e. Wave breaking effects in the entrance and harbor cannot be considered.

f. No nonlinear effects are considered.

g. Diffraction around structure ends is represented by diffraction around a blunt vertical wall with specified reflection coefficient.

Despite limitations imposed by the above assumptions, HARBD is considered suitable for meeting the numerical modeling objectives of the Kahului Harbor study.

The harbor wave response model is presented in the following section, including a general description of the HARBD model and implementation of the model at Kahului Harbor. Validation was accomplished with a combination of storm wave events selected from available field data and with statistical summaries of a wide range of field cases. The final section of this chapter describes the test procedures and calculations. Procedures for evaluating operational performance at a pier are discussed.

As part of the test procedures, a suite of incident wave conditions must be specified at the seaward boundary of the area covered by HARBD. Incident short waves are determined by consideration of measurements outside the harbor. Incident long waves are specified over a broad range of frequencies but only a normally incident direction to identify possible harbor resonant responses.

The existing harbor and 11 proposed modifications were studied. Results for wind waves and swell are presented in Chapter 5. Harbor oscillation results are presented in Chapter 6. The presentation focuses on wave conditions in the vicinity of existing or proposed piers, but results over the full harbor area are also given.

Model Description

Model formulation

The numerical wave model HARBD is a steady-state hybrid element model used in the calculation of linear wave response in harbors of varying size and depth (Chen 1986, Chen and Houston 1987, Lillycrop and Thompson 1996). Originally developed for use with long-period waves (Chen and Mei 1974), HARBD has since been adapted to include capabilities for modeling wind waves and swell (Houston 1981), bottom friction, and partially reflective boundaries (Chen 1986). The model is based on a linearized mild slope equation. An overview of the model and its applications is given by Thompson and Hadley (1995).

The HARBD model has been shown to perform satisfactorily in comparison to analytic solutions and laboratory data for a variety of wind wave and swell cases (Houston 1981; Crawford and Chen 1988; Thompson, Chen, and Hadley 1996) and long wave cases (Chen 1986; Chen and Houston 1987; Houston 1981; Thompson, Chen, and Hadley 1993). As a result, it has been used with confidence in both long wave and short wave studies. Studies encompassing both long (harbor oscillations) and short waves are Harkins et al. (1996) and Thompson and Hadley (1994b). Additional long wave studies have included harbor oscillations (Briggs et al. 1994; Briggs, Lillycrop, and McGehee 1992; Mesa 1992; Sargent 1989; Weishar and Aubrey 1986; Houston 1976) and tsunamis (Farrar and Houston 1982, Houston and Garcia 1978, Houston 1978). Additional wind wave and swell studies include Thompson and Hadley (1994a); Lillycrop et al. (1993); Lillycrop and Boc (1992); Lillycrop, Bratos, and

Thompson (1990); Kaihatu, Lillycrop, and Thompson (1989); Farrar and Chen (1987); Clausner and Abel (1986); and Bottin, Sargent, and Mize (1985).

The HARBD model covers in detail a domain including the harbor and a portion of the adjacent nearshore area (Figure 37). This domain is bounded by a 180-deg semicircle in the water region seaward of the harbor entrance (∂A in Figure 37) and the land-water interface along the shoreline and harbor (∂C in Figure 37). The region defined by these boundaries is denoted Region A. If possible, the semicircle radius should be at least twice the wavelength of the longest incident wave to be modeled (using a typical water depth within the semicircle). Also, the semicircle should encompass any complex offshore bathymetry which strongly influences waves entering the harbor. In general, the semicircle should be as large as practical constraints on grid size and resolution will allow.
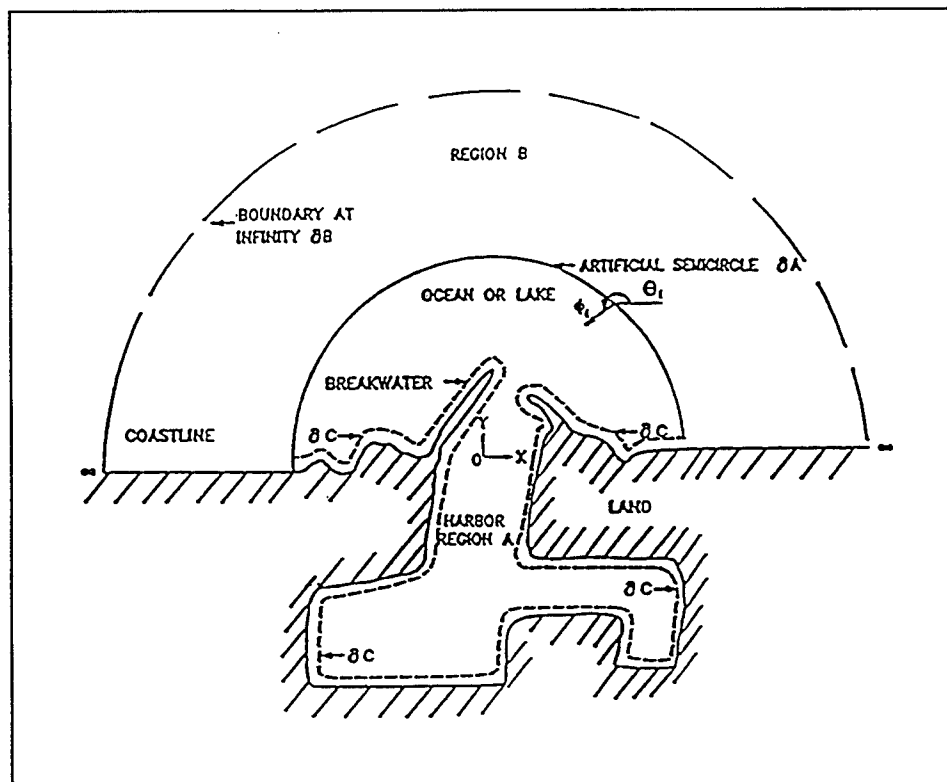
Figure 37. Representation of HARBD domain

The area outside the semicircle is treated as a semi-infinite region which extends from a straight coastline seaward to infinity (Region B). This region is assumed to have a constant water depth and no bottom friction.

Assuming linear, regular waves propagating over mild slope in arbitrary water depth, Chen (1986) derived the governing equation as

$$\nabla \cdot (\lambda \, c \, c_g \nabla\phi) \; + \; \frac{\omega^2 \, c_g}{c} \, \phi \; = \; 0 \qquad\qquad (2)$$

where

∇ = horizontal gradient operator

λ = complex bottom friction factor

c = wave phase speed

c_g = wave group speed

ϕ = velocity potential

ω = angular frequency

This equation is identical to Berkhoff's (1972) equation except for addition of the bottom friction factor λ. The factor λ, which is a complex number with magnitude greater than zero and less than or equal to one, is specified as

$$\lambda \; = \; \frac{1}{1 \; + \; \dfrac{i\beta a_i}{d \, \sinh \kappa d} \, e^{i\gamma}} \qquad\qquad (3)$$

where

i = $(-1)^{1/2}$

β = dimensionless bottom friction coefficient that can vary in space

a_i = incident wave amplitude

d = water depth

κ = wave number

γ = phase shift between stress and flow velocity

The bottom friction factor is a factor tending to reduce local velocities proportionately through the relationships

$$u = \lambda \frac{\partial \phi}{\partial x}$$

$$v = \lambda \frac{\partial \phi}{\partial y} \tag{4}$$

where

u,v = local horizontal velocity components

x,y = horizontal coordinates

Boundary conditions are specified in Regions A and B. At the solid boundary ∂C, a reflection/absorption boundary condition is used similar to the impedance condition in acoustics. The condition is specified as

$$\frac{\partial \phi}{\partial n} - \alpha \phi = 0 \tag{5}$$

with

$$\alpha = i\kappa \frac{1 - K_r}{1 + K_r} \tag{6}$$

where

n = unit normal vector directed into the solid region

K_r = reflection coefficient of the boundary

Values of K_r for wind waves and swell are normally chosen based on the boundary material and shape. General guidelines for K_r can be assembled from laboratory and field data (Thompson, Chen, and Hadley 1996). In wind wave and swell studies, K_r is generally chosen to be consistent with this guidance. Effects such as slope, permeability, relative depth, wave period, breaking, and overtopping can be considered in selecting values within these fairly wide ranges. For long wave studies, K_r is generally set equal to 1.0, representing full reflection.

The second boundary condition is imposed in the far region (Region B) at infinity. It requires that the scattered wave, defined as the difference between the total wave and incident wave, behave as a classical outgoing wave at infinity. This radiation condition may be expressed as

$$\lim_{r \to \infty} \sqrt{r} \left(\frac{\partial}{\partial r} - i\kappa \right) \phi^s = 0 \tag{7}$$

where

r = radial polar coordinate

ϕ^s = velocity potential of the scattered wave

The complete boundary value problem is specified by Equations 2, 5, and 7. A hybrid element method is employed to solve the boundary value problem. A conventional finite element grid is developed and solved in Region A. The triangular elements allow detailed representation of harbor features and bathymetry within Region A. An analytical solution with unknown coefficients in a Hankel function series is used to describe Region B. For a given grid, short wave period tests (relatively large values of κ) require more terms than long period tests to adequately represent the series. A variational principle with a proper functional is established such that matching conditions are satisfied along ∂A. Details are given by Chen (1986) and Lillycrop and Thompson (1996).

Experience with the model has indicated that the element size Δx and local wavelength L should be related by

$$\Delta x \leq \frac{L}{6} \tag{8}$$

Typically, harbor domains include some shallow areas in which many elements would be needed to satisfy the constraint in Equation 8. In practice, Equation 8 is at least satisfied in the harbor channel and basin depths. If additional elements can be accomodated, it is generally preferred to extend the semicircle further seaward rather than to greatly refine shallow harbor regions.

Input information for HARBD must be carefully assembled. In addition to developing the finite element grid to suit HARBD requirements, a number of parameters must be specified. Critical input parameters and ranges of typical values are summarized in Table 8.

The principal output information available from HARBD consists of amplification factor and phase at each node. These are defined as

$$A_{amp} = \left| \frac{a}{a_i} \right| = \left| \frac{H}{H_i} \right| = |\phi| \tag{9}$$

$$\theta = \tan^{-1} \left[\frac{Im \, \{\phi\}}{Re \, \{\phi\}} \right]$$

Table 8
Critical HARBD Input Parameters and Ranges of Typical Values

Parameter	Where Specified	Typical Values	
		Short Waves	**Long Waves**
Bottom friction, β	Every element	0.0	0.0-0.1
Boundary reflection, K_r	Every element on solid boundary	0.0 - 1.0	1.0
Coastline reflection, $K_{r,coast}$	Single value	1.0	1.0
Depth in infinite region, d_{far}	Single value	Between avg. & max. on semicircle	
Number of terms in Hankel function series	Single value	8 - 100[1]	8

[1] The number of terms needed increases as wave period decreases.

where

A_{amp} = amplification factor

a, a_i = local and incident wave amplitudes

H, H_i = local and incident wave heights

θ = phase relative to the incident wave

$Im\{\phi\}$ = imaginary part of ϕ

$Re\{\phi\}$ = real part of ϕ

Amplification factors are easily interpreted. Phases are helpful in viewing wind wave and swell propagation characteristics and in interpreting standing wave patterns. In long wave applications, phases prove useful for determining relative phase differences within the harbor, interpreting harbor oscillation patterns, and identifying potentially troublesome nodal areas.

Spectral adaptation

HARBD computes harbor response to specified wave period and direction combinations. However, the model is often used to approximate irregular wind wave and swell behavior, as in physical model tests with irregular waves and all field cases. More realistic numerical model simulations can be obtained by linearly combining HARBD results from a range of regular wave frequencies and directions in the irregular wave spectrum. With proper weighting, regular wave results represent a desired spectral distribution of energy.

Spectral adaptation of the HARBD model is done as a post-processing step using the standard, regular wave output from the model. For a given set of incident wave directions representing the range of possible approach directions, HARBD is run for a number of wave periods spread between the shortest period satisfying the grid resolution constraint of Equation 8 and the longest swell period of interest.

Spectral post-processing is based on the assumption that a consistent spectral form can be applied at every node. This major assumption provides the basis for a workable, reasonable spectral weighting which improves on the traditional regular wave approach. The spectrum is represented as the product of two functions:

$$S(f,\theta) \quad = \quad S(f) \; D(f,\theta) \tag{10}$$

where

$S(f, \theta)$ = directional spectral energy density function

$S(f)$ = spectral energy density function

$D(f, \theta)$ = angular spreading function

The JONSWAP spectral form was chosen for $S(f)$ (Hasselmann et al. 1973). The JONSWAP spectrum is specified as (U.S. Army Corps of Engineers 1989)

$$S(f_i) \quad = \quad \frac{\alpha \; g^2}{(2\pi)^4 \; f_i^5} \; e^a \; \gamma^b \tag{11}$$

where $S(f_i)$ = spectral energy density at frequency f_i.

The parameters a and b are given by the following relationships:

$$a \; = \; \frac{-1.25}{f_i \; T_p^4}$$

$$b \; = \; e^{\frac{-1}{2\sigma^2} (f_i T_p - 1)^2} \tag{12}$$

$$\sigma \; = \; 0.07 \quad \text{for} \quad f_i \le f_p$$

$$= \; 0.09 \quad \text{for} \quad f_i \ge f_p$$

48

where

T_p = peak spectral period

f_p = peak spectral frequency = $\dfrac{1}{T_p}$

Parameters α and γ are calculated as

$$\alpha = 157.9 \, \epsilon^2$$

$$\gamma = 6614 \, \epsilon^{1.59}$$

$$\epsilon = \frac{H_s}{4 \, L_p}$$

(13)

where

H_s = significant wave height

L_p = wavelength for waves at peak frequency

The parameter ϵ is a significant wave steepness. The parameter γ, called the peak enhancement factor, controls the sharpness of the spectral peak.

Although the JONSWAP spectrum was developed primarily for actively growing wind waves, it can be used with appropriate choice of γ to approximate any single-peaked spectrum, including old swell which has travelled a great distance from the generation area (e.g. Goda 1985) (Table 9).

Table 9
Guidance for
Choosing γ

Wave Condition	γ
Growing sea	3.3
Old swell	8-10

The angular spreading function in Equation 10 is described by the commonly used expression

$$D(\theta) = G(s) \, \cos^{2s}\left(\frac{\theta - \theta_0}{2}\right)$$

(14)

where

$G(s)$ = normalizing function

s = constant-valued spreading parameter

θ_0 = primary wave direction

$\theta - \theta_0$ = wave direction difference, ranging from $-\pi/2$ to $+\pi/2$

The spreading parameter s controls the magnitude of directional spread. As the value of s increases, directional spread narrows. Wind waves are typically represented by broad spreads and swell by narrow spreads. Recommended representative values for each are given in Table 10 (Goda 1985).

Table 10 Guidance for Choosing s	
Wave Condition	s
Wind waves	10
Swell	25 - 75

Spectral post-processing begins with specification of the desired $H_s, T_p,$ γ, and s and the arrays of HARBD amplification factors. A refined JONSWAP spectrum is computed with 1,000 points, where the f_i's in Equation 11 are

$$f_1 = 0.5 * f_p, \quad f_2 = 0.502 * f_p, \quad f_3 = 0.504 * f_p, \dots, f_{1000} = 2.498 * f_p$$

The number of wave periods computed with HARBD is always much smaller than 1,000, typically less than 20. These periods, converted to frequency (reciprocal of period), can be used to define bands in the JONSWAP spectrum. Bands are bounded by the midpoints between HARBD computational frequencies. The highest and lowest frequency bands are assumed to be centered on the highest and lowest HARBD computational frequencies, respectively. A weighting factor for each HARBD-defined band is computed by summing values from the refined JONSWAP spectrum which fall within the band and normalizing by the total spectral energy.

$$w_k = \frac{\sum_{i=N_{k1}}^{N_{k2}} S(f_i)}{\sum_{i=1}^{1,000} S(f_i)} \tag{15}$$

where

w_k = weighting factor for k'th HARBD computational frequency

N_{k1} = index of lowest JONSWAP frequency f_i satisfying $f_i > \dfrac{f_{k-1} + f_k}{2}$

N_{k2} = index of highest JONSWAP frequency f_i satisfying $f_i < \dfrac{f_k + f_{k+1}}{2}$

50

f_{k-1}, f_k, f_{k+1} = $(k-1)$'th, k'th, and $(k+1)$'th HARBD computational frequencies, with $f_{k-1} < f_k < f_{k+1}$

Though not shown in the equation, the weighting factor also includes fractional energy interpolated across JONSWAP frequencies bracketing the two end points of each HARBD band.

Directional spread is also calculated over 1,000 points, covering a range of $-\pi/2$ to $+\pi/2$. The midpoints between HARBD wave directions are used to define directional bands. The weighting factor for each HARBD-defined directional band becomes:

$$w_n = \frac{\sum_{i=N_{n1}}^{N_{n2}} D(\theta_i)}{\sum_{i=1}^{1,000} D(\theta_i)} \tag{16}$$

where

w_n = weighting factor for n'th HARBD computational direction

N_{n1} = index of lowest spreading direction θ_i satisfying $\theta_i > \dfrac{\theta_{n-1} + \theta_n}{2}$

N_{n2} = index of highest spreading direction θ_i satisfying $\theta_i < \dfrac{\theta_n + \theta_{n+1}}{2}$

$\theta_{n-1}, \theta_n, \theta_{n+1}$ = $(n-1)$'th, n'th, $(n+1)$'th HARBD computational directions, with $\theta_{n-1} < \theta_n < \theta_{n+1}$

The width of the lowest HARBD-defined directional band is assumed to be twice the difference between the HARBD direction and the first midpoint. The width of the highest HARBD-defined directional band is defined similarly.

The effective amplification factor at each node can then be computed as

$$(A_{amp})_{eff} = \sqrt{\sum_{k=1}^{N_T} \sum_{n=1}^{N_D} w_n \, w_k \, A_{amp}^2(f_k, \theta_n)} \tag{17}$$

where

$(A_{amp})_{eff}$ = effective, or spectral, amplification factor at a node

$A_{amp}(f_k, \theta_n)$ = nodal amplification factor for HARBD computational
frequency f_k and direction θ_n

N_T = number of HARBD computational wave periods

N_D = number of HARBD computational wave directions

Finite element grids

The finite element numerical grid depicting existing conditions at Kahului
Harbor was created using WES's finite element grid development software
(Turner and Baptista 1993) (Figure 38). The grid covers the entire Kahului
Harbor area and extends somewhat seaward into Kahului Bay. The land
boundary was digitized from an aerial photograph. Grid element size is based on
the criterion of 6 elements per wavelength (the minimum recommended resolu-
tion with HARBD) for a 10-sec wave in 15-ft water depth. Depths for virtually
all areas of interest exceed 15 ft. For the longer period waves, the grid gives a
high degree of resolution. Grid characteristics are summarized in Table 11.

The radius of the seaward semicircle is 2,307 ft. This is equivalent to 2.9 and
9.7 wavelengths for the longest and shortest short wave periods considered,
assuming a representative water depth of 35 ft. The semicircle size and location
were chosen to include both breakwaters and the immediate nearshore area. The
semicircle extends sufficiently far seaward to cover the most important nearshore
bathymetry while maintaining a reasonable number of grid elements.

Bathymetric data were obtained from National Oceanic and Atmospheric
Administration hydrographic chart 19342 and WES bathymetric survey data.
Digitized depths were transferred onto the finite element grid using the WES grid
software package. A contour plot of bathymetry is given in Figure 39.

Reflection coefficients K_r are needed for all solid boundaries. For the short
wave tests, K_r values were estimated from existing Corps of Engineers guidance,
photos, and field notes from a recent site visit by WES personnel, and past
experience. The solid boundary was divided into 13 zones and a reflection
coefficient was estimated for each zone (Figure 40). Reflection coefficients
ranged from 0.2 for the shallow sandy beach along the southwest shore of the
existing harbor to 0.5 for all pier areas and 0.9 for the grouted revetment along
the western side of Pier 2. Additional parameter values used in the numerical
model are summarized in Table 12.

Different parameters are used for the long wave tests. The reflection
coefficient was set to 1.0 for all boundaries, since long waves generally reflect
very well from a coastal boundary. Long waves are more affected by bottom
friction than short waves, so a value of β greater than zero is appropriate. The
value of β is best determined by calibration with field data, as discussed in the
following section. A value of $\beta=0.032$ was selected. This and other parameters
are summarized in Table 12.

52
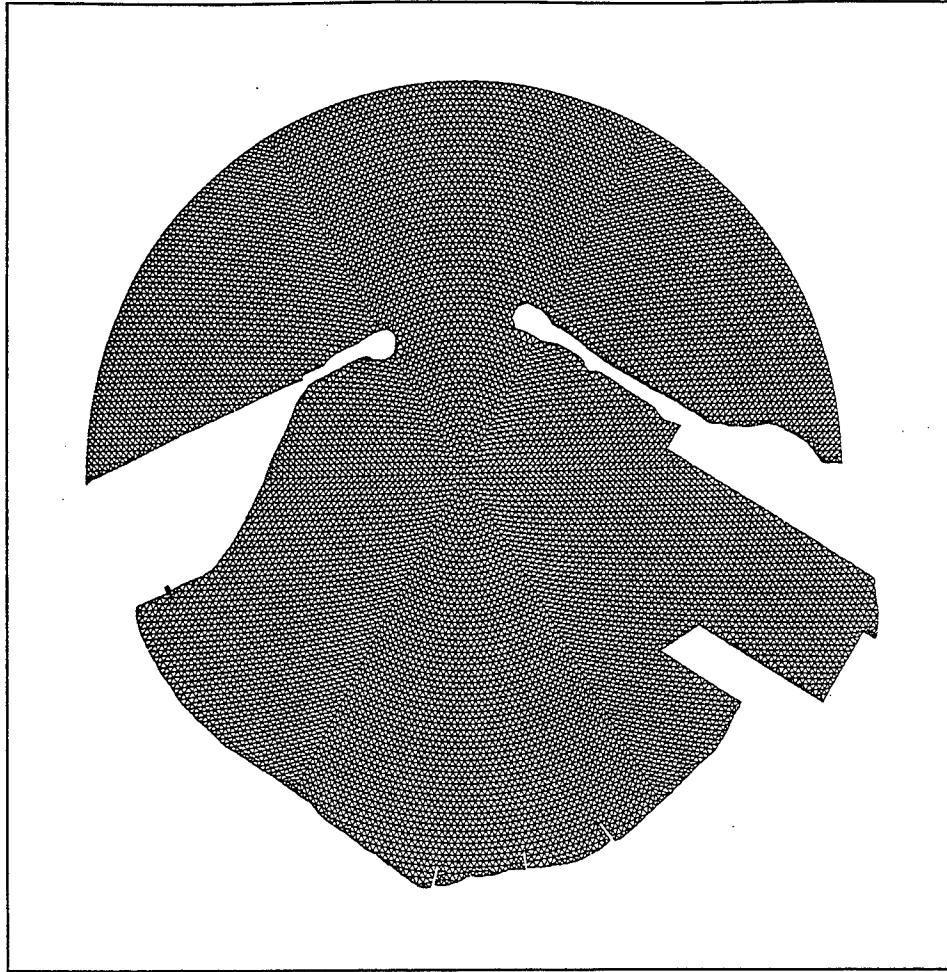
Figure 38. Grid of existing harbor

In addition to existing conditions, 11 harbor modification plans were specified for evaluation, as discussed in Chapter 1 and summarized in Table 13. The existing harbor grid was modified to represent each alternative configuration. Grid characteristics for each configuration are included in Table 11. Short wave reflection coefficients were modified as appropriate for the plan grids. General guidelines were $K_r = 0.5$ along piers (mainly due to steep, partially revetted slopes under piers) and $K_r = 0.35$ along breakwater extensions.

Table 11
Grid Sizes

Harbor Plan	Number of:				
	Elements	Nodes	Solid Boundary Nodes	Semicircle Boundary Nodes	Length of Typical Element (ft)
Existing	22908	11801	497	196	35.5
Plan 1	23351	12045	542	196	35.5
Plan 2	23468	12106	547	196	35.5
Plan 3a	23393	12053	516	196	35.5
Plan 3b	23331	12036	544	196	35.5
Plan 3c	23286	12024	565	196	35.5
Plan 4a	22562	11627	495	196	35.5
Plan 4b	22500	11610	523	196	35.5
Plan 4c	22455	11598	544	196	35.5
Plan 5	21696	11216	539	196	35.5
Plan 6	22500	11610	523	196	35.5
Plan 7	21239	10998	560	196	35.5
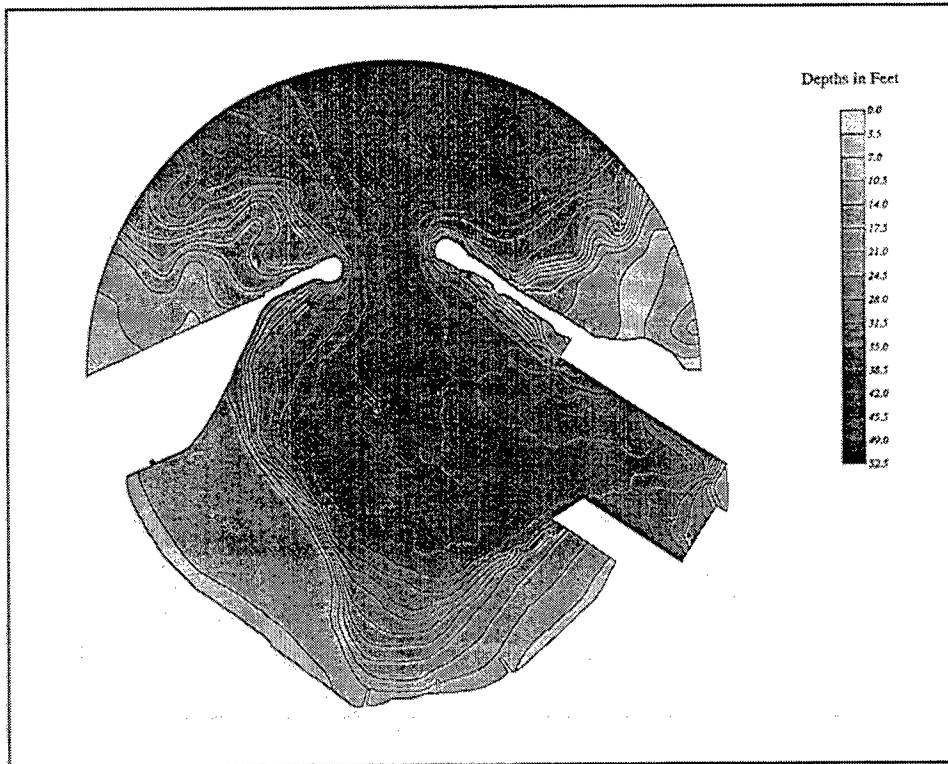
Figure 39. Bathymetry, existing harbor
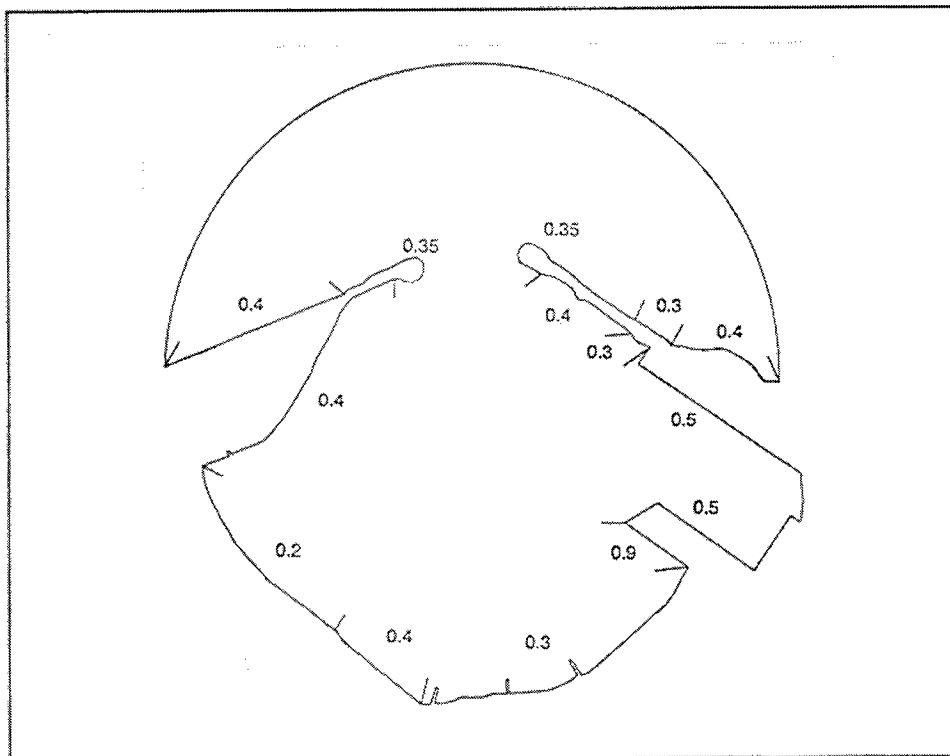
Figure 40. Wave reflection coefficient values, short waves, existing harbor

Table 12
Parameter Values Used in HARBD

Parameter	Value	
	Short Waves	Long Waves
Bottom friction, β	0.0	0.032
Coastline reflection, $K_{r,coast}$	1.0	1.0
Depth in infinite region, d_{far}	45.5 ft	45.5 ft

Table 13
Harbor Alternatives for Numerical Modeling

Features	Alternative Plan						
	1	2	3	4	5	6	7
Passenger Ship Pier							
Slip cut into existing fill	x	x					
Notch cut into existing fill			x				
Pier adjacent to existing fill				x		x	x
New fill area in SW area of harbor					x		x
Protective Stub Added to End of West Breakwater (test lengths of 0, 600, 1,000 ft)			x	x		x[1]	x[1]
Barge Pier in Canoe Club Area							
Aligned north/south (Concept C)	x						
Parallel to Pier 2 (Concept 12)		x	x	x	x	x	x
Pier 1 Extension	x	x	x	x	x	x	x
T-Pier for Fuel Barges (dredge & revet between Piers 1 & 3)	x	x	x	x	x	x	x
Areas with 35-ft Project Depth Dredged to 38-ft Depth						x	x
Selected Combination of Features							x

[1] Breakwater stub of 600-ft length only.

Calibration and validation

The availability of extensive field data at Kahului Harbor allowed a detailed calibration and validation of the numerical harbor response model. Both short and long wave responses were considered. Data from the time period Nov 93 - Sep 94 were used for calibration and validation, as discussed in Chapter 2.

Short waves. Four high wave events during January and March 1994 were selected for short wave calibration (Table 14). HARBD was run for the incident wave periods and directions described in the following section and the output was post-processed to give spectral estimates of the four events. Reflection coefficients were adjusted within reasonable ranges to achieve a good fit between field data and model results (Figure 41). The principal adjustment was the reflection coefficient used along the piers. As-built plans for the commercial piers and laboratory studies of a similar configuration of pile-supported pier with underlying slope (Allsop 1990) were used to determine reasonable ranges for reflection coefficient. Only the 192-, 203-, and 214-deg incident wave directions were used during the calibration and validation phase of the study. The remaining two directions were added later to more completely represent the range of diffraction possibilities for alternatives involving the western portion of the harbor.
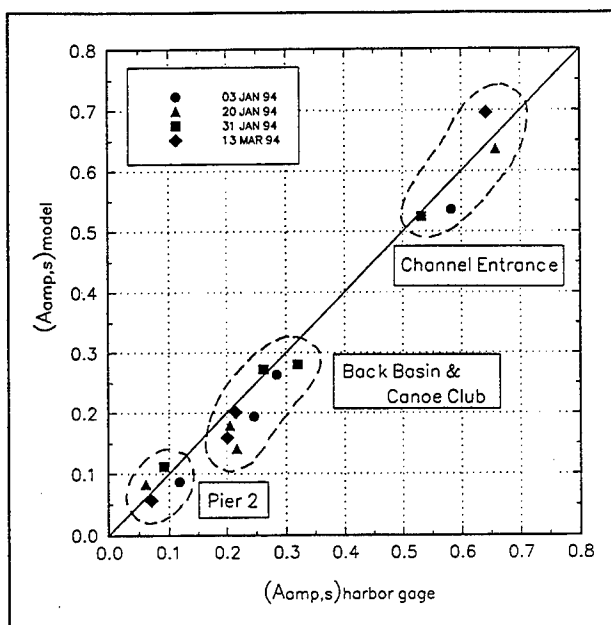
Figure 41. Model short wave calibration to four storm events

Table 14 Field Cases for Short Wave Model Calibration, Array				
Date	Hour	H_s cm	T_p sec	θ_m deg
3 Jan 94	1300	212	14.8	194
20 Jan 94	1300	247	10.1	202
31 Jan 94	0700	162	17.9	191
13 Mar 94	1300	195	8.9	205

A comparison of HARBD results and field data with published diffraction patterns through a breakwater gap, done as part of the calibration process, showed the dominance of diffraction between the entrance and interior harbor locations. Goda (1985) gives diffraction of a directional spectrum through a gap between two straight, colinear breakwaters in uniform depth. Bowers and Welsby (1982) report on laboratory tests of several other breakwater gap

configurations, including one similar to the Kahului breakwaters. Their tests, as well as others by Blue and Johnson (1949), show that the relative rotation of the breakwaters makes little difference in the diffraction pattern for wave periods of concern here. However, the presence of rubble on the inside of the breakwaters causes significant absorption and dissipation relative to the classical vertical wall breakwater. Appropriate adjustment factors taken from Bowers and Welsby (1982) were applied to the spectral diffraction results of Goda (1985) for comparison to two of the field calibration events.

The calibrated short wave model was run in a spectral mode for the T_p and θ_m combinations represented in the field data summaries of Appendix B. Comparing the model results to field data validates the numerical model against an 11-month summary of gage data (Figure 42). The validation comparison is generally comparable to the calibration results. The agreement at Pier 2 is excellent. The model shows a persistent tendency to underestimate the amplification factor at the other gages. The tendency is more

Figure 42. Model short wave validation to 11 months of gage data

evident than in the initial storm calibration, particularly at Canoe Club and Back Basin. In most cases, it is greater than one standard deviation of the field data. The possibility of incorrect reflection coefficients and/or bathymetry in these shallow areas was explored within reasonable ranges, but the general level of agreement could not be improved.

Long waves. Long wave calibration was aimed at adjusting bottom friction β to approximately match amplification factors between model and data. The reflection coefficient K_r was set to 1.0. Only the lower frequencies (0.003-0.010 Hz or 100- to 333-sec period) were considered because most prominent resonant peaks are in this range and K_r=1.0 is more strictly correct at low frequencies. Only resonant peaks were considered in calibration because they are the features of greatest interest and are most sensitive to the choice of β. A value of β=0.032 was found to give a reasonably good match at all peaks in the selected frequency range and at all harbor gages, as illustrated in Figure 43.

58

Figure 43. Model long wave calibration

Field and model amplification factors over the full range of long wave frequencies are compared in Figure 44. The general agreement is reasonable. The model shows several overly large peaks, especially at frequencies higher than the 0.01-Hz limit considered in calibration.
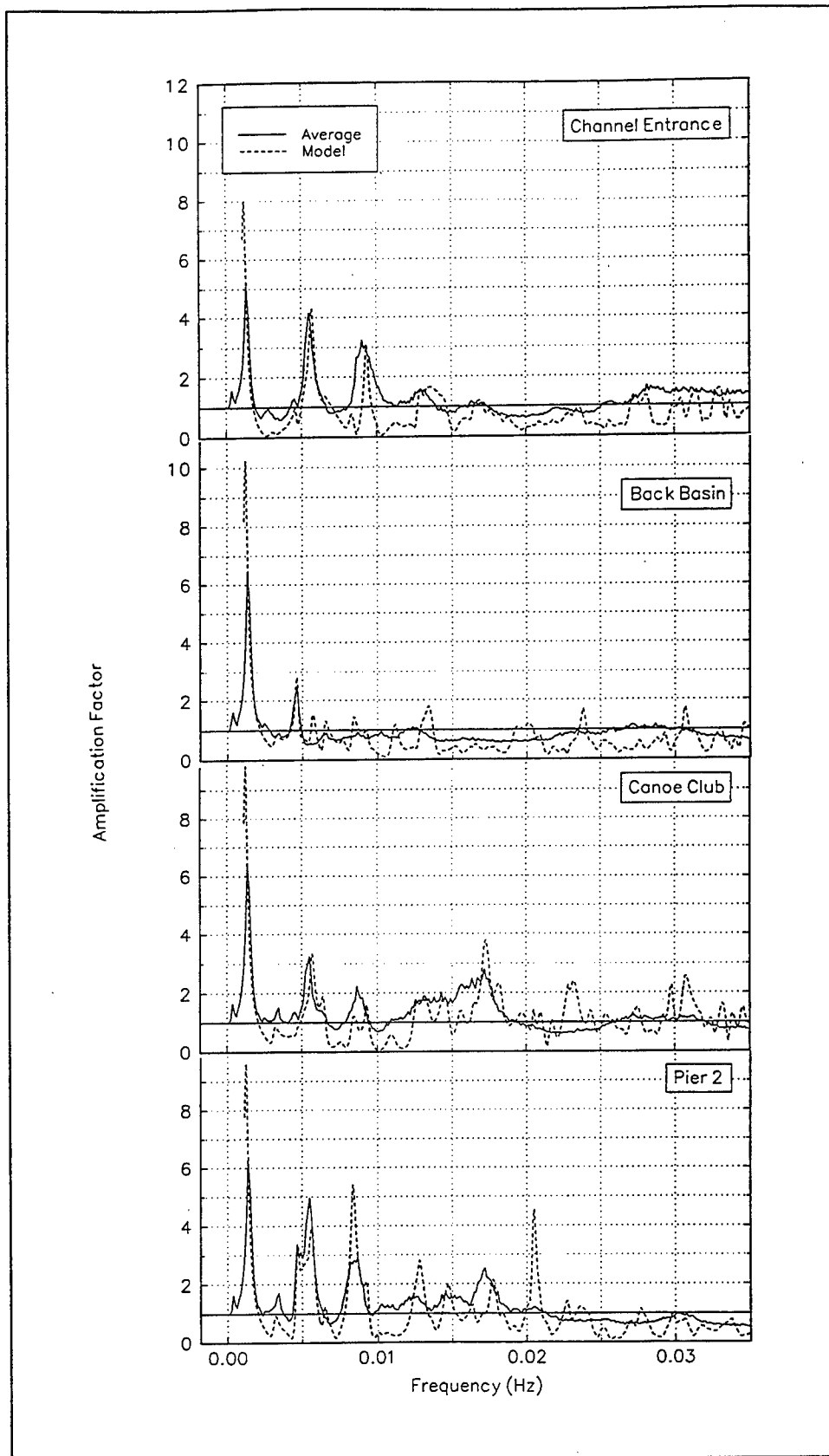
Figure 44. Long wave comparison of average gage spectra and model

Test Procedures and Calculations

Incident wave conditions

A range of short and long wave conditions incident to Kahului Harbor was considered. A representative range of wave periods and directions which could cause damaging waves inside the harbor was included, based on field measurements.

The short wave periods and approach directions considered are given in Table 15. These conditions provide reasonable coverage of the field measurements summarized in Figures 18 and 19. The shortest wave period, representative of strong local storms, is 2 sec shorter than the grid design period. Past experience has shown that the model still provides adequate results for small increments below the grid design period. The longest period represents a very long swell condition. Directions were chosen to include likely approach directions to the harbor entrance and to give adequate representation of the directional spectrum in post-processing. They were also chosen after review of directional response sensitivity runs at a selected swell period. Test directions were reckoned in 11-deg increments beginning with 192 deg (coming from, relative to true north). Incident wave directions and the angular orientation of the seaward semicircular model boundary are illustrated in Figure 45.

Table 15 Summary of Incident Short Wave Conditions		
Wave Period (sec)		**Wave Direction (deg, going toward)**
8	17	192
9	18	203
10	19	214
11	20	225
12	21	236
13	22	
14	23	
15	24	
16		

For the study of existing harbor conditions and comparison of alternatives, HARBD was run with the full set of short wave periods and directions in all possible combinations. Model results were then evaluated for directional spectra with T_p and θ_m values equivalent to the period and direction values used in the initial HARBD runs (Table 15).

Incident long wave conditions considered are given in Table 16. A fine resolution in wave frequency was used over the full range of possible resonant conditions to ensure that all important peaks were identified. A total of 468 periods were considered. Only one approach direction is included, since past studies have indicated that harbor response is relatively insensitive to incident long wave direction. This direction represents a wave directly approaching the harbor entrance from deep water.

One water level was tested. The tide range at Kahului Harbor is relatively small, with a mean range of 1.9 ft. Harbor wave response is unlikely to vary much with water level over this tidal range. The water level was selected as mean lower low water, the reference datum for bathymetric data.

Table 16 Summary of Incident Long Wave Conditions	
Wave Period (sec)	Wave Direction (deg, going toward)
25.00	180
25.06	
25.13	
...[1]	
1000.0	

[1] Frequency increments are 0.0001 Hz for periods of 25-80 sec and 0.00006 Hz for periods of 80-1000 sec.
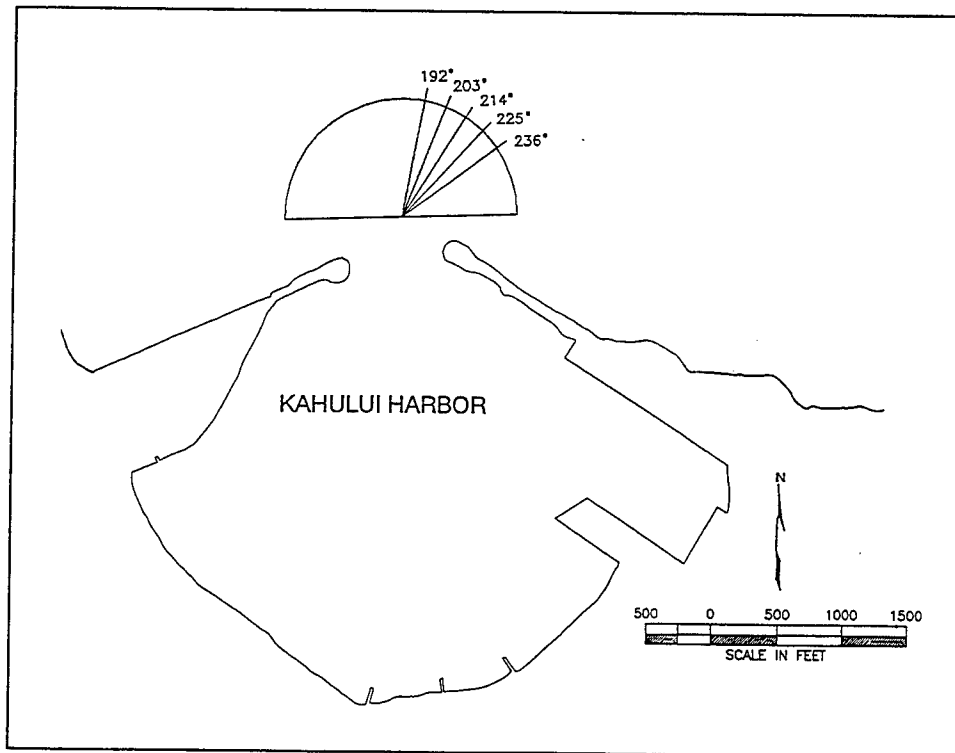
Figure 45. Incident wave directions

Calculation of spectra

Numerical model test results for short waves in Kahului Harbor are all based on spectral post-processing of the initial HARBD runs. Hence, short wave amplification factors are all in the form of $(A_{amp})_{eff}$ in Equation 17. This approach requires, first, that HARBD be run with the range of wave periods and directions to be considered in the spectral calculations. Second, values of peak wave period T_p corresponding to the peak spectral frequency, wave approach direction θ_m, spectral peak enhancement factor γ, and directional spreading factor s must be specified. The T_p and θ_m values were chosen to represent wind wave and swell conditions at the harbor, as discussed in the section "Incident wave conditions" (pages 61 and 62).

Values for γ and s were approximated by relating the guidance in Tables 9 and 10 to T_p values. High energy waves, of concern for harbor design, with T_p up to 10 sec were assumed to be growing seas. Parameters γ and s were set to 3.3 and 10, respectively. Waves with T_p greater than 10 sec were treated as swell. As swell T_p increases, the swell is expected to have an increasingly peaked frequency spectrum and narrow directional spread. To represent the spectrum for the range of swell considered, values of γ and s were scaled to fall between the values for growing seas and maximum values established for old swell (Table 17).

Output basins

In order to get special coverage of areas where harbor traffic would most likely be affected by wave conditions, 38 possible output locations or "basins" were selected to cover all harbor layouts. A basin is a small cluster of elements over which the HARBD response is averaged to give a more representative output. Whenever possible, basins were positioned to coincide with basins of other plans, particularly those of the existing harbor (Figure 46). Basin locations for alternative plans are given in Appendix E. In general, primary output basins define five areas of interest: Pier 1 (Basins 2-6), Piers 2 and 3 (Basins 7-10), recreational boat ramp (Basin 21), modified barge pier, and proposed passenger pier. Locations

**Table 17
Approximate Relationships Among T_p, γ, and s**

T_p (sec)	γ	s
8	3.3	10
9	3.3	10
10	3.3	10
11	4	15
12	4	20
13	5	25
14	5	30
15	6	35
16	6	40
17	7	45
18	7	50
19	8	55
20	8	60
21	9	65
22	9	70
23	10	75
24	10	75

and defining basins of barge and passenger piers vary with plan. Each basin in this study contains 22-28 elements. HARBD output information was saved at each of these locations in addition to the detailed output at nodes.
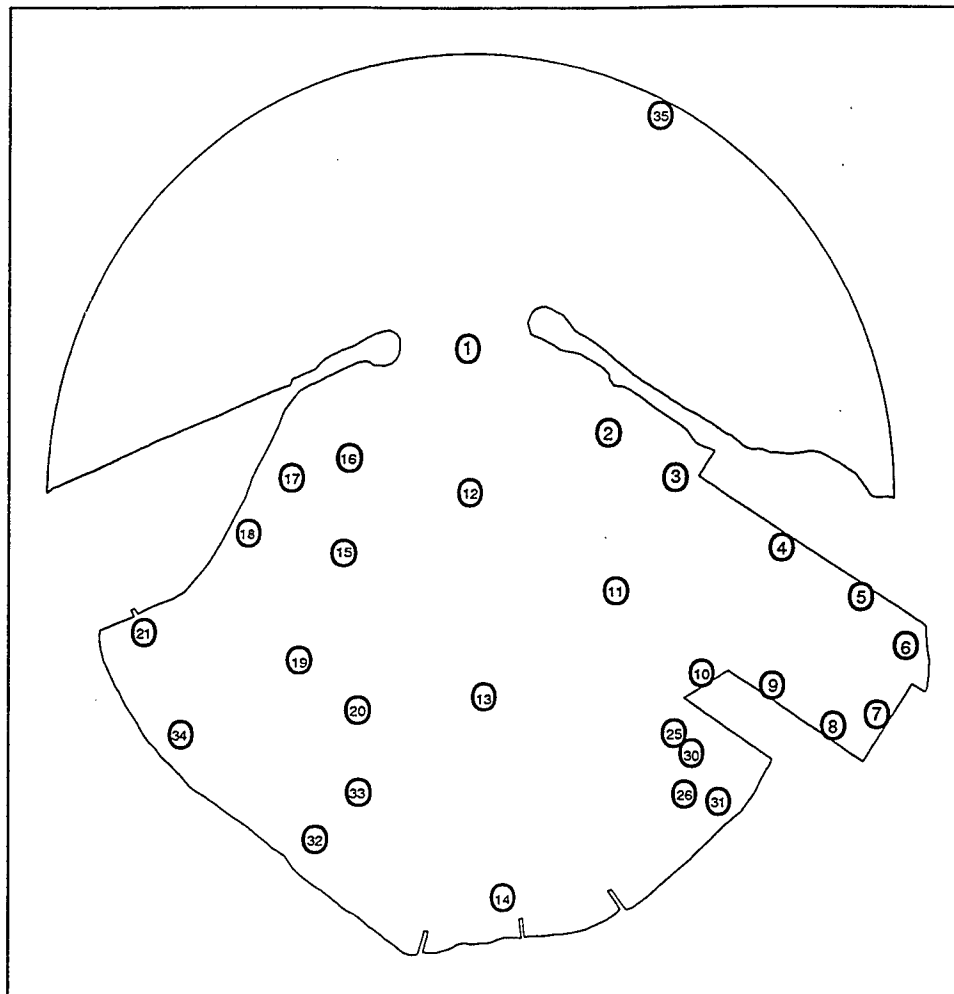
Figure 46. Output basins, existing harbor

Procedures for evaluating operational performance at a pier

One objective of this study was to develop and implement a more quantitative procedure for comparing the operational acceptability of different harbor plans subjected to long waves using HARBD. The procedures are described in the following paragraphs.

Existing criteria. The following criteria are relevant to operational performance at a pier:

1. Wilson (1967) suggests that a wharf will be operationally acceptable if

$$\frac{H}{T} < 0.0038 \ \text{ft/sec}$$

$$\frac{H}{T} < 0.0012 \ \text{m /s} \tag{18}$$

where H and T are long wave height and period measured in an adjacent corner. He refers to this as a *slope criterion* since it was derived from H/L for a shallow-water wave. The H and T combinations for threshold damage are shown in Figure 47.
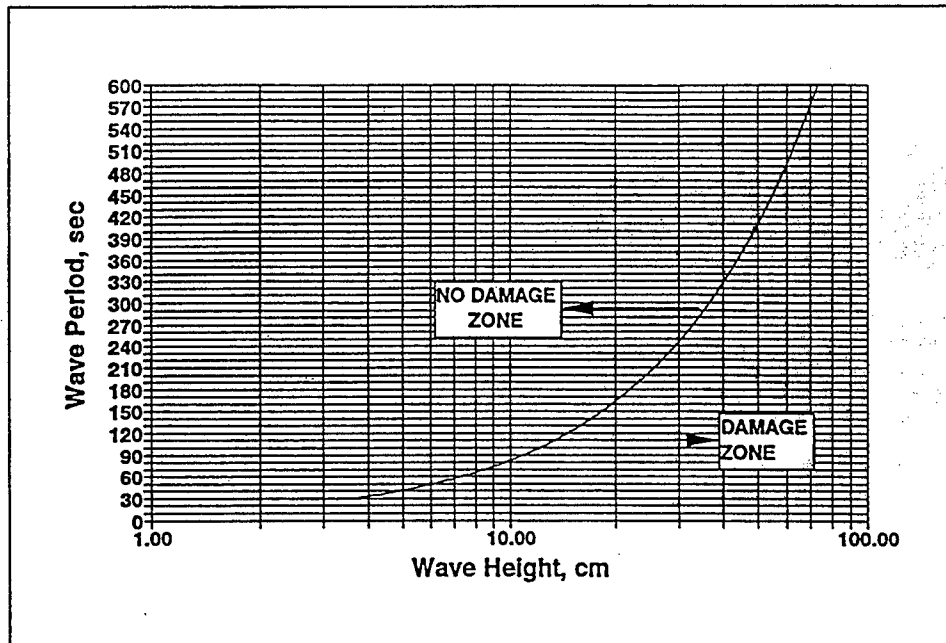
Figure 47. Wilson's threshold of surge damage for moored ships (from Seabergh and Thomas (1995))

2. Seabergh and Thomas (1995) reference unpublished long-wave *significant* height criteria suggested by Walker and Szwetlot ($H_{s,long}$<5-10 cm for 100 percent operational efficiency with man-made fiber mooring lines; $H_{s,long}$<10-15 cm with steel wire mooring lines) and Burke for the Los Angeles Long Beach Harbor complex. Based on these and Wilson's (1967) published criterion, Seabergh and Thomas use the following criteria as indicators of successful operational conditions:

$$H_{s,long} < 5 \ \text{cm} \quad \text{for } T=41-205 \ \text{sec}$$

$$H_{s,long} < 10 \ \text{cm} \quad \text{for } T=205-1,024 \ \text{sec} \tag{19}$$

3. The Permanent International Association of Navigation Congresses (PIANC) (1995) gives criteria for each degree of freedom of a moored ship (surge, sway, heave, etc.). The criteria for horizontal translational motions

are given in terms of distance and velocity. Since horizontal motions are highly constrained by mooring lines, the velocity criteria seem more useful for present purposes (though they are stated to be applicable only for fishing vessels, coasters, freighters, ferries, and Ro-Ro vessels). Velocity criteria vary with size of ship, but they are as follows:

$$u_{max} < 0.3\text{-}0.6 \quad m\ /s$$

$$u_{max} < 1.0\text{-}2.0 \quad ft/sec \tag{20}$$

4. Damage at a wharf presumably occurs when *forces* (in mooring lines, against fenders, against ship hull, etc.) are too great. Since force is equal to mass times acceleration, it seems that an operational criterion based on long wave *accelerations* would be most relevant to the physical problem.

Intercomparison of existing criteria. It is useful to consider how consistent the above four criteria are with each other. Slope, velocity, and acceleration criteria can be inter-related by using equations for an idealized two-dimensional standing wave. Velocity can be expressed as (Sorensen 1993)

$$u = \frac{Hc}{d} \ \sin kx \ \sin \sigma t \tag{21}$$

where

k = wave number, $= \dfrac{2\pi}{L}$

x = horizontal coordinate

σ = frequency

t = time

Differentiating with respect to time gives an expression for acceleration, a

$$a = \frac{du}{dt} = \frac{Hc}{d} \ \sigma \ \sin kx \ \cos \sigma t$$

$$= \frac{2\pi Hc}{Td} \ \sin kx \ \cos \sigma t \tag{22}$$

$$= \left(2\pi \sqrt{\frac{g}{d}} \right) \frac{H}{T} \ \sin kx \ \cos \sigma t$$

The term in parentheses is relatively constant (assuming that d is relatively constant). The key variable is H/T. Thus it is clear that Wilson's slope criterion

is basically an acceleration criterion as well. Maximum acceleration can also be written as

$$a_{max} = \frac{Hc}{d} \frac{2\pi}{T} = 2\pi \frac{u_{max}}{T} \tag{23}$$

Thus the acceleration criterion is similar to the velocity criterion with the addition of a scaling by the wave period T. A critical threshold acceleration for harbor operations can be defined from Wilson's slope criterion as

$$a_{crit} = 2\pi \sqrt{\frac{g}{d}} \left(\frac{H}{T}\right)_{crit} = 2\pi \sqrt{\frac{g}{d}} \times (0.0038 \quad ft/sec) \tag{24}$$

Now the velocity criterion (No. 3) is examined. Maximum velocity in a standing wave (from Equation 21) is

$$u_{max} = \frac{Hc}{d} = \frac{H\sqrt{gd}}{d} = H\sqrt{\frac{g}{d}} \tag{25}$$

or, rearranging terms,

$$H = u_{max} \sqrt{\frac{d}{g}} \tag{26}$$

Putting this expression for H into Wilson's criterion gives

$$\frac{u_{max}}{T} \sqrt{\frac{d}{g}} < 0.0038 \quad ft/sec \tag{27}$$

or

$$u_{max} < 0.0038 \, T \sqrt{\frac{g}{d}} \quad , \quad u_{max} \quad in \quad ft/sec \tag{28}$$

If representative values for T and d are taken, this expression can be evaluated and compared to PIANC's criterion. Assume d=32 ft and $\sqrt{\frac{g}{d}}$ = 1, and T ranges from 40 sec to 400 sec. Then

$$u_{max} = 0.15 - 1.50 \quad \text{ft/sec}$$

which is reasonably consistent with the PIANC criterion in Equation 20 (though the threshold velocity for damage at the shorter periods is much lower than the PIANC values).

Seabergh and Thomas' criteria (No. 2) can be compared directly with Wilson's criterion (No. 1) (Table 18). Slope values at the high end of the range defined by Seabergh and Thomas' criteria are reasonably comparable to Wilson's criterion.

In conclusion, the four criteria are reasonably consistent. Considering the major simplifications in the overall problem (particularly the lack of explicit consideration of the type of vessel and mooring system), differences between criteria seem relatively minor.

Table 18 Slope[1] Values Defined By Seabergh and Thomas' (1995) Long Wave Criteria			
$H_{s,long}$ (cm)	Wave Period, T (sec)		
	41	205	1,024
5	0.0040	0.0008	
10		0.0016	0.0003

[1] Slope values are defined as $H_{s,long}/T$, in ft/sec for comparison with Wilson's criterion of $H/T < 0.0038$ ft/sec

Adaptation of HARBD output for comparing harbor plans to operational criteria. None of the criteria seems ideally suited to the physical problem and HARBD's capabilities, but HARBD output can be adapted to give quantitative insight relative to the criteria. More importantly, the criteria provide a convenient yardstick for comparing operational performance of alternative plans to the existing harbor. Thus operational experience at existing piers can be applied to piers in the alternative plans. The Wilson and Seabergh and Thomas criteria (Nos. 1 and 2) were used in this study because they are best suited to the standard HARBD output.

68

5 Harbor Response to Wind Waves and Swell

Numerical model studies of the harbor response to wind waves and swell were directed primarily toward assessing the operational performance of alternative harbor modifications. Results, especially at existing and proposed new pier areas, are summarized in this chapter. Amplification factors are presented in the following section. The final section gives H_s values exceeded 10 percent and 1 percent of the time, a result more directly applicable to operational performance. The H_s values are derived from a combination of amplification factors from the numerical model and wave measurements at the directional array outside the harbor. They are compared to operational criteria for wind waves and swell.

Amplification Factors

Amplification factors, representing directionally spread short wave spectra in the form of $(A_{amp})_{eff}$ in Equation 17, were calculated for a variety of wind wave and swell conditions. Figure 48 shows examples of a short period swell and a long period swell coming from two different directions. Tables of $(A_{amp})_{eff}$ in the existing harbor for various incident peak wave periods and directions (T_p and θ_m) are given in Appendix F.

For a more concise comparison between the existing harbor and alternative plans, average values of $(A_{amp})_{eff}$ were computed for each basin across wave periods ranging from 10 sec through 20 sec. Figure 49 shows results for the existing harbor and three plans. The $(A_{amp})_{eff}$ changes progressively as incident wave direction changes. As would be expected, amplification tends to be greater for directions of more direct approach to the basins. Also it is evident that the proposed new passenger pier locations in these particular plans have an exposure to wind waves and swell which is significantly greater than that at the existing Pier 1 (Basins 4-6).

As illustrated in Figure 49, the average amplification factor changes between plans only if there are significant changes in basin location (as in the passenger
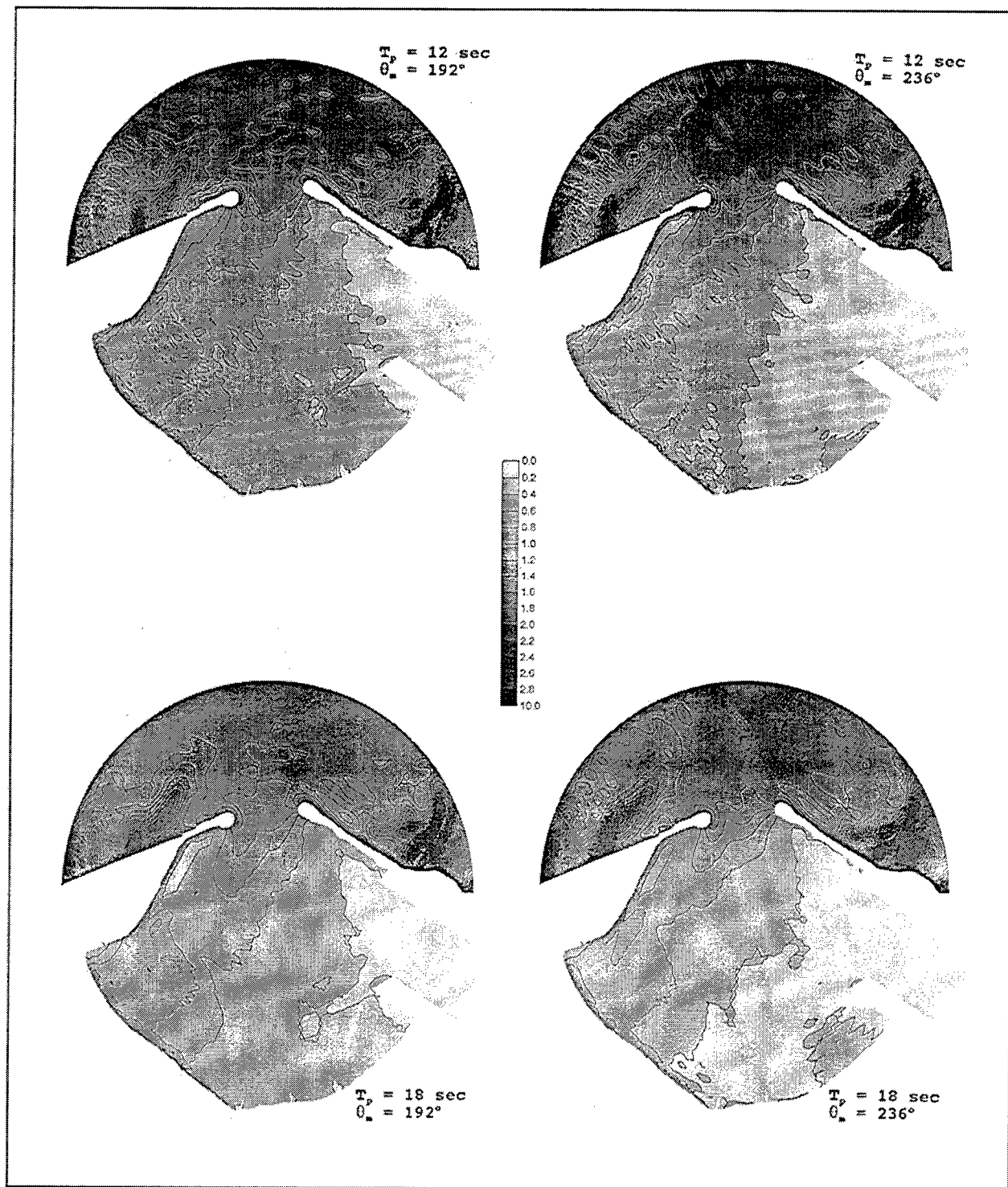
Figure 48. Example swell amplification factor contours, existing harbor

pier moving to different locations) or sheltering by the breakwater extension.
Piers 1-3 behave similarly in the various plans. The wind wave and swell
response in the harbor is basically a result of diffraction through the breakwater
gap. Boundary reflection characteristics have a localized effect on the waves, but

changes in the western half of the harbor have virtually no effect on the existing pier areas.

An even more concise description of $(A_{amp})_{eff}$ at each basin can be obtained by considering wave climate as well. A climate-based amplification factor is calculated for each basin as

$$(A_{amp})_{climate} = \sum_{j=1}^{N_T} \sum_{k=1}^{N_D} ((A_{amp})_{eff})_{jk} \frac{N_{jk}}{N_{total}} \qquad (30)$$

where

jk = indices denoting the jth period interval and k^{th} direction interval, where the intervals are based on the incident wave conditions in Table 15

$((A_{amp})_{eff})_{jk}$ = spectral amplification factor for the jth period and k^{th} direction

N_{jk} = number of array records with T_p and θ_m in the jth and k^{th} period and direction intervals

N_{total} = total number of records from the array gage

This climate-based amplification factor is given in Appendix F for every basin and harbor plan. Array data used in the calculation were from Nov 93 - Sep 94, as discussed in Chapter 2.

One complication which arose during the wind wave and swell studies was inconsistent results at the boat ramp (Basin 21) between some of the plans. After investigation, it was discovered that bottom friction has a signficant effect at this location because of the expanse of very shallow water approaching it. Rough correction factors were developed from a small number of runs with $\beta=0.032$ and applied to Basin 21 for all plans. Results presented here include that correction.

Evaluation Against Operational Criteria for Wind Waves and Swell

Standard operational criteria used by the U.S. Army Corps of Engineers (USACE) for wind waves and swell in *shallow draft* harbors are:

a. Wave height in berthing areas will not exceed 1 ft more than 10 percent of the time.

b. Wave height in entrance and access channels and turning basins will not exceed 2 ft more than 10 percent of the time.
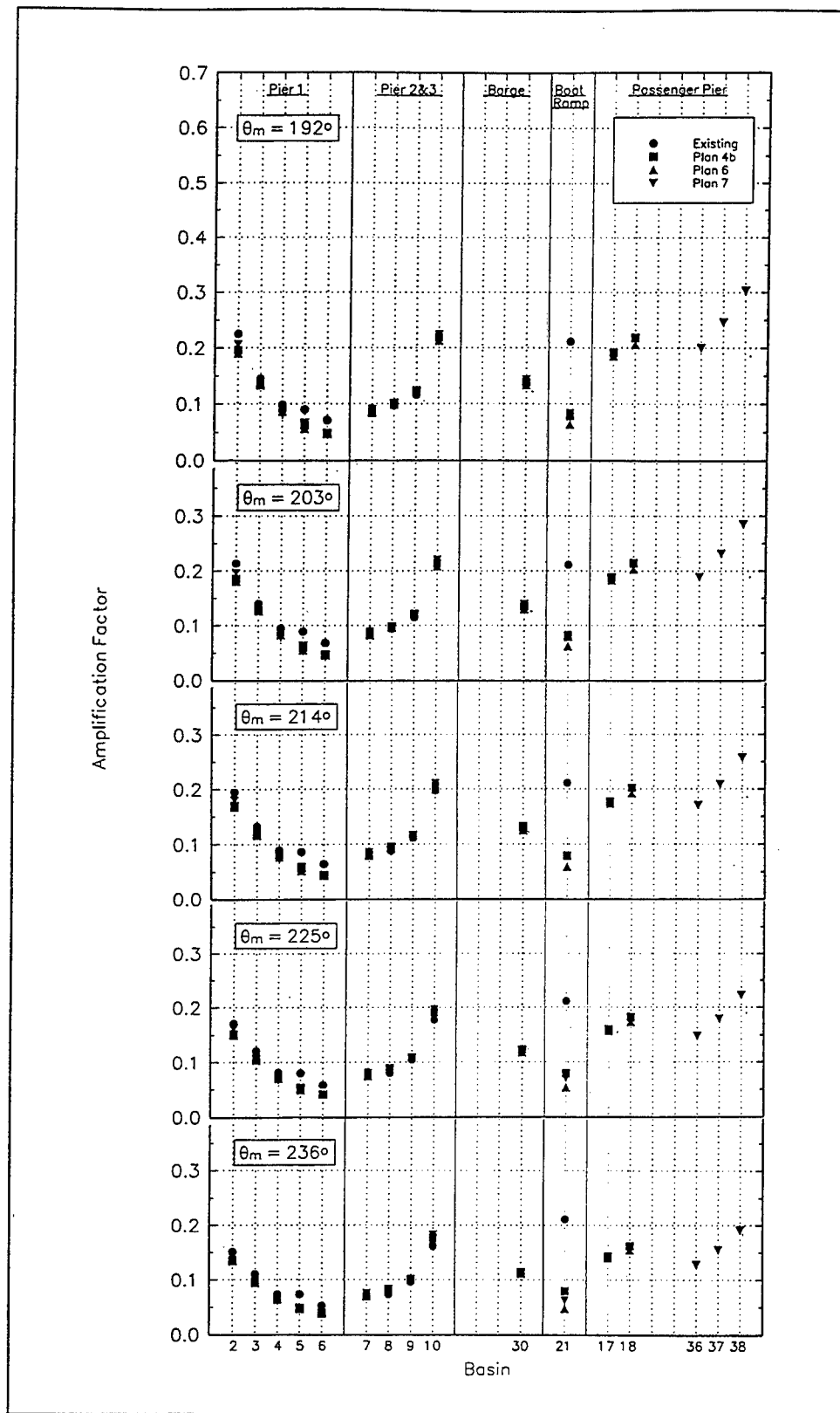
Figure 49. Comparison of $(A_{amp})_{eff}$ averaged over periods of 10-20 sec at piers, existing harbor and Plans 4b, 6, and 7 (see Figure 46 and Appendix E for basin locations)

Standard criteria for wind waves and swell in *deep draft* harbors, such as Kahului Harbor, are not so well established. However, the criteria for shallow draft harbors can provide a useful basis for comparing alternative plans at Kahului Harbor.

Another, perhaps more valuable, criterion for evaluating proposed new pier areas is to conduct comparisons with existing piers. Many years of practical experience at Piers 1 and 2 can then be approximately transferred to new plans.

Wave heights for assessing the USACE criteria were computed by combining the time-history of array gage parameters over the time period November 1993 through September 1994 with numerical model results to create a time-history of wave heights at each harbor basin. For each array record, the corresponding wave height at a harbor basin is

$$(H_s)_{harbor} = (A_{amp})_{eff} \times (H_s)_{array} \tag{31}$$

where

$(H_s)_{harbor} = $ significant wave height at a harbor basin

$(A_{amp})_{eff} = $ spectral amplification factor interpolated between values for periods and directions in Table 15 to represent T_p and θ_m at the array

$(H_s)_{array} = $ significant wave height at the array

The 11-month time-history of $(H_s)_{harbor}$ at each basin was sorted into descending order and the value of H_s which was exceeded 10 percent of the time was identified. The H_s value exceeded 1 percent of the time was also identified. The H_s with 1 percent exceedance relates to a more demanding operational condition, which may be more applicable to large commercial vessels.

Significant wave heights exceeded 10 percent of the time are less than 1 ft at all existing and most proposed pier areas (Figure 50). The existing harbor is included in each panel of the figure to give a common reference. Existing Piers 1-3 extend approximately between Basins 3-9. Basin 3, which is centered on the proposed extension of Pier 1, has higher wave conditions than any basins along existing piers. Basin 2, the location of a possible future extension of Pier 1, has wave heights approximately twice as high as the main existing Pier 1 (Basins 4 and 5). Wave heights at the exposed end of Pier 2 (Basin 10) also approach this level. The significant wave height exceeded 10 percent of the time computed directly from Pier 2 wave gage results is 0.39 ft, which compares well with corresponding numerical model results at Basin 8 in the existing harbor and helps to validate the model wave heights (Table 19).

Except for Plan 2, wave heights at the proposed new barge pier (Basins 25, 26, and 30) range between those near the center of Pier 2 (Basin 9) to the exposed end of Pier 2 (Basin 10), depending on the harbor plan. The boat ramp is considerably more protected in most plans relative to the existing harbor. Proposed passenger pier locations in the alternative plans have a wide range of protection. The best protected alternatives give wave conditions similar to the existing Pier 1. The most exposed alternative (Plan 4a) gives waves signficantly higher than at any existing pier locations.

Table 19 Significant Wave Heights Exceeded 10 Percent and 1 Percent of the Time at Field Gages		
Gage	H_s with 10% Exceedance (ft)	H_s with 1% Exceedance (ft)
Pier 2	0.39	0.63
Canoe Club	1.15	1.65
Back Basin	1.26	1.99
Channel Entrance	3.10	4.63

The H_s values exceeded 1 percent of the time are considerably higher than those exceeded 10 percent of the time, but show similar relative trends (Figure 51). Existing pier areas still fall below the 1-ft wave height threshold, with the exception of the exposed end of Pier 2 (Basin 10) and, possibly, the northwest end of Pier 1. Proposed new barge and passenger piers are below the threshold in some plans and above in others.

74
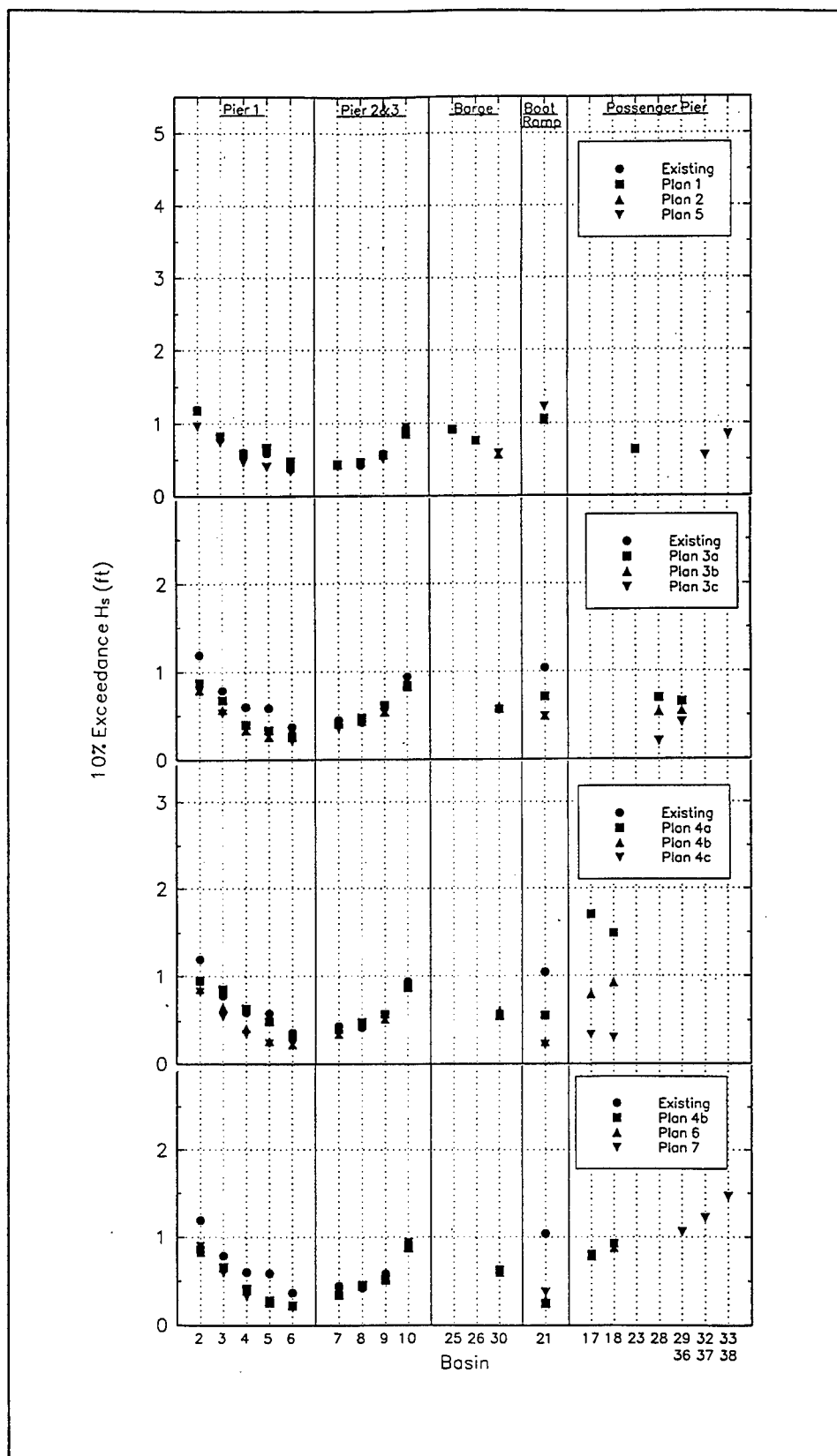
Figure 50. Comparison of H_s exceeded 10 percent of the time at piers
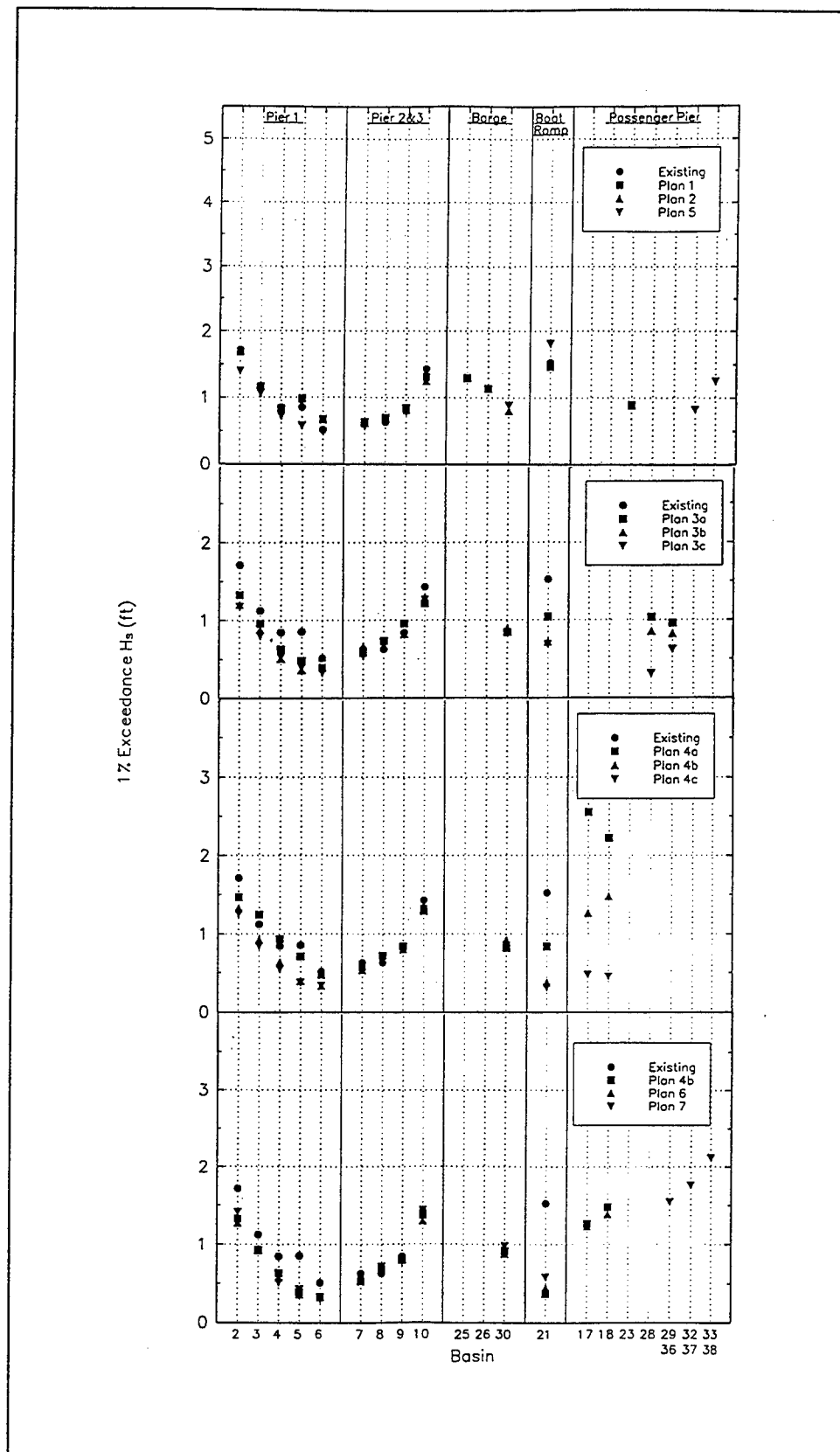
Figure 51. Comparison of H_s exceeded 1 percent of the time at piers

6 Harbor Oscillations

To evaluate harbor resonance characteristics, the HARBD numerical model was run for the existing harbor and all alternative plans. Incident long wave periods ranged from 25 sec to 1,000 sec in very fine increments, as discussed in Chapter 4. These evaluations were included because oscillations are an important part of interpreting the existing harbor wave response (as evidenced by gage data in the harbor), and modifications to the harbor can potentially lead to increased operational problems due to harbor oscillations. Amplification factor results are presented in the following section. Additional results more closely related to operational performance criteria are given in the final section.

Amplification Factors

Amplification factors for the long waves involved in harbor oscillation behave differently than those for wind waves and swell. Long waves, because of their length relative to harbor dimensions and their reflectivity from harbor boundaries, form *standing wave* patterns in the harbor. Standing wave behavior in a simple closed basin of uniform depth is illustrated in Figure 52. In the fundamental mode of oscillation, *antinodes* occur at both basin walls and a *node* midway between walls. Second and third modes of oscillation are also illustrated. Antinodes always occur at the walls. Additional antinodes and nodes occur at regular
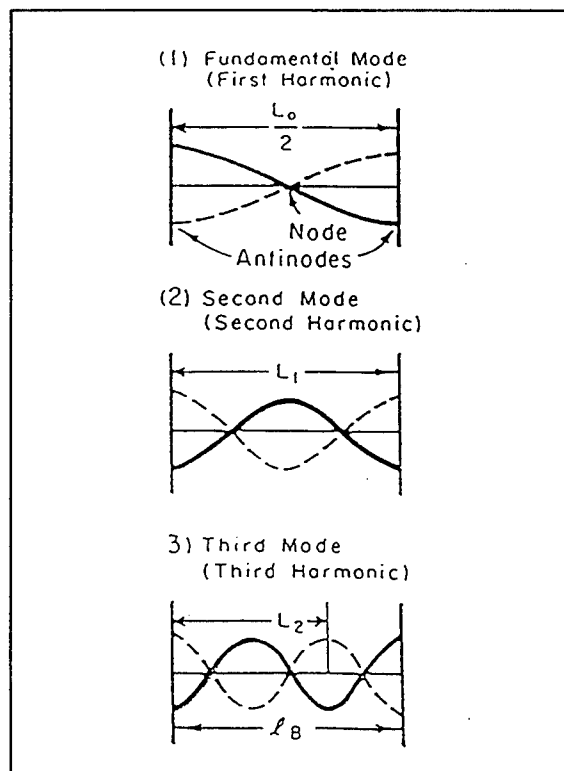
Figure 52. Harbor oscillation definitions

intervals between walls, with the number of antinodes and nodes dependent on the mode of oscillation.

The water surface in a standing wave has its greatest vertical motion at antinodes. There is no vertical movement at an ideal node, but horizontal velocities reach a maximum there. In terms of amplification factors, this behavior gives large values of $A_{amp,l}$ at antinodes and small values around nodes. Contrary to wind waves and swell, small values of $A_{amp,l}$ are not necessarily indicative of a tranquil harbor area.

Phases in a standing wave also behave differently than for typical wind waves and swell. For example, the water surface in the fundamental mode of oscillation in Figure 52 simultaneously reaches a maximum at every point to the left of the node. These points are all in phase. At the same time, every point to the right of the node reaches a minimum value. These points are also in phase with each other but exactly out of phase with the points to the left of the node. Thus phases in a simple standing wave are constant between an antinode and node. They quickly change by 180 deg (or π radians) across the node and remain constant up to the next node or boundary.

Amplification factors for pier areas in the existing harbor are shown as a function of wave frequency in Figure 53. Some frequencies produce a strong resonant amplification, with peak amplification factors between about 2 and 10. Many of the same resonant frequencies appear at all basins, though the strength of amplification can vary considerably between basins. A large peak at very low frequency (0.0007 Hz or 1,500-sec period) shows at every basin and plan. This peak represents the Helmholtz (or *grave*) mode of oscillation, in which the entire harbor rises and falls in unison. Phase is constant over the whole harbor. This peak also dominates long wave spectra at the array (Figure 20).

Amplification factor and phase contour plots for the four highest resonant peaks (excluding Helmholtz resonance) show oscillation patterns in the existing harbor. In the amplification factor plots, areas of high amplification are evident as darker shades of gray (Figure 54). Corresponding phase contours are shown in Figure 55. Areas in which phase contours are tightly bunched indicate nodal areas. As would be expected for standing waves, nodal lines in Figure 55 coincide with low amplification factors in Figure 54. The phase plots also indicate areas of the harbor which rise and fall together during the resonant condition (same gray shade). Thus the oscillation patterns can be interpreted.

The 212.77-sec resonant period, peak A, shown in Figure 54 represents a relatively simple rocking oscillation between Piers 1-3, the south end of the harbor, and the boat ramp area. A single nodal line runs across the harbor in a generally east-west direction. The 176.99-sec resonance, peak B, is primarily a rocking between Piers 1-3 and the coral stockpile along the west breakwater. The shorter period oscillations are more complex patterns, though they generally indicate a strong nodal area at or near Pier 1 and the seaward end of Pier 2. The peak D resonance is an interesting pattern between the corners of Pier 1 and Pier 2.

78
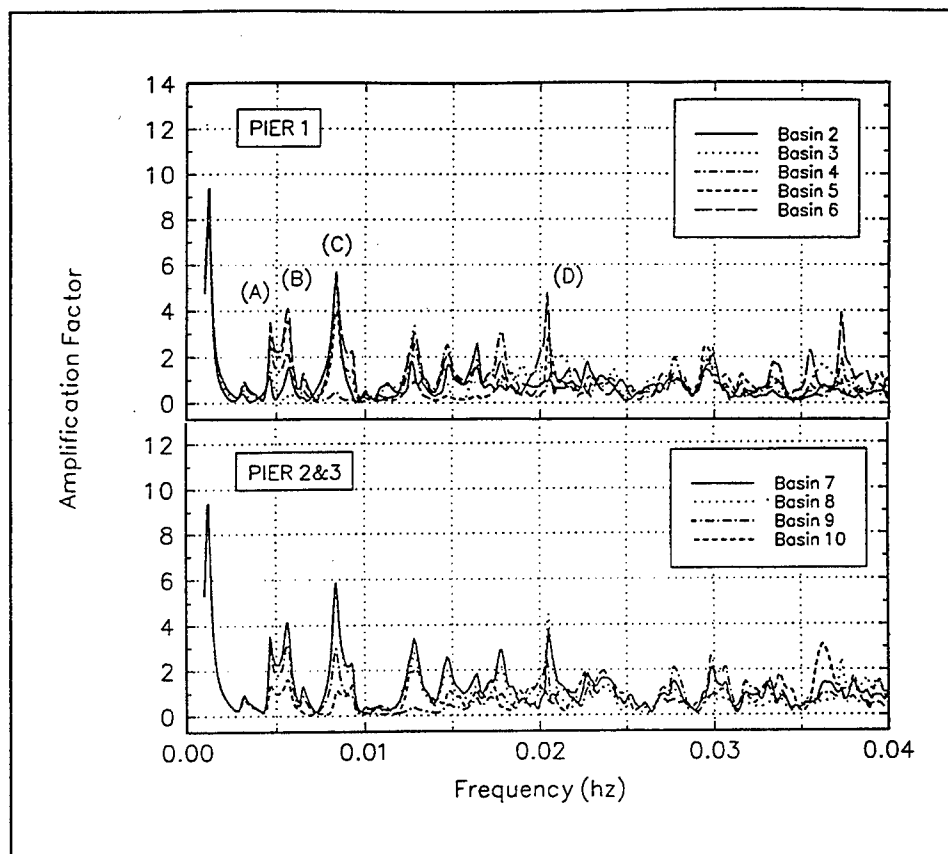
Figure 53. Long wave response, existing harbor, Piers 1-3

The long wave amplification factors shown here may be overestimated for resonant peaks at periods less than about 100 sec. The wave reflection coefficient at all solid boundaries was set to 1.0 for all long wave runs, but Figure 44 shows some evidence that peaks at the shorter long wave periods tend to be overestimated. The peak D case is particularly evident. Some reduction in reflection coefficient as wave period decreases could be expected physically. This case was rerun with $K_r=0.95$ along all boundaries. The height of peak D was reduced from 4.5 to near 1.0. Additional tests with $K_r=0.95$ helped confirm that this choice would improve the long wave calibration at periods between 25 sec and 100 sec. It was not practical to refine K_r values and revise long wave runs for all plans, and the initial runs with $K_r=1.0$ are considered adequate for evaluating alternative plans.

Amplification factor plots for alternative plans are given in Appendices G and H. Plots of $A_{amp,l}$ versus frequency (Appendix G) are grouped so that the existing and proposed harbor plans can be easily compared at each pier area. Amplification factor and phase contour plots for the main resonant frequencies are given in Appendix H.

A more quantitative comparison between the existing harbor and alternative plans can be obtained by averaging amplification factors across a range of long wave frequencies. The root-mean-square (RMS) amplification factor was

computed for each plan (Figure 56). The RMS is used because squared amplification factors are indicative of wave energy, a more relevant basis for comparison than wave height. In computing the RMS, frequencies lower than 0.0025 Hz (400 sec) were not included to avoid domination by the Helmholtz peak common to all plans.

The existing harbor and all plans show minimum values of the RMS amplification factor around the middle of Pier 1 and end of Pier 2 (Basins 4 and 10). Thus, these tend to be nodal areas. Another notable feature of the figure is the exceptionally high amplifications at the proposed passenger pier in Plans 1 and 2. Basin 30, representing the proposed barge pier for most plans, was inadvertently omitted in Plan 2 long wave runs. Basin 31, which was very similar to Basin 30 in other long wave runs, is used in its place in the long wave summaries in this report.

Evaluation Against Operational Criteria for Long Waves

Procedures for evaluating the operational acceptability of different harbor plans subjected to long waves are reviewed in Chapter 4. This study used a variation of the most direct procedure (Seabergh and Thomas 1995). The percent of observations with $H_{s,long}$ greater than 10 cm was computed for each basin and plan. However, the range of long wave frequencies was divided into two segments having periods ranging from 30-100 sec and 100-400 sec. The choice of 100 sec as the dividing point was based on an expected sensitivity of barges to periods in the shorter period range and a lower confidence in that range because of the concern that K_r may be slightly high. $H_{s,long}$ is calculated as

$$H_{s,long} = 4 \sqrt{\sum_{i=N_1}^{N_2} \left[\frac{(A_{amp})_{harbor}}{(A_{amp})_{array}} \right]_i \times E_{array}(f_i)}$$

(32)

where

$N_1, N_2 =$ spectral line numbers in model corresponding to the period range being considered (30-100 sec or 100-400 sec)

$(A_{amp})_{harbor}, (A_{amp})_{array} =$ amplification factors for i^{th} spectral line in model

$E_{array}(f_i) =$ spectral energy at array for i^{th} spectral line in model (interpolated from gage data), in units of cm^2

Amplification factor at the array is needed as a divisor because long waves can easily reflect back to the array. Spectral energy at the array cannot be considered
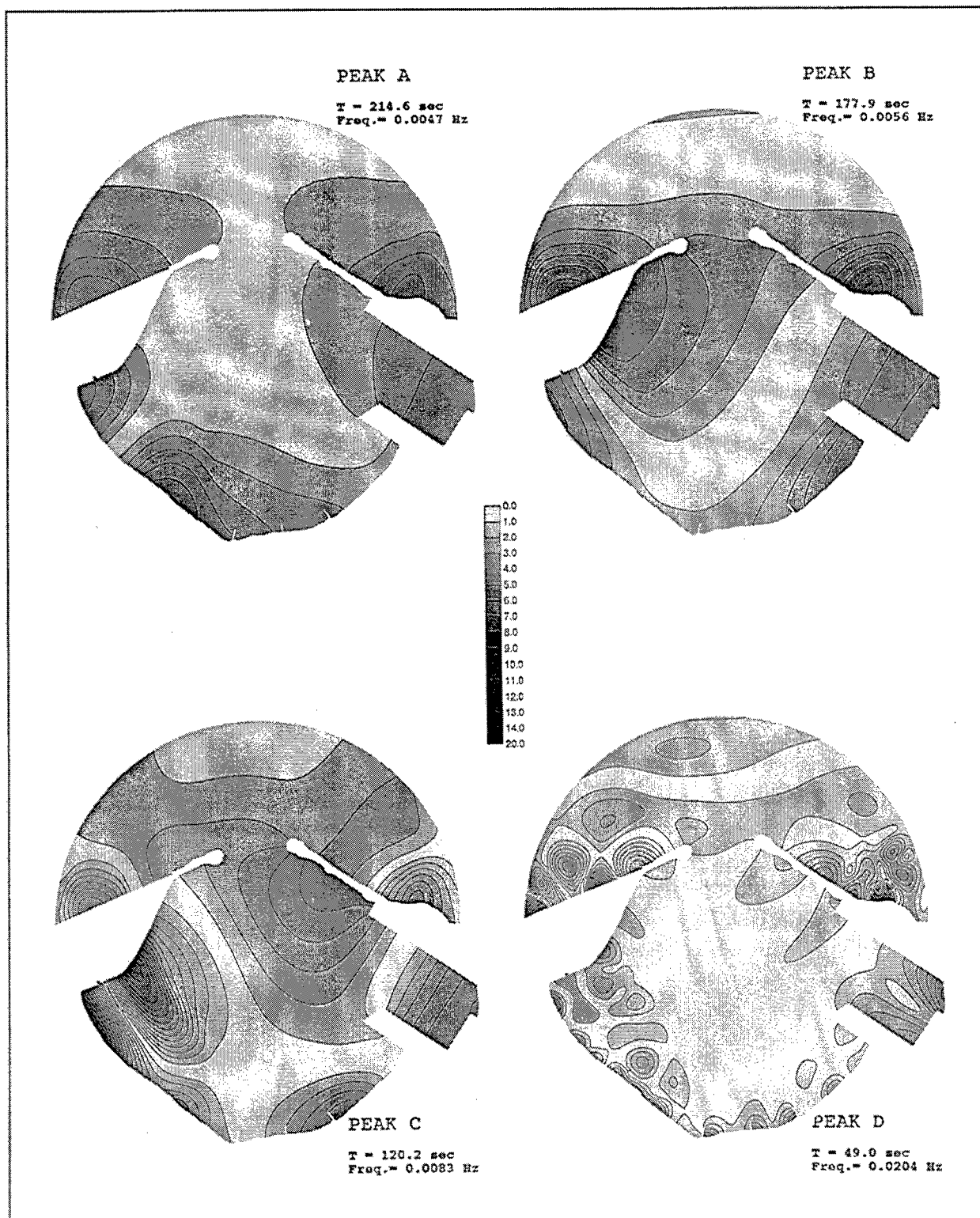
Figure 54. Resonant long wave amplification factor contours, existing harbor
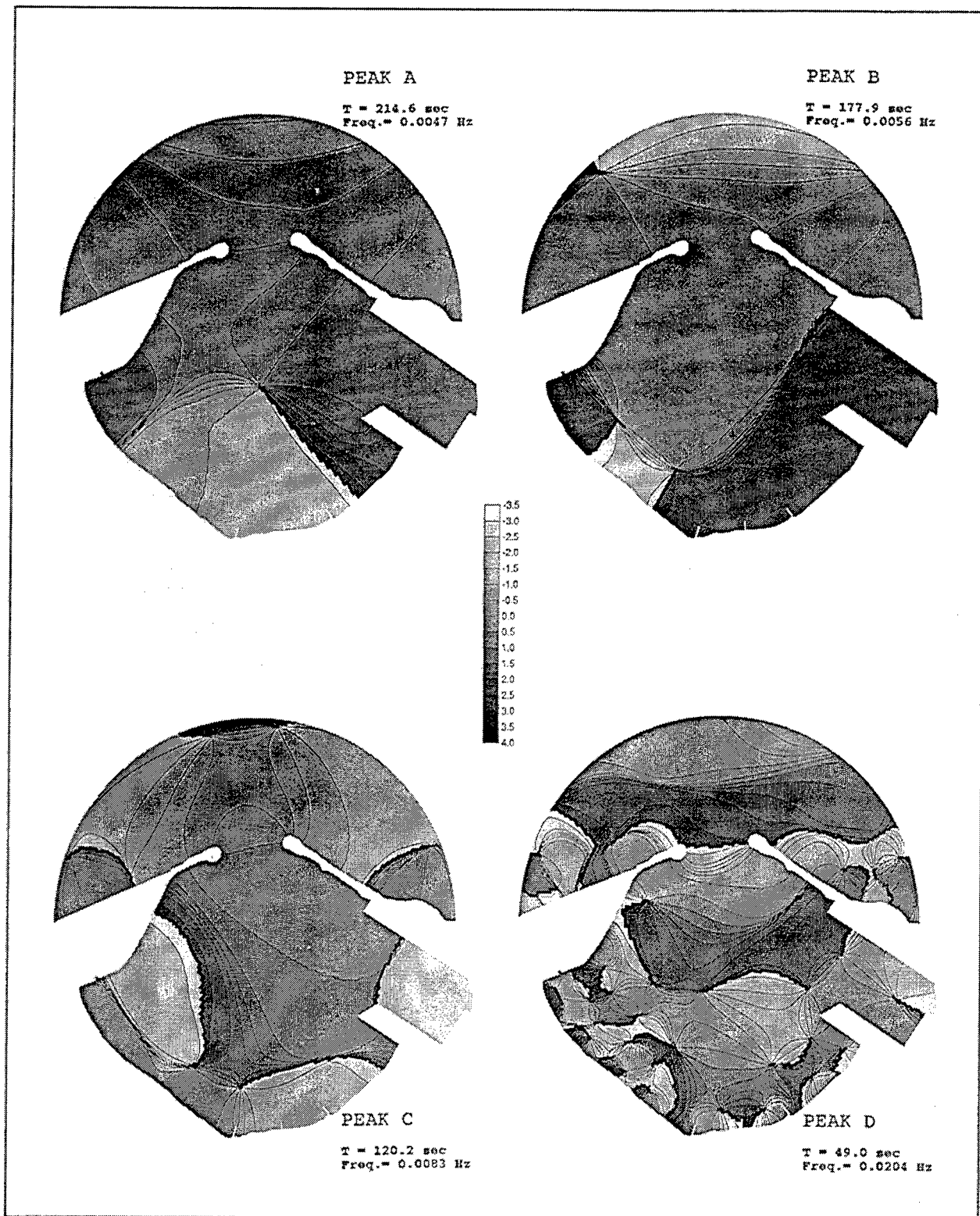
Figure 55. Resonant long wave phase contours, existing harbor
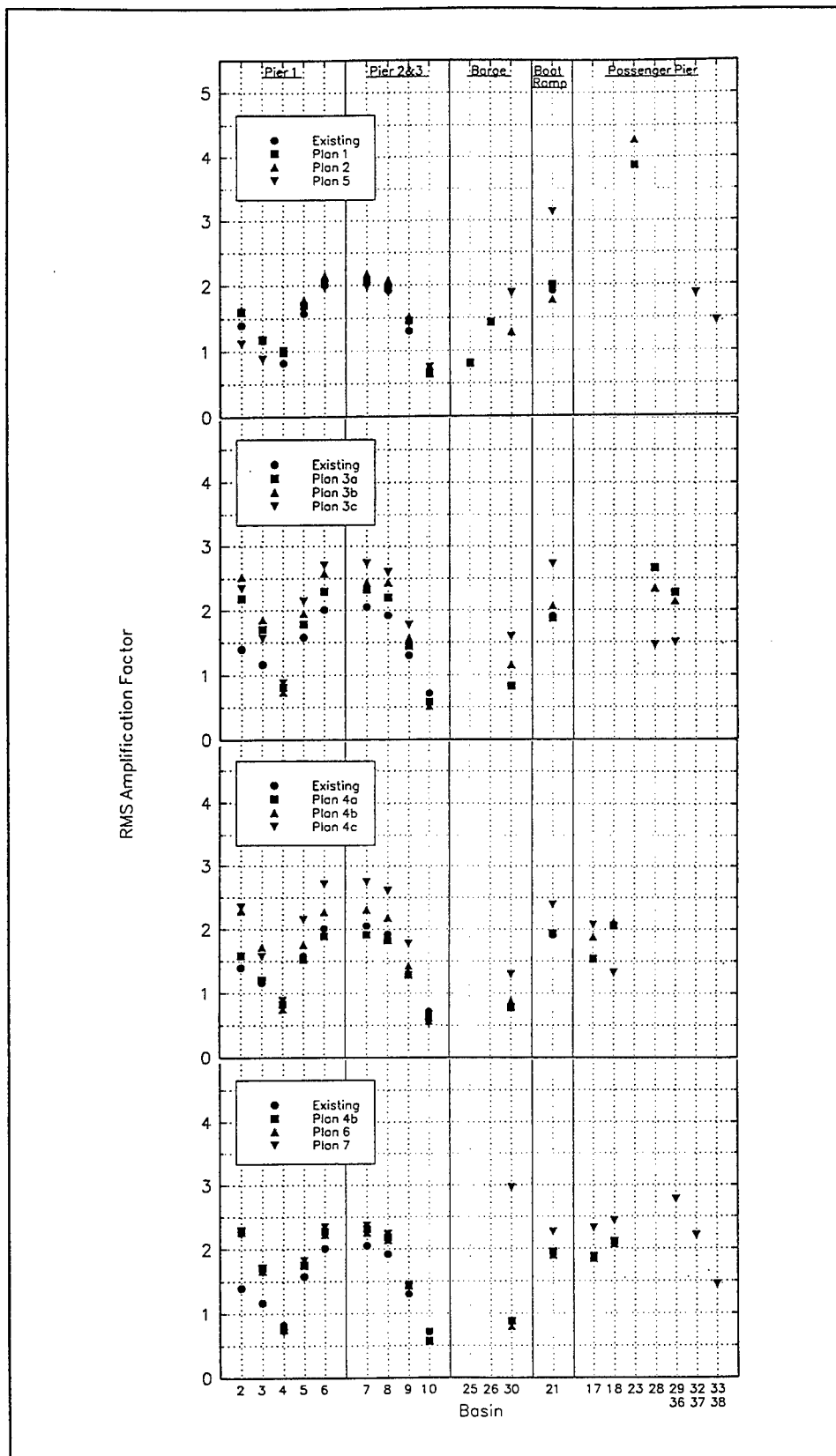
Figure 56. Long wave RMS amplification factor comparison at piers, *T*=100-400 sec

as purely incident energy. $(A_{amp})_{array}$ was constrained to be greater than or equal to 1.0 in this calculation.

Using Equation 32 and the 11-month field data set, the percent of observations with $H_{s,long} \geq 10$ cm was calculated. Results for the 100-sec to 400-sec range are similar to the RMS amplification factor results (Figure 57). Results for the 30-sec to 100-sec range are more scattered (Figure 58). Corresponding information from the field gages is given in Table 20 for comparison.

A slope criterion as suggested by Wilson (1967) was also evaluated. Wave height for the criterion was an $H_{s,long}$ as in Equation 32, with the summation taken over nine successive model frequencies. The number nine was chosen because nine successive frequencies encompass a broad enough band to include most or all of any peak in the model spectral response. The $H_{s,long}$ was multiplied by the center frequency to give a slope. If any combination of nine successive frequencies gave a slope exceeding Wilson's criterion, the record was counted as having exceeded the threshold. Period ranges of 30-100 sec and 100-400 sec were evaluated separately as before. Results are given in Appendix G.

Table 20 Percent Occurrence of $H_{s,long} \geq 10$ cm at Field Gages		
Gage	Wave Period Range (sec)	
	100-400	30-100
Pier 2	3.8	1.4
Canoe Club	0.8	2.1
Back Basin	0.1	0.2
Channel Entrance	2.2	1.6
Array	0.4	3.0

An additional operational guideline is based on the value of $A_{amp,l}$ for the higher resonant peaks. Experience with Los Angeles and Long Beach Harbors has indicated that if $A_{amp,l}$ is greater than about 5, some operational difficulties may be encountered. If $A_{amp,l}$ is greater than 10, major operational problems can be expected.[1] This guideline may be applied to the plots in Appendix G. If the very low frequency Helmholtz peak is excluded, Plans 1, 2, 5, and 7 all appear to be operationally unacceptable as presently formulated. They all have basins at which $A_{amp,l}$ exceeds 10.

Results are best judged by comparison to the existing piers. Plans 1 and 2 clearly have potential problems at the passenger pier (Basin 23) in the 100- to 400-sec range. The magnitude of response in a range which affects ships of this size is large enough that this facility would likely be unacceptable. Plans 5 and 7 also tend toward elevated responses.

---

[1] Personal Communication, William C. Seabergh, Research Hydraulic Engineer, U.S. Army Engineer Waterways Experiment Station, Vicksburg, MS.

Most plans indicate improved conditions at the new barge facility on the south side of Pier 2 relative to existing piers. The 30- to 100-sec period range is considered especially important for barge response. Most plans show improved conditions for passenger vessels, too. The 100- to 400-sec range is probably more critical for these vessels.
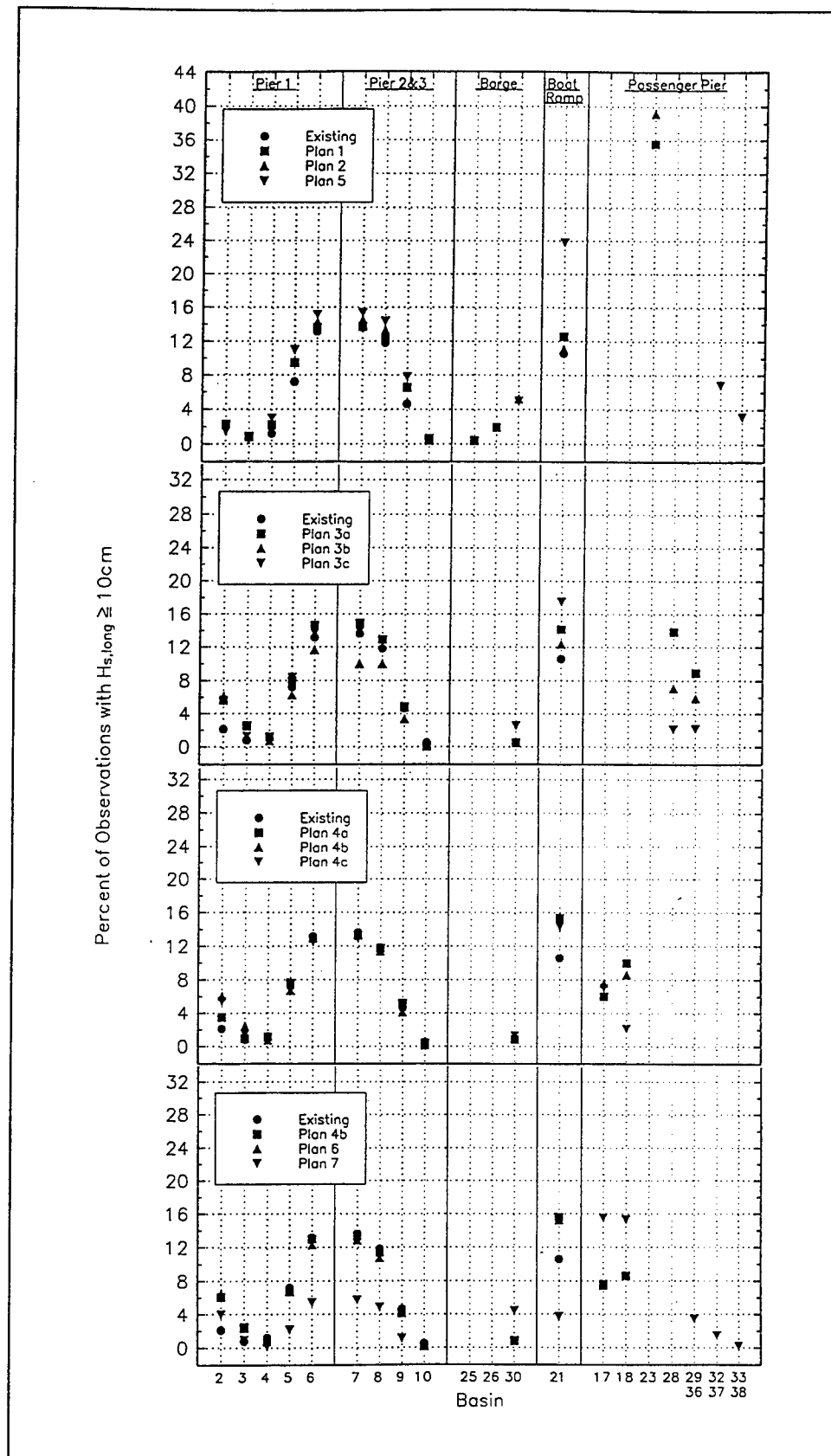
Figure 57. Percent occurrence of $H_{s,long}$ ≥ 10 cm at piers, T=100-400 sec
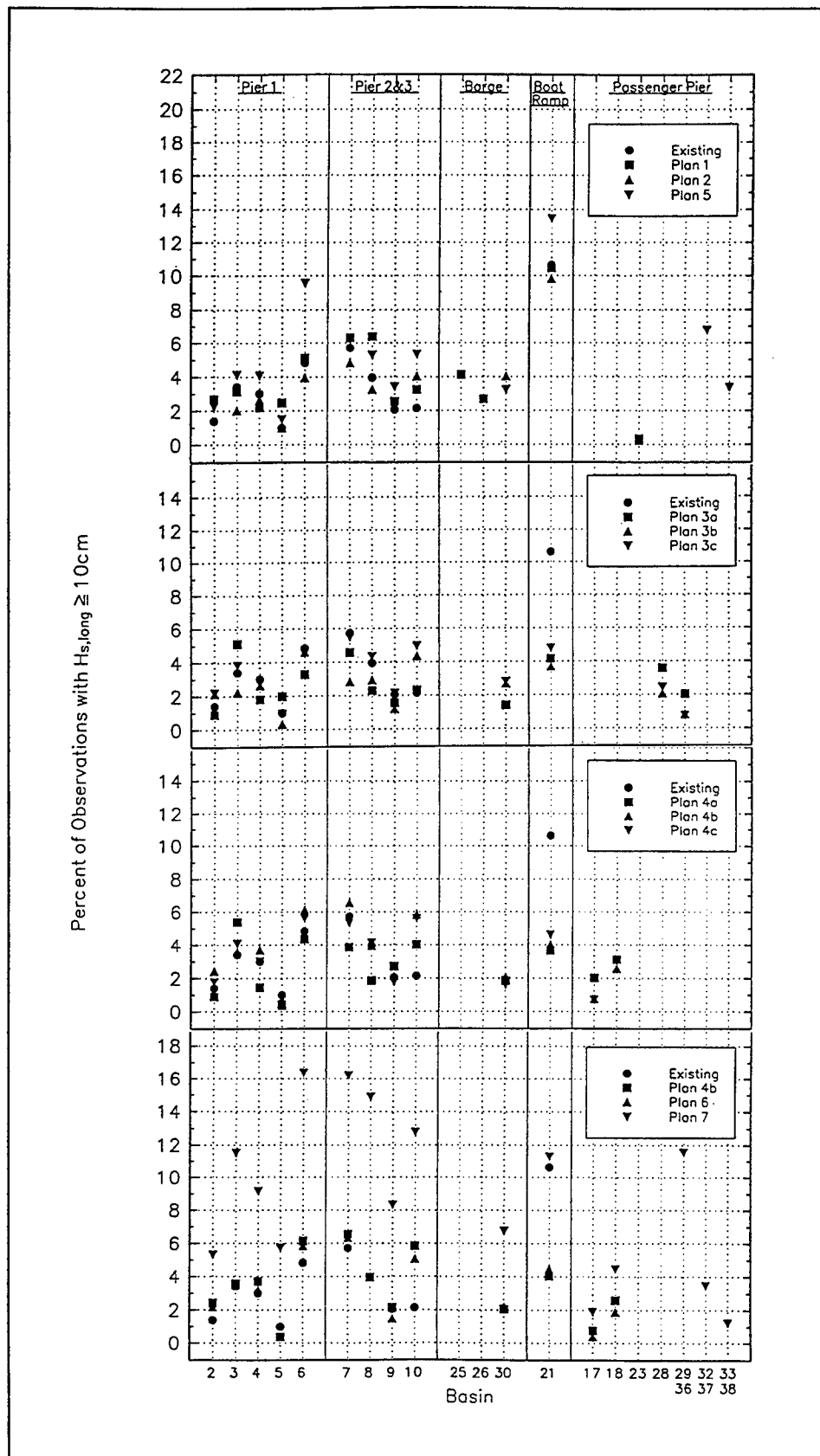
Figure 58. Percent occurrence of $H_{s,long} \geq 10$ cm at piers, T=30-100 sec

7 Conclusions and Recommendations

Studies of the wave response of Kahului Harbor have produced valuable information about the existing harbor and possible modifications. Field measurements taken over a period of 18 months at a deepwater directional buoy, a directional array outside the harbor, and four gages inside the harbor were extremely helpful in understanding present harbor behavior. Numerical modeling of the existing harbor also helped to explain the response to short and long waves.

The numerical model was used to simulate the behavior of 11 alternative modifications to the harbor. Model results are compared with criteria for operational acceptability and with experience in the existing harbor to the extent possible. The effectiveness of proposed new harbor areas for wind wave and swell protection often has little relationship to protection from oscillations. These two aspects of pier operability must both be considered in judging success of the alternative plans.

An overview of performance of the alternative plans is given by their success relative to a simple, meaningful criterion. For wind waves and swell, success was defined as having $H_s > 1$ ft less than 1 percent of the time at all basins along the pier (Table 21). The 1 percent level was chosen because the existing Piers 1 and 2 (which are considered successful) meet this criterion but the seaward ends of Piers 1 and 2 (which are believed to be marginal) slightly exceed the criterion. Thus successful piers in Table 21 should be comparable or better than the existing facilities for wind waves and swell.

A similar overview of plan performance for harbor oscillations is given in Tables 22 and 23. The criteria are expressed in terms of percent exceedances of $H_{s,long} = 10$ cm. The threshold percent values were selected to be slightly higher than the existing harbor facilities.

Specific conclusions and recommendations are as follows:

a. *Plan 1.* Not recommended because of large long wave amplifications at proposed passenger pier.

b. *Plan 2.* Not recommended because of large long wave amplifications at proposed passenger pier.

c. *Plan 3a.* Generally acceptable for both short and long waves. The long wave amplification factor at one resonance is quite high at Piers 1-3 and the proposed passenger pier.

d. *Plan 3b.* Generally acceptable.

e. *Plan 3c.* Generally acceptable.

f. *Plan 4a.* Not recommended because of large wind waves and swell at the proposed passenger pier.

g. *Plan 4b.* Generally acceptable. Fairly large wind waves and swell can be expected at the proposed passenger pier.

h. *Plan 4c.* Generally acceptable.

i. *Plan 5.* Not recommended because of large long wave amplifications at proposed barge and passenger piers.

j. *Plan 6.* Generally acceptable. Fairly large wind waves and swell can be expected at the proposed passenger pier.

k. *Plan 7.* Not recommended because of large long wave amplifications at proposed barge and passenger piers.

All of the plans, including those designated as acceptable, include some long wave resonant peaks which are larger than in the existing harbor. These seem to be a likely consequence of creating new pier areas. It is assumed that peaks with amplification factors well under 10 will not cause any major operational difficulties.

Some of the limitations in the plans tested may be overcome by prudent design. For example, the fill area in the southwest area of the harbor created strong oscillations. However, the same facility could be designed as a pile-supported structure and the strong oscillations would be avoided. The breakwater extension present in some of the plans might be designed without a core, allowing it to block wind waves and swell but remain transparent to long waves.

A physical model study to refine and validate the preferred plan(s) is strongly recommended as a final phase of the studies. The physical modeling component was part of the originally proposed WES study.

Table 21
Plans with H_s>1 ft Less Than 1 Percent of the Time

Plan	Area				
	Pier 1	Piers 2 & 3	Barge	Boat Ramp	Passenger Pier
Existing	x	x			
1		x			x
2		x	x		x
3a	x	x	x		
3b	x	x	x	x	x
3c	x	x	x	x	x
4a		x	x	x	
4b	x	x	x	x	
4c	x	x	x	x	x
5		x	x		
6	x	x	x	x	
7	x	x	x	x	

Table 22
Plans with $H_{s,long}$≥ 10 cm Less Than 16 Percent of the Time, 100- to 400-sec Periods

Plan	Area				
	Pier 1	Piers 2 & 3	Barge	Boat Ramp	Passenger Pier
Existing	x	x		x	
1	x	x	x	x	
2	x	x	x	x	
3a	x	x	x	x	x
3b	x	x	x	x	x
3c	x	x	x		x
4a	x	x	x	x	x
4b	x	x	x	x	x
4c	x	x	x	x	x
5	x	x	x		x
6	x	x	x	x	x
7	x	x	x	x	x

Table 23					
Plans with $H_{s,long} \geq 10$ cm Less Than 7 Percent of the Time, 30- to 100-sec Periods					
Plan	Area				
	Pier 1	Piers 2 & 3	Barge	Boat Ramp	Passenger Pier
Existing	x	x			
1	x	x	x		x
2	x	x	x		x
3a	x	x	x	x	x
3b	x	x	x	x	x
3c	x	x	x	x	x
4a	x	x	x	x	x
4b	x	x	x	x	x
4c	x	x	x	x	x
5		x	x		x
6	x	x	x	x	x
7			x		

References

Allsop, N. W. H. (1990). "Reflection performance of rock armoured slopes in random waves." *Proceedings of the 22nd International Conference on Coastal Engineering.* American Society of Civil Engineers, Vol 2, 1460-1472.

Basco, D. R., and McGehee, D. D. (1990). "A methodology to select nearshore wave gauge sites: The Virginia wave gauge study," Report No. 90-1, Coastal Engineering Institute, Old Dominion University, Norfolk, VA.

Berkhoff, J. C. W. (1972). "Computation of combined refraction-diffraction." *Proceedings of the 13th International Conference on Coastal Engineering.* American Society of Civil Engineers, Vol 1, 471-490.

Blue, F. L., and Johnson, J. W. (1949). "Diffraction of water waves passing through a breakwater gap." *Transactions, American Geophysical Union.* Vol 30, No. 5, 705-718.

Bottin, R. R., Jr., Sargent, F. E., and Mize, M. G. (1985). "Fisherman's Wharf area, San Francisco Bay, California, design for wave protection: Physical and numerical model investigation," Technical Report CERC-86-7, U.S. Army Engineer Waterways Experiment Station, Vicksburg, MS.

Bowers, E. C., and Welsby, J. (1982). "Experimental study of diffraction through a breakwater gap," Report No. IT 229, Hydraulics Research Station, Wallingford, England.

Briggs, M. J., Lillycrop, L. S., and McGehee, D. D. (1992). "Comparison of model and field results for Barbers Point Harbor." *Proceedings, Coastal Engineering Practice.* American Society of Civil Engineers, 387-99.

Briggs, M. J., Lillycrop, L. S., Harkins, G. R., Thompson, E. F., and Green, D. R. (1994). "Physical and numerical model studies of Barbers Point Harbor, Oahu, Hawaii," Technical Report CERC-94-14, U.S. Army Engineer Waterways Experiment Station, Vicksburg, MS.

Chen, H. S. (1986). "Effects of bottom friction and boundary absorption on water wave scattering," *Applied Ocean Research* 8 (2), 99-104.

Chen, H. S., and Houston, J. R. (1987). "Calculation of water oscillation in coastal harbors: HARBS and HARBD user's manual," Instruction Report CERC-87-2, U.S. Army Engineer Waterways Experiment Station, Vicksburg, MS.

Chen, H. S., and Mei, C. C. (1974). "Oscillations and wave forces in an offshore harbor," Report No. 190, Department of Civil Engineering, Massachusetts Institute of Technology, Cambridge, MA.

Clausner, J. E., and Abel, C. E. (1986). "Contained aquatic disposal: Site location and cap material investigations for Outer Indiana Harbor, IN, and Southern Lake Michigan," Technical Report EL-87-9, Vol II, Appendix J, U.S. Army Engineer Waterways Experiment Station, Vicksburg, MS.

Coastal Engineering Research Center. (1996). "Compendium of U.S. wave data, summary statistics, January 1996," U.S. Army Engineer Waterways Experiment Station and U.S. Department of Commerce, National Oceanic and Atmospheric Administration. To obtain copies, contact U.S. Army Engineer Waterways Experiment Station, CD-P, 3909 Halls Ferry Road, Vicksburg, MS 39180.

Corson, W. D., Abel, C. E., Brooks, R. M., Farrar, P. D., Groves, B. J., Jensen, R. E., Payne, J. B., Ragsdale, D. S., and Tracy, B. A. (1986). "Pacific Coast hindcast deepwater wave information," WIS Report 14, U.S. Army Engineer Waterways Experiment Station, Vicksburg, MS.

Crawford, P. L., and Chen, H. S. (1988). "Comparison of numerical and physical models of wave response in a harbor," Miscellaneous Paper CERC-88-11, U.S. Army Engineer Waterways Experiment Station, Vicksburg, MS.

Farrar, P. D., and Chen, H. S. (1987). "Wave response of the proposed harbor at Agat, Guam: Numerical model investigation," Technical Report CERC-87-4, U.S. Army Engineer Waterways Experiment Station, Vicksburg, MS.

Farrar, P. D., and Houston, J. R. (1982). "Tsunami response of Barbers Point Harbor, Hawaii," Miscellaneous Paper HL-82-1, U.S. Army Engineer Waterways Experiment Station, Vicksburg, MS.

Goda, Y. (1985). *Random seas and design of maritime structures.* University of Tokyo Press, Tokyo, Japan.

Harkins, G., Smith, E., McGehee, D., Thompson, E., and Hadley, L. (1996). "Wave response of Kaumalapau Harbor, Lanai, Hawaii," in preparation, U.S. Army Engineer Waterways Experiment Station, Vicksburg, MS.

Hasselmann, K., Barnett, T. P., Bouws, E., Carlson, H., Cartwright, D. E., Enke, K., Ewing, J. A., Gienapp, H., Hasselmann, D. E., Kruseman, D., Meerburg, A., Muller, D., Olberg, D. J., Richter, K., Sell, W., and Walden, H. (1973). "Measurements of wind wave growth and swell decay during the Joint North Sea Wave Project (JONSWAP)," Deutsches Hydrographisches Institut, Hamburg, Germany.

Houston, J. R. (1976). "Long Beach Harbor numerical analysis of harbor oscillation; Report 1, Existing conditions and proposed improvements," Miscellaneous Paper H-76-20, U.S. Army Engineer Waterways Experiment Station, Vicksburg, MS.

_____. (1978). "Interaction of tsunamis with the Hawaiian Islands calculated by a finite-element numerical model," *Journal of Physical Oceanography* 8 (1), 93-101.

_____. (1981). "Combined refraction and diffraction of short waves using the finite element method," *Applied Ocean Research* 3 (4), 163-170.

Houston, J. R., and Garcia, A. W. (1978). "Type 16 flood insurance study: Tsunami predictions for the west coast of the continental United States," Technical Report H-78-26, U.S. Army Engineer Waterways Experiment Station, Vicksburg, MS.

Kaihatu, J. M., Lillycrop, L. S., and Thompson, E. F. (1989). "Effects of entrance channel dredging at Morro Bay, California," Miscellaneous Paper CERC-89-3, U.S. Army Engineer Waterways Experiment Station, Vicksburg, MS.

Lillycrop, L. S., and Boc, S. J. (1992). "Numerical modeling of proposed Kawaihae Harbor, HI." *Proceedings, Coastal Engineering Practice.* American Society of Civil Engineers, 412-24.

Lillycrop, L. S., and Thompson, E. F. (1996). "Harbor wave oscillation model (HARBD) theory and program documentation," *Coastal Modeling System (CMS) User's Manual,* Instruction Report CERC-91-1, M. A. Cialone, ed., U.S. Army Engineer Waterways Experiment Station, Vicksburg, MS.

Lillycrop, L. S., Bratos, S. M., and Thompson, E. F. (1990). "Wave response of proposed improvements to the shallow-draft harbor at Kawaihae, Hawaii," Miscellaneous Paper CERC-90-8, U.S. Army Engineer Waterways Experiment Station, Vicksburg, MS.

Lillycrop, L. S., Bratos, S. M., Thompson, E. F., and Rivers, P. (1993). "Wave response of proposed improvements to the small boat harbor at Maalaea, Maui, Hawaii," Miscellaneous Paper CERC-93-4, U.S. Army Engineer Waterways Experiment Station, Vicksburg, MS.

References

Markle, D. G., and Boc, S. J. (1994). "Periodic inspections of Kahului and Laupahoehoe Breakwaters, Hawaii; Report 1, base conditions," Technical Report CERC-94-12, U.S. Army Engineer Waterways Experiment Station, Vicksburg, MS.

McGehee, D. D. (1995). "Requirement for FY95 wave measurements in Kahului Harbor," Memorandum for Record, U.S. Army Engineer Waterways Experiment Station, Vicksburg, MS.

McGehee, D. D., and McKinney, J. P. "Tsunami detection and warning capability using nearshore submerged pressure transducers; Case study of the 4 October 1994 Shikotan tsunami." *Proceedings, IUGG Tsunami Symposium.* In preparation, Boulder, CO.

Merrifield, M. A., and Okihiro, M. S. "Correlations between infragravity energy at Kahului Harbor and deep ocean wave buoy measurements," in preparation, U.S. Army Engineer Waterways Experiment Station, Vicksburg, MS.

Mesa, C. (1992). "A dual approach to low frequency energy definition in a small craft harbor." *Proceedings, Coastal Engineering Practice.* American Society of Civil Engineers, 400-11.

Okihiro, M. S., and Guza, R. T. (1996). "Observations of seiche forcing and amplification in three small harbors," *J. Waterway, Port, Coastal and Ocean Engineering* 122 (5), 232-238, American Society of Civil Engineers.

Okihiro, M. S., Guza, R. T., O'Reilly, W. C., and McGehee, D. D. (1994). "Selecting wave gauge sites for monitoring harbor oscillations: A case study for Kahului Harbor, Hawaii," Miscellaneous Paper CERC-94-10, U.S. Army Engineer Waterways Experiment Station, Vicksburg, MS.

Permanent International Association of Navigation Congresses. (1995). "Criteria for movements of moored ships in harbours, a practical guide," Report of Working Group No. 24, Supplement to Bulletin No. 88, Brussels, Belgium.

Sargent, F. E. (1989). "Los Angeles - Long Beach Harbor Complex 2020 Plan harbor resonance analysis: Numerical model investigation," Technical Report CERC-89-16, U.S. Army Engineer Waterways Experiment Station, Vicksburg, MS.

Sargent, F. E., Markle, D. G., and Grace, P. J. (1988). "Case histories of Corps breakwater and jetty structures; Report 4, Pacific Ocean Division," Technical Report REMR-CO-3, U.S. Army Engineer Waterways Experiment Station, Vicksburg, MS.

Seabergh, W. C., and Thomas, L. J. (1995). "Los Angeles Harbor Pier 400 harbor resonance model study," Technical Report CERC-95-8, U.S. Army Engineer Waterways Experiment Station, Vicksburg, MS.

Seymour, R., Castel, D., McGehee, D., Thomas, J., and O'Reilly, W. (1993). "New technology in coastal wave monitoring." *Proceedings of the 2nd International Symposuim on Ocean Wave Measurement and Analysis.* American Society of Civil Engineers, 105-123.

Sorensen, R. M. (1993). *Basic wave mechanics for coastal and ocean engineers.* Wiley, New York.

Steele, K. E., and Mettlach, T. (1993). "NDBC wave data - current and planned." *Proceedings of the 2nd International Symposium on Ocean Wave Measurement and Analysis.* American Society of Civil Engineers, 198-207.

Thompson, E. F. (1980). "Energy spectra in shallow U.S. coastal waters," Technical Paper 80-2, U.S. Army Engineer Waterways Experiment Station, Vicksburg, MS.

_____. (1995). "Estimation of peak period in wave data from Kahului Harbor," Memorandum for Record, U.S. Army Engineer Waterways Experiment Station, Vicksburg, MS.

Thompson, E. F., and Hadley, L. L. (1994a). "Wave response of Port Allen Harbor, Kauai, Hawaii" Miscellaneous Paper CERC-94-9, U.S. Army Engineer Waterways Experiment Station, Vicksburg, MS.

_____. (1994b). "Wave response of proposed improvement plan 6 to the small boat harbor at Maalaea, Maui, Hawaii" Miscellaneous Paper CERC-94-17, U.S. Army Engineer Waterways Experiment Station, Vicksburg, MS.

_____. (1995). "Numerical modeling of harbor response to waves," *J. Coastal Research* 11(3), 744-753.

Thompson, E. F., Chen, H. S., and Hadley, L. L. (1993). "Numerical modeling of waves in harbors," *Proceedings, WAVES 93.* American Society of Civil Engineers, 590-601.

_____. (1996). "Validation of a numerical model for wind waves and swell in harbors," *J. Waterway, Port, Coastal and Ocean Engineering* 122 (5), 245-257, American Society of Civil Engineers.

Turner, P. J., and Baptista, A. M. (1993). "ACE/gredit User's Manual," Center for Coastal and Land-Margin Research, Oregon Graduate Institute of Science and Technology, Beaverton, OR.

U.S. Army Corps of Engineers. (1989). "Water levels and wave heights for coastal engineering design," Engineer Manual 1110-2-1414, Washington, DC.

Weishar, L. L., and Aubrey, D. G. (1986). "A study of inlet hydraulics at Green Harbor, Marshfield, Mass.," Miscellaneous Paper CERC 88-10, U.S. Army Engineer Waterways Experiment Station, Vicksburg, MS.

Wilson, B. W. (1967). "The threshold of surge damage for moored ships." *Proceedings of the Institute of Civil Engineers*. London, Vol. 38, 107-132.

Appendix A
Field Data Summary

Table A1
Number of Occurrences of T_p and θ_m Array

T_p (sec)	θ_m (deg azimuth)											
	<190	190-	192-	194-	196-	198-	200-	202-	204-	206-	208-	210-
<8	0	2	1	7	4	3	10	36	43	49	32	33
8-	0	0	1	2	1	10	21	39	42	39	33	14
9-	3	1	0	2	7	16	46	22	35	25	13	6
10-	2	1	3	3	9	19	37	42	36	15	8	4
11-	13	5	12	14	18	27	33	29	26	7	4	2
12-	6	9	3	8	20	24	27	29	17	8	2	0
13-	5	5	3	5	14	12	24	8	8	1	0	8
14-	3	10	25	11	15	19	20	16	4	11	11	2
15-	5	3	5	6	7	7	4	6	7	2	0	6
16-	3	2	3	2	1	16	7	2	5	1	1	0
17-	0	3	7	2	1	1	5	1	2	0	1	0
18-	0	0	2	6	2	5	2	1	1	0	1	1
19-	0	0	0	2	2	7	3	1	0	0	0	0
≥20	0	0	0	0	0	0	0	0	0	0	0	0
Tot.	40	41	65	70	101	166	239	232	226	158	106	76
%	2.2	2.3	3.6	3.9	5.7	9.3	13.4	13.0	12.6	8.8	5.9	4.3

(Continued)

A2

Table A1 (Concluded)

T_p (sec)	θ_m (deg azimuth)										Total	
	212-	214-	216-	218-	220-	222-	224-	226-	228-	≥230	No.	%
<8	11	5	3	1	2	2	1	0	1	10	256	14.3
8-	4	3	5	0	0	1	1	0	0	3	219	12.3
9-	5	3	4	2	0	1	3	0	0	7	201	11.3
10-	3	4	2	3	1	3	4	0	1	4	204	11.4
11-	2	0	4	2	0	3	1	1	1	19	223	12.5
12-	4	4	1	1	2	4	1	1	2	14	187	10.5
13-	0	3	6	0	1	0	2	0	0	11	116	6.5
14-	0	4	1	0	4	2	6	1	0	22	187	10.4
15-	2	0	1	0	1	0	1	0	1	6	70	3.9
16-	1	0	1	0	1	1	0	1	0	9	57	3.2
17-	5	1	0	0	0	0	0	0	0	2	31	1.7
18-	0	0	0	0	0	0	0	0	0	0	21	1.2
19-	0	0	0	0	0	0	0	0	0	0	15	0.8
≥20	0	0	0	0	0	0	0	0	0	0	0	0
Tot.	37	27	28	9	12	17	20	4	6	107	1787	
%	2.1	1.5	1.6	0.5	0.7	1.0	1.1	0.2	0.3	6.0		100.0

NDBC 51026, N. MOLOKAI   (21.37N 156.96W)

NUMBER OF RECORDS WITH HMO BY MONTH FOR 1993 – 1996

YEAR	JAN	FEB	MAR	APR	MAY	JUN	JUL	AUG	SEP	OCT	NOV	DEC	TOTAL
1993	331	574	681	485	0	151	700	686	677	708	700	701	6394
1994	701	591	697	712	172	0	0	0	325	727	701	486	5112
1995	137	646	727	701	733	707	728	727	709	729	703	715	7962
1996	716	680	0	0	0	0	0	0	0	0	0	0	1396

NUMBER OF RECORDS WITH HMO AND Tp BY MONTH FOR 1993 – 1996

YEAR	JAN	FEB	MAR	APR	MAY	JUN	JUL	AUG	SEP	OCT	NOV	DEC	TOTAL
1993	331	574	681	485	0	151	700	686	677	708	700	701	6394
1994	701	591	697	712	172	0	0	0	325	727	701	486	5112
1995	137	646	727	701	733	707	728	727	709	729	703	715	7962
1996	716	680	0	0	0	0	0	0	0	0	0	0	1396

NUMBER OF RECORDS WITH HMO, Tp, AND Dp BY MONTH FOR 1993 – 1996

YEAR	JAN	FEB	MAR	APR	MAY	JUN	JUL	AUG	SEP	OCT	NOV	DEC	TOTAL
1993	331	574	681	485	0	151	700	686	677	708	700	701	6394
1994	701	591	697	712	172	0	0	0	325	727	701	486	5112
1995	137	646	727	701	733	707	728	727	709	729	703	715	7962
1996	716	680	0	0	0	0	0	0	0	0	0	0	1396

MEAN Hm0(METRES) BY MONTH AND YEAR
NDBC BUOY 51026 (21.37 N, 156.96 W)

MONTH

	JAN	FEB	MAR	APR	MAY	JUN	JUL	AUG	SEP	OCT	NOV	DEC		MEAN
YEAR														
1993	2.0	2.9	2.6	2.7	.	1.7	1.9	2.0	1.4	2.1	2.8	3.2		2.3
1994	2.9	2.4	2.9	2.5	2.1	.	.	.	1.6	2.0	2.8	3.1		2.5
1995	2.3	2.2	2.3	2.4	1.8	1.6	1.8	1.9	1.7	2.0	2.3	2.5		2.0
1996	2.4	3.4	.	.	.	.	.	.	.	.	.	.		2.9
MEAN	2.5	2.7	2.6	2.5	1.9	1.6	1.9	1.9	1.6	2.0	2.6	2.9		

LARGEST Hm0(METRES) BY MONTH AND YEAR
NDBC BUOY 51026 (21.37 N, 156.96 W)

MONTH

	JAN	FEB	MAR	APR	MAY	JUN	JUL	AUG	SEP	OCT	NOV	DEC
YEAR												
1993	3.5	6.8	5.0	4.4	.	2.3	4.0	4.7	2.6	3.9	4.8	5.0
1994	5.6	4.6	6.0	4.5	2.6	.	.	.	2.4	3.7	4.8	5.0
1995	4.5	5.5	4.6	4.8	3.4	2.5	2.9	2.8	3.9	3.4	7.3	5.0
1996	5.0	5.9	.	.	.	.	.	.	.	.	.	.

4 YR. STATISTICS FOR NDBC BUOY 51026   (21.37 N, 156.96 W)

THE MEAN SIGNIFICANT WAVE HEIGHT(METRES)=   2.3

THE MEAN PEAK WAVE PERIOD (SECONDS)=   10.7

THE MOST FREQUENT 22.5(CENTER) DIRECTION BAND (DEGREES)=   90.0

THE STANDARD DEVIATION OF Hm0(METRES)=   0.8

THE STANDARD DEVIATION OF TP(SECONDS)=   2.9

THE LARGEST Hm0(METRES)=   7.3

THE TP(SECONDS)ASSOC. WITH THE LARGEST Hm0=   16.7

THE PEAK DIRECTION (DEGREES) ASSOC. WITH THE LARGEST Hm0=   344.0

THE DATE OF LARGEST Hm0 OCCURRENCE IS   95114350

BUOY STATION 51026 21.37 N, 156.96 W   AZIMUTH(DEGREES) = 0.0
PERCENT OCCURRENCE(X1000) OF HEIGHT AND PERIOD BY DIRECTION

HEIGHT(METRES)				PEAK PERIOD(SECONDS)							TOTAL
	<6.9	6.9- 8.0	8.1- 8.7	8.8- 9.5	9.6- 10.5	10.6- 11.7	11.8- 13.3	13.4- 15.3	15.4- 18.1	18.2- LONGER	
0.0-0.9	.	14	23	28	4	14	.	.	.	.	83
1.0-1.9	4	43	186	493	1064	929	464	110	14	4	3311
2.0-2.9	9	28	86	153	301	867	1020	220	71	9	2764
3.0-3.9	.	.	9	23	105	162	522	412	119	.	1352
4.0-4.9	.	.	.	.	9	4	86	115	81	4	299
5.0-5.9	.	.	.	.	.	.	.	.	28	9	37
6.0-6.9	.	.	.	.	.	.	.	.	9	4	13
7.0-7.9	.	.	.	.	.	.	.	.	.	.	0
8.0-8.9	.	.	.	.	.	.	.	.	.	.	0
9.0-9.9	.	.	.	.	.	.	.	.	.	.	0
10.0+	.	.	.	.	.	.	.	.	.	.	0
TOTAL	13	85	304	697	1483	1976	2092	857	322	30	

MEAN Hm0(M) = 2.3 LARGEST Hm0(M) = 6.3 MEAN TP(SEC)= 11.5 NO. OF CASES= 1645.

BUOY STATION 51026 21.37 N, 156.96 W   AZIMUTH(DEGREES) = 22.5
PERCENT OCCURRENCE(X1000) OF HEIGHT AND PERIOD BY DIRECTION

HEIGHT(METRES)				PEAK PERIOD(SECONDS)							TOTAL
	<6.9	6.9- 8.0	8.1- 8.7	8.8- 9.5	9.6- 10.5	10.6- 11.7	11.8- 13.3	13.4- 15.3	15.4- 18.1	18.2- LONGER	
0.0-0.9	.	23	38	14	38	.	.	.	.	.	113
1.0-1.9	4	76	268	680	824	311	67	.	.	.	2230
2.0-2.9	19	138	167	186	258	532	560	76	14	.	1950
3.0-3.9	4	9	43	206	162	110	158	158	23	.	873
4.0-4.9	.	.	.	.	28	.	.	33	67	.	128
5.0-5.9	.	.	.	.	.	.	.	.	19	14	33
6.0-6.9	.	.	.	.	.	.	.	.	.	.	0
7.0-7.9	.	.	.	.	.	.	.	.	.	.	0
8.0-8.9	.	.	.	.	.	.	.	.	.	.	0
9.0-9.9	.	.	.	.	.	.	.	.	.	.	0
10.0+	.	.	.	.	.	.	.	.	.	.	0
TOTAL	27	246	516	1086	1310	953	785	267	123	14	

MEAN Hm0(M) = 2.2 LARGEST Hm0(M)= 5.8 MEAN TP(SEC)= 10.5 NO. OF CASES= 1115.

BUOY STATION 51026 21.37 N, 156.96 W   AZIMUTH(DEGREES) = 45.0
PERCENT OCCURRENCE(X1000) OF HEIGHT AND PERIOD BY DIRECTION

HEIGHT(METRES)				PEAK PERIOD(SECONDS)							TOTAL
	<6.9	6.9-8.0	8.1-8.7	8.8-9.5	9.6-10.5	10.6-11.7	11.8-13.3	13.4-15.3	15.4-18.1	18.2-LONGER	
0.0-0.9	.	38	86	100	23	.	.	.	.	.	247
1.0-1.9	95	690	666	949	642	162	9	9	9	.	3231
2.0-2.9	67	474	517	661	522	340	67	71	14	.	2733
3.0-3.9	4	71	148	268	258	19	4	.	.	.	772
4.0-4.9	.	4	.	23	19	38	4	23	.	.	111
5.0-5.9	.	.	.	.	9	23	.	.	.	.	32
6.0-6.9	.	.	.	.	.	.	.	.	.	.	0
7.0-7.9	.	.	.	.	.	.	.	.	.	.	0
8.0-8.9	.	.	.	.	.	.	.	.	.	.	0
9.0-9.9	.	.	.	.	.	.	.	.	.	.	0
10.0+	.	.	.	.	.	.	.	.	.	.	0
TOTAL	166	1277	1417	2001	1473	582	84	103	23	0	

MEAN Hm0(M) = 2.1   LARGEST Hm0(M)=   5.2 MEAN TP(SEC)= 9.1 NO. OF CASES=   1491.

BUOY STATION 51026 21.37 N, 156.96 W   AZIMUTH(DEGREES) = 67.5
PERCENT OCCURRENCE(X1000) OF HEIGHT AND PERIOD BY DIRECTION

HEIGHT(METRES)				PEAK PERIOD(SECONDS)							TOTAL
	<6.9	6.9-8.0	8.1-8.7	8.8-9.5	9.6-10.5	10.6-11.7	11.8-13.3	13.4-15.3	15.4-18.1	18.2-LONGER	
0.0-0.9	23	76	71	33	.	.	.	.	.	.	203
1.0-1.9	1318	3168	2367	1433	450	210	4	.	.	.	8950
2.0-2.9	416	1787	2276	1974	637	100	33	4	.	.	7227
3.0-3.9	.	134	273	632	508	67	23	9	.	.	1646
4.0-4.9	.	.	14	105	287	292	33	19	.	.	750
5.0-5.9	.	.	.	4	33	76	.	.	.	.	113
6.0-6.9	.	.	.	.	.	.	.	.	.	.	0
7.0-7.9	.	.	.	.	.	.	.	.	.	.	0
8.0-8.9	.	.	.	.	.	.	.	.	.	.	0
9.0-9.9	.	.	.	.	.	.	.	.	.	.	0
10.0+	.	.	.	.	.	.	.	.	.	.	0
TOTAL	1757	5165	5001	4181	1915	745	93	32	0	0	

MEAN Hm0(M) = 2.2   LARGEST Hm0(M)=   6.0 MEAN TP(SEC)= 8.4 NO. OF CASES=   3945.

HEIGHT(METRES)   PEAK PERIOD(SECONDS)   TOTAL

	<6.9	6.9-8.0	8.1-8.7	8.8-9.5	9.6-10.5	10.6-11.7	11.8-13.3	13.4-15.3	15.4-18.1	18.2-LONGER	TOTAL
0.0-0.9	81	81	105	28	.	4	.	.	.	.	299
1.0-1.9	1615	3091	3589	2175	282	402	206	4	.	.	11364
2.0-2.9	493	1615	2324	3311	1926	287	9	9	28	.	10002
3.0-3.9	4	81	263	661	1231	579	38	91	47	.	2995
4.0-4.9	.	.	4	14	244	369	19	28	.	.	678
5.0-5.9	.	.	.	.	.	.	.	.	.	.	0
6.0-6.9	.	.	.	.	.	.	.	.	.	.	0
7.0-7.9	.	.	.	.	.	.	.	.	.	.	0
8.0-8.9	.	.	.	.	.	.	.	.	.	.	0
9.0-9.9	.	.	.	.	.	.	.	.	.	.	0
10.0+	.	.	.	.	.	.	.	.	.	.	0
TOTAL	2193	4868	6285	6189	3683	1641	272	132	75	0	

MEAN Hm0(M) = 2.2   LARGEST Hm0(M) =   4.9   MEAN TP(SEC) = 8.7   NO. OF CASES=   5291.

HEIGHT(METRES)   PEAK PERIOD(SECONDS)   TOTAL

	<6.9	6.9-8.0	8.1-8.7	8.8-9.5	9.6-10.5	10.6-11.7	11.8-13.3	13.4-15.3	15.4-18.1	18.2-LONGER	TOTAL
0.0-0.9	.	.	.	.	.	4	.	.	.	.	4
1.0-1.9	47	28	23	38	4	4	43	.	.	.	187
2.0-2.9	.	19	4	62	62	19	.	.	.	.	166
3.0-3.9	.	.	.	.	9	.	.	.	.	.	9
4.0-4.9	.	.	.	.	.	.	.	.	.	.	0
5.0-5.9	.	.	.	.	.	.	.	.	.	.	0
6.0-6.9	.	.	.	.	.	.	.	.	.	.	0
7.0-7.9	.	.	.	.	.	.	.	.	.	.	0
8.0-8.9	.	.	.	.	.	.	.	.	.	.	0
9.0-9.9	.	.	.	.	.	.	.	.	.	.	0
10.0+	.	.	.	.	.	.	.	.	.	.	0
TOTAL	47	47	27	100	75	27	43	0	0	0	

MEAN Hm0(M) = 2.0   LARGEST Hm0(M) =   3.6   MEAN TP(SEC) = 9.1   NO. OF CASES=   78.

BUOY STATION 51026 21.37 N, 156.96 W   AZIMUTH(DEGREES) =135.0
PERCENT OCCURRENCE(X1000) OF HEIGHT AND PERIOD BY DIRECTION

HEIGHT (METRES)				PEAK PERIOD (SECONDS)							TOTAL
	<6.9	6.9-8.0	8.1-8.7	8.8-9.5	9.6-10.5	10.6-11.7	11.8-13.3	13.4-15.3	15.4-18.1	18.2-LONGER	
0.0-0.9	.	.	.	.	.	.	.	.	.	.	0
1.0-1.9	.	.	.	.	.	.	.	.	.	.	0
2.0-2.9	.	.	.	.	.	.	.	.	.	4	4
3.0-3.9	.	.	.	.	.	.	.	.	.	4	4
4.0-4.9	.	.	.	.	.	.	.	.	.	.	0
5.0-5.9	.	.	.	.	.	.	.	.	.	.	0
6.0-6.9	.	.	.	.	.	.	.	.	.	.	0
7.0-7.9	.	.	.	.	.	.	.	.	.	.	0
8.0-8.9	.	.	.	.	.	.	.	.	.	.	0
9.0-9.9	.	.	.	.	.	.	.	.	.	.	0
10.0+	.	.	.	.	.	.	.	.	.	.	0
TOTAL	0	0	0	0	0	0	0	0	0	8	

MEAN Hm0(M) = 3.1 LARGEST Hm0(M) = 3.5 MEAN TP(SEC)= 22.5 NO. OF CASES=   2.

BUOY STATION 51026 21.37 N, 156.96 W   AZIMUTH(DEGREES) =157.5
PERCENT OCCURRENCE(X1000) OF HEIGHT AND PERIOD BY DIRECTION

HEIGHT (METRES)				PEAK PERIOD (SECONDS)							TOTAL
	<6.9	6.9-8.0	8.1-8.7	8.8-9.5	9.6-10.5	10.6-11.7	11.8-13.3	13.4-15.3	15.4-18.1	18.2-LONGER	
0.0-0.9	.	.	.	.	.	.	.	.	.	.	0
1.0-1.9	.	.	.	.	.	.	.	.	.	.	0
2.0-2.9	.	.	.	.	.	.	.	.	.	.	0
3.0-3.9	.	.	.	.	.	.	.	.	.	.	0
4.0-4.9	.	.	.	.	.	.	.	.	.	.	0
5.0-5.9	.	.	.	.	.	.	.	.	.	.	0
6.0-6.9	.	.	.	.	.	.	.	.	.	.	0
7.0-7.9	.	.	.	.	.	.	.	.	.	.	0
8.0-8.9	.	.	.	.	.	.	.	.	.	.	0
9.0-9.9	.	.	.	.	.	.	.	.	.	.	0
10.0+	.	.	.	.	.	.	.	.	.	.	0
TOTAL	0	0	0	0	0	0	0	0	0	0	

MEAN Hm0(M) = 0.0 LARGEST Hm0(M) = 0.0 MEAN TP(SEC)= 0.0 NO. OF CASES=   0.

BUOY STATION 51026   21.37 N, 156.96 W   AZIMUTH(DEGREES) =180.0
PERCENT OCCURRENCE(X1000) OF HEIGHT AND PERIOD BY DIRECTION

HEIGHT(METRES)   PEAK PERIOD(SECONDS)   TOTAL

	<6.9	6.9-8.0	8.1-8.7	8.8-9.5	9.6-10.5	10.6-11.7	11.8-13.3	13.4-15.3	15.4-18.1	18.2-LONGER	
0.0-0.9	.	.	.	.	.	.	.	.	.	.	0
1.0-1.9	.	.	.	.	.	.	.	.	.	.	0
2.0-2.9	.	.	.	.	.	.	.	.	.	.	0
3.0-3.9	.	.	.	.	.	.	.	.	.	.	0
4.0-4.9	.	.	.	.	.	.	.	.	.	.	0
5.0-5.9	.	.	.	.	.	.	.	.	.	.	0
6.0-6.9	.	.	.	.	.	.	.	.	.	.	0
7.0-7.9	.	.	.	.	.	.	.	.	.	.	0
8.0-8.9	.	.	.	.	.	.	.	.	.	.	0
9.0-9.9	.	.	.	.	.	.	.	.	.	.	0
10.0+	.	.	.	.	.	.	.	.	.	.	0
TOTAL	0	0	0	0	0	0	0	0	0	0	

MEAN Hm0(M) = 0.0   LARGEST Hm0(M) = 0.0   MEAN TP(SEC) = 0.0   NO. OF CASES=   0.

BUOY STATION 51026   21.37 N, 156.96 W   AZIMUTH(DEGREES) =202.5
PERCENT OCCURRENCE(X1000) OF HEIGHT AND PERIOD BY DIRECTION

HEIGHT(METRES)   PEAK PERIOD(SECONDS)   TOTAL

	<6.9	6.9-8.0	8.1-8.7	8.8-9.5	9.6-10.5	10.6-11.7	11.8-13.3	13.4-15.3	15.4-18.1	18.2-LONGER	
0.0-0.9	.	.	.	.	.	.	.	.	.	.	0
1.0-1.9	.	.	.	.	.	.	.	.	.	.	0
2.0-2.9	.	.	.	.	.	.	.	.	.	.	0
3.0-3.9	.	.	.	.	.	.	.	.	.	.	0
4.0-4.9	.	.	.	.	.	.	.	.	.	.	0
5.0-5.9	.	.	.	.	.	.	.	.	.	.	0
6.0-6.9	.	.	.	.	.	.	.	.	.	.	0
7.0-7.9	.	.	.	.	.	.	.	.	.	.	0
8.0-8.9	.	.	.	.	.	.	.	.	.	.	0
9.0-9.9	.	.	.	.	.	.	.	.	.	.	0
10.0+	.	.	.	.	.	.	.	.	.	.	0
TOTAL	0	0	0	0	0	0	0	0	0	0	

MEAN Hm0(M) = 0.0   LARGEST Hm0(M) = 0.0   MEAN TP(SEC) = 0.0   NO. OF CASES=   0.

BUOY STATION 51026   21.37 N, 156.96 W   AZIMUTH(DEGREES) =225.0
PERCENT OCCURRENCE(X1000) OF HEIGHT AND PERIOD BY DIRECTION

HEIGHT(METRES)				PEAK PERIOD(SECONDS)							TOTAL
	<6.9	6.9-8.0	8.1-8.7	8.8-9.5	9.6-10.5	10.6-11.7	11.8-13.3	13.4-15.3	15.4-18.1	18.2-LONGER	
0.0-0.9	.	.	.	.	.	.	.	.	.	.	0
1.0-1.9	.	4	.	4	.	.	. .	.	.	4	12
2.0-2.9	.	.	.	.	.	.	.	.	.	.	0
3.0-3.9	.	.	.	.	.	.	.	.	.	.	0
4.0-4.9	.	.	.	.	.	.	.	.	.	.	0
5.0-5.9	.	.	.	.	.	.	.	.	.	.	0
6.0-6.9	.	.	.	.	.	.	.	.	.	.	0
7.0-7.9	.	.	.	.	.	.	.	.	.	.	0
8.0-8.9	.	.	.	.	.	.	.	.	.	.	0
9.0-9.9	.	.	.	.	.	.	.	.	.	.	0
10.0+	.	.	.	.	.	.	.	.	.	.	0
TOTAL	0	4	0	4	0	0	0	0	0	4	

MEAN Hm0(M) = 1.4   LARGEST Hm0(M) =   1.7   MEAN TP(SEC)= 12.1   NO. OF CASES=   3.

BUOY STATION 51026   21.37 N, 156.96 W   AZIMUTH(DEGREES) =247.5
PERCENT OCCURRENCE(X1000) OF HEIGHT AND PERIOD BY DIRECTION

HEIGHT(METRES)				PEAK PERIOD(SECONDS)							TOTAL
	<6.9	6.9-8.0	8.1-8.7	8.8-9.5	9.6-10.5	10.6-11.7	11.8-13.3	13.4-15.3	15.4-18.1	18.2-LONGER	
0.0-0.9	.	.	.	.	.	.	.	.	.	.	0
1.0-1.9	.	14	4	4	.	.	.	.	4	.	26
2.0-2.9	.	.	.	.	.	.	.	.	.	.	0
3.0-3.9	.	.	.	.	.	.	.	.	.	.	0
4.0-4.9	.	.	.	.	.	.	.	.	.	.	0
5.0-5.9	.	.	.	.	.	.	.	.	.	.	0
6.0-6.9	.	.	.	.	.	.	.	.	.	.	0
7.0-7.9	.	.	.	.	.	.	.	.	.	.	0
8.0-8.9	.	.	.	.	.	.	.	.	.	.	0
9.0-9.9	.	.	.	.	.	.	.	.	.	.	0
10.0+	.	.	.	.	.	.	.	.	.	.	0
TOTAL	0	14	4	4	0	0	0	0	4	0	

MEAN Hm0(M) = 1.3   LARGEST Hm0(M) =   1.9   MEAN TP(SEC)= 9.4   NO. OF CASES=   6.

BUOY STATION 51026 21.37 N, 156.96 W   AZIMUTH(DEGREES) =270.0
PERCENT OCCURRENCE(X1000) OF HEIGHT AND PERIOD BY DIRECTION

HEIGHT(METRES)				PEAK PERIOD(SECONDS)						TOTAL
	<6.9	6.9- 8.0	8.1- 8.7	8.8- 9.5	9.6- 10.5	10.6- 11.7	11.8- 13.3	13.4- 15.3	15.4- 18.1	18.2- LONGER	
0.0-0.9	.	.	4	.	.	.	4	.	.	.	8
1.0-1.9	.	.	.	4	.	4	14	.	.	4	26
2.0-2.9	.	.	.	.	.	.	.	4	.	.	4
3.0-3.9	.	.	.	.	.	.	.	.	.	.	0
4.0-4.9	.	.	.	.	.	.	.	.	.	.	0
5.0-5.9	.	.	.	.	.	.	.	.	.	.	0
6.0-6.9	.	.	.	.	.	.	.	.	.	.	0
7.0-7.9	.	.	.	.	.	.	.	.	.	.	0
8.0-8.9	.	.	.	.	.	.	.	.	.	.	0
9.0-9.9	.	.	.	.	.	.	.	.	.	.	0
10.0+	.	.	.	.	.	.	.	.	.	.	0
TOTAL	0	0	4	4	0	4	18	4	0	4	

MEAN Hm0(M) = 1.4 LARGEST Hm0(M)= 2.9 MEAN TP(SEC)= 12.5 NO. OF CASES= 9.

BUOY STATION 51026 21.37 N, 156.96 W   AZIMUTH(DEGREES) =292.5
PERCENT OCCURRENCE(X1000) OF HEIGHT AND PERIOD BY DIRECTION

HEIGHT(METRES)				PEAK PERIOD(SECONDS)						TOTAL
	<6.9	6.9- 8.0	8.1- 8.7	8.8- 9.5	9.6- 10.5	10.6- 11.7	11.8- 13.3	13.4- 15.3	15.4- 18.1	18.2- LONGER	
0.0-0.9	.	.	.	:	9	9	9	9	.	.	36
1.0-1.9	.	.	.	.	38	86	282	225	86	38	755
2.0-2.9	.	.	.	.	19	91	138	273	254	76	851
3.0-3.9	.	.	.	.	.	.	19	105	124	28	276
4.0-4.9	.	.	.	.	.	.	.	.	62	9	71
5.0-5.9	.	.	.	.	.	.	.	.	.	.	0
6.0-6.9	.	.	.	.	.	.	.	.	.	.	0
7.0-7.9	.	.	.	.	.	.	.	.	.	.	0
8.0-8.9	.	.	.	.	.	.	.	.	.	.	0
9.0-9.9	.	.	.	.	.	.	.	.	.	.	0
10.0+	.	.	.	.	.	.	.	.	.	.	0
TOTAL	0	0	0	0	66	186	448	612	526	151	

MEAN Hm0(M) = 2.3 LARGEST Hm0(M)= 4.9 MEAN TP(SEC)= 14.5 NO. OF CASES= 417.

A12

BUOY STATION 51026   21.37 N, 156.96 W   AZIMUTH(DEGREES) =315.0
PERCENT OCCURRENCE(X1000) OF HEIGHT AND PERIOD BY DIRECTION

HEIGHT(METRES)   PEAK PERIOD(SECONDS)   TOTAL

	<6.9	6.9-8.0	8.1-8.7	8.8-9.5	9.6-10.5	10.6-11.7	11.8-13.3	13.4-15.3	15.4-18.1	18.2-LONGER	TOTAL
0.0-0.9	.	.	4	.	28	38	14	.	.	.	84
1.0-1.9	.	.	23	110	273	1073	1744	1068	349	86	4726
2.0-2.9	23	9	14	38	100	388	1816	2664	1380	306	6738
3.0-3.9	.	.	9	9	28	76	325	1289	1279	292	3307
4.0-4.9	.	.	.	.	.	.	57	215	532	23	827
5.0-5.9	.	.	.	.	.	.	.	9	43	.	52
6.0-6.9	.	.	.	.	.	.	.	.	.	.	0
7.0-7.9	.	.	.	.	.	.	.	.	.	.	0
8.0-8.9	.	.	.	.	.	.	.	.	.	.	0
9.0-9.9	.	.	.	.	.	.	.	.	.	.	0
10.0+	.	.	.	.	.	.	.	.	.	.	0
TOTAL	23	9	50	157	429	1575	3956	5245	3583	707	

MEAN Hm0(M) = 2.5 LARGEST Hm0(M)= 5.5 MEAN TP(SEC)= 14.1 NO. OF CASES= 3287.

BUOY STATION 51026   21.37 N, 156.96 W   AZIMUTH(DEGREES) =337.5
PERCENT OCCURRENCE(X1000) OF HEIGHT AND PERIOD BY DIRECTION

HEIGHT(METRES)   PEAK PERIOD(SECONDS)   TOTAL

	<6.9	6.9-8.0	8.1-8.7	8.8-9.5	9.6-10.5	10.6-11.7	11.8-13.3	13.4-15.3	15.4-18.1	18.2-LONGER	TOTAL
0.0-0.9	.	14	.	4	43	9	4	.	.	.	74
1.0-1.9	.	.	23	364	925	1878	1653	354	95	28	5320
2.0-2.9	4	43	43	71	182	977	2856	2008	555	129	6868
3.0-3.9	.	9	4	23	62	277	819	1759	642	95	3690
4.0-4.9	.	.	.	.	.	28	158	369	349	9	913
5.0-5.9	.	.	.	.	.	4	28	28	81	4	145
6.0-6.9	.	.	.	.	.	.	.	.	86	4	90
7.0-7.9	.	.	.	.	.	.	.	.	9	.	9
8.0-8.9	.	.	.	.	.	.	.	.	.	.	0
9.0-9.9	.	.	.	.	.	.	.	.	.	.	0
10.0+	.	.	.	.	.	.	.	.	.	.	0
TOTAL	4	66	70	462	1212	3173	5518	4518	1817	269	

MEAN Hm0(M) = 2.5 LARGEST Hm0(M)= 7.3 MEAN TP(SEC)= 13.0 NO. OF CASES= 3575.

Appendix A Field Data Summary   A13

BUOY STATION 51026 21.37 N, 156.96 W   FOR ALL DIRECTIONS
PERCENT OCCURRENCE(X1000) OF HEIGHT AND PERIOD

HEIGHT(METRES)				PEAK PERIOD(SECONDS)						TOTAL
	<6.9	6.9-8.0	8.1-8.7	8.8-9.5	9.6-10.5	10.6-11.7	11.8-13.3	13.4-15.3	15.4-18.1	18.2-LONGER	
0.0-0.9	105	249	335	210	148	81	33	9	.	.	1170
1.0-1.9	3086	7117	7155	6259	4505	5066	4490	1773	560	167	40178
2.0-2.9	1035	4117	5435	6460	4011	3604	6504	5334	2319	527	39346
3.0-3.9	14	306	752	1826	2367	1294	1912	3824	2238	421	14954
4.0-4.9	.	4	19	143	589	733	359	805	1092	47	3791
5.0-5.9	.	.	.	4	43	105	28	38	172	28	418
6.0-6.9	.	.	.	.	.	.	.	.	95	9	104
7.0-7.9	.	.	.	.	.	.	.	.	9	.	9
8.0-8.9	.	.	.	.	.	.	.	.	.	.	0
9.0-9.9	.	.	.	.	.	.	.	.	.	.	0
10.0+	.	.	.	.	.	.	.	.	.	.	0
TOTAL	4240	11793	13696	14902	11663	10883	13326	11783	6485	1199	

MEAN Hm0 (M) = 2.3   LARGEST Hm0 (M) = 7.3   MEAN TP (SEC) = 10.7   TOTAL CASES= 20864.

Appendix B
Means and Standard Deviations of $A_{amp,s}$ from Field Wave Gages

---

Table B1
Mean $A_{amp,s}$, Nov 93-Sep 94, Pier 2 (Only Cases with 8 or More Observations are Shown)

T_p (sec)	θ_m (deg going toward, referenced to true north)					
	<195	195-205	205-215	215-225	225-235	235-245
< 8		0.07	0.08	0.09		
8-9		0.07	0.07	0.07		
9-10	0.12	0.10	0.10			
10-11	0.10	0.09	0.09	0.08		0.10
11-12	0.09	0.09	0.09	0.10		
12-13	0.09	0.08	0.08	0.10	0.10	
13-14	0.09	0.08	0.08	0.08		
14-15	0.09	0.07	0.07	0.08		
15-16		0.07	0.07	0.07		
16-17	0.14	0.11	0.12			
17-18	0.11	0.10				
18-19		0.09				
19-20		0.09				
20-21						
>21						

Table B2
Mean $A_{amp,s}$, Nov 93-Sep 94, Canoe Club (Only Cases with 8 or More Observations are Shown)

T_p (sec)	θ_m (deg going toward, referenced to true north)					
	<195	195-205	205-215	215-225	225-235	235-245
< 8		0.23	0.23	0.24		
8-9		0.23	0.22	0.23		
9-10	0.30	0.26	0.28			
10-11	0.30	0.26	0.28	0.26		0.30
11-12	0.31	0.27	0.29	0.31		
12-13	0.30	0.25	0.26	0.28	0.31	
13-14	0.31	0.24	0.25	0.30		
14-15	0.31	0.25	0.25	0.27		
15-16		0.24	0.24	0.25		
16-17	0.32	0.26	0.25			
17-18	0.31	0.26				
18-19		0.30				
19-20		0.30				
20-21						
>21						

Table B3
Mean $A_{amp,s}$, Nov 93-Sep 94, Back Basin (Only Cases with 8 or More Observations are Shown)

T_p (sec)	θ_m (deg going toward, referenced to true north)					
	<195	195-205	205-215	215-225	225-235	235-245
< 8		0.26	0.25	0.25		
8-9		0.24	0.23	0.25		
9-10	0.33	0.28	0.27			
10-11	0.32	0.28	0.28	0.28		0.31
11-12	0.35	0.29	0.31	0.33		
12-13	0.33	0.27	0.26	0.31	0.33	
13-14	0.34	0.26	0.26	0.33		
14-15	0.33	0.25	0.24	0.27		
15-16		0.25	0.24	0.25		
16-17	0.35	0.26	0.26			
17-18	0.32	0.29				
18-19		0.29				
19-20		0.30				
20-21						
>21						

Table B4
Mean $A_{amp,s}$, Nov 93-Sep 94, Channel Entrance (Only Cases with 8 or More Observations are Shown)

T_p (sec)	θ_m (deg going toward, referenced to true north)					
	<195	195-205	205-215	215-225	225-235	235-245
< 8		0.68	0.76	0.78		
8-9		0.66	0.71	0.65		
9-10	0.66	0.69	0.73			
10-11	0.62	0.67	0.74	0.74		0.69
11-12	0.57	0.65	0.69	0.68		
12-13	0.59	0.63	0.71	0.69	0.73	
13-14	0.62	0.64	0.66	0.62		
14-15	0.66	0.68	0.72	0.71		
15-16		0.67	0.72	0.67		
16-17	0.66	0.66	0.69			
17-18	0.61	0.66				
18-19		0.62				
19-20		0.67				
20-21						
>21						

T_p (sec)	θ_m (deg going toward, referenced to true north)					
	<195	195-205	205-215	215-225	225-235	235-245
< 8		0.01	0.01	0.01		
8-9		0.01	0.01	0.00		
9-10	0.01	0.02	0.01			
10-11	0.02	0.01	0.02	0.01		0.01
11-12	0.01	0.01	0.01	0.01		
12-13	0.01	0.01	0.01	0.01	0.01	
13-14	0.01	0.01	0.01	0.01		
14-15	0.00	0.01	0.01	0.01		
15-16		0.01	0.01	0.01		
16-17	0.02	0.02	0.02			
17-18	0.02	0.01				
18-19		0.01				
19-20		0.01				
20-21						
>21						

Table B5
Standard Deviation of $A_{amp,s}$, Nov 93-Sep 94, Pier 2 (Only Cases with 8 or More Observations are Shown)

Table B6
Standard Deviation of $A_{amp,s}$, Nov 93-Sep 94, Canoe Club (Only Cases with 8 or More Observations are Shown)

T_p (sec)	θ_m (deg going toward, referenced to true north)					
	<195	195-205	205-215	215-225	225-235	235-245
< 8		0.02	0.02	0.02		
8-9		0.02	0.02	0.02		
9-10	0.02	0.03	0.04			
10-11	0.04	0.03	0.05	0.02		0.02
11-12	0.04	0.04	0.05	0.04		
12-13	0.04	0.03	0.04	0.05	0.05	
13-14	0.05	0.03	0.03	0.06		
14-15	0.04	0.02	0.02	0.04		
15-16		0.02	0.02	0.02		
16-17	0.03	0.04	0.04			
17-18	0.04	0.01				
18-19		0.05				
19-20		0.04				
20-21						
>21						

Table B7
Standard Deviation of $A_{amp,s}$ Nov 93-Sep 94, Back Basin (Only Cases with 8 or More Observations are Shown)

T_p (sec)	θ_m (deg going toward, referenced to true north)					
	<195	195-205	205-215	215-225	225-235	235-245
< 8		0.03	0.08	0.02		
8-9		0.02	0.02	0.03		
9-10	0.03	0.03	0.04			
10-11	0.04	0.04	0.05	0.04		0.04
11-12	0.04	0.04	0.05	0.03		
12-13	0.03	0.04	0.04	0.05	0.04	
13-14	0.04	0.03	0.04	0.06		
14-15	0.02	0.03	0.03	0.04		
15-16		0.03	0.02	0.02		
16-17	0.03	0.04	0.06			
17-18	0.03	0.01				
18-19		0.03				
19-20		0.02				
20-21						
>21						

Table B8
Standard Deviation of $A_{amp,s}$ Nov 93-Sep 94, Channel Entrance
(Only Cases with 8 or More Observations are Shown)

T_p (sec)	θ_m (deg going toward, referenced to true north)					
	<195	195-205	205-215	215-225	225-235	235-245
< 8		0.06	0.07	0.05		
8-9		0.05	0.05	0.06		
9-10	0.08	0.06	0.07			
10-11	0.06	0.08	0.06	0.04		0.05
11-12	0.07	0.08	0.06	0.10		
12-13	0.04	0.07	0.05	0.09	0.08	
13-14	0.07	0.05	0.07	0.05		
14-15	0.08	0.05	0.05	0.05		
15-16		0.05	0.04	0.03		
16-17	0.08	0.03	0.01			
17-18	0.05	0.02				
18-19		0.03				
19-20		0.05				
20-21						
>21						

Appendix C
Summary Tables of Extreme Events of H_s and $H_{s,long}$

Table C1
Extreme Short Wave Cases (Observations with H_s Greater Than 200 cm at Array)

Date	Array $H_{s,long}$ (cm)	$T_{p,long}$ (sec)	H_s (cm)	T_p (sec)	θ_m (deg)	N_p	Water Level	Pier 2 $H_{s,long}$ (cm)	$T_{p,long}$ (sec)	H_s (cm)	T_p (sec)	$A_{amp,l}$	$A_{amp,s}$
0100 10 Nov 93	25.2	158	284	14.1	206	1	433	29.1	178	26.5	13.9	1.15	0.09
0400 10 Nov 93	30.2	67	300	13.8	198	1	452	30.2	210	28.3	13.9	1.00	0.09
0700 10 Nov 93	26.5	64	296	13.7	224	1	431	25.9	195	26.6	13.9	0.98	0.09
1000 10 Nov 93	24.9	56	283	13.5	202	1	426	23.1	210	23.4	13.9	0.93	0.08
1300 10 Nov 93	21.6	64	270	13.0	201	1	449	19.9	191	22.1	13.2	0.92	0.08
1600 10 Nov 93	19.2	67	255	12.4	203	1	444	21.0	178	23.7	12.9	1.09	0.09
1900 10 Nov 93	19.4	1638	257	12.1	199	1	404	18.9	191	21.3	11.9	0.97	0.08
2200 10 Nov 93	19.7	65	257	11.9	201	1	399	19.0	178	19.1	11.9	0.96	0.07
0100 11 Nov 93	17.9	1638	248	12.0	198	1	438	22.1	195	22.5	12.0	1.23	0.09
0400 11 Nov 93	15.4	65	223	12.1	199	1	466	19.8	178	17.3	12.2	1.29	0.08
0700 11 Nov 93	15.1	1638	226	11.9	202	1	443	19.1	178	17.4	11.7	1.26	0.08
1000 11 Nov 93	13.6	1638	225	11.8	197	1	421	15.6	182	18.7	11.7	1.15	0.08
0100 12 Nov 93	12.8	1365	201	11.3	...	...	...	...	...	...	...	...	...
0400 12 Nov 93	14.4	1638	202	11.5	200	1	473	17.3	178	15.9	11.9	1.20	0.08
0700 12 Nov 93	15.0	1365	210	11.9	202	1	458	16.7	1365	15.0	12.0	1.11	0.07
2200 23 Nov 93	9.9	2048	219	9.0	197	1	413	10.4	1170	17.1	3.3	1.05	0.08
1000 24 Nov 93	13.6	1638	211	11.6	196	1	431	17.9	191	18.6	11.7	1.32	0.09
1300 24 Nov 93	14.4	1638	212	12.1	198	1	441	17.0	1638	19.8	11.6	1.18	0.09
1600 24 Nov 93	15.2	1638	223	12.0	196	1	431	17.3	910	18.8	11.6	1.14	0.08
1900 24 Nov 93	15.4	1365	226	12.0	199	1	402	16.3	1170	18.1	11.7	1.06	0.08
2200 24 Nov 93	14.5	1024	218	11.7	199	1	404	17.0	182	18.1	11.8	1.17	0.08

(Sheet 1 of 3)

Table C1 (Continued)

Date	Array						Water Level	Pier 2					
	$H_{s,long}$ (cm)	$T_{p,long}$ (sec)	H_s (cm)	T_p (sec)	θ_m (deg)	N_p		$H_{s,long}$ (cm)	$T_{p,long}$ (sec)	H_s (cm)	T_p (sec)	$A_{amp,l}$	$A_{amp,s}$
1600 25 Nov 93	15.0	61	210	11.6	195	1	437	17.1	819	19.5	11.6	1.14	0.09
1900 25 Nov 93	18.8	57	250	12.2	195	1	408	18.5	186	21.8	11.8	0.98	0.09
2200 25 Nov 93	20.7	63	265	12.4	215	1	401	20.0	182	26.3	12.0	0.96	0.10
0100 26 Nov 93	18.6	72	256	12.2	200	1	437	19.5	910	22.7	11.8	1.05	0.09
0400 26 Nov 93	18.5	1638	264	12.2	197	1	467	19.3	1638	21.3	12.1	1.04	0.08
0700 26 Nov 93	15.1	1365	224	12.1	201	1	451	18.3	819	19.8	11.7	1.21	0.09
1000 26 Nov 93	12.6	1638	206	11.4	200	1	429	12.8	200	18.7	11.6	1.02	0.09
1900 26 Nov 93	11.5	1638	200	11.0	199	1	407	12.0	178	13.9	11.8	1.04	0.07
2200 26 Nov 93	12.1	1638	204	10.8	200	1	394	13.9	1365	13.6	11.7	1.14	0.07
0100 27 Nov 93	10.3	1638	200	11.0	200	1	432	11.3	910	17.1	11.5	1.10	0.09
1900 11 Dec 93	16.1	1638	201	15.0	197	1	406	18.1	216	15.9	14.1	1.12	0.08
0400 3 Jan 94	19.2	303	204	15.6	194	1	424	25.9	745	27.2	16.7	1.35	0.13
0700 3 Jan 94	18.6	1638	209	15.1	190	1	452	28.5	178	23.3	15.9	1.53	0.11
1300 3 Jan 94	20.5	167	212	14.8	194	1	429	32.9	819	25.0	15.8	1.60	0.12
1000 20 Jan 94	14.4	1170	243	9.9	202	1	443	17.7	1365	14.0	9.9	1.23	0.06
1300 20 Jan 94	19.3	4096	247	10.1	202	1	434	18.3	182	15.1	17.1	0.95	0.06
1600 20 Jan 94	14.6	1170	231	9.7	203	1	417	16.1	1170	14.3	16.7	1.10	0.06
1900 20 Jan 94	14.0	1365	209	9.4	202	1	411	15.4	819	14.5	16.5	1.10	0.07

(Sheet 2 of 3)

Table C1 (Concluded)

Date	Array						Water Level	Pier 2					
	$H_{s,long}$ (cm)	$T_{p,long}$ (sec)	H_s (cm)	T_p (sec)	θ_m (deg)	N_p		$H_{s,long}$ (cm)	$T_{p,long}$ (sec)	H_s (cm)	T_p (sec)	$A_{amp,l}$	$A_{amp,s}$
2200 28 Jan 94	18.7	48	207	12.9	192	1	409	20.5	186	20.5	13.7	1.09	0.10
0100 29 Jan 94	19.4	315	205	12.4	196	1	398	19.5	745	21.7	17.5	1.00	0.11
0400 29 Jan 94	19.3	72	208	12.2	191	1	443	22.7	178	19.7	16.5	1.17	0.09
0700 29 Jan 94	19.2	256	204	12.4	194	1	476	25.8	178	18.7	16.7	1.34	0.09
0600 15 Mar 94	14.9	1170	212	10.3	205	1	436	15.0	1638	12.6	11.5	1.01	0.06
0700 15 Mar 94	14.3	1365	204	10.7	204	1	447	14.1	1170	12.7	11.5	0.99	0.06
0400 17 Mar 94	18.4	1638	231	10.7	210	1	434	21.4	1638	15.2	11.4	0.16	0.07
0400 12 Apr 94	10.1	1365	201	9.2	206	1	443	12.5	910	13.4	4.4	1.23	0.07
0400 21 Apr 94	13.5	29	209	14.6	203	2	454	15.6	819	18.3	14.3	1.16	0.09
0700 21 Apr 94	14.0	56	216	13.9	199	1	417	13.7	1365	19.3	13.9	0.98	0.09
1000 21 Apr 94	13.4	1024	204	13.3	202	1	419	14.9	1638	19.1	13.8	1.11	0.09

(Sheet 3 of 3)

C4

Table C2
Extreme Long Wave Cases (Observations with $H_{s,long}$ Greater Than 20 cm at Array or Pier 2)

Date	Array						Water Level	Pier 2					
	$H_{s,long}$ (cm)	$T_{p,long}$ (sec)	H_s (cm)	T_p (sec)	θ_m (deg)	N_p		$H_{s,long}$ (cm)	$T_{p,long}$ (sec)	H_s (cm)	T_p (sec)	$A_{amp,l}$	$A_{amp,s}$
0100 10 Nov 93	25.2	158	284	14.1	206	1	433	29.1	178	26.5	13.9	1.15	0.09
0400 10 Nov 93	30.2	67	300	13.8	198	1	452	30.2	210	28.3	13.9	1.00	0.09
0700 10 Nov 93	26.5	64	296	13.7	224	1	431	25.9	195	26.6	13.9	0.98	0.09
1000 10 Nov 93	24.9	56	283	13.5	202	1	426	23.1	210	23.4	13.9	0.93	0.08
1300 10 Nov 93	21.6	64	270	13.1	201	1	449	19.9	191	22.1	13.2	0.92	0.08
1600 10 Nov 93	19.2	67	255	12.4	203	1	444	21.0	178	23.7	12.9	1.09	0.09
0100 11 Nov 93	17.9	1638	248	12.0	198	1	438	22.1	195	22.5	12.0	1.23	0.09
2200 25 Nov 93	20.7	63	265	12.4	215	1	401	20.0	182	26.3	12.0	0.96	0.10
0000 3 Jan 94	20.7	248	193	16.1	192	1	427	26.5	178	29.7	16.5	1.28	0.15
0400 3 Jan 94	19.2	303	204	15.6	194	1	424	25.9	745	27.2	16.7	1.35	0.13
0700 3 Jan 94	18.6	1638	209	15.1	190	1	452	28.5	178	23.3	15.9	1.53	0.11
1000 3 Jan 94	18.9	1170	193	15.4	202	1	459	30.0	819	23.5	15.8	1.59	0.12
1300 3 Jan 94	20.5	167	212	14.8	194	1	429	32.9	819	25.0	15.8	1.60	0.12
1600 3 Jan 94	17.9	1638	191	14.7	193	1	404	22.6	186	20.4	15.8	1.26	0.11
1900 3 Jan 94	14.5	910	173	14.8	198	1	418	23.9	910	17.3	14.4	1.65	0.10
2200 12 Jan 94	10.4	1170	93	15.5	195	1	398	20.0	910	15.2	16.6	1.92	0.16
2200 28 Jan 94	18.7	48	207	12.9	192	1	409	20.5	186	20.5	13.7	1.09	0.10
0400 29 Jan 94	19.3	72	208	12.2	191	1	443	22.7	178	19.7	16.5	1.17	0.09
0700 29 Jan 94	19.2	256	204	12.4	194	1	476	25.8	178	18.7	16.7	1.34	0.09
1000 29 Jan 94	16.9	910	195	12.4	196	1	446	21.3	910	18.9	16.5	1.26	0.10

(Continued)

Table C2 (Concluded)

Date	Array						Water Level	Pier 2					
	$H_{s,long}$ (cm)	$T_{p,long}$ (sec)	H_s (cm)	T_p (sec)	θ_m (deg)	N_p		$H_{s,long}$ (cm)	$T_{p,long}$ (sec)	H_s (cm)	T_p (sec)	$A_{amp,l}$	$A_{amp,s}$
0400 31 Jan 94	16.2	1638	148	18.6	192	1	432	22.5	819	14.3	17.8	1.39	0.10
0700 31 Jan 94	17.4	248	162	17.9	191	1	467	27.0	210	14.9	17.4	1.55	0.09
1000 31 Jan 94	14.8	241	146	17.5	193	1	455	21.1	683	14.3	17.4	1.43	0.10
1300 31 Jan 94	13.3	1170	139	17.1	192	1	414	20.4	910	18.0	16.7	1.53	0.13
0400 17 Mar 94	18.4	1638	231	10.7	210	1	434	21.4	1638	15.2	11.4	1.16	0.07
1600 31 Mar 94	13.7	455	128	15.8	190	1	403	22.7	745	18.3	15.8	1.66	0.14
1900 31 Mar 94	15.0	248	134	15.5	189	1	440	22.9	200	16.5	16.5	1.53	0.12
2200 31 Mar 94	12.9	1638	126	15.1	217	0	458	22.6	819	12.4	15.4	1.76	0.10
0100 1 Apr 94	11.7	819	124	15.0	192	1	442	20.5	819	11.7	15.3	1.76	0.09
1600 5 Apr 94	14.6	174	171	15.0	195	1	432	20.4	910	19.0	15.8	1.40	0.11

Table C3
Extreme Long Cases all Gages (Observations with $H_{s,long}$ Greater Than 20 cm at Array or Pier 2)

Date	Array		Pier 2		Canoe Club		Back Basin		Channel Entrance	
	$H_{s,long}$ (cm)	$T_{p,long}$ (sec)	$A_{amp,l}$	$T_{p,long}$ (sec)	$A_{amp,l}$	$T_{p,long}$ (sec)	$A_{amp,l}$	$T_{p,long}$ (sec)	$A_{amp,l}$	$T_{p,long}$ (sec)
0100 10 Nov 93	25.2	157.5	1.15	178.1	1.03	819.2	0.69	819.2	1.10	178.1
0400 10 Nov 93	30.2	67.1	1.00	210.1	0.85	60.7	0.60	210.1	0.96	174.3
0700 10 Nov 93	26.5	64.0	0.98	195.0	0.93	64.0	0.67	221.4	0.93	195.0
1000 10 Nov 93	24.9	56.1	0.93	210.1	0.82	910.2	0.57	1024.0	0.87	178.1
1300 10 Nov 93	21.6	63.5	0.92	190.5	0.85	1024.0	0.55	1024.0	0.94	106.4
1600 10 Nov 93	19.2	67.1	1.09	178.1	1.00	273.1	0.67	221.4	1.11	178.1
0100 11 Nov 93	17.9	1638.4	1.23	195.0	1.11	221.4	0.76	221.4	1.09	195.0
2200 25 Nov 93	20.7	62.5	0.96	182.0	0.85	819.2	0.61	819.2	0.92	182.0
0000 3 Jan 94	20.7	248.2	1.28	178.1	1.13	744.7	0.91	744.7	1.06	174.3
0400 3 Jan 94	19.2	303.4	1.35	744.7	1.23	744.7	1.00	744.7	1.11	744.7
0700 3 Jan 94	18.6	1638.4	1.53	178.1	1.27	910.2	1.04	910.2	1.29	178.1
1000 3 Jan 94	18.9	1170.3	1.59	819.2	1.36	819.2	1.11	819.2	1.33	819.2
1300 3 Jan 94	20.5	167.2	1.60	819.2	1.42	819.2	1.23	819.2	1.29	819.2
1600 3 Jan 94	17.9	1638.4	1.26	186.2	1.08	1170.3	0.84	1170.3	0.99	1170.3
1900 3 Jan 94	14.5	910.2	1.65	910.2	1.54	910.2	1.29	910.2	1.40	910.2
2200 12 Jan 94	10.4	1170.3	1.92	910.2	1.80	910.2	1.44	910.2	1.64	910.2
2200 28 Jan 94	18.7	47.9	1.09	186.2	1.03	819.2	0.78	819.2	1.01	186.2
0400 29 Jan 94	19.3	72.5	1.17	178.1	1.02	1024.0	0.79	1024.0	0.97	178.1
0700 29 Jan 94	19.2	256.0	1.34	178.1	1.12	910.2	0.79	910.2	1.17	178.1
1000 29 Jan 94	16.9	910.2	1.26	910.2	1.15	910.2	0.86	910.2	1.09	910.2

(Continued)

Table C3 (Concluded)

Date	Array $H_{s,long}$ (cm)	Array $T_{p,long}$ (sec)	Pier 2 $A_{amp,l}$	Pier 2 $T_{p,long}$ (sec)	Canoe Club $A_{amp,l}$	Canoe Club $T_{p,long}$ (sec)	Back Basin $A_{amp,l}$	Back Basin $T_{p,long}$ (sec)	Channel Entrance $A_{amp,l}$	Channel Entrance $T_{p,long}$ (sec)
0400 31 Jan 94	16.2	1638.4	1.39	819.2	1.33	819.2	1.10	819.2	1.17	819.2
0700 31 Jan 94	17.4	248.2	1.55	210.1	1.35	682.7	1.11	682.7	1.29	178.1
1000 31 Jan 94	14.8	240.9	1.43	682.7	1.33	682.7	1.08	682.7	1.19	1024.0
1300 31 Jan 94	13.3	1170.3	1.53	910.2	1.48	910.2	1.25	910.2	1.27	910.2
0400 17 Mar 94	18.4	1638.4	1.16	1638.4	1.07	1638.4	0.81	1638.4	1.20	1638.4
1600 31 Mar 94	13.7	455.1	1.66	744.7	1.55	744.7	1.23	744.7	1.36	744.7
1900 31 Mar 94	15.0	248.2	1.53	199.8	1.29	910.2	1.01	910.2	1.21	178.1
2200 31 Mar 94	12.9	1638.4	1.76	819.2	1.55	819.2	1.32	819.2	1.52	819.2
0100 1 Apr 94	11.7	819.2	1.76	819.2	1.74	819.2	1.51	819.2	1.52	819.2
1600 5 Apr 94	14.6	174.3	1.40	910.2	1.29	910.2	0.98	910.2	1.12	910.2

Appendix D
Wave Climate Summary

List of Figures

List of Tables

Figure D1. Wave height time series plot for November 1994
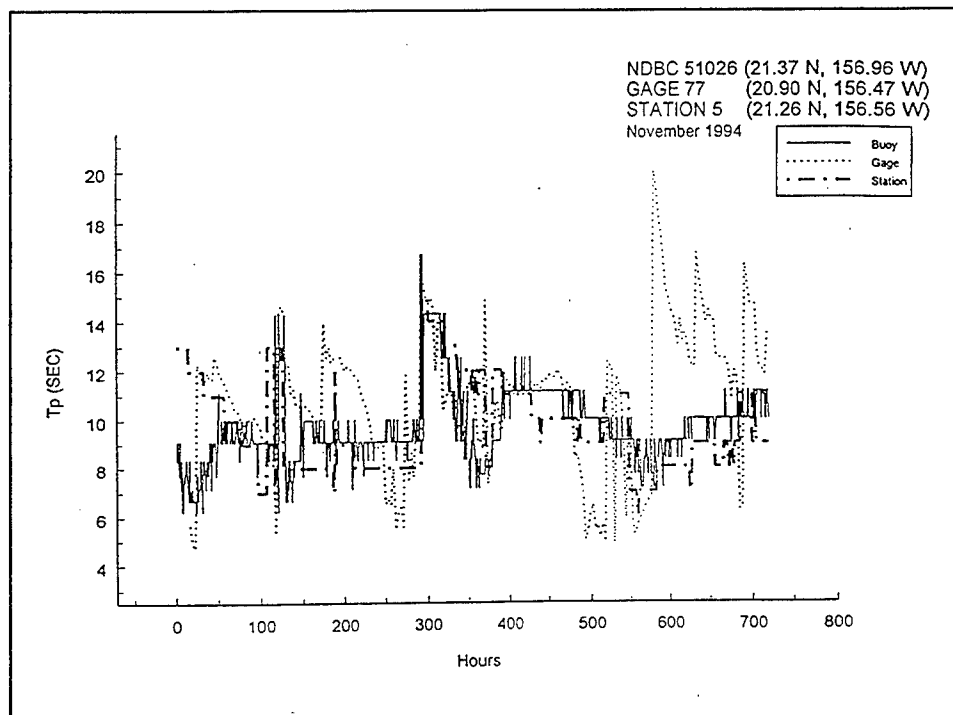
Figure D2. Wave period time series plot for November 1994
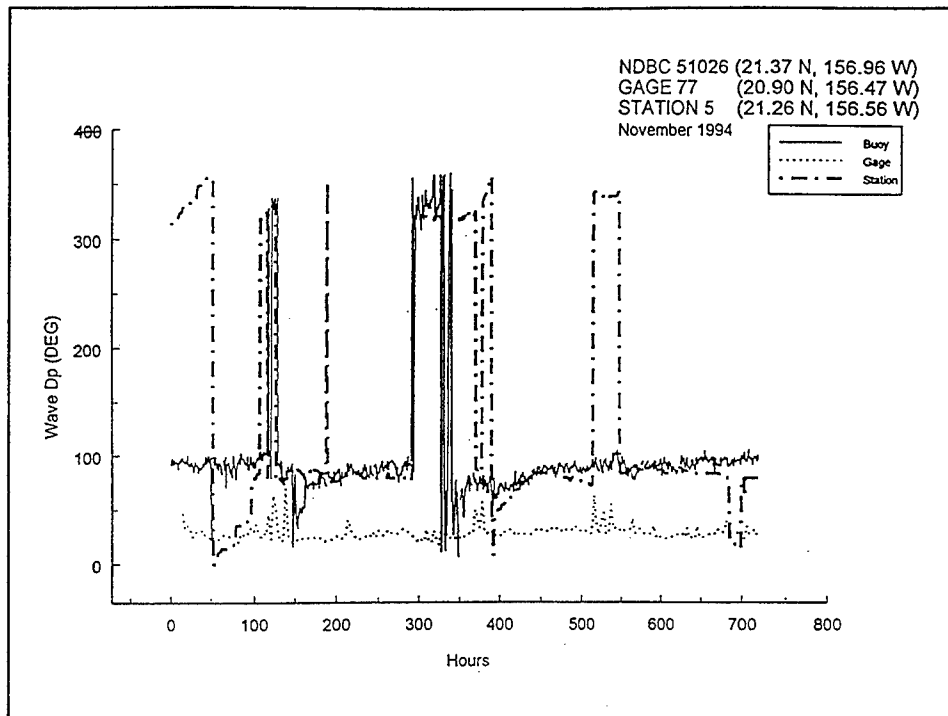
Figure D3. Wave direction time series plot for November 1994

KAHULUI HARBOR, HAWAII 1993 - 1994
LAT: 21.37 N, LONG:156.96 W, BUOY 51026
SUMMARY OF WAVE INFORMATION BY MONTH

OCCURRENCES OF WAVE HEIGHT BY MONTH FOR ALL YEARS

Hmo(m)	JAN	FEB	MAR	APR	MAY	JUN	JUL	AUG	SEP	OCT	NOV	DEC	TOTAL
0.00 - 0.49	.	.	.	.	.	.	.	.	.	.	.	.	0
0.50 - 0.99	.	.	.	.	.	.	.	.	.	16	.	.	16
1.00 - 1.49	39	24	61	16	.	.	.	.	135	231	.	13	519
1.50 - 1.99	90	127	159	170	42	.	.	.	153	510	80	44	1375
2.00 - 2.49	106	191	80	167	127	.	.	.	37	448	438	185	1779
2.50 - 2.99	176	207	75	144	3	.	.	.	.	172	497	257	1531
3.00 - 3.49	139	37	113	178	.	.	.	.	.	50	196	300	1013
3.50 - 3.99	73	3	91	30	.	.	.	.	.	8	95	243	543
4.00 - 4.49	42	1	51	6	.	.	.	.	.	.	69	116	285
4.50 - 4.99	26	1	36	1	.	.	.	.	.	.	26	28	118
5.00 - 5.49	9	.	26	.	.	.	.	.	.	.	.	1	36
5.50 - 5.99	1	.	5	.	.	.	.	.	.	.	.	.	6
6.00 - 6.49	.	.	.	.	.	.	.	.	.	.	.	.	0
6.50 - 6.99	.	.	.	.	.	.	.	.	.	.	.	.	0
7.00 - 7.49	.	.	.	.	.	.	.	.	.	.	.	.	0
7.50 - 7.99	.	.	.	.	.	.	.	.	.	.	.	.	0
8.00 - 8.49	.	.	.	.	.	.	.	.	.	.	.	.	0
8.50 - 8.99	.	.	.	.	.	.	.	.	.	.	.	.	0
9.00 - 9.49	.	.	.	.	.	.	.	.	.	.	.	.	0
9.50 - 9.99	.	.	.	.	.	.	.	.	.	.	.	.	0
10.00 - GREATER	.	.	.	.	.	.	.	.	.	.	.	.	0
TOTAL	701	591	697	712	172	0	0	0	325	1435	1401	1187	7221

OCCURRENCES OF PEAK PERIOD BY MONTH FOR ALL YEARS

Tp(sec)	JAN	FEB	MAR	APR	MAY	JUN	JUL	AUG	SEP	OCT	NOV	DEC	TOTAL
3.0 - 3.9	.	.	.	.	.	.	.	.	.	.	.	.	0
4.0 - 4.9	.	.	.	.	.	.	.	.	.	3	.	.	3
5.0 - 5.9	2	13	.	7	3	.	.	.	2	37	.	.	51
6.0 - 6.9	5	.	.	5	15	.	.	.	1	21	19	8	87
7.0 - 7.9	58	48	30	31	15	.	.	.	31	211	68	45	537
8.0 - 8.9	82	58	77	97	27	.	.	.	76	273	133	93	916
9.0 - 9.9	40	151	89	235	63	.	.	.	86	236	373	146	1419
10.0 - 10.9	30	34	121	125	5	.	.	.	71	90	276	300	1052
11.0 - 11.9	28	31	136	36	3	.	.	.	21	106	251	116	728
12.0 - 12.9	116	84	106	63	9	.	.	.	25	213	160	104	880
13.0 - 13.9	.	.	.	.	.	.	.	.	.	.	.	.	0
14.0 - 14.9	182	88	76	87	21	.	.	.	12	161	80	197	904
15.0 - 15.9	.	.	.	.	.	.	.	.	.	.	.	.	0
16.0 - 16.9	135	67	55	19	11	.	.	.	.	76	39	140	542
17.0 - 17.9	.	.	.	.	.	.	.	.	.	.	.	.	0
18.0 - 18.9	.	.	.	.	.	.	.	.	.	.	.	.	0
19.0 - 19.9	.	.	.	.	.	.	.	.	.	.	.	.	0
20.0 - LONGER	23	17	7	7	.	.	.	.	.	8	2	38	102
TOTAL	701	591	697	712	172	0	0	0	325	1435	1401	1187	7221

OCCURRENCES OF PEAK DIRECTION BY MONTH FOR ALL YEARS

Dp(deg) DIRECTION BAND & CENTER	JAN	FEB	MAR	APR	MAY	JUN	JUL	AUG	SEP	OCT	NOV	DEC	TOTAL
348.75 - 11.24 (0.0)	59	26	50	35	1	.	.	.	34	109	104	56	474
11.25 - 33.74 (22.5)	40	23	9	54	.	.	.	.	7	69	153	1	356
33.75 - 56.24 (45.0)	41	58	78	132	2	.	.	.	30	105	136	14	596
56.25 - 78.74 (67.5)	79	189	196	67	26	.	.	.	40	297	268	147	1309
78.75 - 101.24 (90.0)	46	45	49	238	100	.	.	.	152	307	557	531	2025
101.25 - 123.74 (112.5)	.	.	2	13	.	.	.	.	.	2	14	4	35
123.75 - 146.24 (135.0)	.	1	.	.	.	.	.	.	.	.	.	.	1
146.25 - 168.74 (157.5)	.	.	.	.	.	.	.	.	.	.	.	.	0
168.75 - 191.24 (180.0)	.	.	.	.	.	.	.	.	.	.	.	.	0
191.25 - 213.74 (202.5)	.	.	.	.	.	.	.	.	.	.	.	.	0
213.75 - 236.24 (225.0)	.	.	.	.	.	.	.	.	.	1	.	.	2
236.25 - 258.74 (247.5)	.	.	.	.	.	.	.	.	1	1	.	.	6
258.75 - 281.24 (270.0)	.	.	.	.	.	.	.	.	.	6	.	.	6
281.25 - 303.74 (292.5)	10	14	25	.	.	.	.	.	1	28	.	23	101
303.75 - 326.24 (315.0)	229	135	190	81	26	.	.	.	13	178	52	222	1126
326.25 - 348.74 (337.5)	197	100	98	92	17	.	.	.	47	327	117	189	1184
TOTAL	701	591	697	712	172	0	0	0	325	1435	1401	1187	7221

D4

KAHULUI HARBOR, HAWAII 1994
LAT: 21.26 N, LONG:156.56 W, STATION 5
SUMMARY OF WAVE INFORMATION BY MONTH

OCCURRENCES OF WAVE HEIGHT BY MONTH FOR ALL YEARS

Hmo(m)	JAN	FEB	MAR	APR	MAY	JUN	JUL	AUG	SEP	OCT	NOV	DEC	TOTAL
0.00 - 0.49													0
0.50 - 0.99								16					16
1.00 - 1.49					41	57	121	375	247	30			871
1.50 - 1.99		16	43		297	377	583	298	356	297			2267
2.00 - 2.49	104	205	122	341	340	286	40	27	103	192	312	54	2126
2.50 - 2.99	375	274	85	331	57			10	14	195	140	313	1794
3.00 - 3.49	210	159	178	48	9			8		30	234	243	1119
3.50 - 3.99	55	18	247					10			34	122	486
4.00 - 4.49			69									7	76
4.50 - 4.99													0
5.00 - 5.49													0
5.50 - 5.99													0
6.00 - 6.49													0
6.50 - 6.99													0
7.00 - 7.49													0
7.50 - 7.99													0
8.00 - 8.49													0
8.50 - 8.99													0
9.00 - 9.49													0
9.50 - 9.99													0
10.00 - GREATER													0
TOTAL	744	672	744	720	744	720	744	744	720	744	720	739	8755

OCCURRENCES OF PEAK PERIOD BY MONTH FOR ALL YEARS

Tp(sec)	JAN	FEB	MAR	APR	MAY	JUN	JUL	AUG	SEP	OCT	NOV	DEC	TOTAL
3.0 - 3.9													0
4.0 - 4.9													0
5.0 - 5.9													0
6.0 - 6.9					76	25	219	229	72		1		622
7.0 - 7.9	21			27	260	468	225	111	48	24	7	6	1197
8.0 - 8.9	57			293	192	30	298	229	153	86	3	87	1428
9.0 - 9.9	125	92	104	106	118	118	2	29	118	152	145	56	1165
10.0 - 10.9	63	157	284	106	31	56		60	186	172	230	138	1483
11.0 - 11.9	152	172	135	71	29	23		59	109	136	224	112	1222
12.0 - 12.9	169	83	82	61	17			27	34	53	64	157	747
13.0 - 13.9	76	104	103	56	21					53	46	134	593
14.0 - 14.9	23	52	36							43		29	183
15.0 - 15.9	19	10								25		12	66
16.0 - 16.9	27	2										8	37
17.0 - 17.9	12												12
18.0 - 18.9													0
19.0 - 19.9													0
20.0 - LONGER													0
TOTAL	744	672	744	720	744	720	744	744	720	744	720	739	8755

OCCURRENCES OF PEAK DIRECTION BY MONTH FOR ALL YEARS

Dp(deg) DIRECTION BAND & CENTER	JAN	FEB	MAR	APR	MAY	JUN	JUL	AUG	SEP	OCT	NOV	DEC	TOTAL
348.75 - 11.24 (0.0)	265	150	262	268	291	217	84	91	286	215	119	245	2493
11.25 - 33.74 (22.5)	40	75	303	111	191	161	54	44	75	341	205	73	1673
33.75 - 56.24 (45.0)	10		56	71	81	50	196	36	8	8	133	16	665
56.25 - 78.74 (67.5)			68	14	36	174	174	79			61		606
78.75 - 101.24 (90.0)					6	59	13	147					225
101.25 - 123.74 (112.5)								15					15
123.75 - 146.24 (135.0)													0
146.25 - 168.74 (157.5)													0
168.75 - 191.24 (180.0)													0
191.25 - 213.74 (202.5)													0
213.75 - 236.24 (225.0)													0
236.25 - 258.74 (247.5)									20				20
258.75 - 281.24 (270.0)								140	72	29			241
281.25 - 303.74 (292.5)		5					77	63	8	13			166
303.75 - 326.24 (315.0)		197		20	60	24	49	35	115	21		48	569
326.25 - 348.74 (337.5)	429	245	55	236	79	35	97	94	136	117	202	357	2082
TOTAL	744	672	744	720	744	720	744	744	720	744	720	739	8755

KAHULUI HARBOR, HAWAII 1956 - 1975
LAT: 21.94 N, LONG:155.69 W, ORIGINAL STATION 31
SUMMARY OF WAVE INFORMATION BY MONTH

OCCURRENCES OF WAVE HEIGHT BY MONTH FOR ALL YEARS

Hmo(m)	JAN	FEB	MAR	APR	MAY	JUN	JUL	AUG	SEP	OCT	NOV	DEC	TOTAL
0.00 - 0.49	.	.	.	.	.	.	.	.	.	.	.	.	0
0.50 - 0.99	1	.	.	.	16	74	29	89	95	44	.	.	348
1.00 - 1.49	18	36	25	38	529	654	537	504	682	189	54	11	3241
1.50 - 1.99	64	.	281	565	1550	1816	1701	2284	2221	1168	328	102	12116
2.00 - 2.49	452	373	949	1377	1680	1640	2335	1723	1539	1692	867	313	14940
2.50 - 2.99	916	1128	1555	1672	1039	551	358	319	230	1252	1371	1067	11458
3.00 - 3.49	1132	1280	1365	800	146	64	.	32	30	430	1237	1531	8047
3.50 - 3.99	1159	913	561	230	.	1	.	9	3	124	577	953	4530
4.00 - 4.49	566	408	149	81	.	.	.	.	.	56	248	494	2002
4.50 - 4.99	327	177	44	16	.	.	.	.	.	5	86	281	936
5.00 - 5.49	171	77	15	19	.	.	.	.	.	.	17	112	411
5.50 - 5.99	92	67	5	2	.	.	.	.	.	.	5	63	234
6.00 - 6.49	52	50	3	.	.	.	.	.	.	.	5	33	143
6.50 - 6.99	9	8	8	.	.	.	.	.	.	.	5	.	30
7.00 - 7.49	1	3	.	.	.	.	.	.	.	.	.	.	4
7.50 - 7.99	.	.	.	.	.	.	.	.	.	.	.	.	0
8.00 - 8.49	.	.	.	.	.	.	.	.	.	.	.	.	0
8.50 - 8.99	.	.	.	.	.	.	.	.	.	.	.	.	0
9.00 - 9.49	.	.	.	.	.	.	.	.	.	.	.	.	0
9.50 - 9.99	.	.	.	.	.	.	.	.	.	.	.	.	0
10.00 - GREATER	.	.	.	.	.	.	.	.	.	.	.	.	0
TOTAL	4960	4520	4960	4800	4960	4800	4960	4960	4800	4960	4800	4960	58440

OCCURRENCES OF PEAK PERIOD BY MONTH FOR ALL YEARS

Tp(sec)	JAN	FEB	MAR	APR	MAY	JUN	JUL	AUG	SEP	OCT	NOV	DEC	TOTAL
3.0 - 3.9	.	.	.	.	.	.	.	.	.	.	.	.	0
4.0 - 4.9	.	.	.	.	.	.	.	.	.	.	.	.	0
5.0 - 5.9	17	4	4	47	388	628	640	1292	794	151	25	1	3991
6.0 - 6.9	53	55	97	466	566	900	1203	1088	529	300	122	80	5459
7.0 - 7.9	182	229	333	958	908	834	1145	946	625	376	407	394	7337
8.0 - 8.9	261	233	470	735	1244	1349	1580	1197	1087	694	331	362	9543
9.0 - 9.9	152	90	329	415	597	587	250	279	670	742	225	114	4450
10.0 - 10.9	293	343	733	730	776	344	82	112	728	1034	657	264	6096
11.0 - 11.9	1366	1181	1314	941	420	134	60	42	304	958	1152	1142	9014
12.0 - 12.9	.	.	.	.	.	.	.	.	.	.	.	.	0
13.0 - 13.9	1850	1806	1310	397	61	24	.	4	63	546	1474	1771	9306
14.0 - 14.9	749	510	322	111	.	.	.	.	.	159	377	762	2990
15.0 - 15.9	.	.	.	.	.	.	.	.	.	.	.	.	0
16.0 - 16.9	.	.	.	.	.	.	.	.	.	.	.	.	0
17.0 - 17.9	37	69	48	.	.	.	.	.	.	.	30	70	254
18.0 - 18.9	.	.	.	.	.	.	.	.	.	.	.	.	0
19.0 - 19.9	.	.	.	.	.	.	.	.	.	.	.	.	0
20.0 - LONGER	.	.	.	.	.	.	.	.	.	.	.	.	0
TOTAL	4960	4520	4960	4800	4960	4800	4960	4960	4800	4960	4800	4960	58440

OCCURRENCES OF PEAK DIRECTION BY MONTH FOR ALL YEARS

Dp(deg) DIRECTION BAND & CENTER	JAN	FEB	MAR	APR	MAY	JUN	JUL	AUG	SEP	OCT	NOV	DEC	TOTAL
348.75 - 11.24 (0.0)	240	121	305	223	203	126	87	80	104	400	257	234	2380
11.25 - 33.74 (22.5)	81	84	125	50	104	17	51	73	48	94	114	65	906
33.75 - 56.24 (45.0)	47	104	152	310	191	266	845	656	380	229	81	146	3407
56.25 - 78.74 (67.5)	105	253	312	926	906	1207	1867	2008	1093	452	442	327	9898
78.75 - 101.24 (90.0)	166	99	292	495	818	872	384	724	445	198	180	179	4852
101.25 - 123.74 (112.5)	14	12	51	67	78	36	5	40	13	23	17	66	422
123.75 - 146.24 (135.0)	29	8	15	11	12	7	12	.	.	.	8	30	152
146.25 - 168.74 (157.5)	35	18	.	.	1	.	.	.	1	3	18	6	94
168.75 - 191.24 (180.0)	33	.	1	.	.	1	9	.	.	1	1	10	46
191.25 - 213.74 (202.5)	42	.	7	.	.	7	.	41	.	5	5	9	119
213.75 - 236.24 (225.0)	30	10	9	.	7	2	.	.	.	4	3	2	56
236.25 - 258.74 (247.5)	58	35	14	7	.	.	.	.	.	3	.	13	100
258.75 - 281.24 (270.0)	48	.	7	.	.	.	.	.	.	.	.	6	96
281.25 - 303.74 (292.5)	1077	1285	1194	312	232	496	1121	385	208	80	75	580	7045
303.75 - 326.24 (315.0)	2662	2287	2201	2020	1976	1543	463	817	1627	2254	2746	3059	23655
326.25 - 348.74 (337.5)	293	203	275	374	435	224	125	136	881	1206	832	228	5212
TOTAL	4960	4520	4960	4800	4960	4800	4960	4960	4800	4960	4800	4960	58440

Appendix D Wave Climate Summary

OCCURRENCES OF WAVE HEIGHT BY MONTH FOR ALL YEARS

Hmo(m)	JAN	FEB	MAR	APR	MAY	JUN	JUL	AUG	SEP	OCT	NOV	DEC	TOTAL
0.00 - 0.49	13	7	33	18	23	24	50	46	65	34	8	5	326
0.50 - 0.99	86	119	44	111	205	194	177	135	153	180	249	229	1882
1.00 - 1.49	90	80	68	77	5	.	.	1	.	14	115	205	655
1.50 - 1.99	31	6	54	23	3	.	.	.	.	.	63	35	215
2.00 - 2.49	11	.	3	4	.	.	.	.	.	.	19	1	38
2.50 - 2.99	.	.	.	.	.	.	.	.	.	.	11	.	11
3.00 - 3.49	.	.	.	.	.	.	.	.	.	.	1	.	1
3.50 - 3.99	.	.	.	.	.	.	.	.	.	.	.	.	0
4.00 - 4.49	.	.	.	.	.	.	.	.	.	.	.	.	0
4.50 - 4.99	.	.	.	.	.	.	.	.	.	.	.	.	0
5.00 - 5.49	.	.	.	.	.	.	.	.	.	.	.	.	0
5.50 - 5.99	.	.	.	.	.	.	.	.	.	.	.	.	0
6.00 - 6.49	.	.	.	.	.	.	.	.	.	.	.	.	0
6.50 - 6.99	.	.	.	.	.	.	.	.	.	.	.	.	0
7.00 - 7.49	.	.	.	.	.	.	.	.	.	.	.	.	0
7.50 - 7.99	.	.	.	.	.	.	.	.	.	.	.	.	0
8.00 - 8.49	.	.	.	.	.	.	.	.	.	.	.	.	0
8.50 - 8.99	.	.	.	.	.	.	.	.	.	.	.	.	0
9.00 - 9.49	.	.	.	.	.	.	.	.	.	.	.	.	0
9.50 - 9.99	.	.	.	.	.	.	.	.	.	.	.	.	0
10.00 - GREATER	.	.	.	.	.	.	.	.	.	.	.	.	0
TOTAL	231	212	202	233	236	218	227	182	218	228	466	475	3128

OCCURRENCES OF PEAK PERIOD BY MONTH FOR ALL YEARS

Tp(sec)	JAN	FEB	MAR	APR	MAY	JUN	JUL	AUG	SEP	OCT	NOV	DEC	TOTAL
3.0 - 3.9	.	.	.	21	20	18	37	36	43	8	5	.	0
4.0 - 4.9	1	.	.	6	24	46	56	71	31	6	18	5	188
5.0 - 5.9	1	.	1	8	19	26	42	42	14	9	13	7	264
6.0 - 6.9	8	11	7	3	29	67	38	21	23	17	13	.	170
7.0 - 7.9	19	18	25	33	6	25	36	10	25	17	40	62	251
8.0 - 8.9	22	35	35	29	14	14	9	2	32	14	61	38	316
9.0 - 9.9	14	22	44	24	25	16	3	.	32	14	83	20	305
10.0 - 10.9	42	32	50	30	48	6	4	.	21	51	108	45	297
11.0 - 11.9	28	34	12	22	21	.	2	.	6	57	44	54	437
12.0 - 12.9	23	16	5	11	10	.	.	.	3	5	23	29	280
13.0 - 13.9	36	20	7	32	11	.	.	.	7	14	30	103	125
14.0 - 14.9	12	12	5	11	3	.	.	.	2	4	11	32	260
15.0 - 15.9	11	6	3	1	4	.	.	.	.	4	7	20	92
16.0 - 16.9	10	3	3	.	2	.	.	.	.	1	2	23	58
17.0 - 17.9	3	2	1	1	.	.	.	.	.	.	2	16	44
18.0 - 18.9	1	1	2	1	.	.	.	.	.	.	2	7	26
19.0 - 19.9	1	1	2	1	.	.	.	.	.	.	2	7	14
20.0 - LONGER	.	.	.	.	.	.	.	.	.	.	.	1	1
TOTAL	231	212	202	233	236	218	227	182	218	228	466	475	3128

OCCURRENCES OF PEAK DIRECTION BY MONTH FOR ALL YEARS

Dp(deg) DIRECTION BAND & CENTER	JAN	FEB	MAR	APR	MAY	JUN	JUL	AUG	SEP	OCT	NOV	DEC	TOTAL
348.75 - 11.24 (0.0)	30	10	6	2	6	.	.	.	.	1	8	18	81
11.25 - 33.74 (22.5)	169	172	158	200	178	203	186	138	187	133	405	362	2491
33.75 - 56.24 (45.0)	9	12	17	14	28	10	36	40	27	23	38	45	299
56.25 - 78.74 (67.5)	12	3	6	7	7	1	1	1	1	6	10	8	63
78.75 - 101.24 (90.0)	7	13	7	4	12	4	4	3	1	63	5	42	165
101.25 - 123.74 (112.5)	4	1	2	3	2	.	.	.	2	2	.	.	16
123.75 - 146.24 (135.0)	.	.	3	1	1	.	.	.	.	.	.	.	5
146.25 - 168.74 (157.5)	.	.	1	1	2	.	.	.	.	.	.	.	4
168.75 - 191.24 (180.0)	.	.	1	1	.	.	.	.	.	.	.	.	2
191.25 - 213.74 (202.5)	.	.	1	.	.	.	.	.	.	.	.	.	1
213.75 - 236.24 (225.0)	.	.	.	.	.	.	.	.	.	.	.	.	0
236.25 - 258.74 (247.5)	.	.	.	.	.	.	.	.	.	.	.	.	0
258.75 - 281.24 (270.0)	.	.	.	.	.	.	.	.	.	.	.	.	0
281.25 - 303.74 (292.5)	.	.	.	.	.	.	.	.	.	.	.	.	0
303.75 - 326.24 (315.0)	.	.	.	.	.	.	.	.	.	.	.	.	0
326.25 - 348.74 (337.5)	.	1	.	.	.	.	.	.	.	.	.	.	1
TOTAL	231	212	202	233	236	218	227	182	218	228	466	475	3128

Appendix E
Basin Locations
for Alternative Plans

Figure E1. Basin locations, Plan 1

Figure E2. Basin locations, Plan 2

Figure E3. Basin locations, Plan 3a

Figure E4. Basin locations, Plan 3b

Figure E5. Basin locations, Plan 3c

Figure E6. Basin locations, Plan 4a

Figure E7. Basin locations, Plans 4b and 6
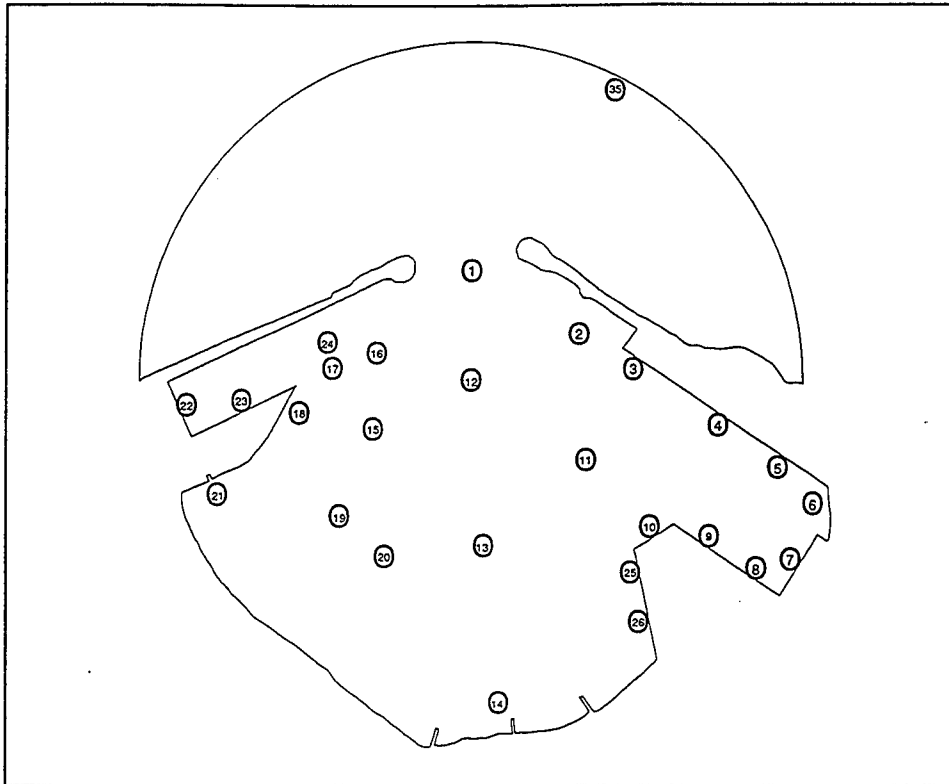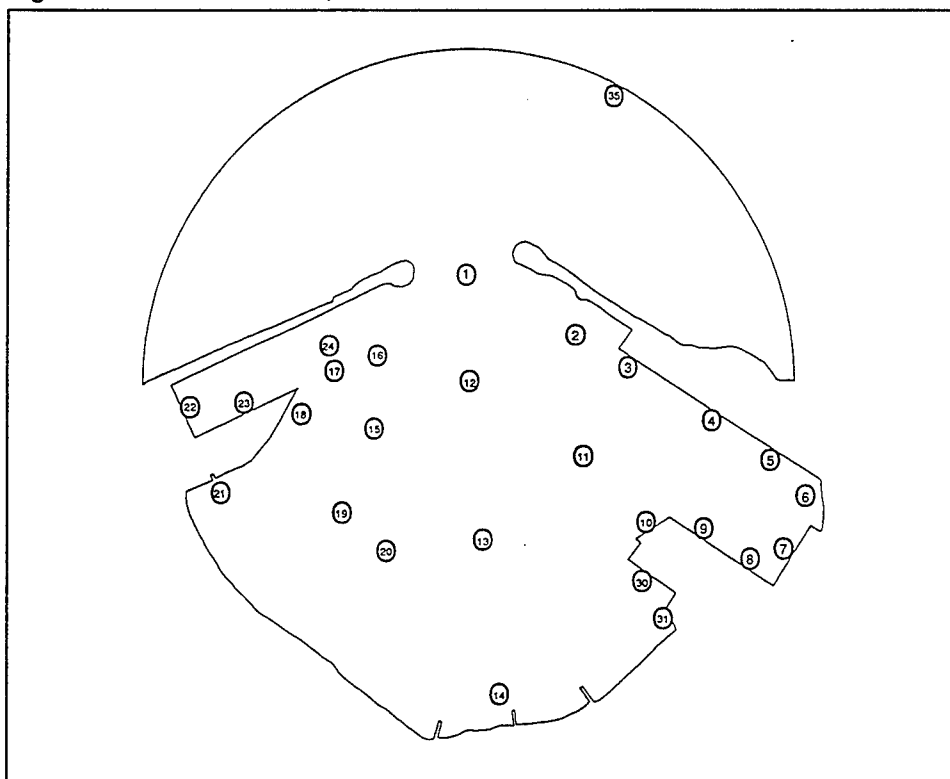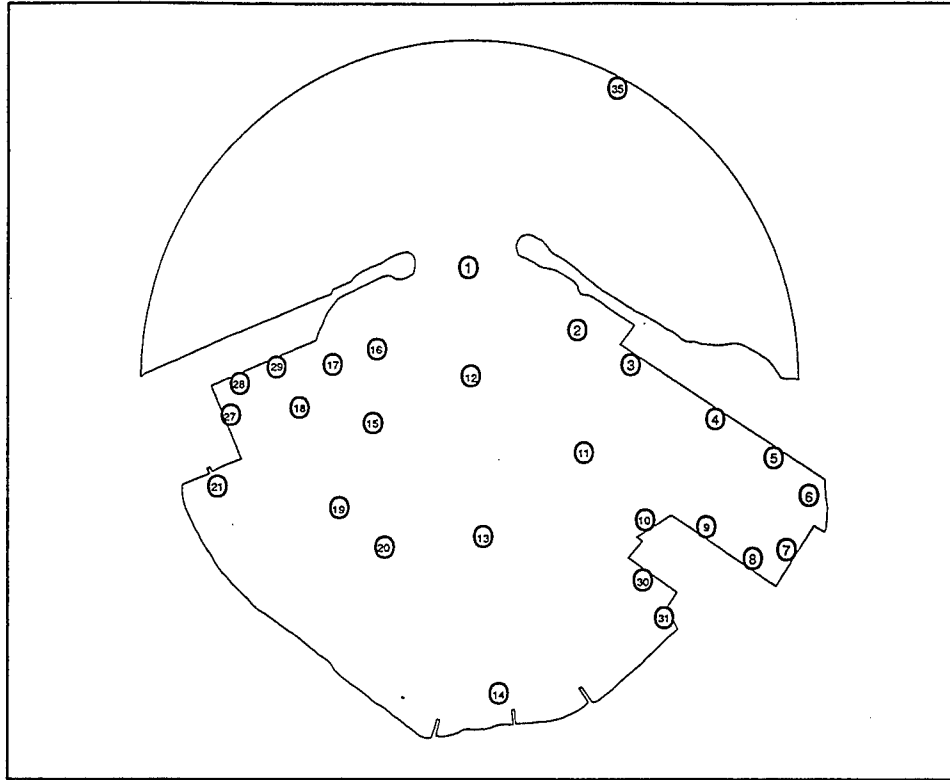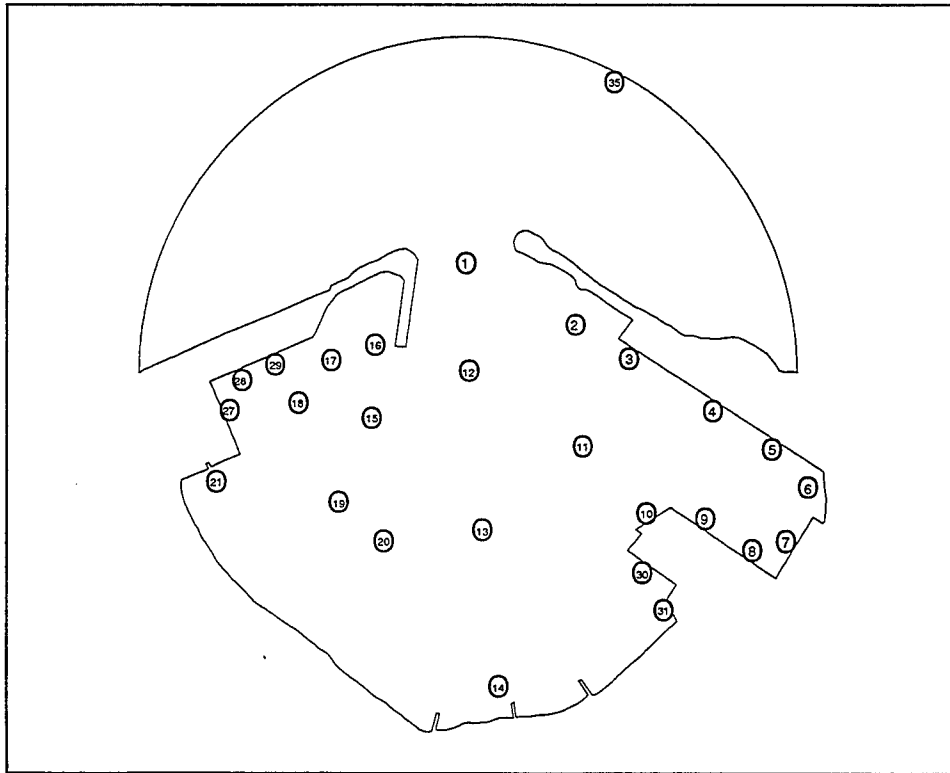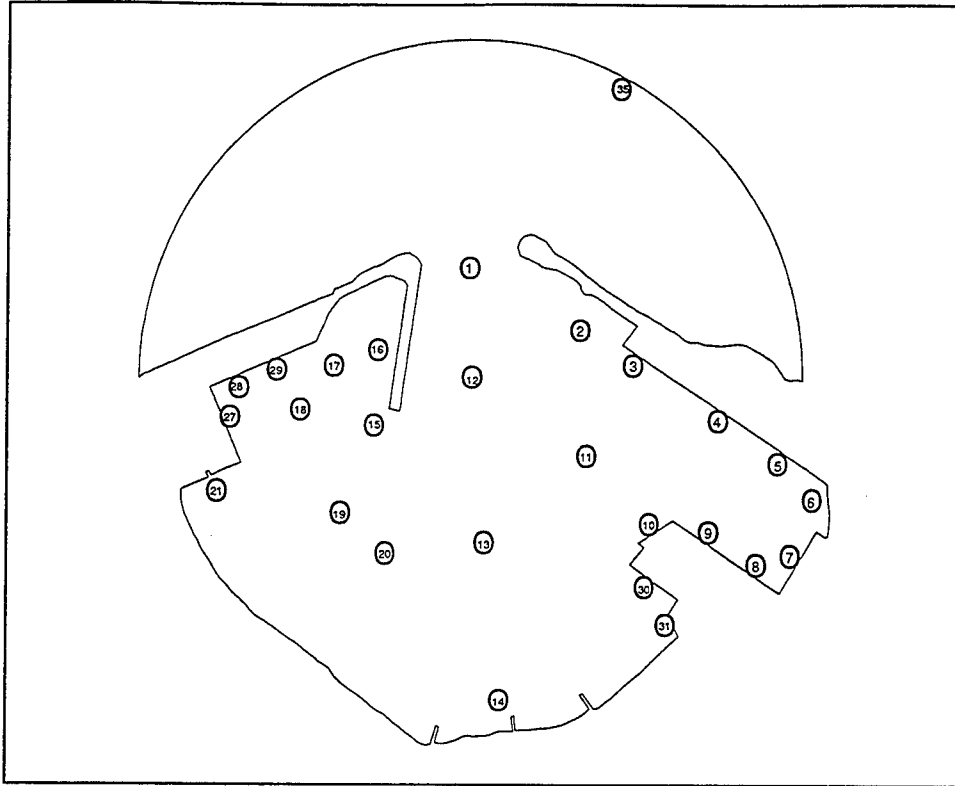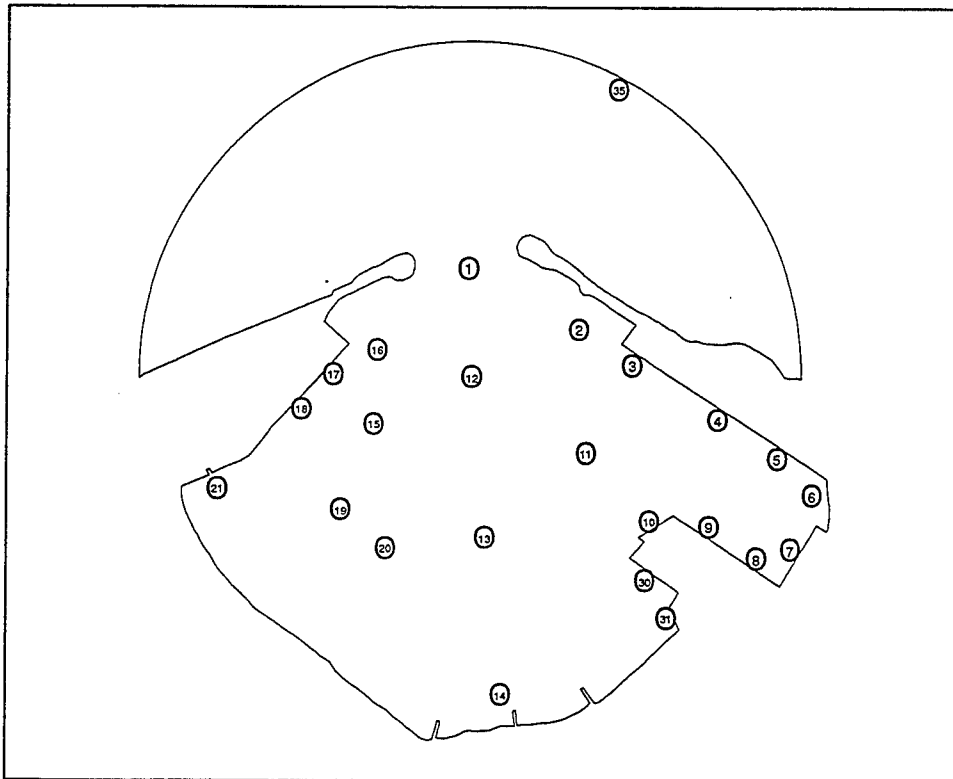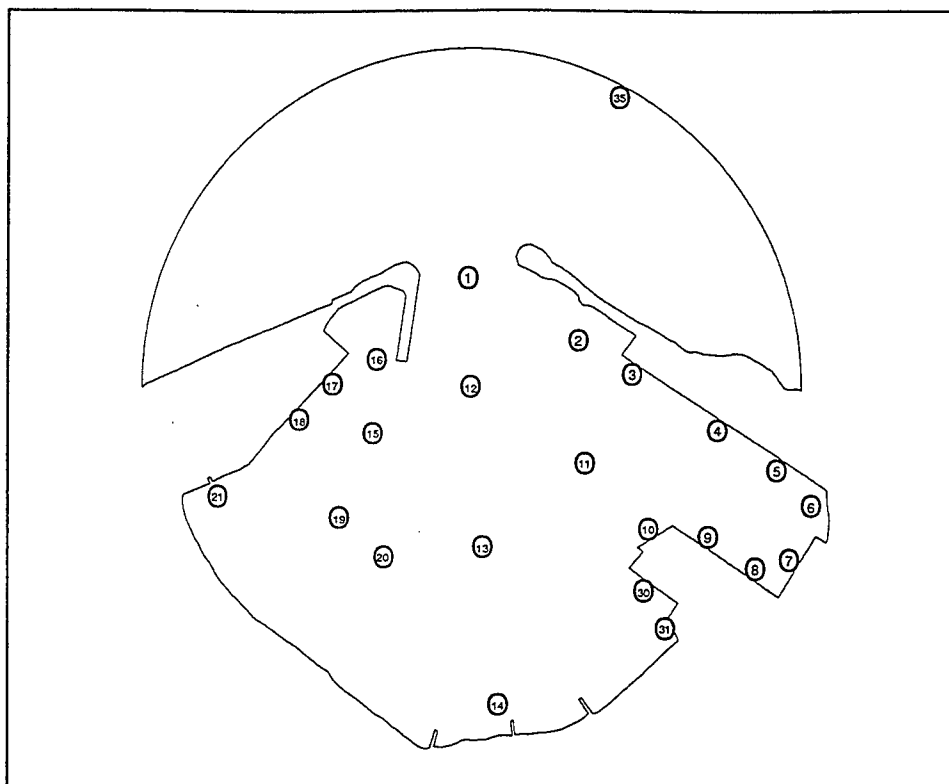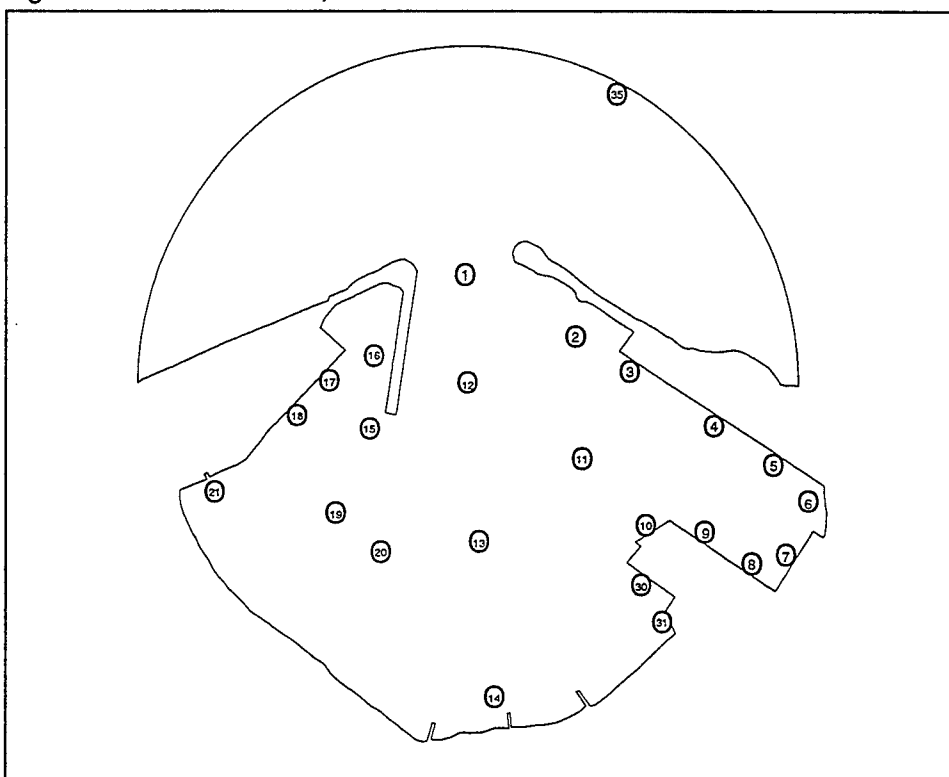

Figure E8. Basin locations, Plan 4c
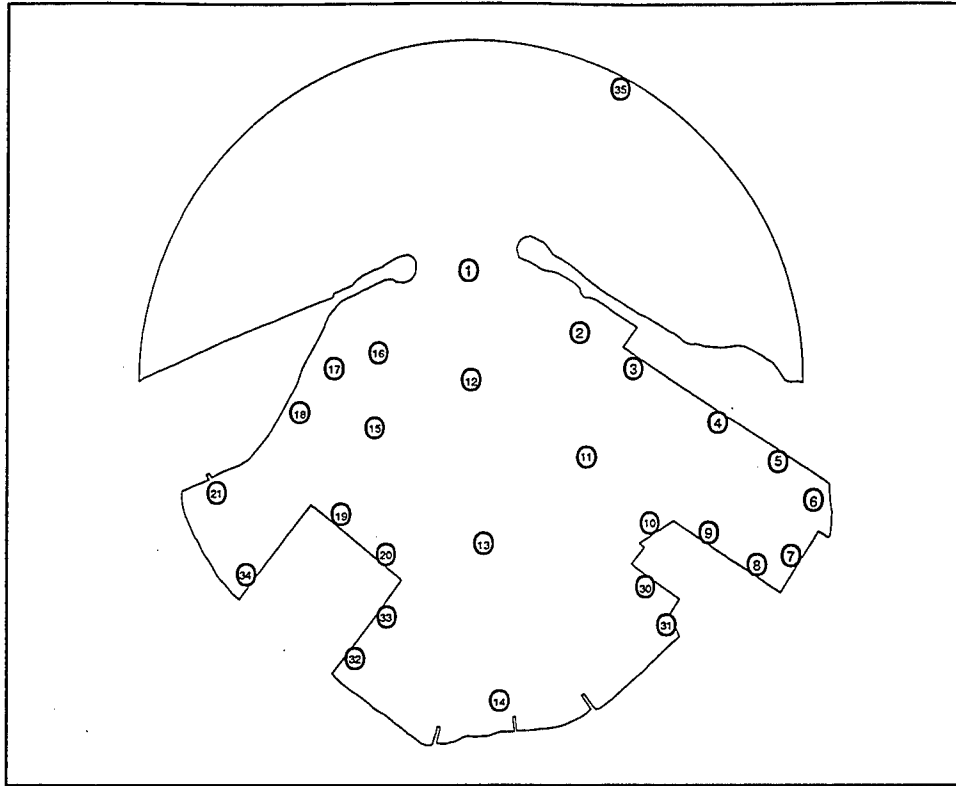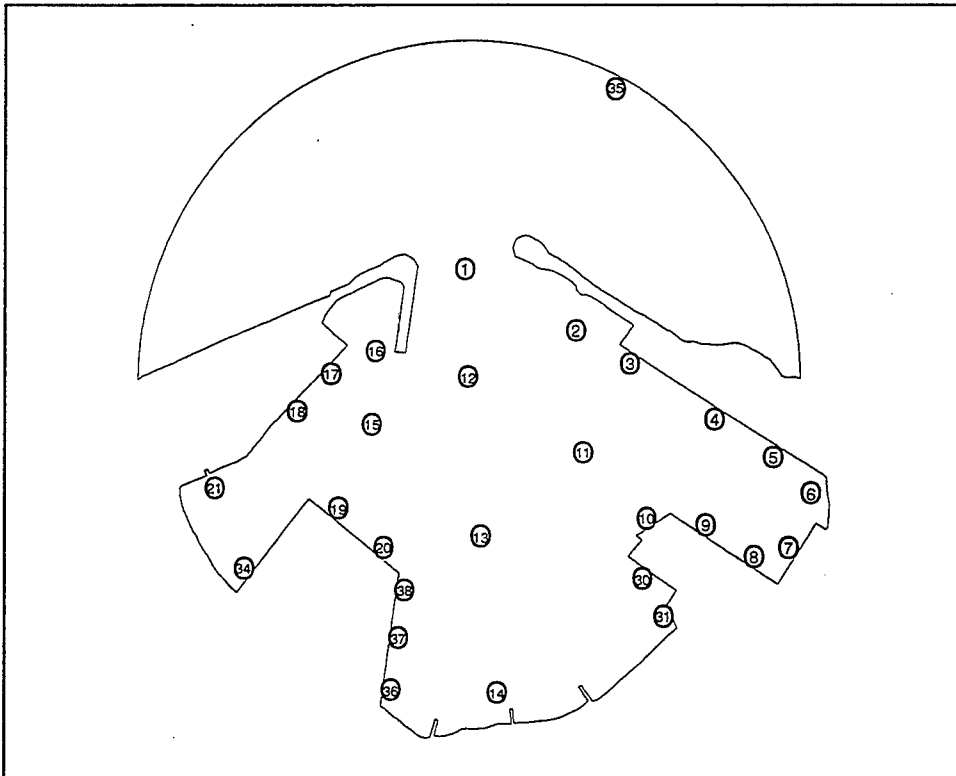
Figure E9. Basin locations, Plan 5

Figure E10. Basin locations, Plan 7

Appendix F
Wind Wave and Swell Summaries from Numerical Model

List of Tables

Table F1
$A_{amp,s}$ Values for $\theta_m = 192$ deg, Existing Harbor

Kahului Harbor - Existing Conditions - 192-deg Angle of Approach

Basin	Wave Period (sec)																
	8	9	10	11	12	13	14	15	16	17	18	19	20	21	22	23	24
1	0.81	0.82	0.81	0.83	0.86	0.88	0.89	0.89	0.90	0.90	0.90	0.89	0.87	0.85	0.83	0.83	0.82
2	0.30	0.28	0.26	0.25	0.23	0.21	0.20	0.20	0.21	0.22	0.23	0.23	0.23	0.24	0.25	0.24	0.24
3	0.19	0.19	0.16	0.15	0.15	0.13	0.13	0.13	0.13	0.14	0.15	0.16	0.17	0.17	0.16	0.16	0.16
4	0.17	0.14	0.12	0.12	0.10	0.09	0.09	0.10	0.10	0.10	0.09	0.09	0.09	0.09	0.10	0.11	0.11
5	0.16	0.15	0.12	0.10	0.09	0.08	0.08	0.08	0.08	0.09	0.10	0.09	0.09	0.09	0.10	0.10	0.10
6	0.09	0.08	0.08	0.07	0.07	0.07	0.07	0.07	0.07	0.08	0.08	0.07	0.07	0.07	0.08	0.08	0.08
7	0.10	0.10	0.09	0.09	0.08	0.08	0.08	0.10	0.09	0.09	0.10	0.10	0.11	0.12	0.12	0.10	0.09
8	0.08	0.09	0.09	0.09	0.09	0.08	0.09	0.11	0.11	0.11	0.11	0.11	0.11	0.11	0.10	0.08	0.08
9	0.13	0.12	0.13	0.12	0.11	0.11	0.11	0.11	0.11	0.11	0.11	0.12	0.13	0.13	0.12	0.11	0.09
10	0.18	0.19	0.18	0.18	0.19	0.21	0.23	0.24	0.24	0.23	0.24	0.24	0.23	0.21	0.18	0.17	0.17
11	0.26	0.23	0.21	0.21	0.22	0.22	0.22	0.23	0.22	0.22	0.22	0.22	0.22	0.20	0.19	0.18	0.17
12	0.51	0.49	0.47	0.48	0.48	0.47	0.46	0.46	0.46	0.46	0.46	0.46	0.48	0.49	0.50	0.51	0.51
13	0.30	0.31	0.29	0.29	0.29	0.30	0.30	0.28	0.28	0.28	0.29	0.31	0.32	0.31	0.31	0.31	0.32
14	0.23	0.24	0.22	0.22	0.23	0.22	0.23	0.23	0.23	0.24	0.25	0.26	0.27	0.27	0.28	0.28	0.28
15	0.52	0.50	0.50	0.53	0.55	0.54	0.53	0.51	0.51	0.50	0.50	0.51	0.52	0.53	0.54	0.56	0.57
16	0.59	0.58	0.59	0.60	0.60	0.60	0.59	0.57	0.56	0.56	0.56	0.56	0.56	0.55	0.56	0.56	0.57
17	0.46	0.46	0.49	0.49	0.50	0.49	0.48	0.46	0.44	0.42	0.40	0.38	0.36	0.34	0.34	0.34	0.34
18	0.70	0.70	0.73	0.71	0.68	0.65	0.61	0.58	0.56	0.53	0.50	0.47	0.45	0.43	0.43	0.43	0.44

(Continued)

Table F1 (Concluded)

Kahului Harbor - Existing Conditions - 192-deg Angle of Approach

Basin	Wave Period (sec)																
	8	9	10	11	12	13	14	15	16	17	18	19	20	21	22	23	24
19	0.81	0.78	0.73	0.73	0.74	0.73	0.70	0.67	0.66	0.66	0.66	0.67	0.68	0.69	0.71	0.71	0.70
20	0.45	0.44	0.44	0.43	0.42	0.42	0.44	0.46	0.47	0.47	0.47	0.47	0.46	0.47	0.48	0.50	0.49
21	0.72	0.68	0.67	0.64	0.62	0.61	0.60	0.58	0.58	0.55	0.52	0.50	0.47	0.45	0.44	0.42	0.42
25	0.21	0.21	0.21	0.21	0.21	0.21	0.22	0.22	0.23	0.24	0.24	0.22	0.20	0.19	0.20	0.23	0.26
26	0.28	0.25	0.24	0.25	0.26	0.28	0.28	0.28	0.28	0.28	0.27	0.25	0.25	0.25	0.26	0.26	0.25
30	0.23	0.22	0.22	0.22	0.22	0.22	0.23	0.23	0.24	0.24	0.24	0.23	0.21	0.19	0.20	0.22	0.24
31	0.34	0.30	0.28	0.28	0.28	0.29	0.29	0.28	0.28	0.29	0.29	0.27	0.24	0.24	0.25	0.26	0.26
32	0.85	0.80	0.77	0.77	0.77	0.74	0.71	0.66	0.64	0.63	0.64	0.65	0.68	0.70	0.71	0.72	0.72
33	0.52	0.51	0.50	0.52	0.52	0.51	0.51	0.52	0.52	0.52	0.53	0.53	0.53	0.53	0.52	0.51	0.49
34	0.47	0.45	0.44	0.46	0.47	0.47	0.47	0.47	0.47	0.47	0.47	0.48	0.48	0.47	0.47	0.47	0.48

Table F2
$A_{amp,s}$ Values for $\theta_m = 203$ deg, Existing Harbor

Kahului Harbor - Existing Conditions - 203-deg Angle of Approach

Basin	Wave Period (sec)																
	8	9	10	11	12	13	14	15	16	17	18	19	20	21	22	23	24
1	0.81	0.82	0.81	0.83	0.86	0.88	0.89	0.90	0.92	0.92	0.91	0.91	0.88	0.86	0.83	0.82	0.81
2	0.29	0.27	0.25	0.24	0.22	0.20	0.19	0.19	0.19	0.20	0.21	0.22	0.22	0.23	0.24	0.24	0.24
3	0.18	0.19	0.16	0.14	0.15	0.13	0.13	0.13	0.12	0.13	0.14	0.15	0.16	0.17	0.16	0.16	0.16
4	0.16	0.13	0.12	0.11	0.10	0.09	0.09	0.09	0.09	0.09	0.09	0.09	0.09	0.09	0.10	0.11	0.11
5	0.15	0.15	0.12	0.10	0.09	0.08	0.08	0.08	0.08	0.09	0.09	0.09	0.09	0.09	0.09	0.10	0.10
6	0.09	0.08	0.08	0.07	0.07	0.06	0.07	0.06	0.06	0.07	0.07	0.07	0.07	0.07	0.08	0.08	0.08
7	0.10	0.10	0.09	0.09	0.09	0.08	0.08	0.08	0.09	0.09	0.10	0.10	0.12	0.13	0.12	0.11	0.10
8	0.08	0.08	0.08	0.09	0.08	0.08	0.08	0.09	0.10	0.11	0.10	0.10	0.11	0.11	0.10	0.09	0.08
9	0.13	0.12	0.12	0.12	0.12	0.11	0.11	0.11	0.11	0.11	0.11	0.12	0.13	0.14	0.13	0.11	0.10
10	0.17	0.18	0.18	0.17	0.18	0.20	0.21	0.22	0.22	0.22	0.23	0.24	0.23	0.21	0.19	0.17	0.16
11	0.25	0.22	0.20	0.20	0.20	0.21	0.21	0.21	0.21	0.21	0.21	0.22	0.21	0.20	0.19	0.17	0.16
12	0.49	0.47	0.45	0.46	0.46	0.45	0.44	0.44	0.44	0.43	0.43	0.42	0.43	0.44	0.45	0.46	0.46
13	0.28	0.29	0.28	0.27	0.28	0.29	0.28	0.27	0.26	0.25	0.27	0.28	0.29	0.28	0.27	0.28	0.29
14	0.21	0.22	0.21	0.21	0.21	0.21	0.21	0.21	0.21	0.22	0.22	0.23	0.24	0.24	0.25	0.25	0.25
15	0.50	0.49	0.48	0.50	0.53	0.52	0.51	0.50	0.49	0.49	0.49	0.50	0.51	0.52	0.53	0.55	0.55
16	0.59	0.59	0.59	0.61	0.62	0.63	0.62	0.60	0.59	0.59	0.59	0.58	0.58	0.58	0.57	0.58	0.58
17	0.48	0.48	0.51	0.52	0.53	0.53	0.51	0.49	0.48	0.45	0.43	0.41	0.39	0.36	0.36	0.35	0.35
18	0.71	0.72	0.74	0.74	0.72	0.69	0.65	0.62	0.59	0.56	0.53	0.49	0.47	0.45	0.45	0.44	0.45

(Continued)

Appendix F Wind Wave and Swell Summaries from Numerical Model

Table F2 (Concluded)

Kahului Harbor - Existing Conditions - 203-deg Angle of Approach

Basin	Wave Period (sec)																
	8	9	10	11	12	13	14	15	16	17	18	19	20	21	22	23	24
19	0.78	0.75	0.70	0.69	0.70	0.69	0.67	0.64	0.63	0.63	0.63	0.65	0.66	0.67	0.68	0.68	0.67
20	0.42	0.42	0.42	0.40	0.39	0.39	0.41	0.43	0.44	0.44	0.43	0.44	0.43	0.43	0.45	0.46	0.46
21	0.71	0.67	0.66	0.64	0.63	0.62	0.61	0.60	0.60	0.57	0.54	0.51	0.49	0.46	0.45	0.42	0.42
25	0.20	0.20	0.20	0.20	0.20	0.20	0.21	0.21	0.22	0.24	0.24	0.22	0.20	0.18	0.18	0.20	0.23
26	0.26	0.24	0.23	0.24	0.25	0.26	0.26	0.26	0.27	0.27	0.27	0.25	0.23	0.23	0.23	0.23	0.22
30	0.21	0.21	0.21	0.21	0.20	0.20	0.21	0.21	0.23	0.24	0.23	0.22	0.21	0.19	0.18	0.20	0.22
31	0.32	0.29	0.27	0.27	0.26	0.27	0.27	0.26	0.27	0.28	0.28	0.26	0.24	0.22	0.23	0.23	0.23
32	0.83	0.78	0.74	0.74	0.74	0.72	0.68	0.64	0.62	0.61	0.63	0.65	0.67	0.69	0.70	0.70	0.71
33	0.49	0.48	0.47	0.49	0.49	0.47	0.47	0.47	0.47	0.47	0.48	0.49	0.49	0.48	0.47	0.46	0.45
34	0.44	0.43	0.41	0.43	0.43	0.43	0.43	0.43	0.43	0.43	0.43	0.44	0.44	0.43	0.43	0.43	0.44

Table F3
$A_{amp,s}$ Values for θ_m = 214 deg, Existing Harbor

Kahului Harbor - Existing Conditions - 214-deg Angle of Approach

Basin	Wave Period (sec)																
	8	9	10	11	12	13	14	15	16	17	18	19	20	21	22	23	24
1	0.81	0.81	0.81	0.82	0.85	0.86	0.87	0.89	0.91	0.91	0.90	0.89	0.87	0.84	0.81	0.78	0.77
2	0.27	0.26	0.24	0.22	0.21	0.19	0.18	0.17	0.17	0.17	0.19	0.20	0.20	0.22	0.23	0.23	0.23
3	0.18	0.18	0.15	0.14	0.14	0.13	0.12	0.12	0.11	0.12	0.13	0.14	0.15	0.16	0.16	0.16	0.16
4	0.16	0.13	0.11	0.11	0.10	0.09	0.08	0.08	0.08	0.08	0.08	0.08	0.09	0.09	0.10	0.10	0.11
5	0.15	0.15	0.12	0.10	0.09	0.08	0.08	0.07	0.07	0.08	0.09	0.09	0.09	0.09	0.09	0.10	0.10
6	0.09	0.08	0.07	0.07	0.07	0.06	0.06	0.06	0.06	0.06	0.07	0.07	0.06	0.07	0.08	0.08	0.09
7	0.10	0.10	0.09	0.09	0.08	0.08	0.08	0.07	0.08	0.08	0.09	0.10	0.12	0.13	0.13	0.12	0.10
8	0.07	0.08	0.08	0.08	0.08	0.08	0.08	0.08	0.09	0.10	0.10	0.10	0.10	0.11	0.10	0.09	0.08
9	0.12	0.12	0.12	0.12	0.11	0.11	0.10	0.10	0.10	0.10	0.11	0.12	0.13	0.14	0.13	0.11	0.10
10	0.17	0.17	0.17	0.17	0.17	0.18	0.19	0.20	0.20	0.21	0.22	0.23	0.23	0.22	0.19	0.16	0.15
11	0.23	0.21	0.19	0.18	0.19	0.19	0.18	0.19	0.19	0.19	0.20	0.21	0.21	0.20	0.18	0.16	0.15
12	0.47	0.44	0.43	0.43	0.44	0.43	0.41	0.40	0.40	0.39	0.37	0.36	0.37	0.37	0.38	0.38	0.39
13	0.26	0.27	0.26	0.25	0.25	0.26	0.25	0.24	0.22	0.22	0.22	0.24	0.24	0.23	0.23	0.23	0.24
14	0.19	0.21	0.20	0.19	0.19	0.20	0.20	0.19	0.19	0.18	0.19	0.19	0.20	0.20	0.20	0.20	0.20
15	0.48	0.47	0.46	0.47	0.49	0.49	0.47	0.46	0.46	0.45	0.45	0.47	0.48	0.49	0.50	0.51	0.52
16	0.59	0.59	0.60	0.62	0.64	0.64	0.63	0.61	0.61	0.60	0.59	0.59	0.59	0.58	0.58	0.57	0.57
17	0.49	0.49	0.52	0.54	0.56	0.56	0.54	0.52	0.51	0.48	0.45	0.42	0.40	0.38	0.37	0.36	0.36
18	0.72	0.72	0.75	0.76	0.74	0.72	0.68	0.64	0.61	0.58	0.54	0.51	0.48	0.46	0.45	0.44	0.44

(Continued)

Table F3 (Concluded)

Kahului Harbor - Existing Conditions - 214-deg Angle of Approach

Basin	Wave Period (sec)																
	8	9	10	11	12	13	14	15	16	17	18	19	20	21	22	23	24
19	0.74	0.71	0.66	0.64	0.64	0.63	0.61	0.58	0.57	0.57	0.57	0.59	0.60	0.61	0.62	0.62	0.61
20	0.39	0.39	0.40	0.38	0.35	0.35	0.36	0.38	0.39	0.38	0.38	0.38	0.37	0.38	0.39	0.40	0.40
21	0.70	0.66	0.65	0.63	0.62	0.62	0.61	0.59	0.59	0.57	0.53	0.51	0.48	0.45	0.44	0.41	0.41
25	0.19	0.19	0.19	0.19	0.18	0.18	0.18	0.19	0.21	0.22	0.23	0.21	0.19	0.17	0.17	0.17	0.19
26	0.25	0.23	0.22	0.22	0.22	0.23	0.23	0.23	0.25	0.26	0.25	0.23	0.22	0.20	0.20	0.19	0.19
30	0.20	0.20	0.20	0.20	0.19	0.18	0.19	0.19	0.21	0.22	0.22	0.22	0.20	0.18	0.17	0.17	0.18
31	0.29	0.27	0.26	0.25	0.24	0.24	0.24	0.23	0.25	0.26	0.27	0.25	0.23	0.20	0.20	0.19	0.19
32	0.81	0.75	0.71	0.70	0.70	0.68	0.64	0.59	0.58	0.57	0.58	0.60	0.63	0.65	0.65	0.65	0.66
33	0.46	0.45	0.44	0.45	0.44	0.42	0.41	0.40	0.40	0.40	0.41	0.41	0.41	0.41	0.40	0.39	0.38
34	0.41	0.40	0.39	0.40	0.40	0.39	0.37	0.37	0.37	0.37	0.37	0.37	0.38	0.37	0.36	0.37	0.37

Table F4
$A_{amp,s}$ Values for θ_m = 225 deg, Existing Harbor

Kahului Harbor - Existing Conditions - 225-deg Angle of Approach

Basin	Wave Period (sec)																
	8	9	10	11	12	13	14	15	16	17	18	19	20	21	22	23	24
1	0.80	0.80	0.80	0.81	0.83	0.83	0.83	0.84	0.87	0.87	0.84	0.81	0.80	0.78	0.75	0.72	0.71
2	0.26	0.24	0.22	0.20	0.19	0.18	0.16	0.15	0.14	0.14	0.16	0.17	0.18	0.19	0.21	0.21	0.21
3	0.17	0.17	0.15	0.13	0.14	0.12	0.11	0.10	0.10	0.10	0.11	0.12	0.14	0.14	0.15	0.15	0.15
4	0.16	0.12	0.11	0.10	0.09	0.08	0.08	0.07	0.07	0.07	0.07	0.07	0.08	0.08	0.09	0.10	0.11
5	0.14	0.14	0.12	0.09	0.08	0.08	0.07	0.06	0.07	0.07	0.08	0.08	0.08	0.08	0.08	0.09	0.09
6	0.09	0.08	0.07	0.07	0.06	0.06	0.05	0.05	0.05	0.06	0.06	0.06	0.06	0.06	0.07	0.08	0.08
7	0.09	0.09	0.08	0.08	0.08	0.08	0.07	0.07	0.07	0.08	0.08	0.09	0.11	0.12	0.12	0.12	0.11
8	0.07	0.07	0.08	0.08	0.08	0.08	0.07	0.07	0.08	0.09	0.09	0.09	0.09	0.10	0.09	0.08	0.07
9	0.12	0.12	0.12	0.12	0.11	0.11	0.10	0.09	0.09	0.09	0.10	0.11	0.13	0.13	0.13	0.11	0.10
10	0.17	0.16	0.16	0.16	0.16	0.16	0.16	0.17	0.17	0.17	0.18	0.19	0.22	0.21	0.18	0.16	0.14
11	0.21	0.19	0.18	0.17	0.17	0.17	0.16	0.16	0.17	0.17	0.18	0.19	0.19	0.19	0.18	0.16	0.14
12	0.44	0.42	0.40	0.40	0.40	0.39	0.37	0.36	0.35	0.34	0.31	0.30	0.29	0.30	0.30	0.31	0.31
13	0.24	0.25	0.24	0.23	0.23	0.23	0.23	0.21	0.19	0.18	0.18	0.19	0.19	0.19	0.18	0.18	0.19
14	0.18	0.19	0.18	0.17	0.18	0.18	0.18	0.17	0.16	0.15	0.15	0.15	0.16	0.16	0.16	0.16	0.16
15	0.46	0.45	0.43	0.43	0.45	0.44	0.42	0.41	0.40	0.40	0.39	0.40	0.42	0.43	0.44	0.45	0.46
16	0.59	0.58	0.59	0.62	0.64	0.64	0.62	0.59	0.59	0.58	0.56	0.55	0.55	0.54	0.54	0.54	0.54
17	0.50	0.50	0.53	0.56	0.58	0.57	0.54	0.52	0.50	0.47	0.44	0.41	0.39	0.36	0.35	0.34	0.34
18	0.72	0.73	0.76	0.76	0.75	0.72	0.67	0.62	0.60	0.56	0.52	0.48	0.45	0.43	0.42	0.41	0.42

(Continued)

Table F4 (Concluded)

Kahului Harbor - Existing Conditions - 225-deg Angle of Approach

Basin	Wave Period (sec)																
	8	9	10	11	12	13	14	15	16	17	18	19	20	21	22	23	24
19	0.70	0.67	0.62	0.58	0.57	0.56	0.52	0.49	0.49	0.48	0.48	0.50	0.51	0.53	0.54	0.53	0.53
20	0.36	0.36	0.37	0.35	0.32	0.30	0.31	0.32	0.32	0.32	0.31	0.30	0.30	0.31	0.33	0.34	0.34
21	0.68	0.64	0.63	0.61	0.60	0.59	0.57	0.56	0.56	0.53	0.49	0.46	0.44	0.41	0.40	0.38	0.37
25	0.18	0.18	0.19	0.18	0.16	0.16	0.16	0.16	0.19	0.20	0.21	0.20	0.18	0.16	0.15	0.14	0.15
26	0.23	0.22	0.21	0.20	0.20	0.20	0.20	0.20	0.22	0.24	0.23	0.22	0.19	0.18	0.17	0.16	0.16
30	0.19	0.19	0.19	0.19	0.17	0.16	0.16	0.17	0.19	0.20	0.21	0.21	0.19	0.17	0.15	0.14	0.15
31	0.27	0.25	0.25	0.23	0.21	0.20	0.20	0.20	0.22	0.24	0.25	0.23	0.21	0.18	0.17	0.16	0.16
32	0.78	0.71	0.67	0.65	0.64	0.61	0.57	0.52	0.50	0.50	0.50	0.52	0.55	0.57	0.58	0.58	0.58
33	0.43	0.42	0.41	0.41	0.40	0.37	0.34	0.33	0.33	0.33	0.32	0.33	0.33	0.32	0.32	0.31	0.31
34	0.38	0.37	0.36	0.36	0.35	0.34	0.31	0.30	0.30	0.30	0.29	0.30	0.30	0.29	0.29	0.30	0.30

Table F5
A_{amps} Values for θ_m = 236 deg, Existing Harbor

Kahului Harbor - Existing Conditions - 236-deg Angle of Approach

Basin	Wave Period (sec)																
	8	9	10	11	12	13	14	15	16	17	18	19	20	21	22	23	24
1	0.79	0.79	0.79	0.79	0.80	0.79	0.78	0.79	0.81	0.82	0.78	0.74	0.72	0.70	0.69	0.67	0.66
2	0.24	0.23	0.20	0.18	0.17	0.16	0.15	0.13	0.12	0.12	0.13	0.14	0.15	0.17	0.19	0.20	0.20
3	0.16	0.17	0.14	0.13	0.13	0.12	0.10	0.09	0.09	0.09	0.10	0.11	0.12	0.13	0.13	0.14	0.15
4	0.15	0.12	0.10	0.09	0.09	0.08	0.07	0.06	0.06	0.06	0.06	0.06	0.07	0.08	0.09	0.10	0.10
5	0.14	0.14	0.11	0.09	0.08	0.07	0.07	0.06	0.06	0.07	0.07	0.07	0.07	0.07	0.08	0.08	0.09
6	0.09	0.07	0.07	0.06	0.06	0.05	0.05	0.04	0.05	0.05	0.05	0.05	0.05	0.06	0.07	0.08	0.08
7	0.09	0.09	0.08	0.08	0.08	0.07	0.07	0.06	0.06	0.07	0.07	0.08	0.10	0.11	0.12	0.11	0.10
8	0.07	0.07	0.07	0.07	0.07	0.07	0.07	0.06	0.07	0.08	0.08	0.08	0.08	0.09	0.09	0.08	0.07
9	0.12	0.12	0.11	0.11	0.10	0.10	0.09	0.08	0.08	0.08	0.09	0.10	0.11	0.12	0.12	0.11	0.09
10	0.16	0.15	0.15	0.15	0.15	0.15	0.14	0.14	0.16	0.17	0.18	0.19	0.20	0.19	0.17	0.15	0.13
11	0.20	0.18	0.17	0.16	0.15	0.15	0.14	0.14	0.15	0.15	0.16	0.17	0.17	0.17	0.16	0.15	0.13
12	0.42	0.39	0.38	0.37	0.37	0.36	0.33	0.32	0.32	0.30	0.27	0.25	0.24	0.24	0.25	0.26	0.26
13	0.22	0.23	0.23	0.21	0.20	0.21	0.20	0.19	0.17	0.16	0.15	0.15	0.16	0.15	0.15	0.15	0.15
14	0.16	0.17	0.17	0.16	0.16	0.17	0.16	0.15	0.14	0.13	0.12	0.12	0.13	0.13	0.13	0.13	0.13
15	0.43	0.42	0.41	0.40	0.40	0.39	0.37	0.35	0.35	0.34	0.33	0.34	0.36	0.38	0.39	0.41	0.42
16	0.58	0.57	0.59	0.61	0.62	0.62	0.58	0.56	0.55	0.54	0.51	0.49	0.49	0.49	0.49	0.49	0.50
17	0.50	0.50	0.53	0.56	0.58	0.56	0.53	0.49	0.48	0.45	0.41	0.37	0.35	0.33	0.32	0.31	0.31
18	0.71	0.72	0.75	0.76	0.74	0.70	0.64	0.59	0.56	0.52	0.48	0.43	0.41	0.39	0.38	0.37	0.38

(Continued)

Table F5 (Concluded)

Kahului Harbor - Existing Conditions - 236-deg Angle of Approach

Basin	Wave Period (sec)																
	8	9	10	11	12	13	14	15	16	17	18	19	20	21	22	23	24
19	0.66	0.62	0.58	0.52	0.50	0.48	0.45	0.42	0.41	0.41	0.40	0.41	0.43	0.45	0.46	0.47	0.47
20	0.33	0.33	0.35	0.32	0.28	0.26	0.26	0.26	0.27	0.26	0.25	0.24	0.25	0.26	0.28	0.29	0.29
21	0.65	0.62	0.61	0.58	0.57	0.56	0.53	0.51	0.51	0.48	0.44	0.41	0.38	0.36	0.35	0.33	0.33
25	0.17	0.17	0.18	0.16	0.15	0.14	0.14	0.14	0.17	0.19	0.19	0.18	0.16	0.15	0.14	0.13	0.13
26	0.21	0.21	0.20	0.19	0.18	0.17	0.17	0.18	0.20	0.23	0.22	0.20	0.18	0.16	0.16	0.15	0.14
30	0.18	0.17	0.18	0.17	0.16	0.14	0.14	0.15	0.17	0.19	0.19	0.19	0.18	0.16	0.14	0.13	0.13
31	0.25	0.23	0.23	0.21	0.19	0.18	0.17	0.18	0.20	0.23	0.23	0.21	0.19	0.17	0.15	0.15	0.14
32	0.74	0.67	0.63	0.59	0.58	0.55	0.49	0.44	0.43	0.42	0.43	0.44	0.47	0.49	0.50	0.51	0.52
33	0.39	0.38	0.38	0.37	0.35	0.32	0.28	0.27	0.26	0.26	0.26	0.26	0.26	0.26	0.26	0.25	0.25
34	0.35	0.34	0.33	0.32	0.31	0.29	0.26	0.25	0.25	0.25	0.24	0.24	0.24	0.24	0.24	0.25	0.26

Table F6
$A_{amp,s}$ Values Weighted by Wind Wave and Swell Climate

Basin	Plan										Remarks
	Existing	1	2	3a	3b	3c	4a	4b	4c	5	
Pier 1											
2	0.25	0.15	0.25	0.17	0.15	0.15	0.18	0.17	0.17	0.20	
3	0.16	0.09	0.17	0.14	0.12	0.11	0.19	0.14	0.11	0.15	
4	0.13	0.06	0.13	0.08	0.06	0.07	0.14	0.08	0.07	0.10	
5	0.12	0.04	0.14	0.07	0.05	0.06	0.11	0.05	0.05	0.09	
6	0.08	0.04	0.10	0.05	0.07	0.04	0.07	0.05	0.05	0.07	
Piers 2 & 3											
7	0.09	0.06	0.09	0.08	0.09	0.07	0.08	0.07	0.07	0.08	
8	0.08	0.08	0.09	0.09	0.09	0.08	0.10	0.09	0.09	0.08	Pier 2 gage
9	0.12	0.09	0.11	0.12	0.11	0.11	0.12	0.11	0.11	0.10	
10	0.18	0.14	0.17	0.16	0.17	0.16	0.17	0.17	0.17	0.19	
Barge Pier (Planned)											
25		0.14									Concept C
26		0.14									Concept C
30			0.12	0.12	0.12	0.11	0.12	0.12	0.11	0.12	Concept 12
Boat Ramp											
21	0.21	0.19	0.19	0.16	0.11	0.06	0.11	0.08	0.04	0.20	Adjusted for β=0.032
Passenger Ship Pier (Planned)											
17							0.35	0.15	0.07		Adjacent to existing fill
18							0.30	0.17	0.06		" " " "
23		0.12	0.14								Slip in existing fill
28				0.14	0.10	0.04					Notch in existing fill
29				0.14	0.11	0.08					" " " "
32										0.11	New fill in SW harbor area
33										0.17	" " " " " "
Other Harbor Areas											
1	0.83	0.81	0.84	0.85	0.84	0.84	0.83	0.83	0.84	0.84	
11	0.22	0.17	0.22	0.19	0.19	0.18	0.24	0.19	0.18	0.20	
12	0.46	0.42	0.46	0.46	0.47	0.46	0.46	0.47	0.46	0.44	
13	0.27	0.23	0.26	0.27	0.29	0.30	0.26	0.28	0.30	0.29	
14	0.21	0.17	0.20	0.21	0.23	0.24	0.21	0.28	0.24	0.23	Back Basin gage

(Continued)

Table F6 (Concluded)

Basin	Plan										Remarks
	Existing	1	2	3a	3b	3c	4a	4b	4c	5	
Other Harbor Areas (concluded)											
15	0.49	0.53	0.58	0.55	0.31	0.13	0.55	0.32	0.16	0.54	
16	0.60	0.52	0.54	0.56	0.17	0.03	0.53	0.16	0.05	0.63	Channel Entrance gage
17	0.50	0.34	0.37	0.40	0.16	0.05				0.52	
18	0.70	0.46	0.53	0.38	0.17	0.05				0.72	
19	0.71	0.64	0.85	0.64	0.41	0.25	0.85	0.53	0.34	0.69	
20	0.40	0.36	0.42	0.46	0.39	0.33	0.48	0.39	0.34	0.41	
22		0.07	0.08								
24		0.22	0.25								
25	0.20										
26	0.25										
27				0.18	0.11	0.05					
30	0.21										Canoe Club gage (approx)
31	0.28		0.11	0.14	0.12	0.09	0.10	0.10	0.10	0.10	
32	0.75										
33	0.47										
34	0.42									0.30	
35	1.09	1.06	1.09	1.08	1.08	1.08	1.08	1.08	1.08	1.08	Array gage

Table F7
H_s Values Exceeded 10 Percent and 1 Percent of the Time at Piers

Basin Number	H_s Values Exceeded 10% and 1% of Time (ft)							
	Existing		Plan 1		Plan 2		Plan 3a	
	10%	1%	10%	1%	10%	1%	10%	1%
Pier 1								
2	1.19	1.71	1.18	1.68	1.19	1.70	0.87	1.33
3	0.79	1.12	0.82	1.16	0.83	1.18	0.68	0.96
4	0.60	0.85	0.58	0.83	0.59	0.83	0.39	0.63
5	0.59	0.85	0.66	0.98	0.67	0.98	0.33	0.48
6	0.37	0.51	0.47	0.67	0.47	0.66	0.25	0.39
Piers 2 & 3								
7	0.44	0.63	0.43	0.62	0.42	0.61	0.40	0.58
8	0.42	0.63	0.46	0.69	0.46	0.68	0.47	0.73
9	0.58	0.84	0.56	0.84	0.56	0.81	0.61	0.95
10	0.94	1.43	0.87	1.31	0.85	1.26	0.83	1.21
Barge Pier (Planned)								
25			0.91	1.29				
26			0.76	1.13				
30					0.57	0.80	0.57	0.84
Boat Ramp								
21	1.04	1.52	1.06	1.50	1.04	1.47	0.71	1.04
Passenger Ship Pier (Planned)								
23			0.63	0.89	0.63	0.89		
28							0.69	1.04
29							0.65	0.96
								(Sheet 1 of 3)

Table F7 (Continued)

Basin Number	H_s Values Exceeded 10% and 1% of Time (ft)							
	Plan 3b		Plan 3c		Plan 4a		Plan 4b	
	10%	1%	10%	1%	10%	1%	10%	1%
Pier 1								
2	0.79	1.20	0.78	1.17	0.95	1.46	0.86	1.33
3	0.57	0.88	0.53	0.80	0.85	1.24	0.66	0.93
4	0.33	0.51	0.34	0.53	0.64	0.93	0.41	0.63
5	0.26	0.36	0.27	0.39	0.49	0.71	0.26	0.39
6	0.34	0.52	0.21	0.32	0.33	0.47	0.22	0.33
Piers 2 & 3								
7	0.43	0.66	0.35	0.53	0.40	0.57	0.34	0.53
8	0.43	0.66	0.43	0.67	0.48	0.72	0.44	0.68
9	0.54	0.82	0.53	0.81	0.57	0.84	0.52	0.80
10	0.87	1.30	0.84	1.26	0.88	1.29	0.88	1.37
Barge Pier (Planned)								
25								
26								
30	0.61	0.90	0.55	0.83	0.55	0.82	0.62	0.92
Boat Ramp								
21	0.49	0.72	0.49	0.69	0.56	0.84	0.24	0.37
Passenger Ship Pier (Planned)								
17					1.71	2.55	0.80	1.27
18					1.49	2.22	0.93	1.48
28	0.53	0.85	0.19	0.31				
29	0.55	0.82	0.41	0.62				

(Sheet 2 of 3)

Table F7 (Concluded)

Basin Number	H_s Values Exceeded 10% and 1% of Time (ft)							
	Plan 4c		Plan 5		Plan 6		Plan 7	
	10%	1%	10%	1%	10%	1%	10%	1%
Pier 1								
2	0.83	1.25	0.96	1.40	0.83	1.27	0.90	1.41
3	0.56	0.85	0.74	1.06	0.65	0.93	0.59	0.92
4	0.34	0.54	0.46	0.71	0.39	0.58	0.33	0.51
5	0.24	0.37	0.40	0.57	0.25	0.36	0.28	0.43
6	0.23	0.33	0.34	0.48	0.22	0.32	0.20	0.30
Piers 2 & 3								
7	0.35	0.53	0.40	0.57	0.34	0.54	0.37	0.56
8	0.46	0.70	0.43	0.65	0.45	0.69	0.45	0.72
9	0.53	0.82	0.51	0.77	0.51	0.80	0.50	0.78
10	0.87	1.32	0.95	1.39	0.87	1.30	0.94	1.44
Barge Pier (Planned)								
30	0.58	0.86	0.58	0.88	0.60	0.88	0.62	0.98
Boat Ramp								
21	0.21	0.31	1.22	1.81	0.29	0.45	0.37	0.58
Passenger Ship Pier (Planned)								
17	0.33	0.47			0.78	1.23		
18	0.29	0.45			0.88	1.39		
32			0.55	0.82				
33			0.84	1.25				
36							1.06	1.54
37							1.22	1.76
38							1.46	2.12

(Sheet 3 of 3)

Appendix G
Harbor Oscillation Summaries from Numerical Model

List of Figures

List of Tables

Figure G1. Long wave response, Pier 1 (Continued)
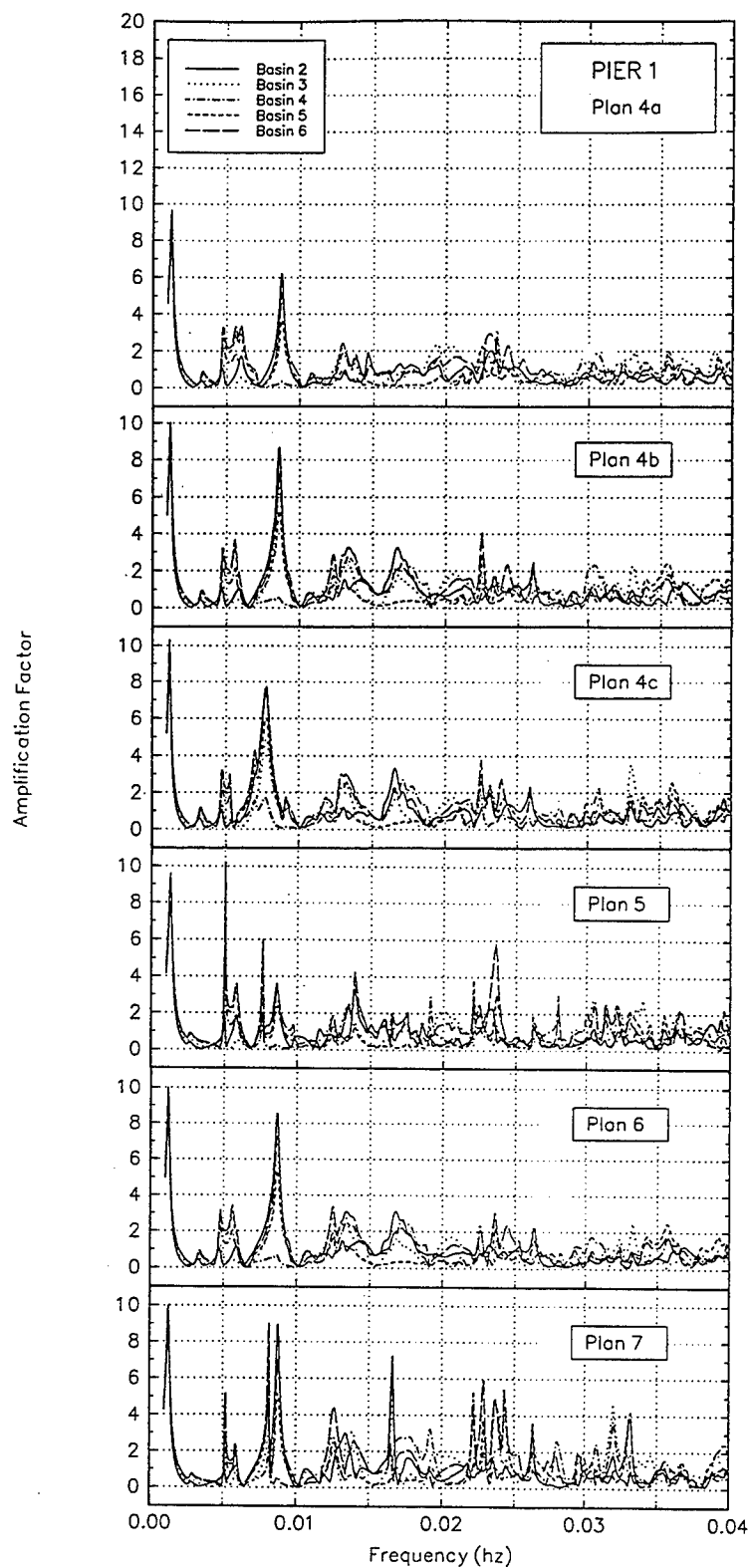
Figure G1. (Concluded)
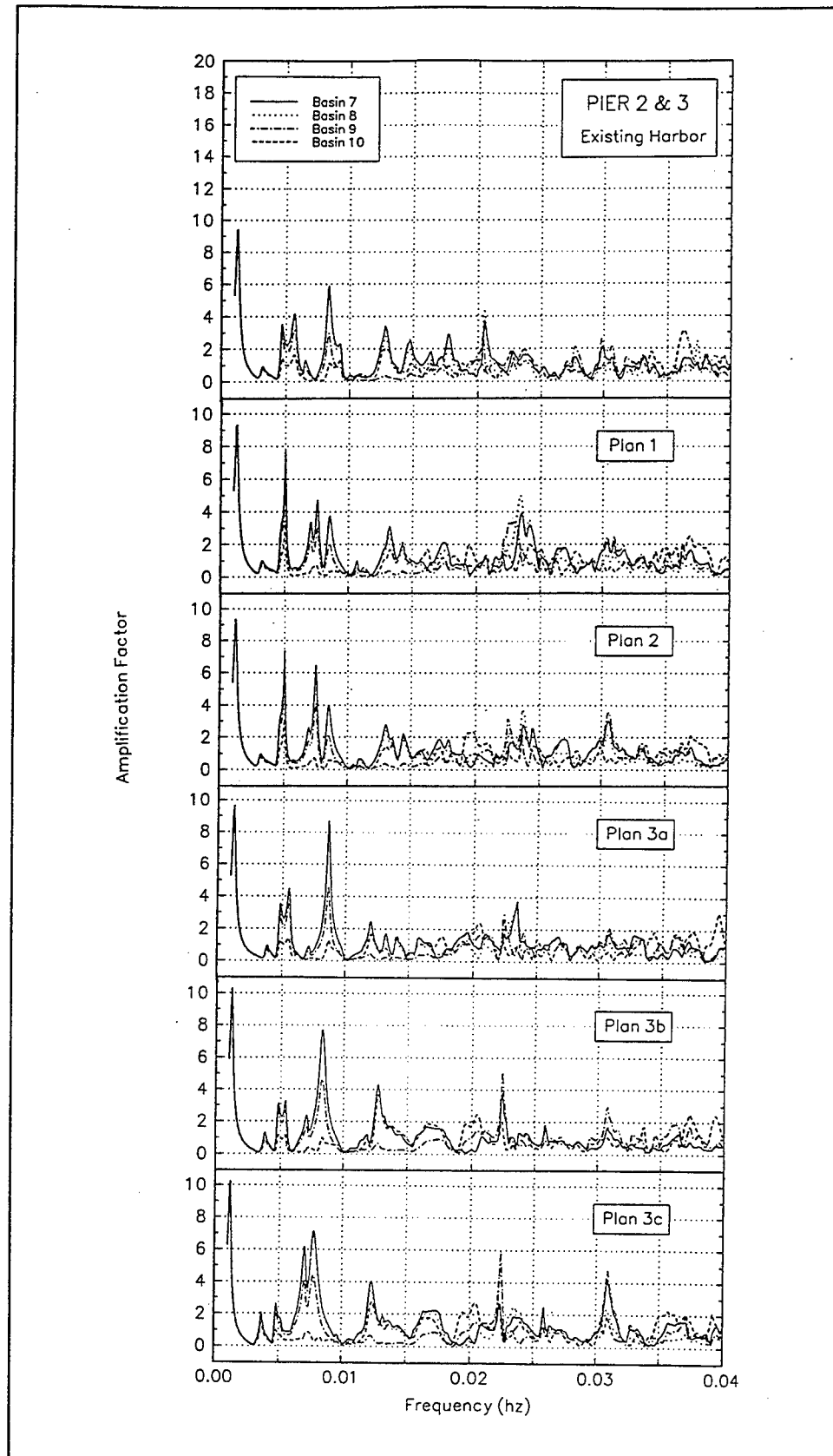
Figure G2. Long wave response, Piers 2 and 3 (Continued)
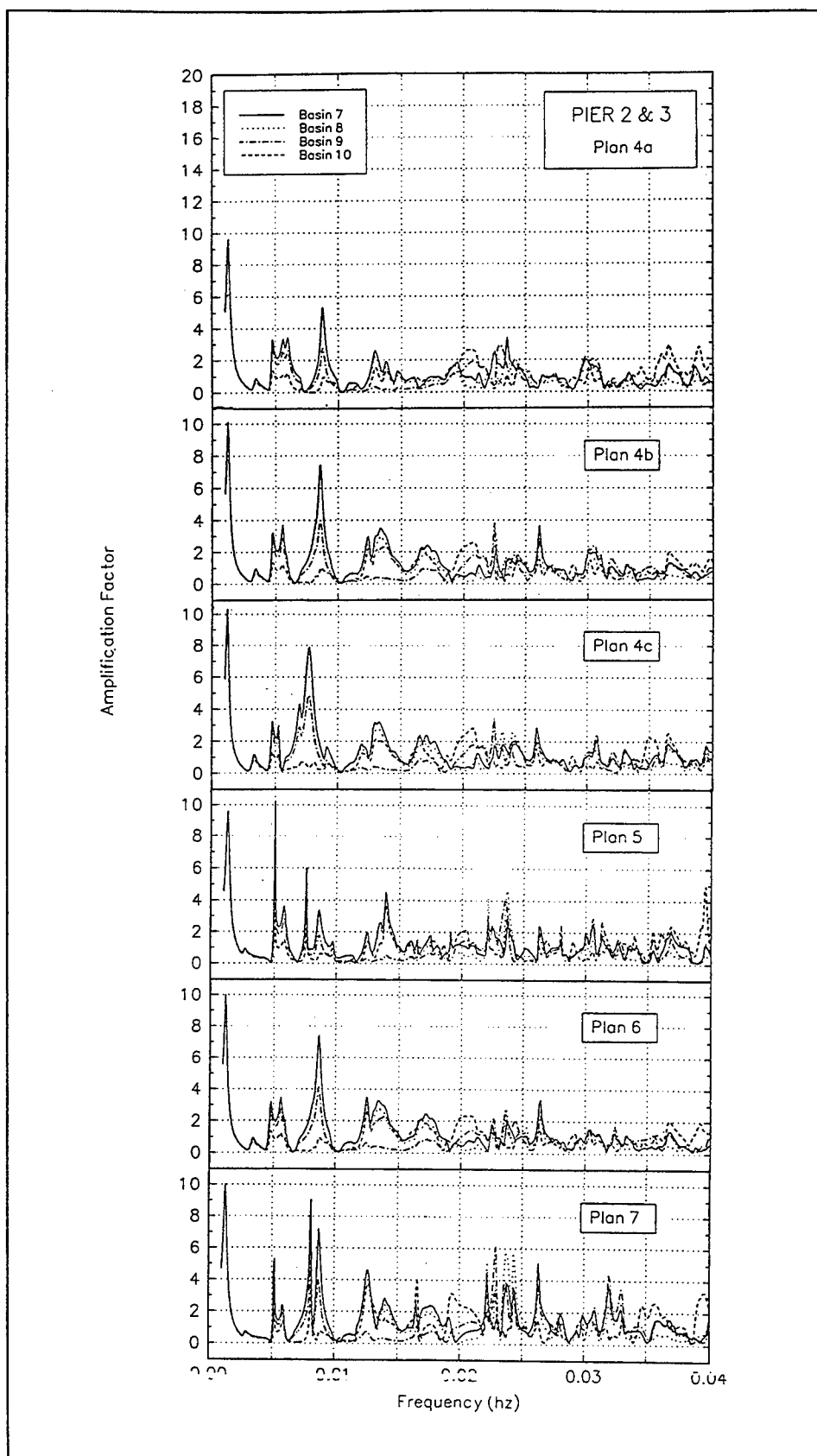
Figure G2. (Concluded)
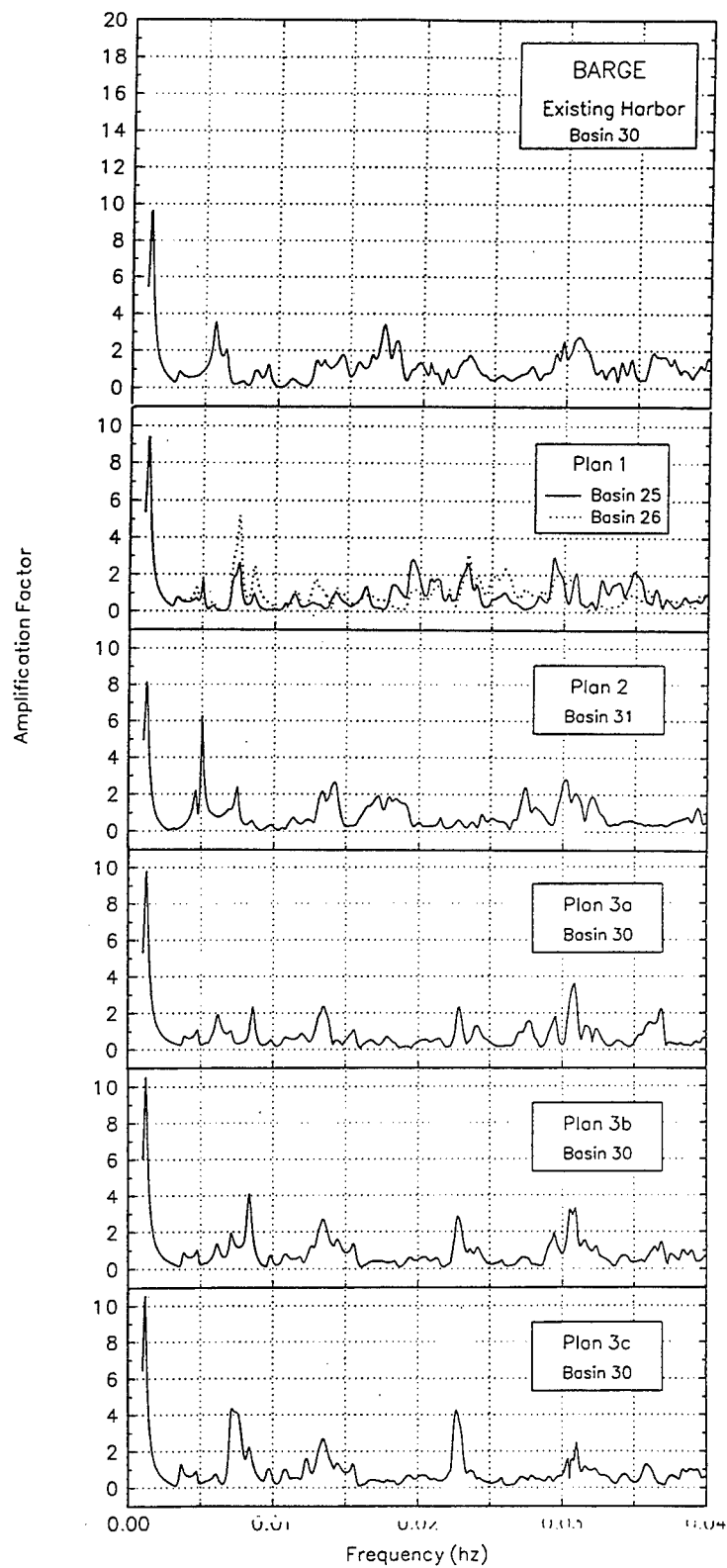
Figure G3. Long wave response, barge pier (Continued)
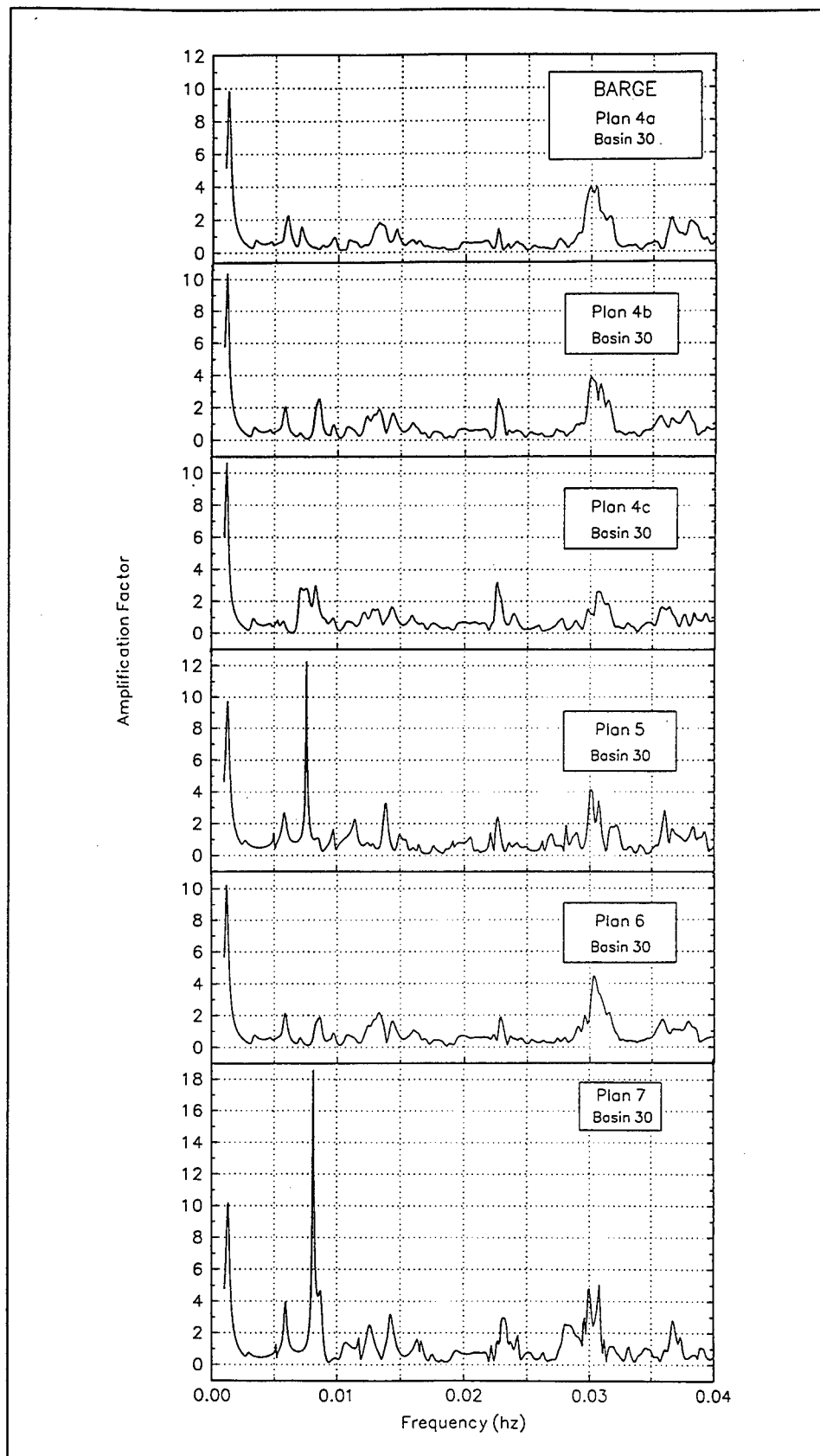
Figure G3. (Concluded)
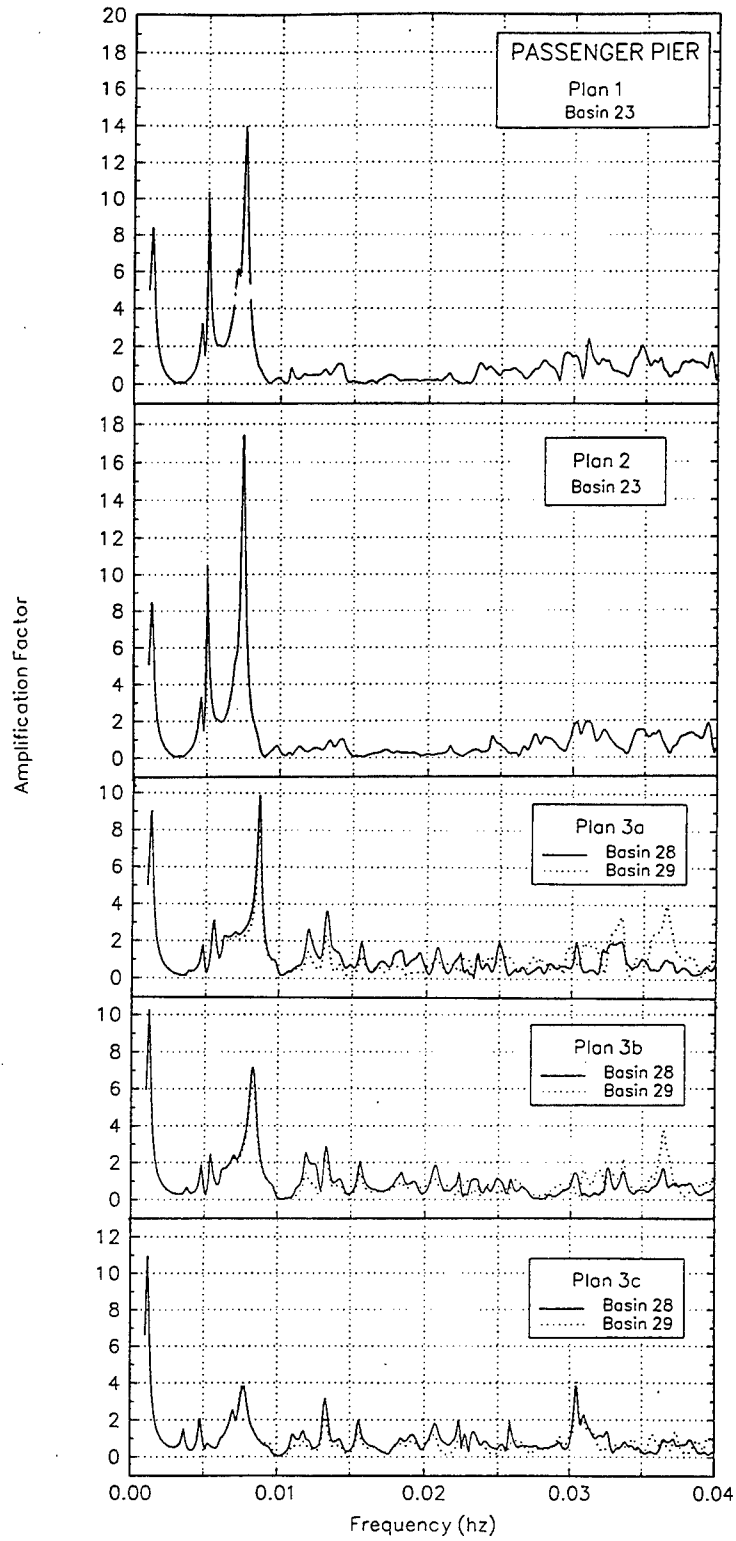
Figure G4. Long wave response, passenger pier (Continued)
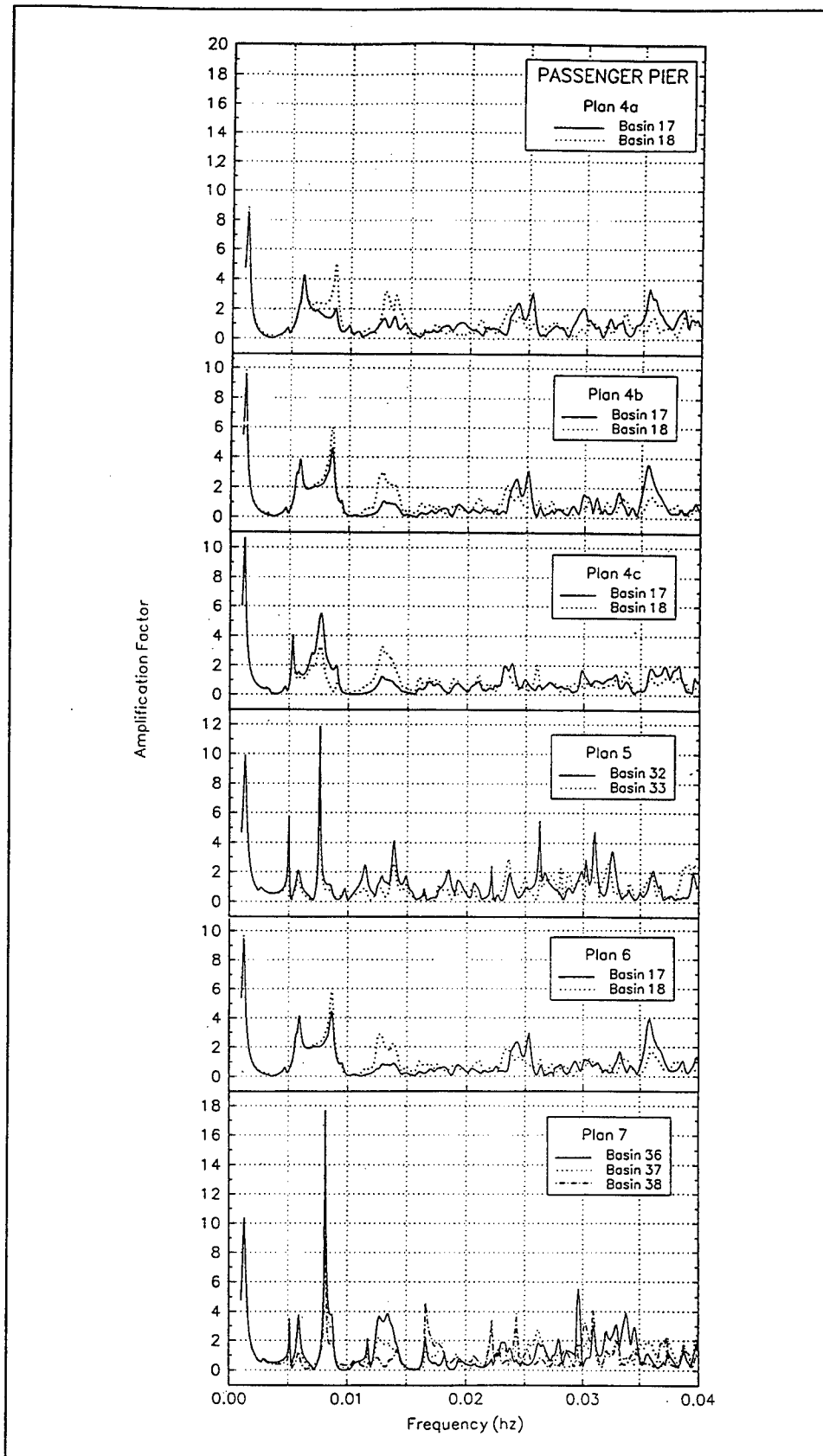
Figure G4. (Concluded)
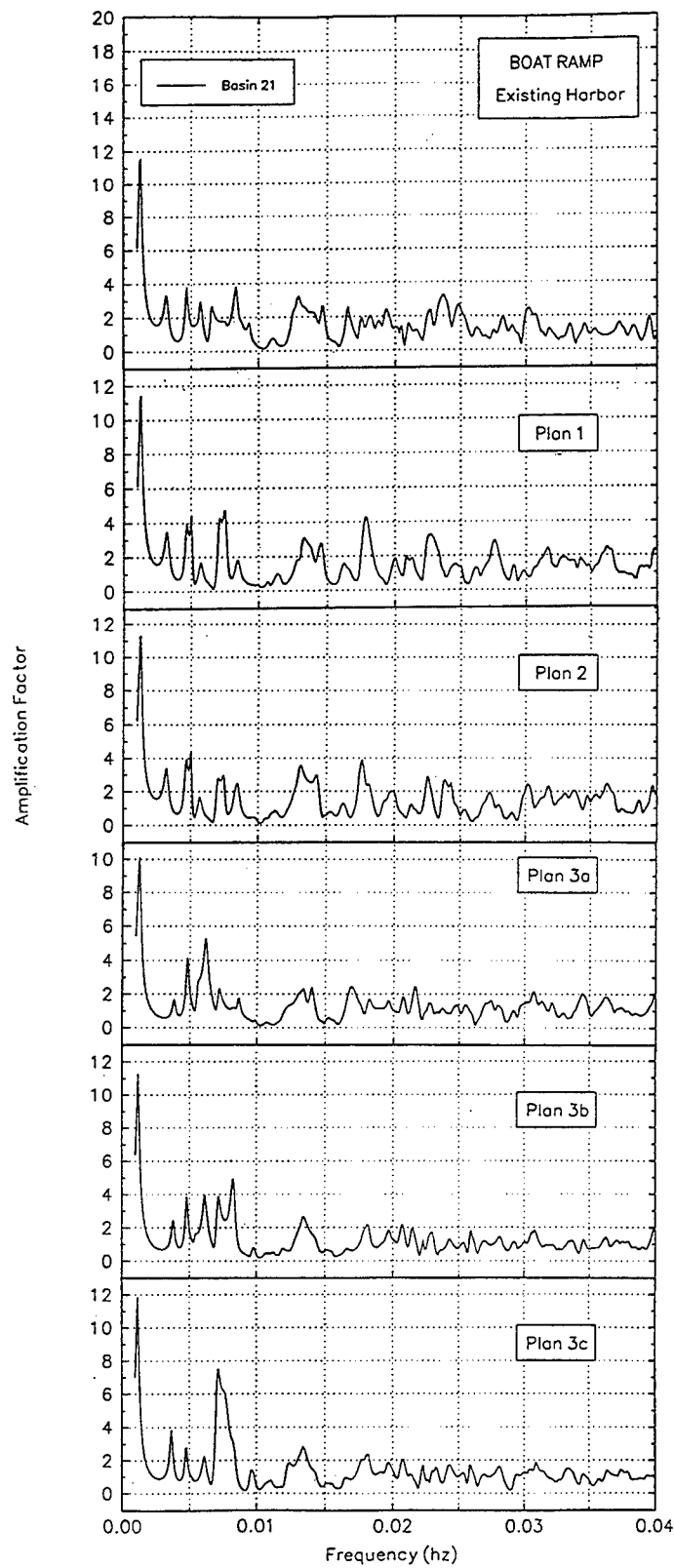
Figure G5. Long wave response, boat ramp (Continued)
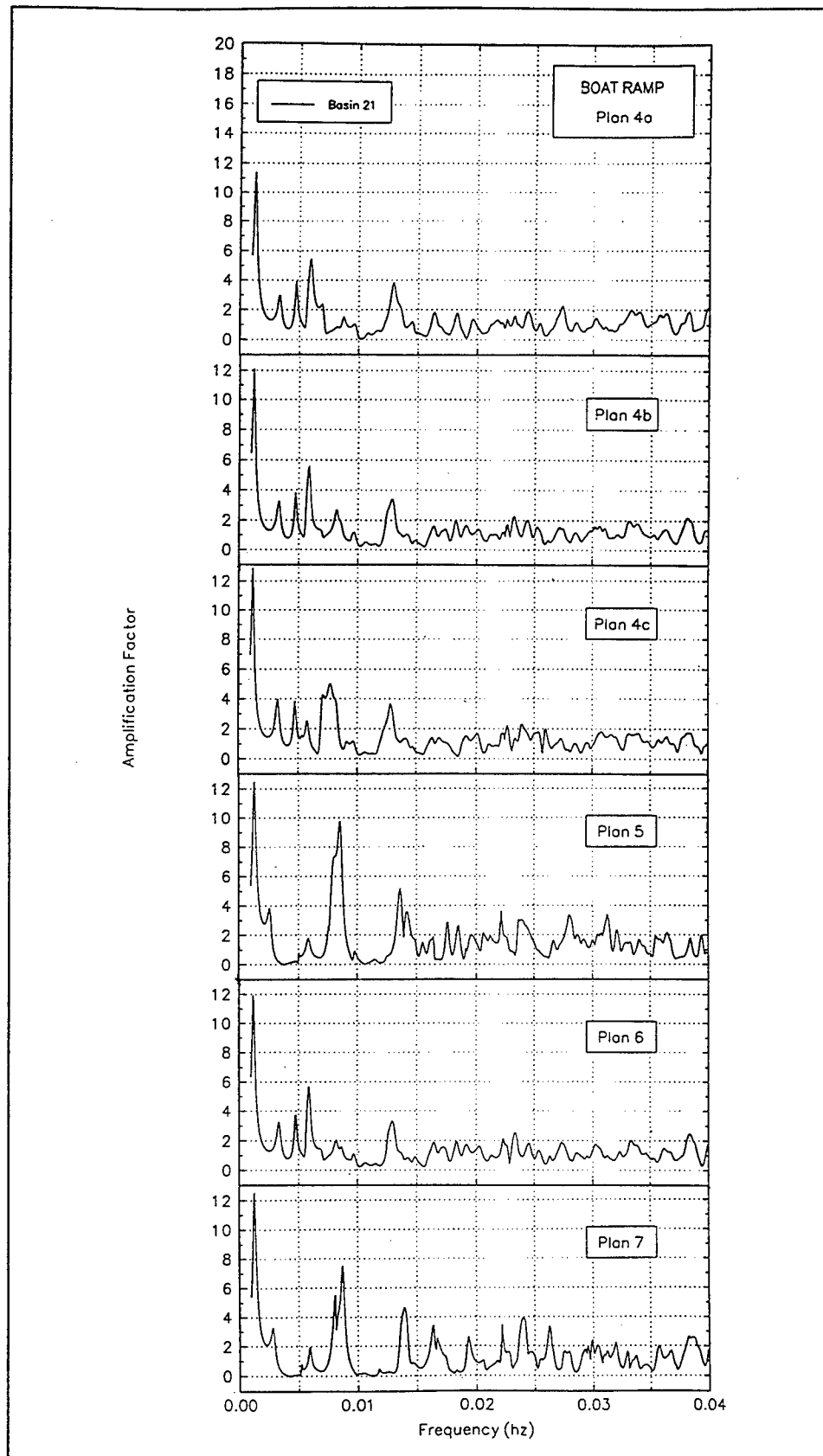
Figure G5. (Concluded)
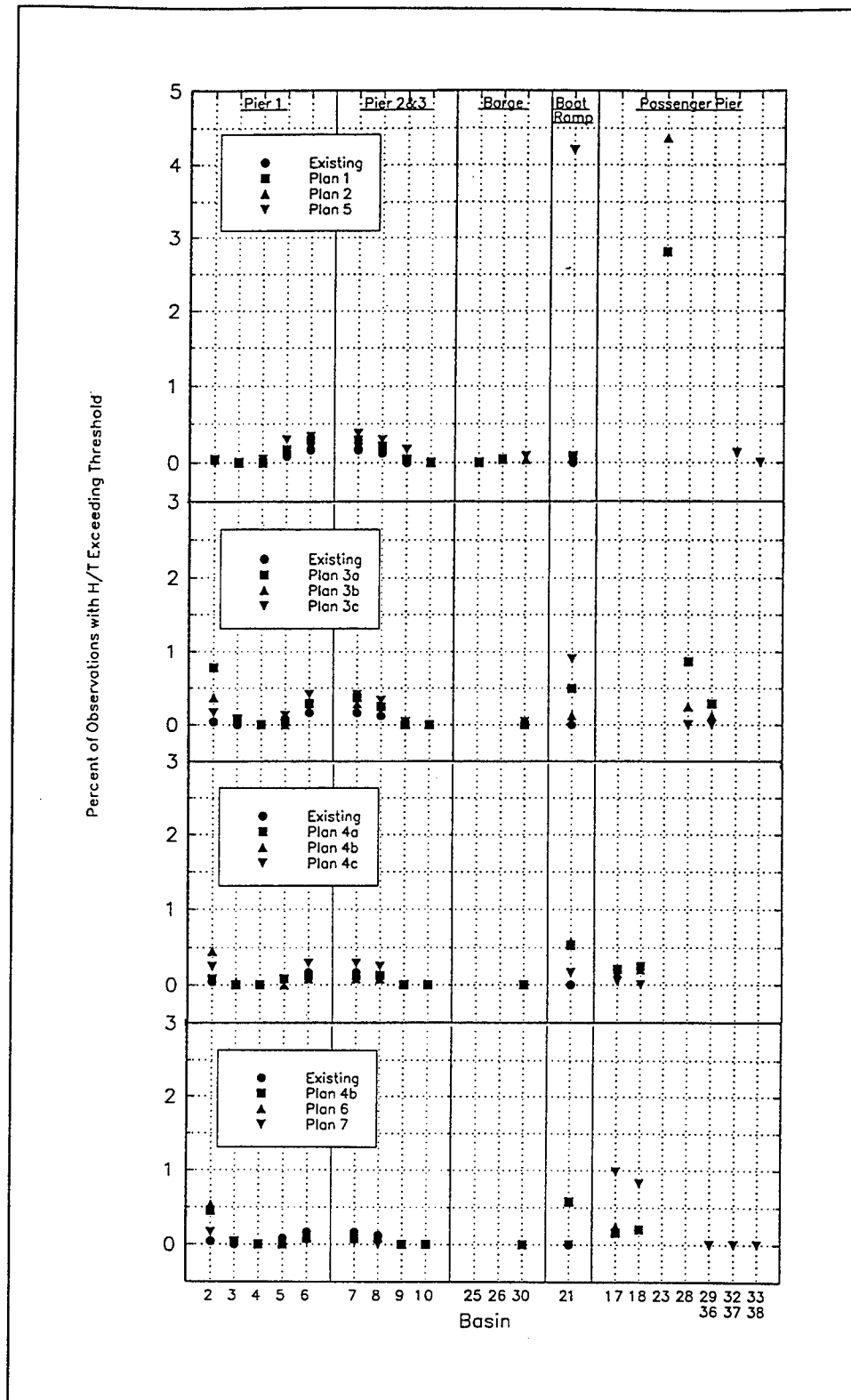
Figure G6. Comparison to Wilson's (1967) slope criterion, 100- to 400-sec period
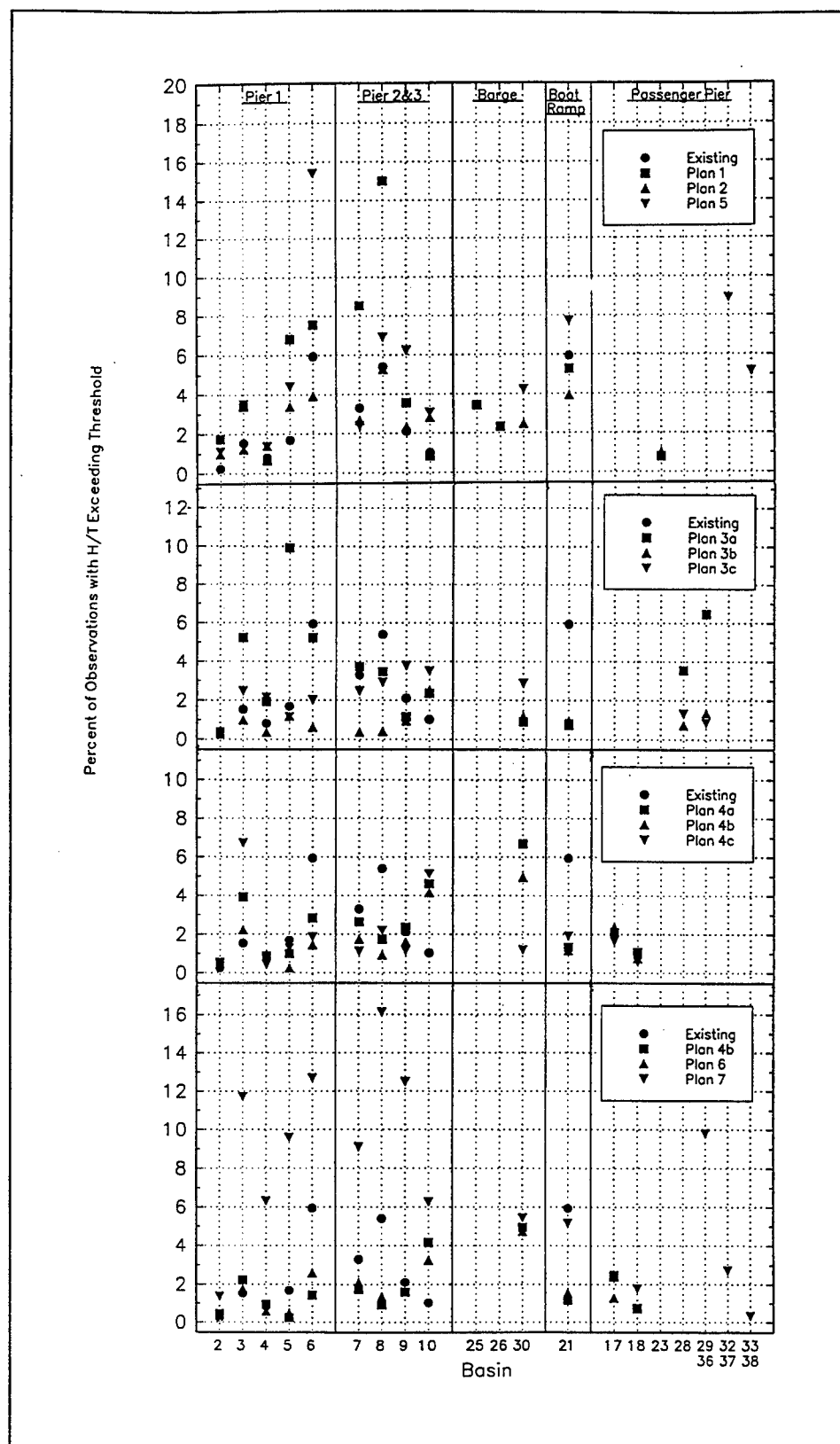
Figure G7. Comparison to Wilson's (1967) slope criterion, 30- to 100-sec period

Table G1
RMS Values of $A_{amp,I}$ at Piers, T=100-400 sec

Basin No.	Harbor Plan											
	Ex.	1	2	3a	3b	3c	4a	4b	4c	5	6	7
Pier 1												
2	1.40	1.60	1.64	2.19	2.53	2.35	1.58	2.29	2.35	1.12	2.27	2.23
3	1.17	1.18	1.19	1.70	1.85	1.57	1.21	1.72	1.58	0.88	1.67	1.64
4	0.82	0.98	0.99	0.81	0.73	0.88	0.83	0.75	0.89	1.01	0.76	0.71
5	1.57	1.69	1.78	1.78	1.95	2.15	1.52	1.75	2.15	1.65	1.75	1.82
6	2.01	2.03	2.15	2.30	2.58	2.70	1.89	2.27	2.71	1.96	2.23	2.34
Piers 2 & 3												
7	2.05	2.05	2.18	2.33	2.43	2.74	1.91	2.31	2.74	1.97	2.26	2.37
8	1.92	1.97	2.08	2.20	2.44	2.60	1.82	2.18	2.61	1.89	2.14	2.24
9	1.31	1.46	1.52	1.45	1.57	1.77	1.29	1.43	1.78	1.42	1.43	1.45
10	0.71	0.64	0.66	0.58	0.51	0.51	0.61	0.57	0.52	0.75	0.57	0.71
Barge Pier (Planned)												
25		0.80										
26		1.43										
30			1.28	0.83	1.16	1.59	0.78	0.88	1.29	1.88	0.80	2.96
Boat Ramp												
21	1.91	2.00	1.77	1.87	2.07	2.72	1.93	1.95	2.39	3.13	1.90	2.26
Passenger Ship Pier (Planned)												
17							1.54	1.88	2.07		1.85	2.32
18							2.06	2.12	1.32		2.07	2.43
23		3.87	4.27									
28				2.66	2.35	1.46						
29				2.28	2.14	1.50						
32										1.87		
33										1.45		
36												2.77
37												2.20
38												1.44

Table G2
Percent Occurrence of $H_{s,long} \geq 10$ cm at Piers, T=100-400 sec

Basin No.	Harbor Plan											
	Ex.	1	2	3a	3b	3c	4a	4b	4c	5	6	7
Pier 1												
2	2.1	2.3	2.4	5.6	6.2	5.5	3.5	6.1	5.4	1.4	6.6	4.0
3	0.8	0.9	0.9	2.6	2.5	1.3	0.9	2.5	1.4	0.5	2.4	0.9
4	1.2	2.2	2.2	1.2	0.7	0.8	1.1	0.7	0.7	3.0	0.9	0.1
5	7.2	9.5	9.6	8.0	6.3	8.4	7.6	6.7	7.5	11.0	6.7	2.2
6	13.1	13.6	14.3	14.6	11.7	13.7	12.9	13.0	12.5	15.1	12.3	5.4
Piers 2 & 3												
7	13.6	13.8	14.6	14.9	10.0	13.9	13.3	13.3	12.9	15.4	12.9	5.7
8	11.8	12.4	13.4	12.9	10.0	12.5	11.7	11.4	11.7	14.4	10.8	4.9
9	4.6	6.6	6.8	4.8	3.3	4.9	5.2	4.1	4.5	7.8	4.2	1.1
10	0.5	0.4	0.4	0.1	0.0	0.1	0.4	0.1	0.0	0.6	0.1	0.1
Barge Pier (Planned)												
25		0.4										
26		1.9										
30			5.2	0.5	0.6	2.6	0.8	0.9	1.3	4.9	0.8	4.4
Boat Ramp												
21	10.6	12.6	11.1	14.1	12.4	17.5	15.4	15.6	14.3	23.8	15.3	3.7
Passenger Ship Pier (Planned)												
17							6.0	7.6	7.0		7.5	15.5
18							10.0	8.6	2.1		8.7	15.3
23		35.6	39.2									
28				13.9	7.1	2.1						
29				8.9	5.9	2.2						
32										6.8		
33										3.2		
36												3.5
37												1.5
38												0.2

Table G3
Percent Occurrence of $H_{s,long} \geq 10$ cm at Piers, T=30-100 sec

Basin No.	Harbor Plan											
	Ex.	1	2	3a	3b	3c	4a	4b	4c	5	6	7
Pier 1												
2	1.4	2.7	2.6	0.9	2.1	2.2	0.9	2.4	1.8	2.2	2.2	5.3
3	3.4	3.1	2.0	5.1	2.2	3.8	5.4	3.6	4.1	4.1	3.5	11.5
4	3.0	2.2	2.7	1.8	2.6	2.8	1.4	3.7	3.0	4.1	3.2	9.2
5	1.0	2.5	1.0	2.0	0.3	0.9	0.5	0.4	0.7	1.5	0.4	5.7
6	4.8	5.1	4.0	3.3	4.6	4.5	4.4	6.1	5.6	9.6	5.9	16.4
Piers 2 & 3												
7	5.7	6.3	4.8	4.6	2.8	5.5	3.9	6.6	5.3	6.2	6.3	16.2
8	4.0	6.4	3.3	2.3	2.9	4.3	1.9	4.0	4.1	5.3	4.0	14.9
9	2.1	2.6	2.4	1.6	1.2	2.1	2.7	2.1	1.8	3.4	1.5	8.3
10	2.1	3.3	4.0	2.3	4.4	4.9	4.0	5.9	5.6	5.3	5.1	12.8
Barge Pier (Planned)												
25		4.1										
26		2.7										
30			4.0	1.4	2.7	2.8	1.9	2.1	1.6	3.3	2.2	6.8
Boat Ramp												
21	10.6	10.5	9.9	4.2	3.7	4.8	3.7	4.0	4.6	13.4	4.5	11.3
Passenger Ship Pier (Planned)												
17							2.0	0.8	0.7		0.4	1.9
18							3.1	2.6	3.0		1.9	4.5
23		0.3	0.2									
28				3.6	2.1	2.4						
29				2.0	0.8	0.7						
32										6.8		
33										3.4		
36												11.5
37												3.5
38												1.2

Table G4
Percent Occurrence of Cases Exceeding Wilson's (1967) Slope Criterion at Piers, T=100-400 sec

Basin No.	Harbor Plan											
	Ex.	1	2	3a	3b	3c	4a	4b	4c	5	6	7
Pier 1												
2	0.04	0.04	0.04	0.78	0.37	0.17	0.08	0.45	0.25	0.00	0.54	0.17
3	0.00	0.00	0.00	0.08	0.04	0.00	0.00	0.04	0.00	0.00	0.04	0.00
4	0.00	0.00	0.00	0.00	0.00	0.00	0.00	0.00	0.00	0.04	0.00	0.00
5	0.08	0.17	0.17	0.04	0.00	0.12	0.08	0.00	0.04	0.29	0.00	0.00
6	0.17	0.29	0.25	0.29	0.33	0.41	0.12	0.08	0.29	0.33	0.12	0.04
Piers 2 & 3												
7	0.17	0.29	0.25	0.37	0.29	0.41	0.12	0.08	0.29	0.37	0.12	0.04
8	0.12	0.21	0.25	0.25	0.29	0.33	0.12	0.08	0.25	0.29	0.12	0.00
9	0.00	0.04	0.04	0.00	0.00	0.04	0.00	0.00	0.00	0.17	0.00	0.00
10	0.00	0.00	0.00	0.00	0.00	0.00	0.00	0.00	0.00	0.00	0.00	0.00
Barge Pier (Planned)												
25		0.00										
26		0.04										
30			0.04	0.00	0.00	0.04	0.00	0.00	0.00	0.08	0.00	0.00
Boat Ramp												
21	0.00	0.08	0.04	0.50	0.12	0.91	0.54	0.58	0.17	4.20	0.58	0.00
Passenger Ship Pier (Planned)												
17							0.21	0.17	0.04		0.25	0.99
18							0.25	0.21	0.00		0.21	0.82
23		2.80	4.37									
28				0.87	0.25	0.00						
29				0.29	0.12	0.00						
32										0.12		
33										0.00		
36												0.00
37												0.00
38												0.00

Table G5
Percent Occurrence of Cases Exceeding Wilson's (1967) Slope Criterion at Piers, *T*=30-100 sec

Basin No.	Harbor Plan											
	Ex.	1	2	3a	3b	3c	4a	4b	4c	5	6	7
Pier 1												
2	0.2	1.7	1.0	0.3	0.5	0.4	0.5	0.5	0.5	1.1	0.5	1.4
3	1.5	3.4	1.2	5.2	1.0	2.5	3.9	2.2	6.7	3.5	1.8	11.7
4	0.8	0.7	1.4	1.9	0.4	2.1	0.9	0.9	0.4	1.4	0.6	6.3
5	1.7	6.8	3.4	9.9	1.2	1.2	1.0	0.2	1.3	4.4	0.5	9.6
6	5.9	7.5	3.9	5.2	0.6	2.0	2.8	1.4	1.9	15.4	2.6	12.7
Piers 2 & 3												
7	3.3	8.5	2.7	3.7	0.4	2.5	2.6	1.7	1.1	2.4	2.1	9.1
8	5.4	15.0	5.3	3.5	0.4	2.9	1.7	0.9	2.2	6.9	1.4	16.1
9	2.1	3.5	2.3	1.2	0.9	3.8	2.4	1.6	1.2	6.2	1.6	12.5
10	1.0	0.9	2.8	2.4	2.5	3.5	4.6	4.2	5.1	3.1	3.3	6.3
Barge Pier (Planned)												
25		3.4										
26		2.3										
30			2.5	0.9	1.2	2.9	6.7	4.9	1.2	4.2	4.7	5.4
Boat Ramp												
21	5.9	5.3	3.9	0.7	0.9	0.8	1.3	1.2	1.9	7.7	1.6	5.2
Passenger Ship Pier (Planned)												
17							2.1	2.4	1.6		1.3	2.5
18							1.1	0.7	0.6		0.7	1.8
23		0.8	1.0									
28				3.5	0.7	1.3						
29				6.5	1.4	0.9						
32										8.9		
33										5.2		
36												9.8
37												2.7
38												0.3

Appendix H
Resonant Amplification Factor and Phase Contour Plots, All Plans

---

List of Figures

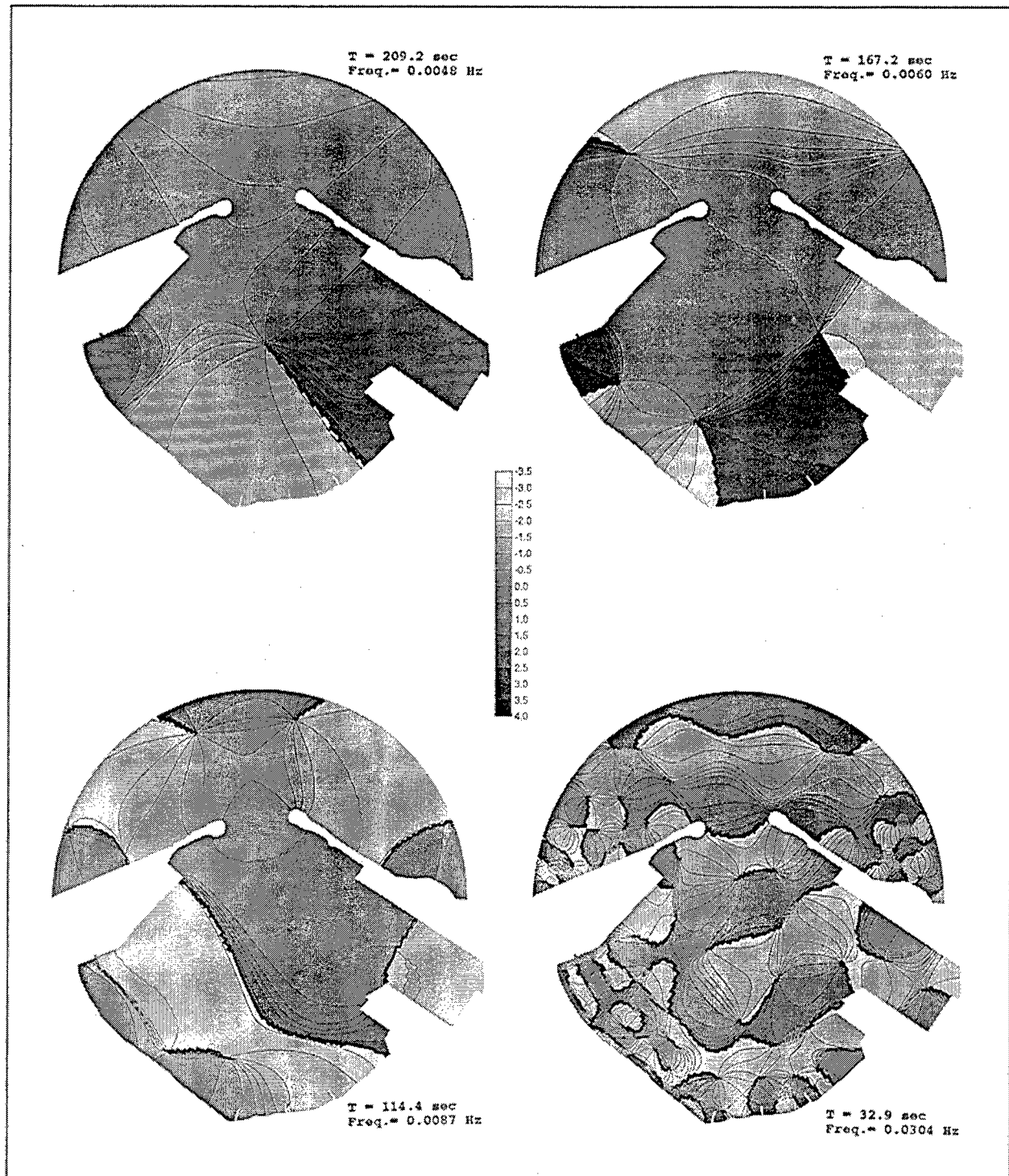Figure H1. Resonant long wave amplification factor contours, Plan 1
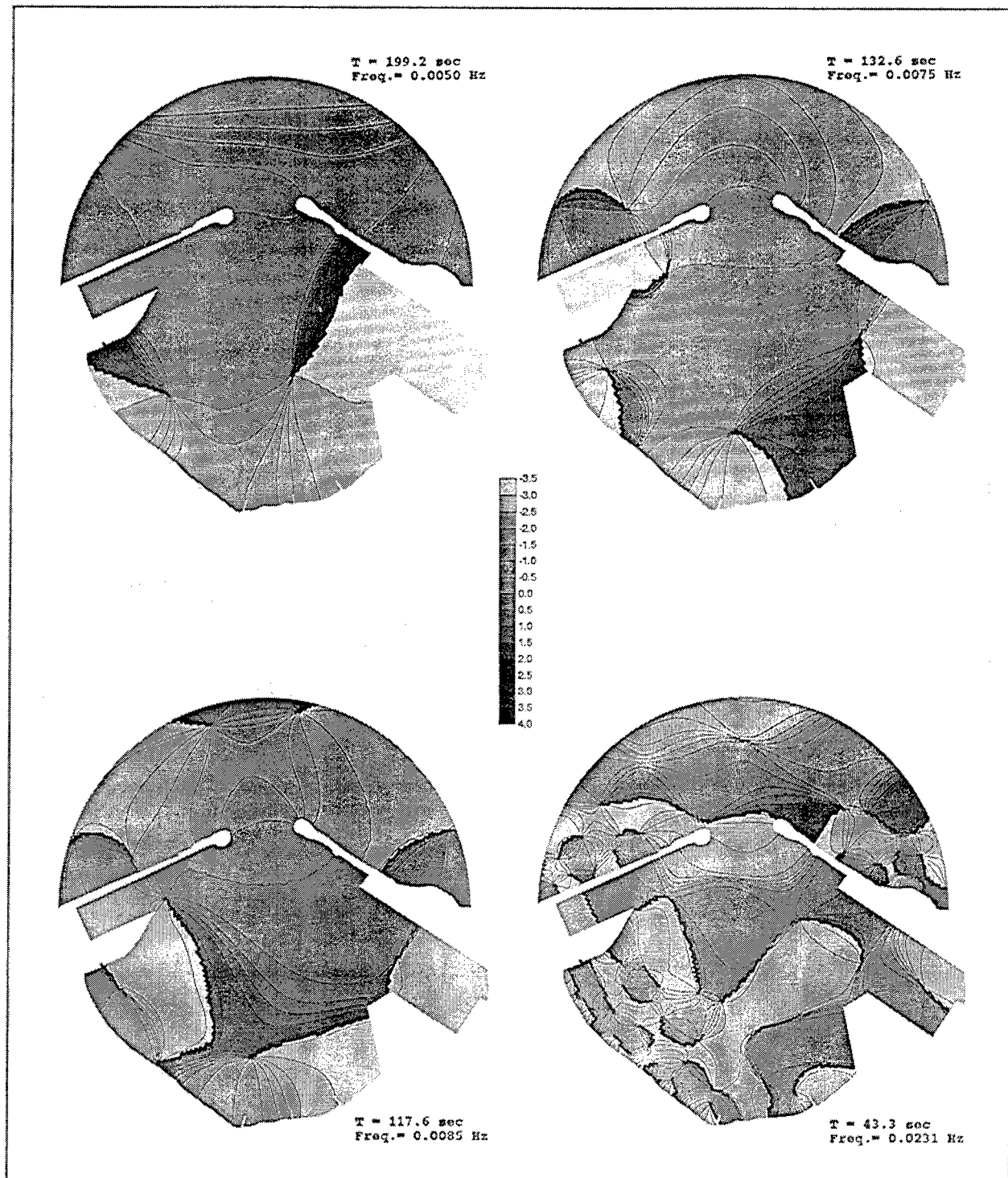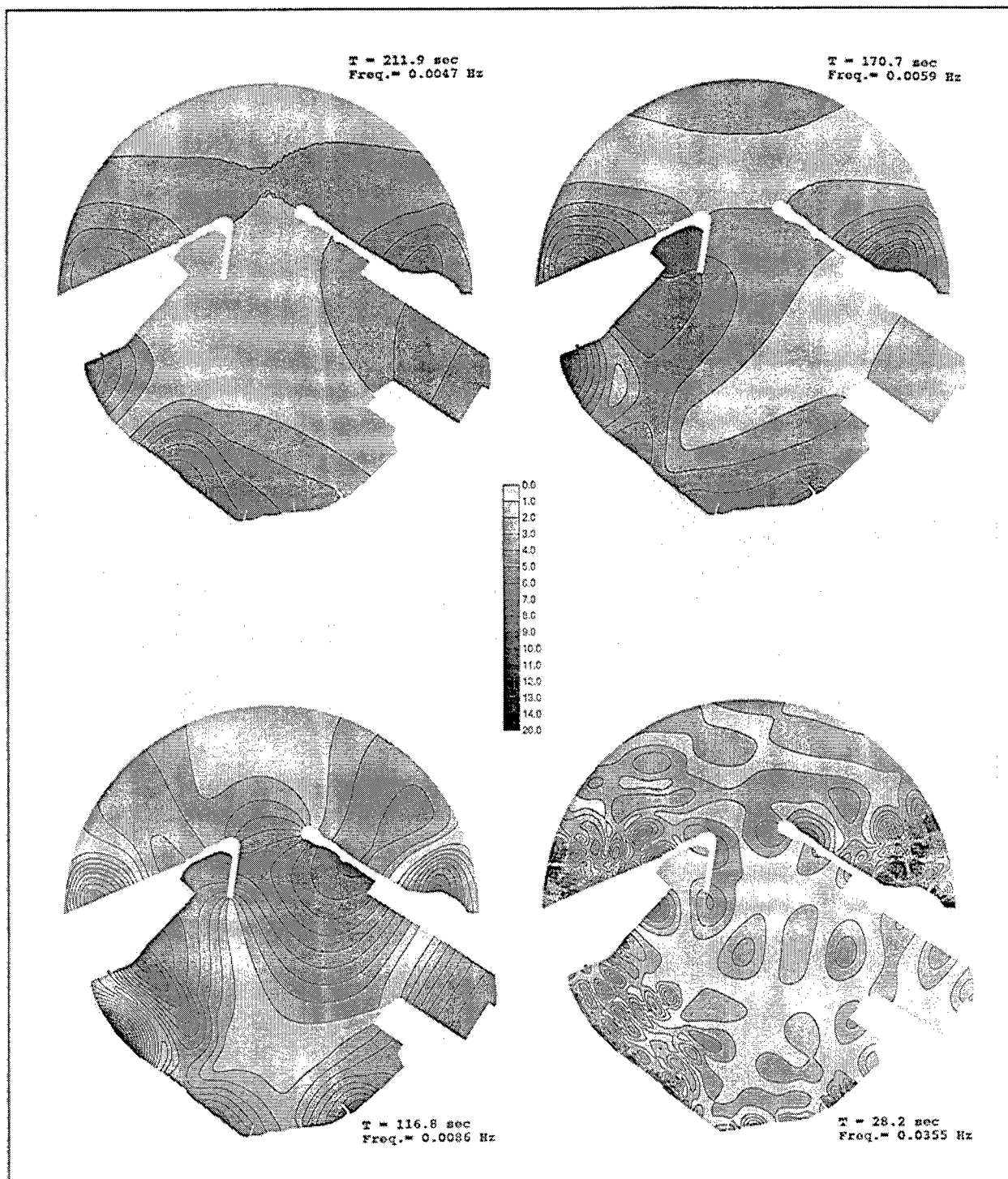
Figure H2. Resonant long wave phase contours, Plan 1
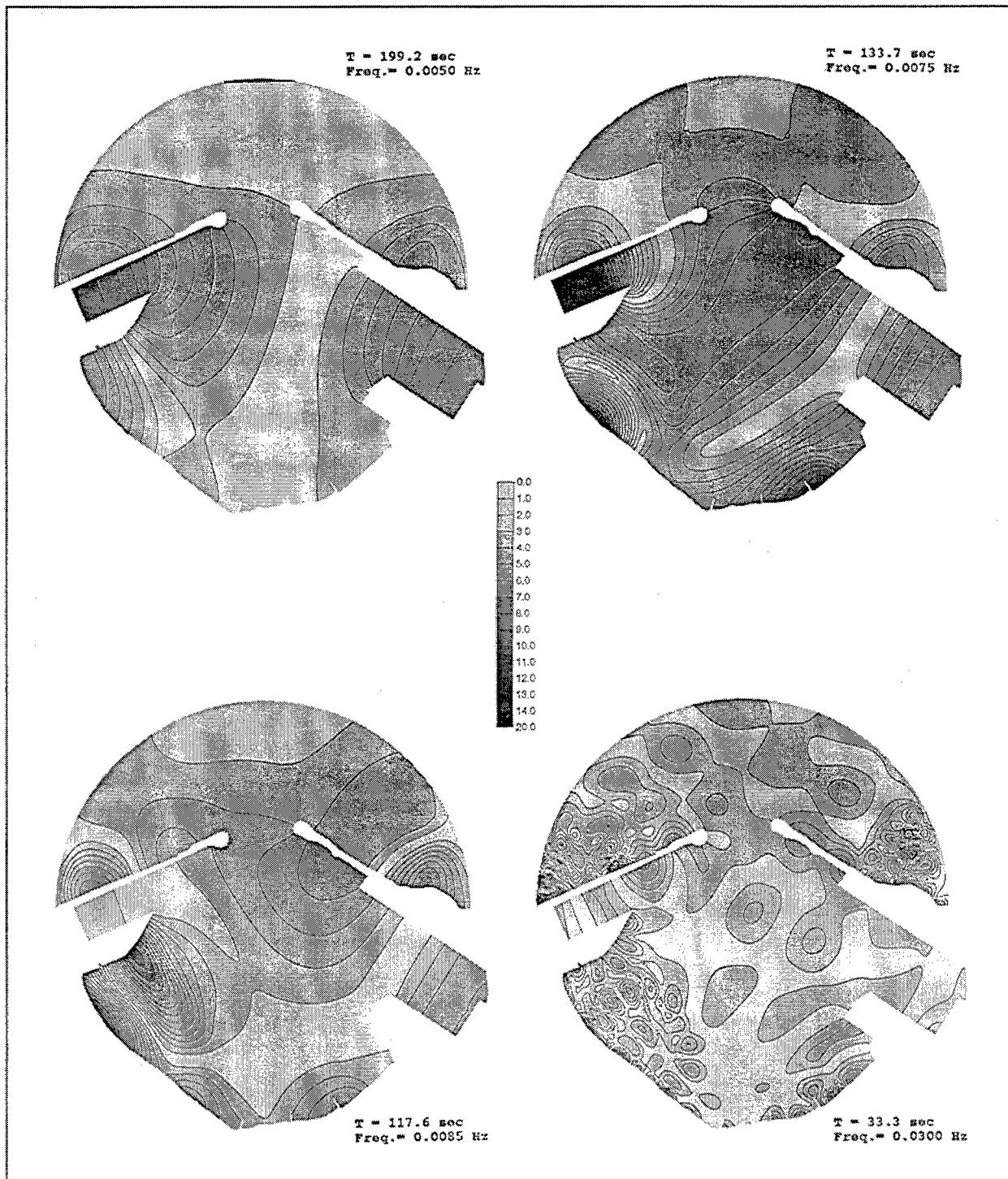
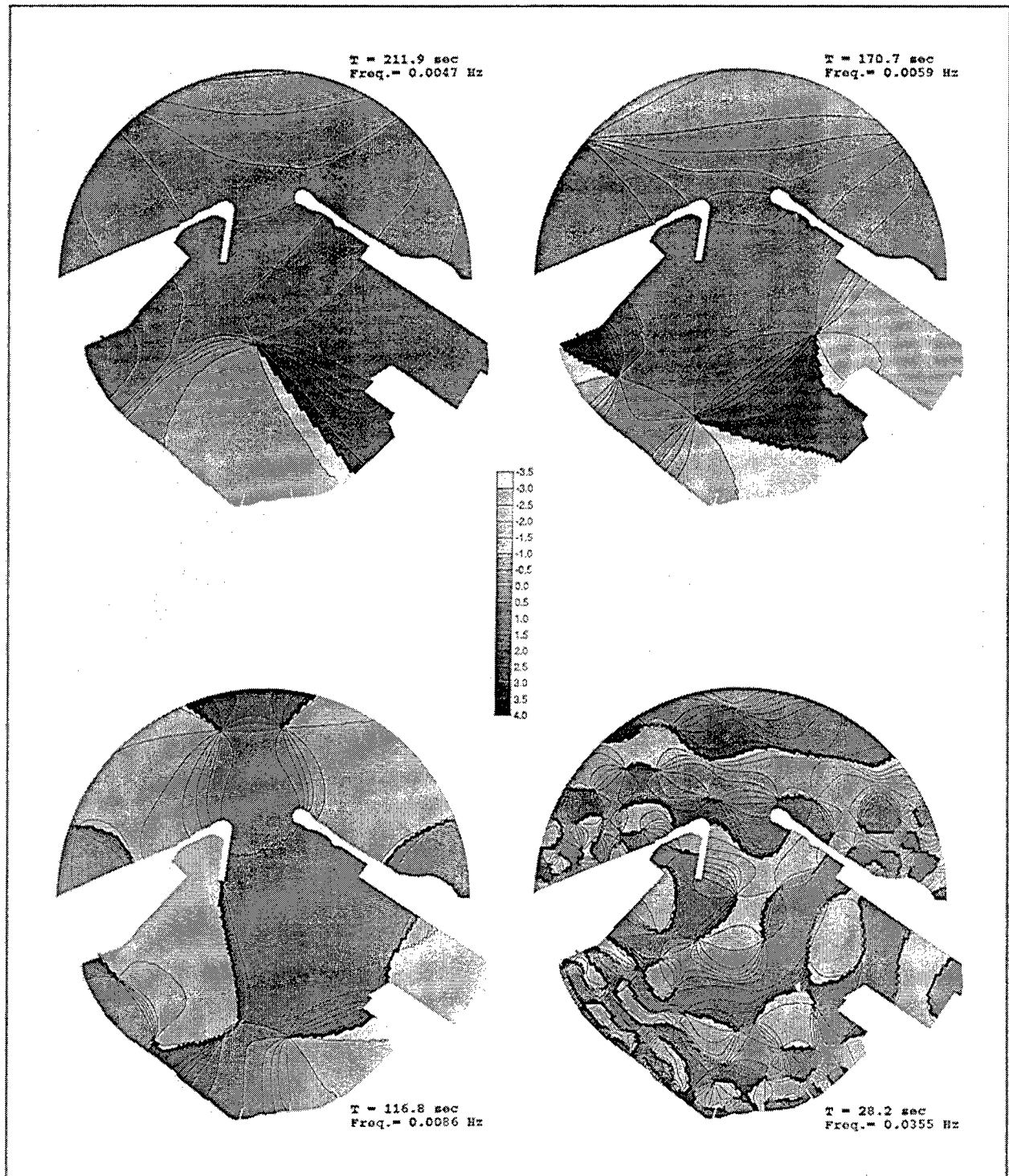Figure H3. Resonant long wave amplification factor contours, Plan 2
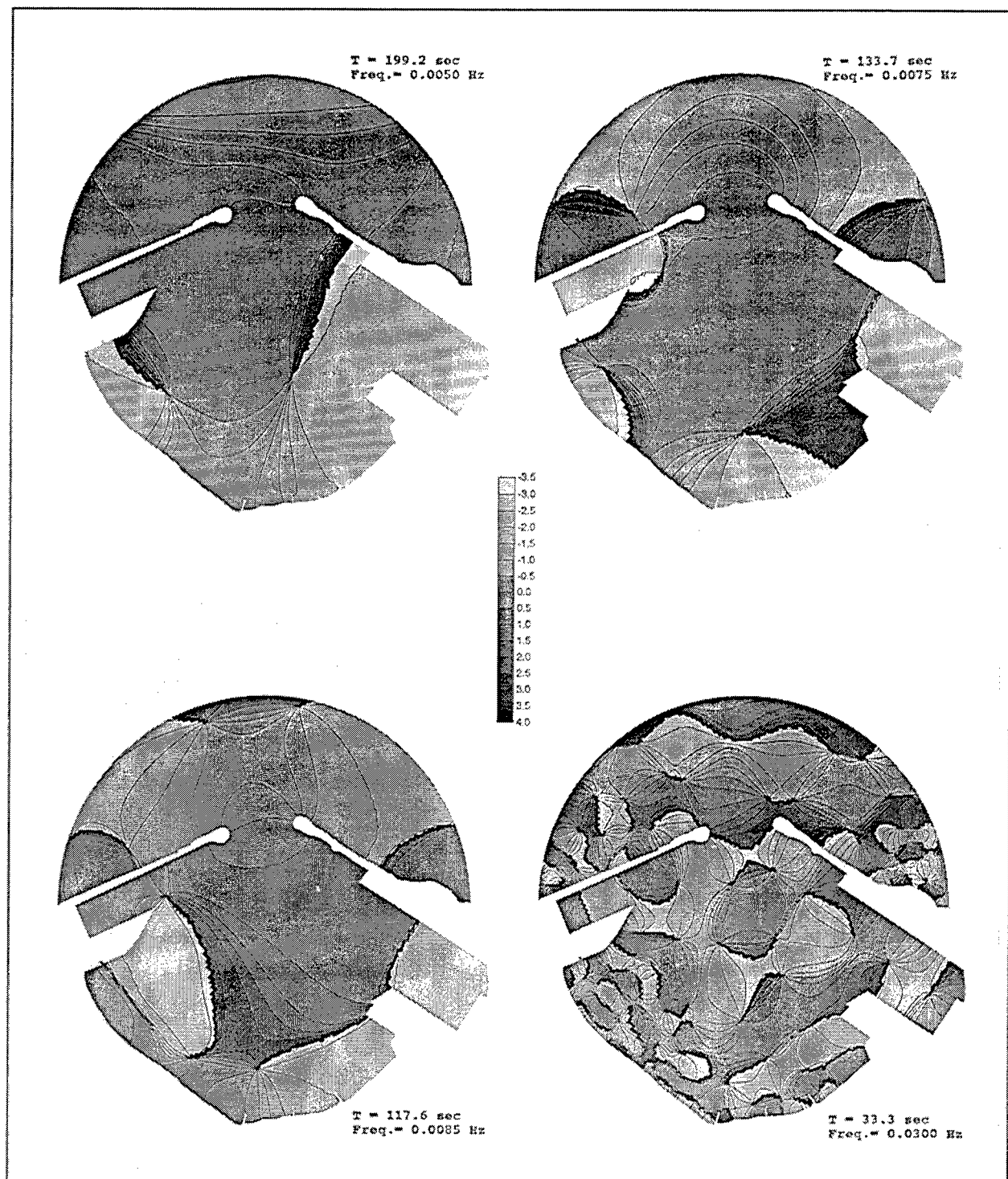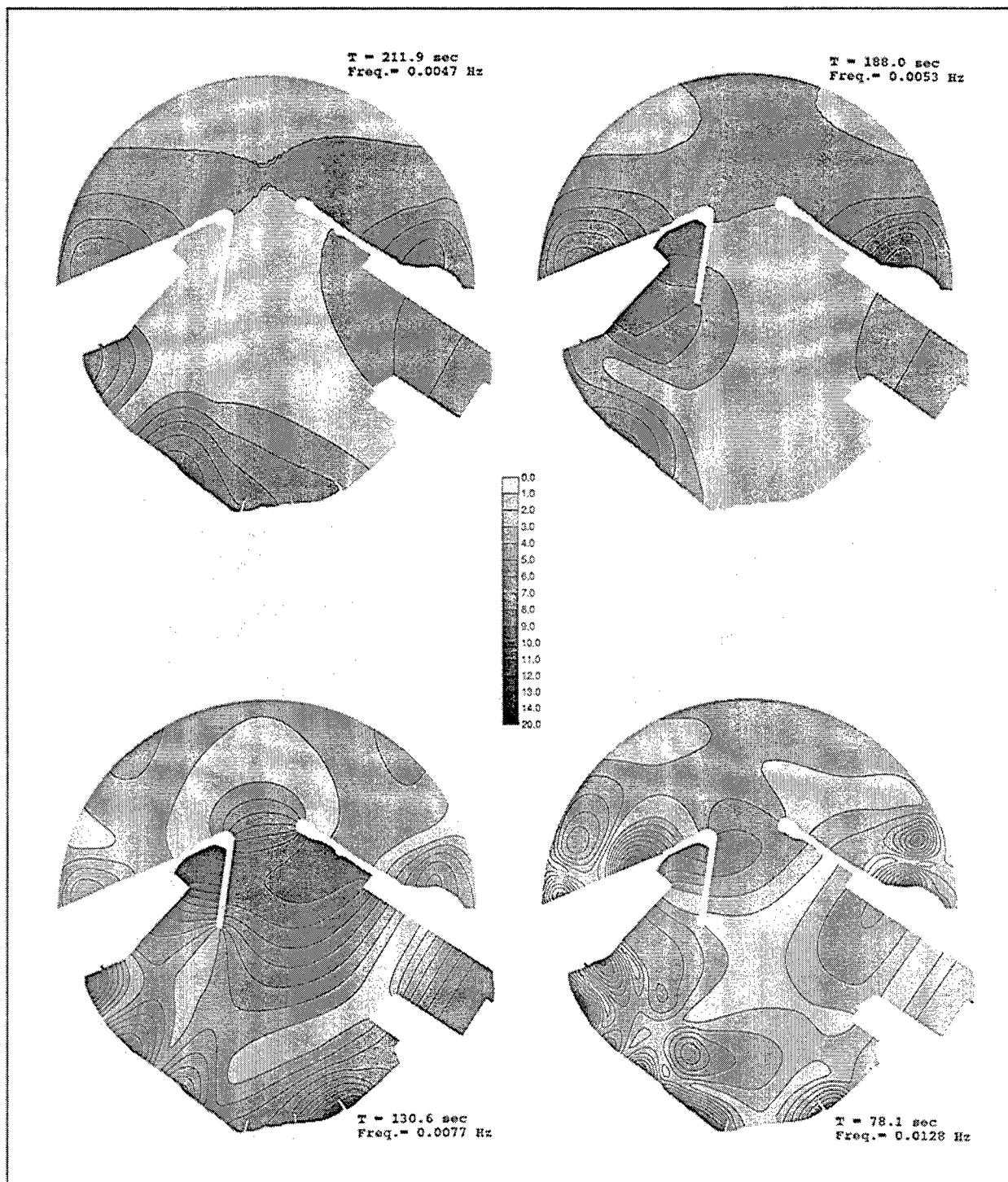
Figure H4. Resonant long wave phase contours, Plan 2
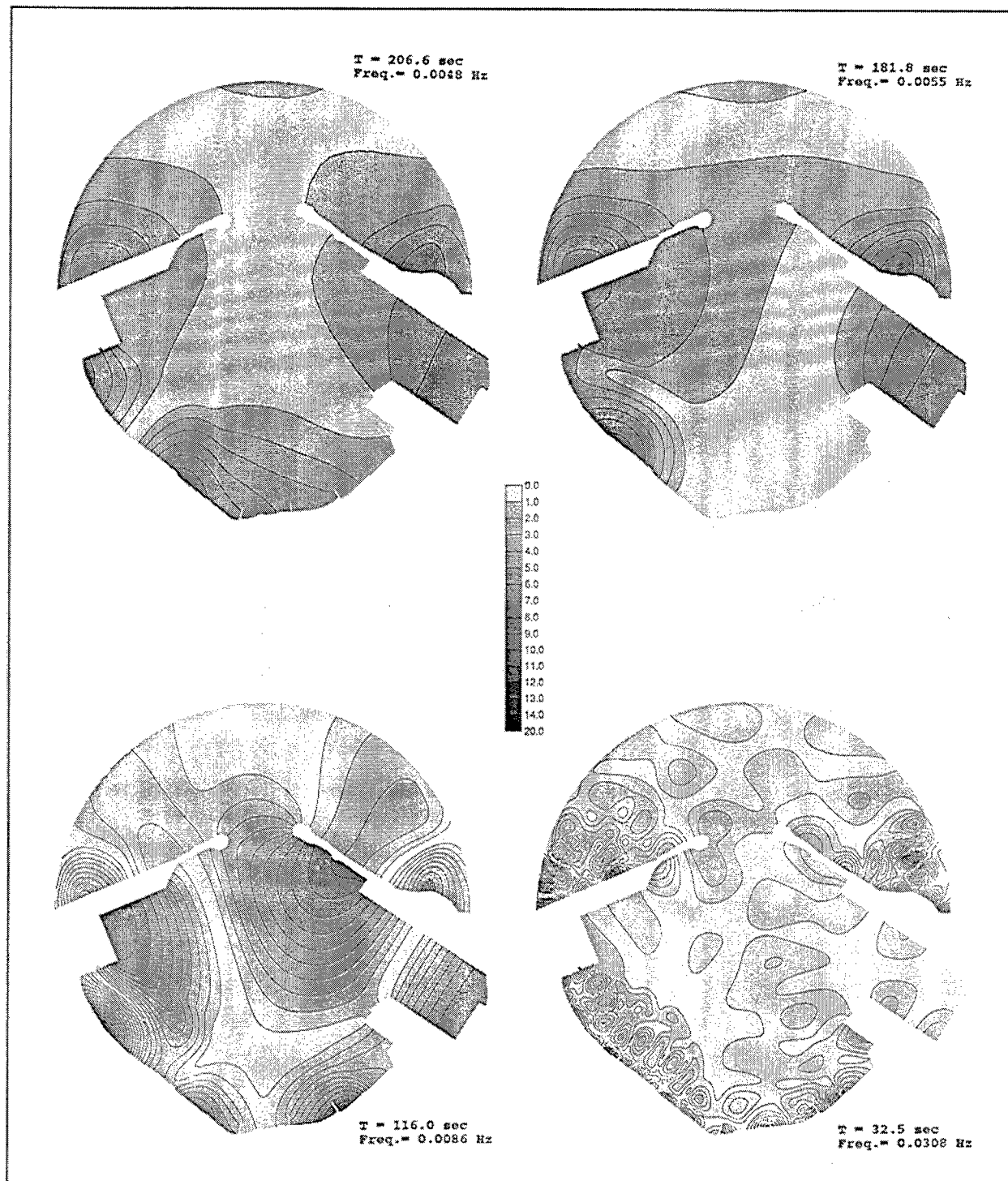
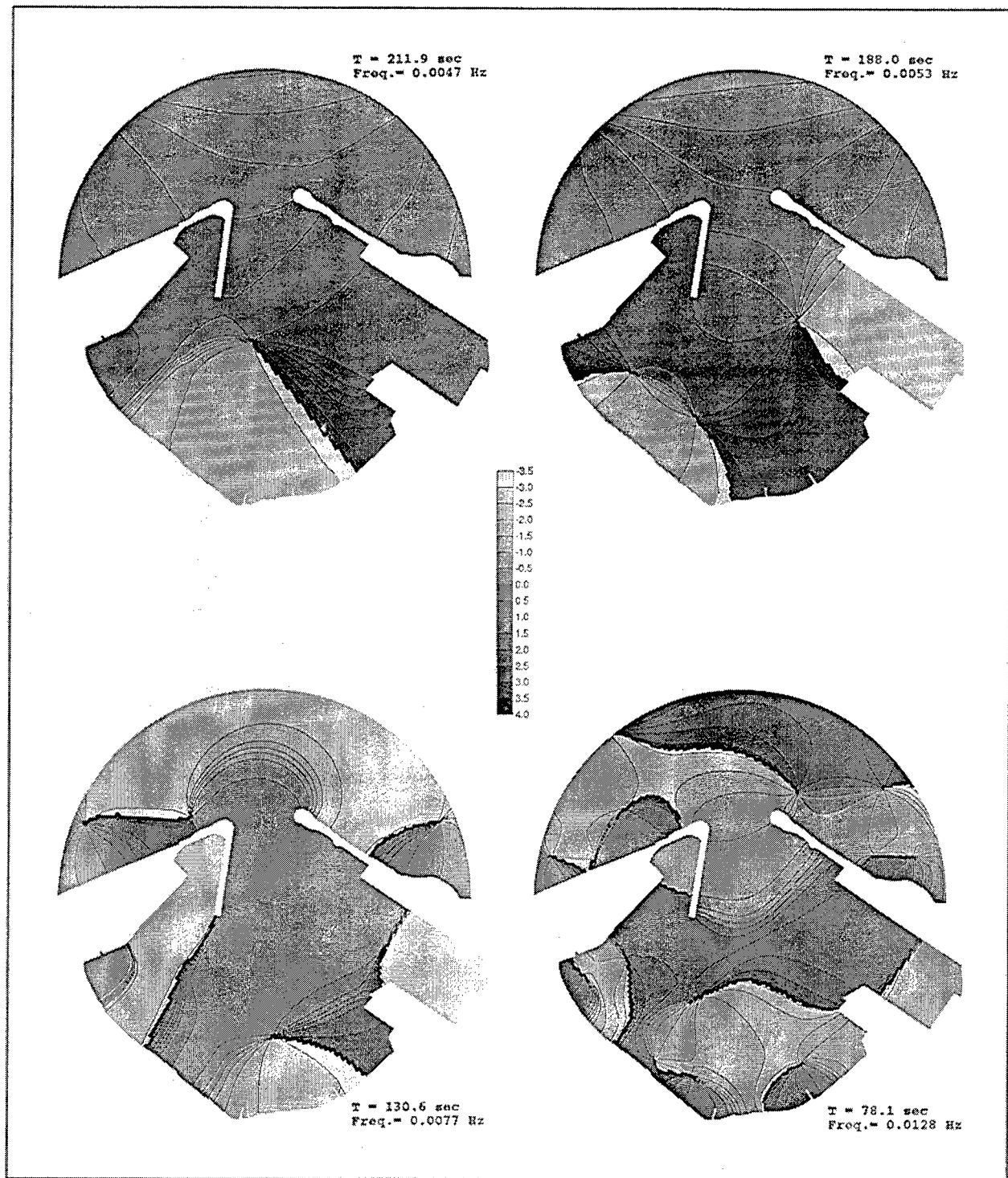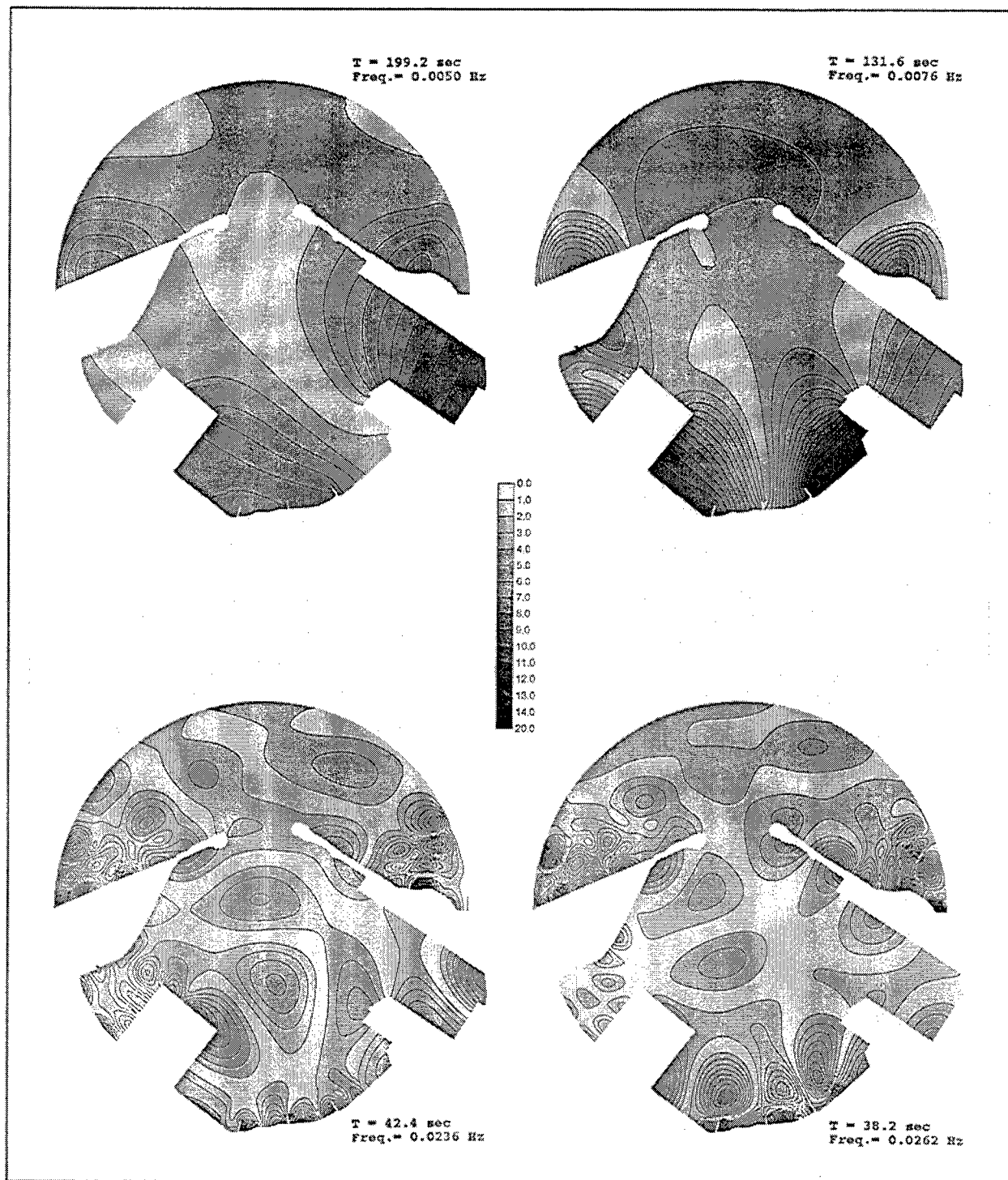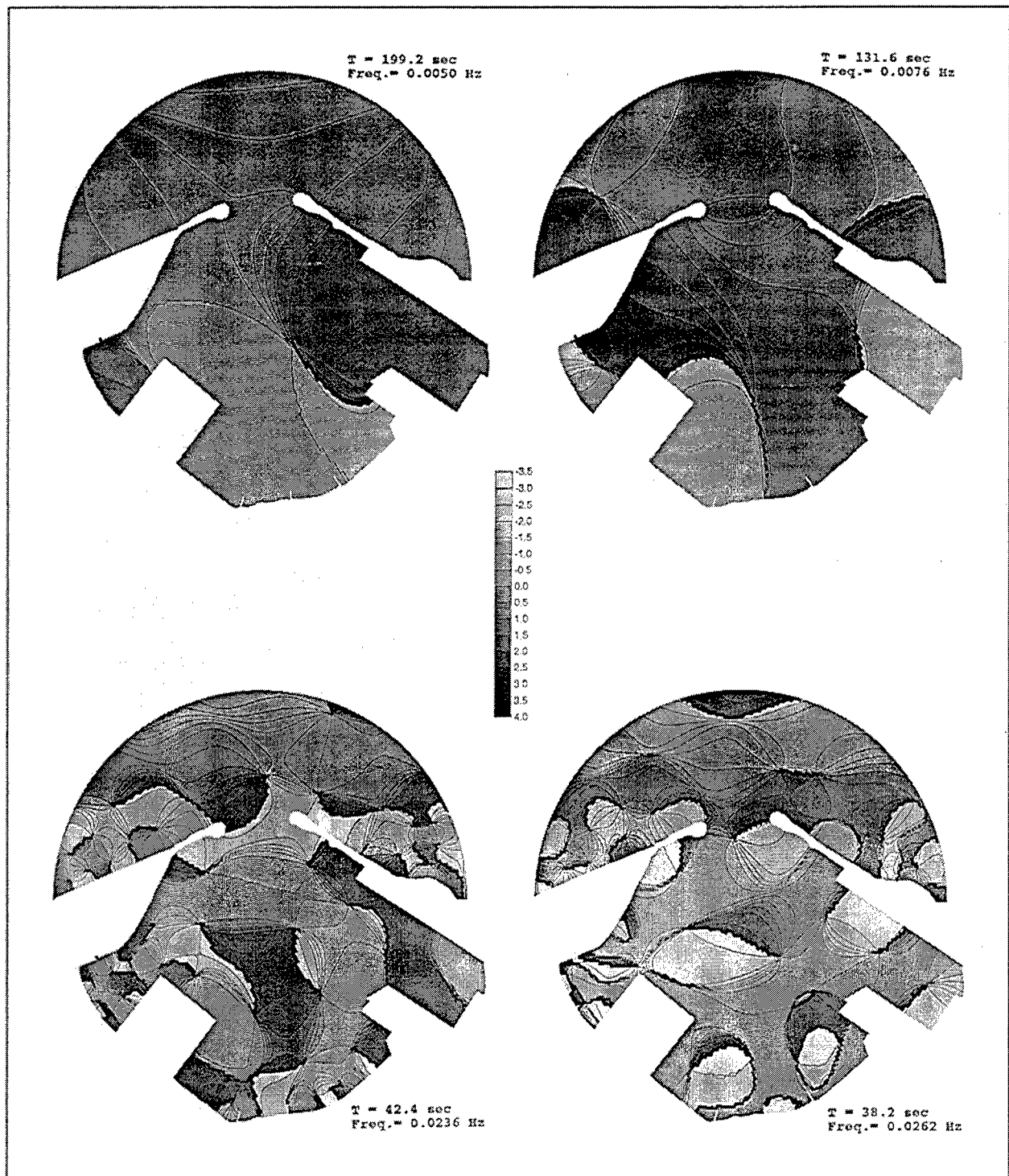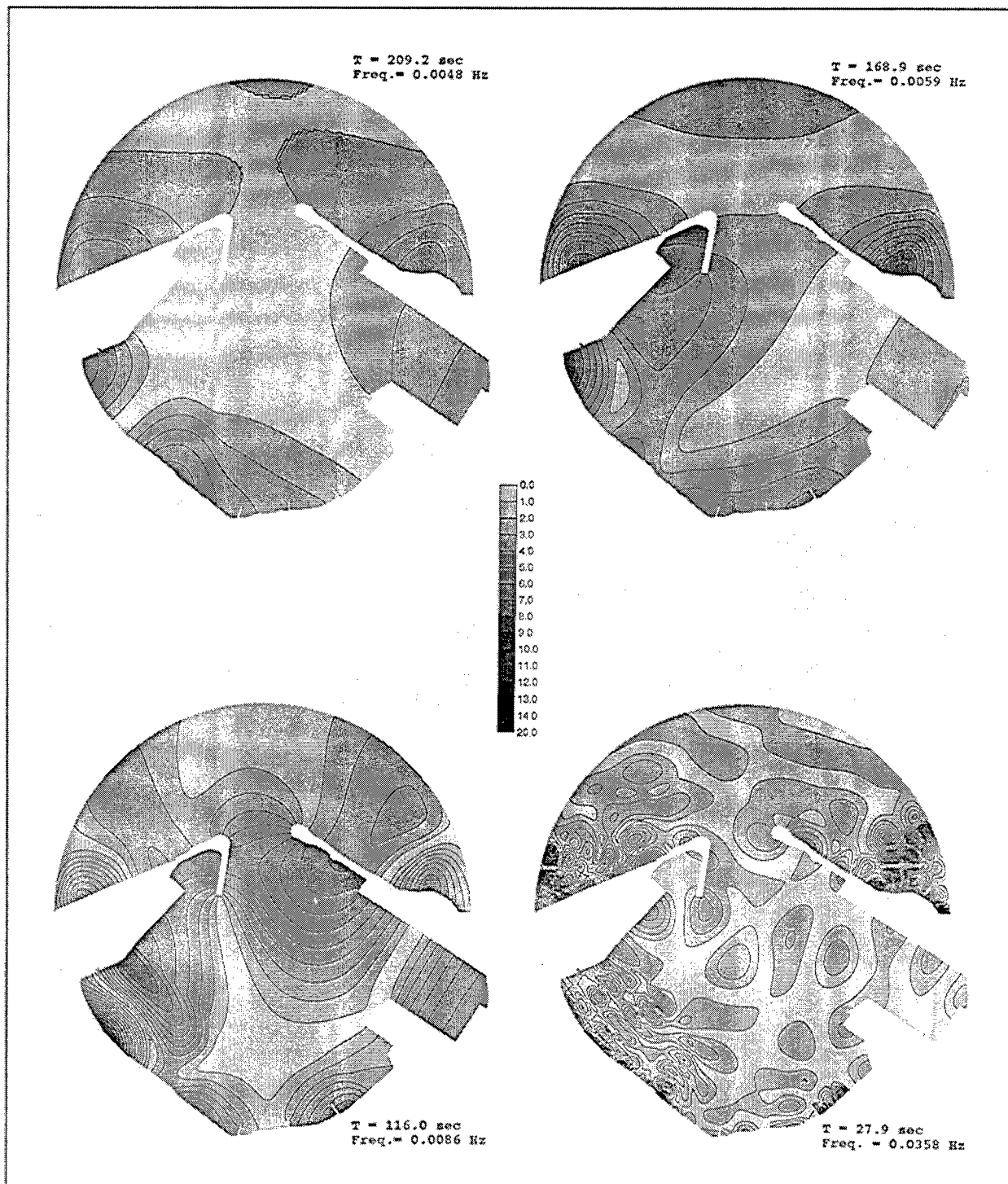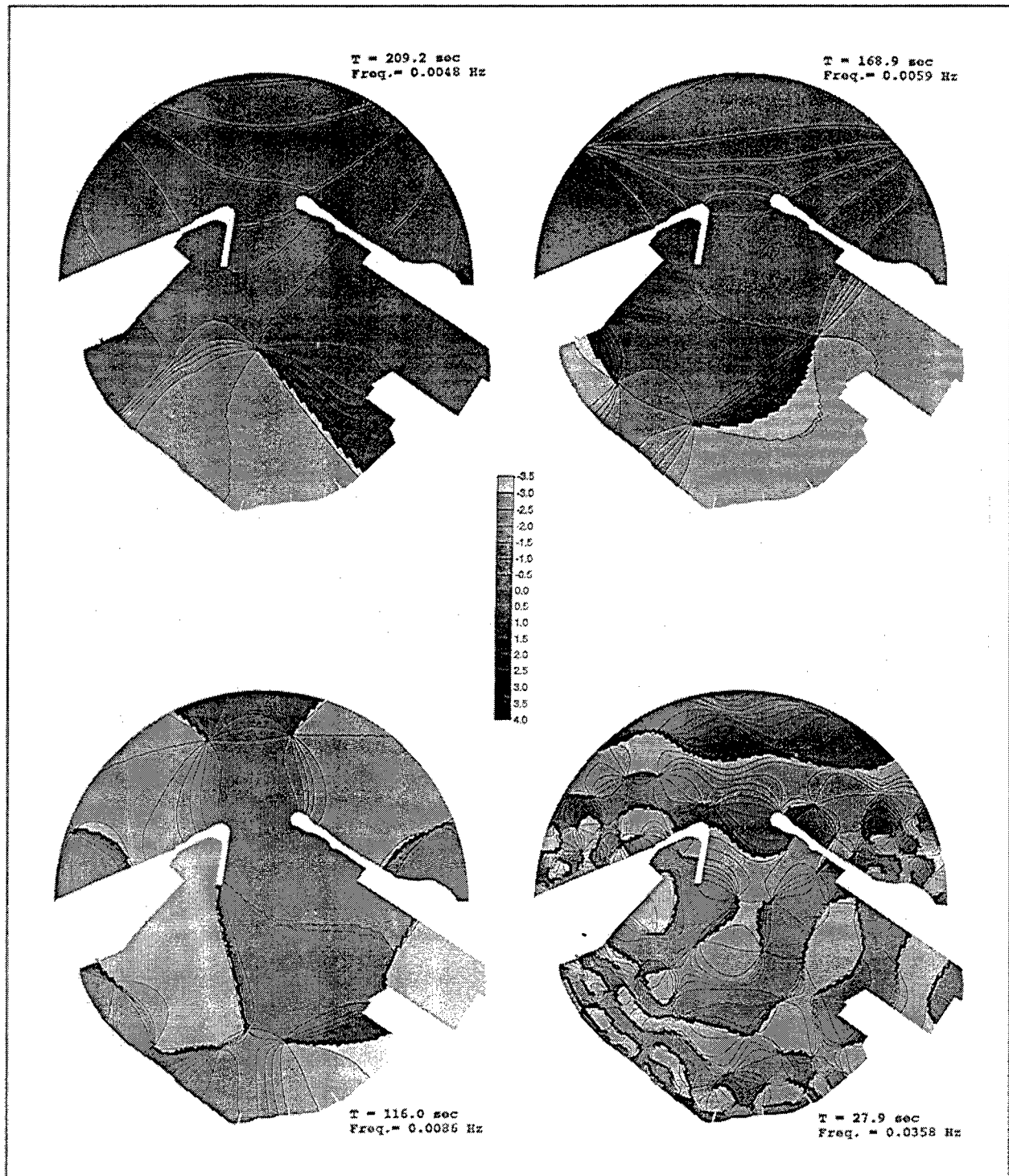Figure H5. Resonant long wave amplification factor contours, Plan 3a
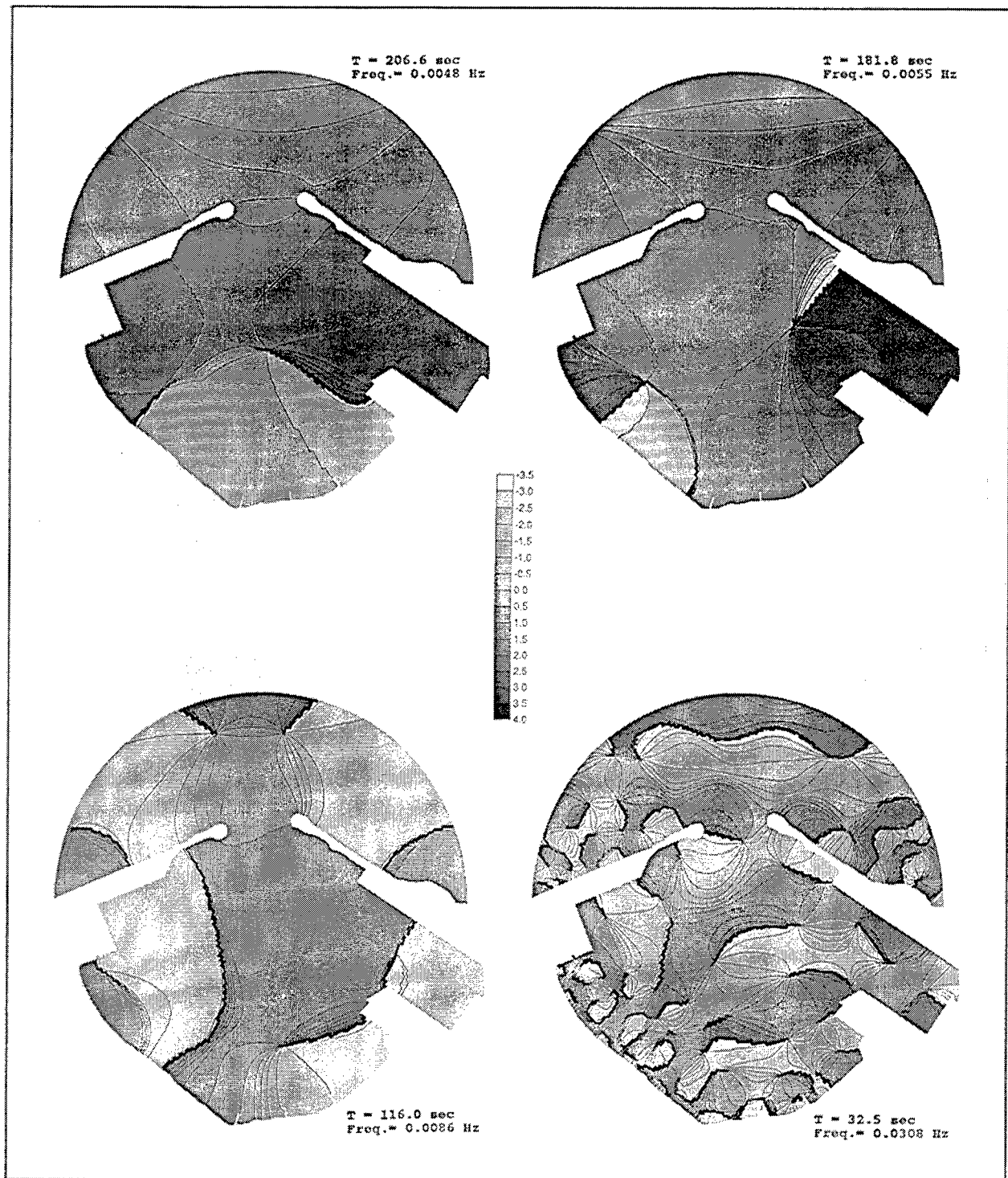
Figure H6. Resonant long wave phase contours, Plan 3a
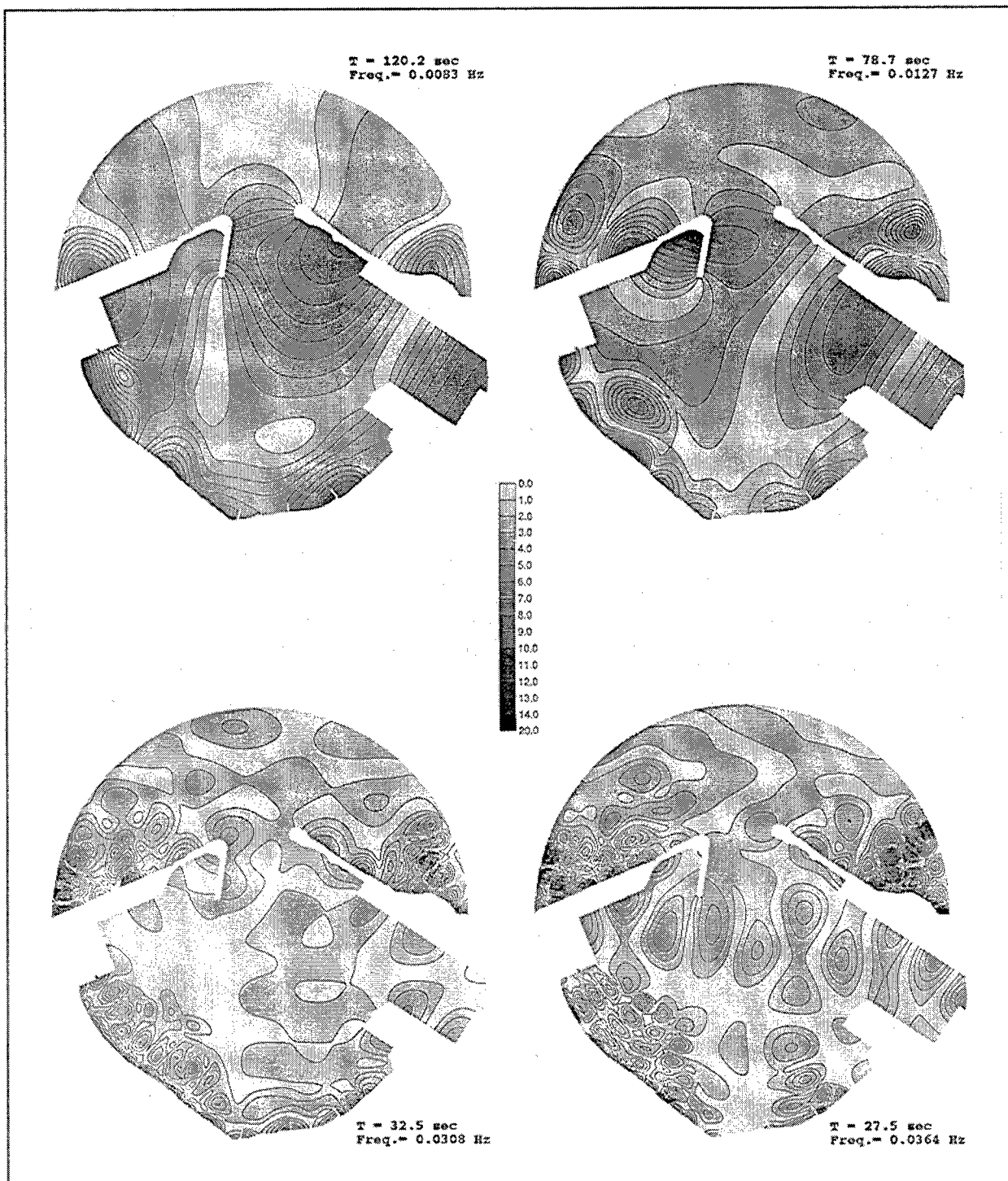
Figure H7. Resonant long wave amplification factor contours, Plan 3b
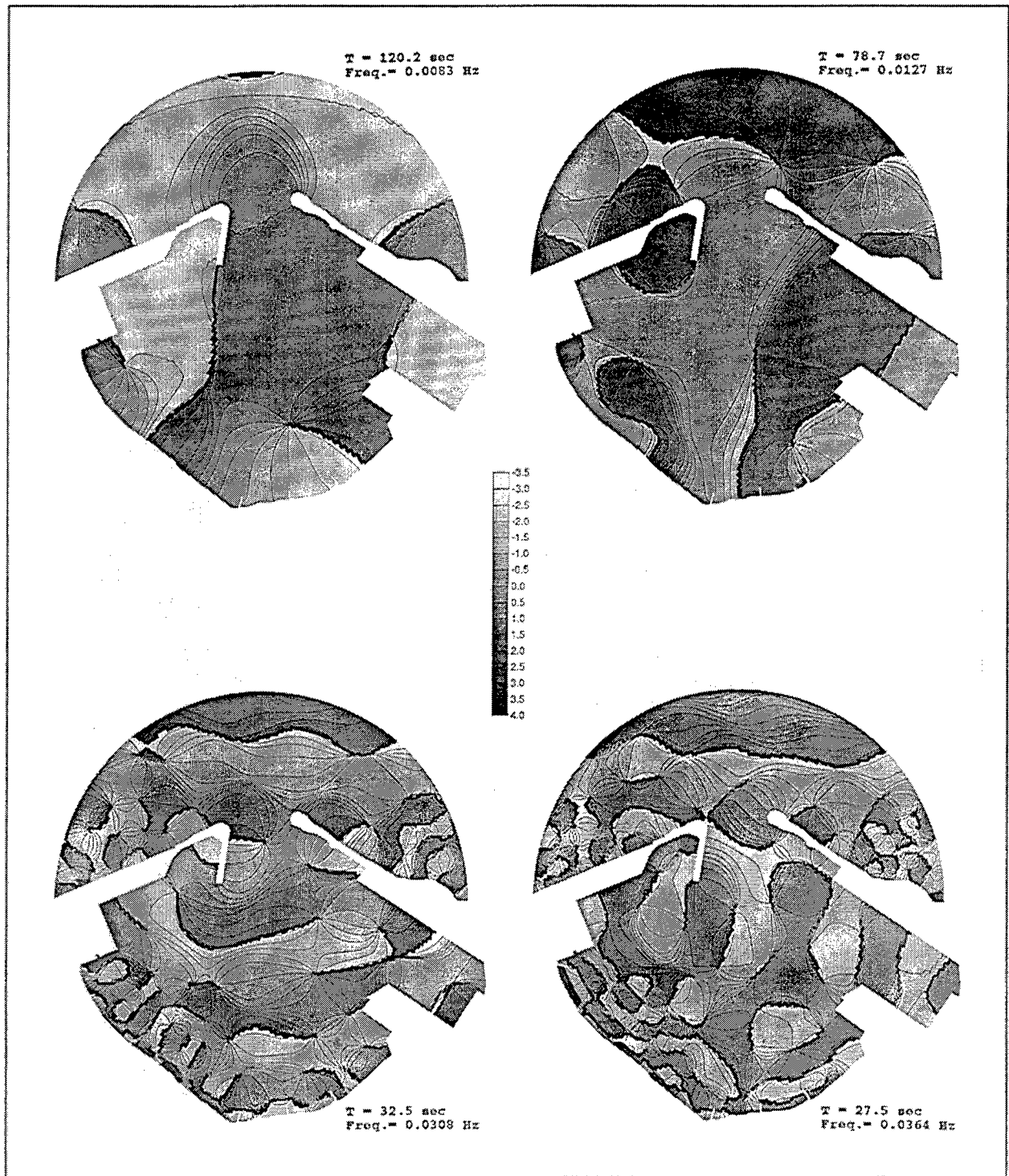
Figure H8. Resonant long wave phase contours, Plan 3b
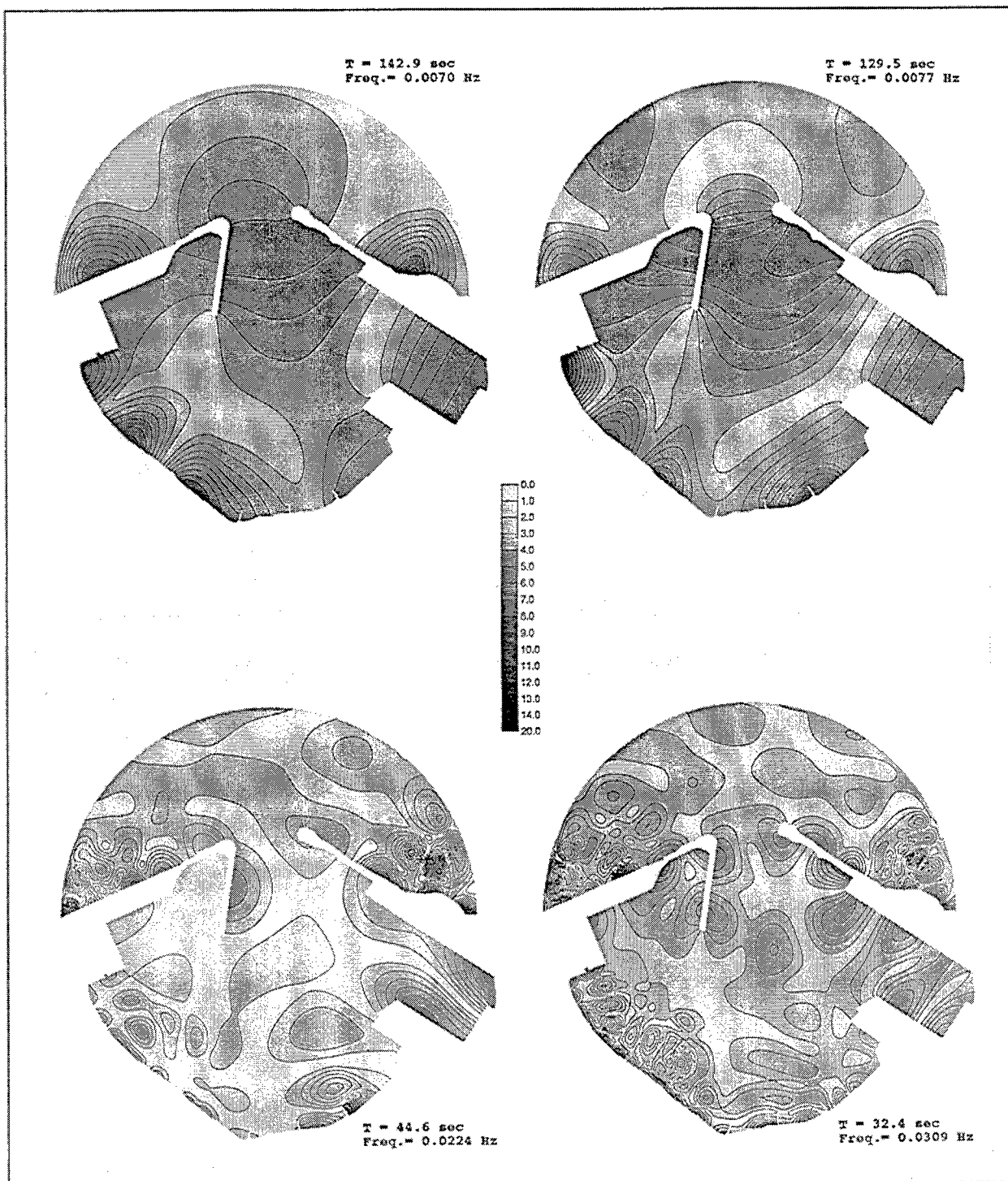
Figure H9. Resonant long wave amplification factor contours, Plan 3c
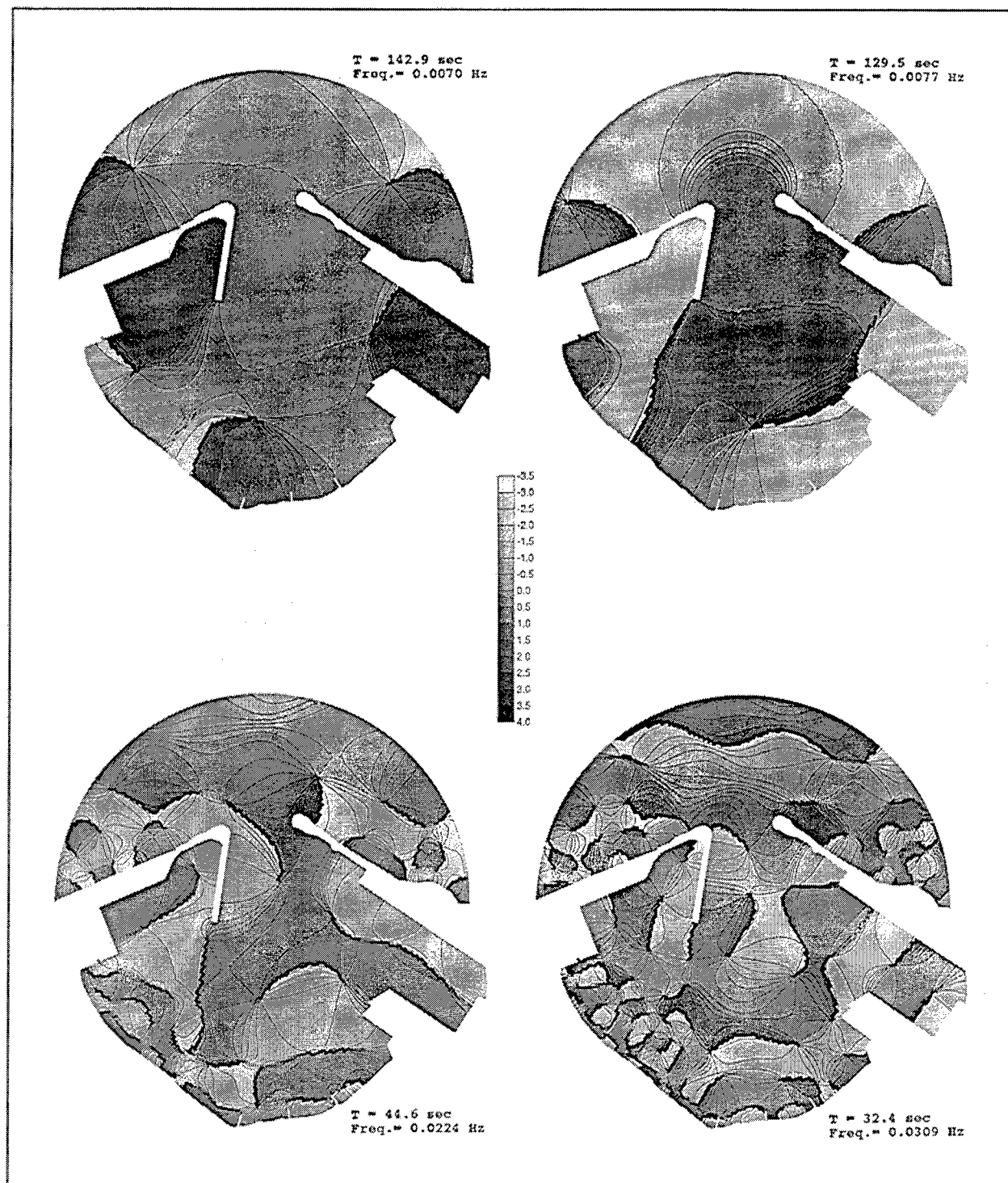
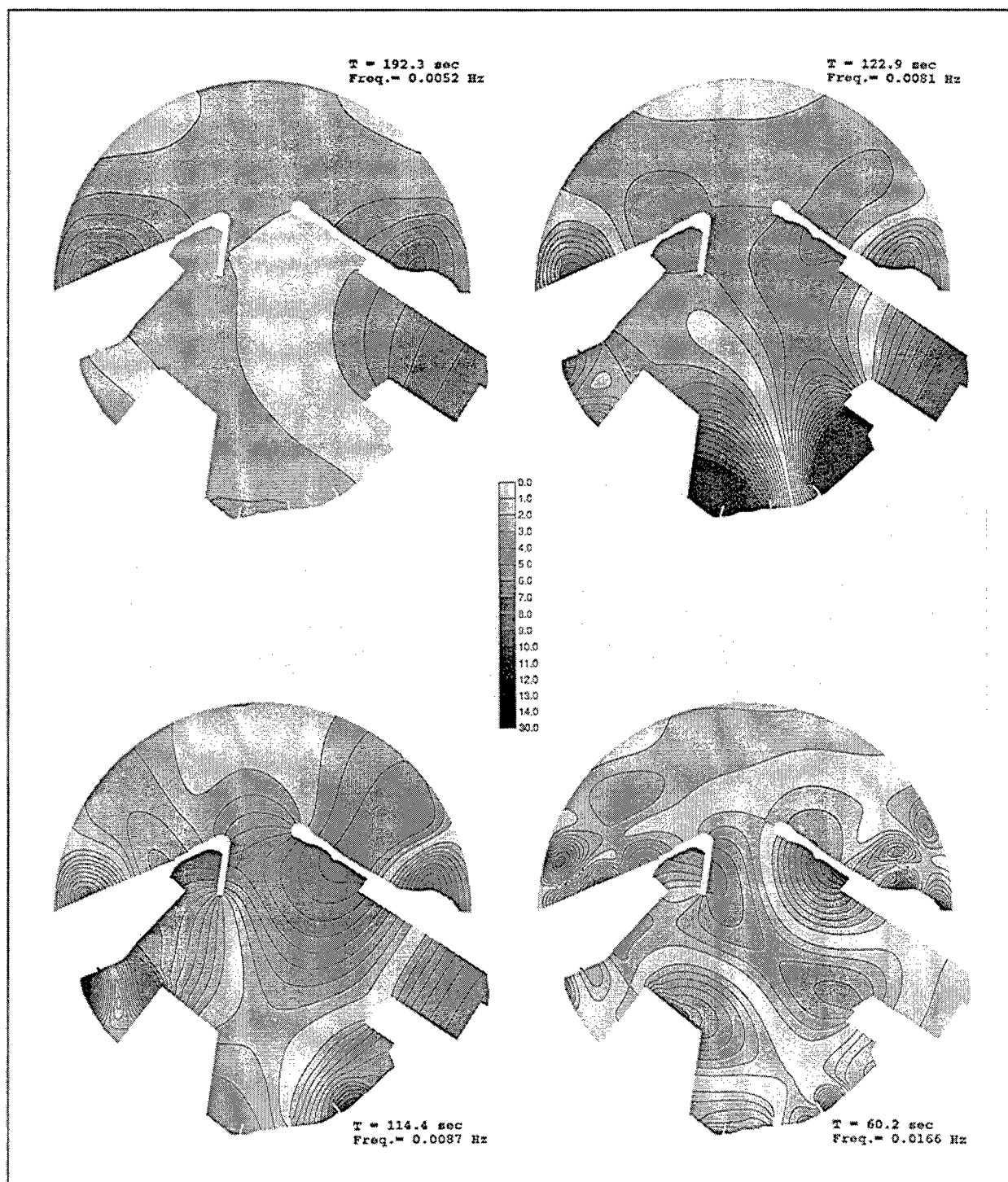Figure H10. Resonant long wave phase contours, Plan 3c
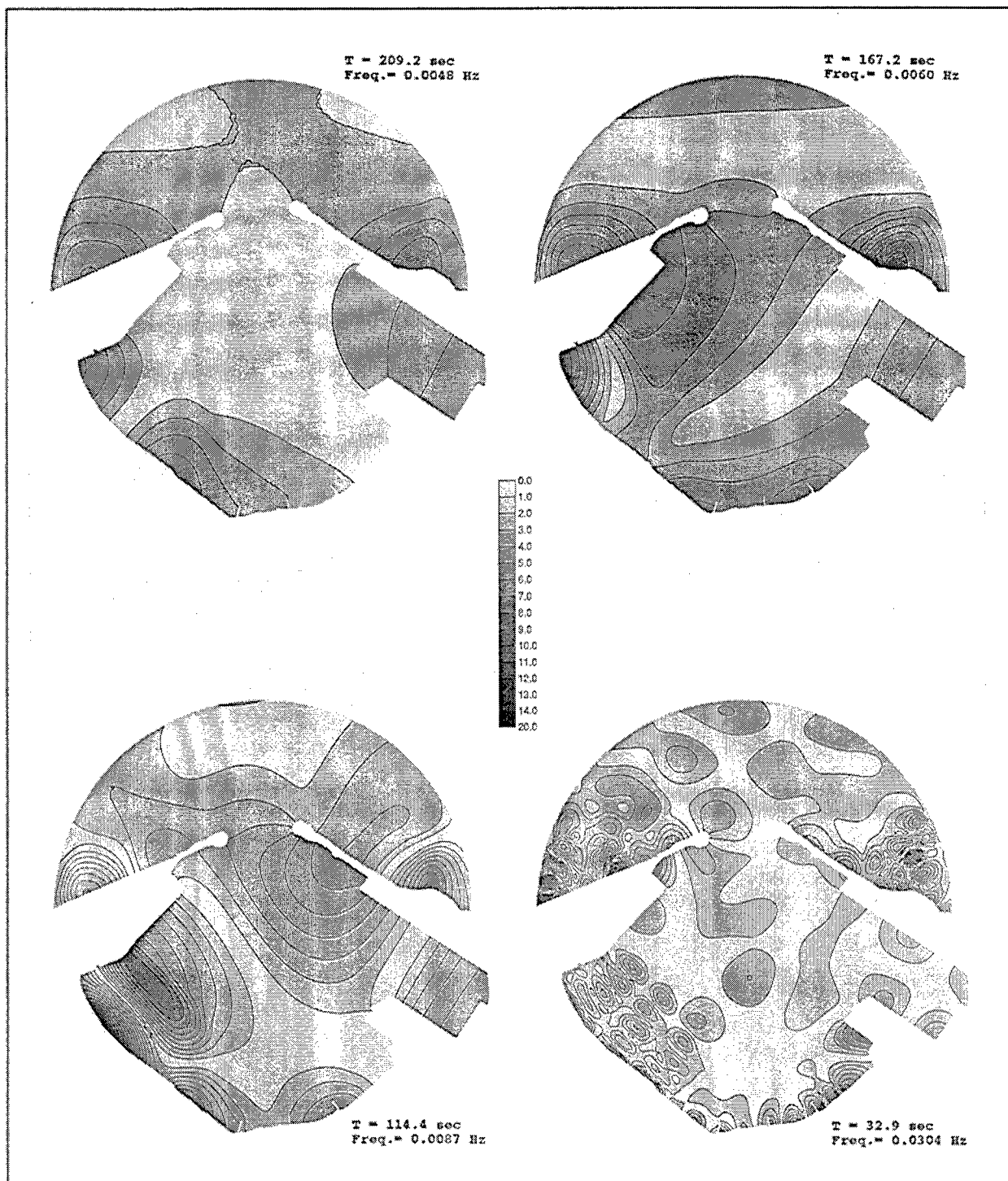
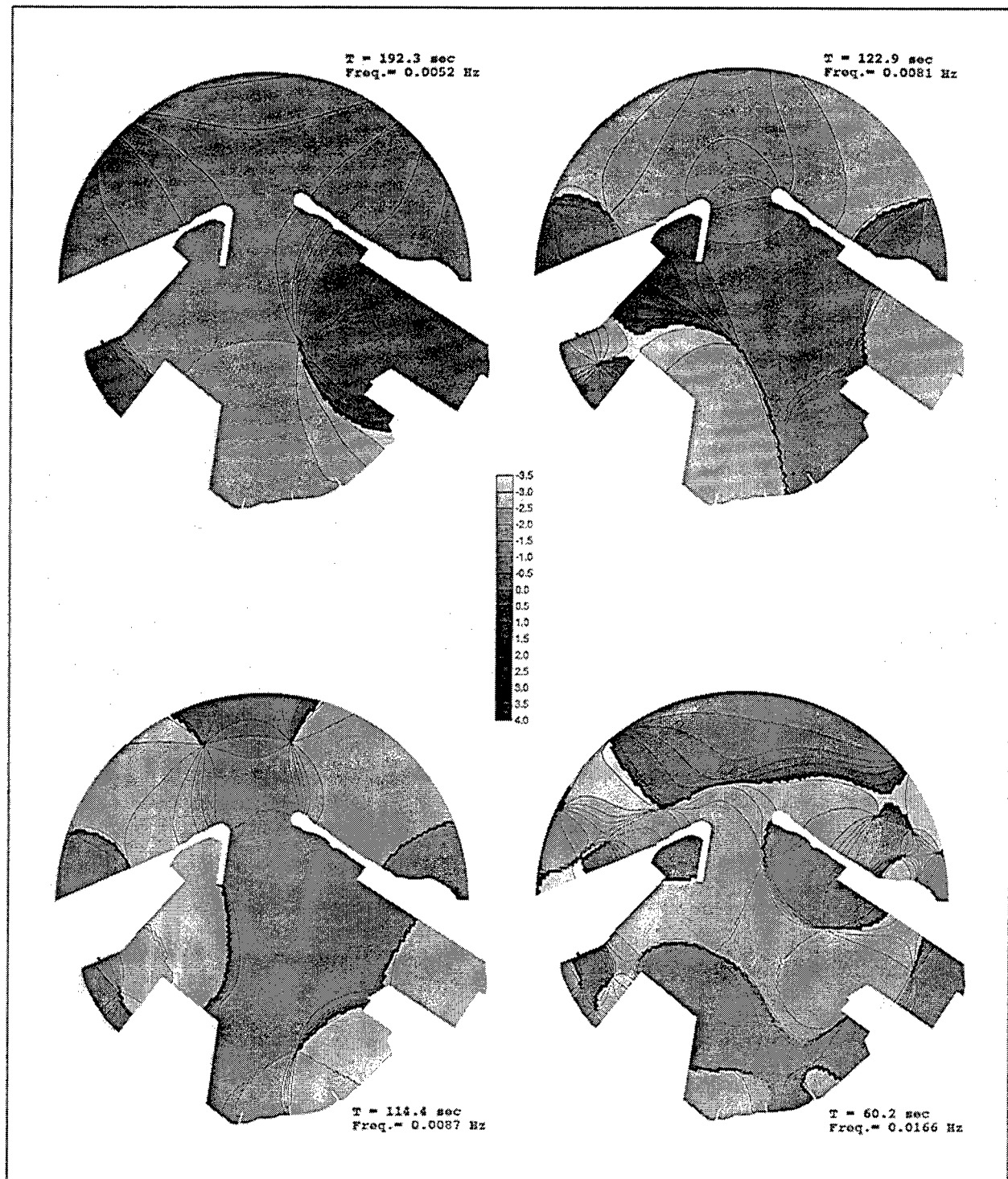Figure H11. Resonant long wave amplification factor contours, Plan 4a

Figure H12. Resonant long wave phase contours, Plan 4a

Figure H13. Resonant long wave amplification factor contours, Plan 4b

Figure H14. Resonant long wave phase contours, Plan 4b

Figure H15. Resonant long wave amplification factor contours, Plan 4c

Figure H16. Resonant long wave phase contours, Plan 4c

Figure H17. Resonant long wave amplification factor contours, Plan 5

Figure H18. Resonant long wave phase contours, Plan 5

Figure H19. Resonant long wave amplification factor contours, Plan 6

Figure H20. Resonant long wave phase contours, Plan 6

Figure H21. Resonant long wave amplification factor contours, Plan 7

Figure H22. Resonant long wave phase contours, Plan 7

Appendix I
Notation

a Wave amplitude, m (ft)

a_i Incident wave amplitude, m (ft)

A_{amp} Wave amplification factor

$(A_{amp})_{eff}$ Effective, or spectral, wave amplification factor

$A_{amp,l}$ Wave amplification factor for long (infragravity) waves

$A_{amp,s}$ Wave amplification factor for wind waves and swell

c Wave phase speed, m/sec (ft/sec)

c_g Wave group speed, m/sec (ft/sec)

d Water depth, m (ft)

d_{far} Water depth, m (ft)

$D(f, \theta)$ Angular spreading function dependent on wave frequency and direction

$D(\theta)$ Angular spreading function dependent only on wave direction

e Constant, 2.7183

f, f_i Wave frequency, sec^{-1}

f_p Peak spectral frequency, sec^{-1}

g Gravitational acceleration, m/sec^2 (ft/sec^2)

H Wave height, m (ft)

H_i Incident wave height, m (ft)

H_{m0} Energy-based, or zero-moment, estimate of significant wave height, m (ft)

H_s Significant wave height for wind waves and swell, m (ft)

$H_{s,long}$ Significant wave height for long (infragravity) waves, m (ft)

i $\sqrt{-1}$

K_r Reflection coefficient of a solid boundary

$K_{r,coast}$ Reflection coefficient of a solid boundary

L Wavelength, m (ft)

L_p Wavelength for waves at peak frequency, m (ft)

n Unit normal vector directed into the solid region

N_D Number of HARBD computational wave directions for spectral approximation

N_p Number of major peaks in wind wave and swell spectrum

N_T Number of HARBD computational wave periods for spectral approximation

r Radial polar coordinate, m (ft)

s Directional spreading parameter

$S(f)$ Spectral energy density function dependent only on frequency

$S(f, \theta)$ Spectral energy density function dependent on frequency and direction

$S(f_i)$ Spectral energy density at frequency, f_i

T Wave period, sec

T_p Peak spectral wave period for wind waves and swell, sec

$T_{p,long}$ Peak spectral wave period for long (infragravity) waves, sec

u, v Horizontal velocity components, m/sec (ft/sec)

w_k Weighting factor for k'th HARBD computational frequency

w_n Weighting factor for n'th HARBD computational direction

x,y Horizontal coordinates, m (ft)

β Dimensionless bottom friction coefficient

γ Spectral peak enhancement factor; phase shift between stress and flow velocity

Δx Grid element dimension

ϵ Significant wave steepness

$\bar{\eta}$ Mean water level reading at Back Basin gage, m (ft)

θ Wave phase; wave direction

θ_0 Primary wave direction, deg

θ_m Incident wave direction for wind waves and swell, deg

κ Wave number, m^{-1} (ft^{-1})

λ Complex bottom friction factor

π Constant, 3.1416

ϕ Velocity potential

ϕ' Velocity potential of the scattered wave

ω Angular wave frequency, radians

∇ Horizontal gradient operator

∂ Partial differentiation symbol

REPORT DOCUMENTATION PAGE

1. AGENCY USE ONLY *(Leave blank)*	2. REPORT DATE December 1996	3. REPORT TYPE AND DATES COVERED Final report

4. TITLE AND SUBTITLE
Wave Response of Kahului Harbor, Maui, Hawaii

5. FUNDING NUMBERS

6. AUTHOR(S)
Edward F. Thompson, Lori L. Hadley, Willie Ann Brandon,
David D. McGehee, Jon M. Hubertz

7. PERFORMING ORGANIZATION NAME(S) AND ADDRESS(ES)
U.S. Army Engineer Waterways Experiment Station
3909 Halls Ferry Road, Vicksburg, MS 39180-6199

8. PERFORMING ORGANIZATION REPORT NUMBER
Technical Report CERC-96-11

9. SPONSORING/MONITORING AGENCY NAME(S) AND ADDRESS(ES)
U.S. Army Engineer Division, Pacific Ocean
Building 230
Ft. Shafter, HI 96858-5440

10. SPONSORING/MONITORING AGENCY REPORT NUMBER

11. SUPPLEMENTARY NOTES
Available from National Technical Information Service, 5285 Port Royal Road, Springfield, VA 22161.

12a. DISTRIBUTION/AVAILABILITY STATEMENT
Approved for public release; distribution is unlimited.

12b. DISTRIBUTION CODE

13. ABSTRACT *(Maximum 200 words)*
Present and projected commercial activities in Kahului Harbor, Maui, Hawaii, indicate that new berths for barge and passenger ship operations will be needed. Deepening of the main harbor areas from 35 ft to 38 ft is also anticipated. The U.S. Army Engineer Division, Pacific Ocean, in coordination with the Harbors Division, Department of Transportation, State of Hawaii, requested field wave measurements and numerical (computer) model studies in support of long-term planning. Field measurements were collected over a period of 18 months at a deepwater directional buoy, a directional array outside the harbor, and four gages inside the harbor. The numerical model, validated with field measurements for short waves (wind waves and swell) and long waves (harbor oscillations), was used to evaluate the technical feasibility of 11 alternative modifications to the harbor. Model results were compared to experience in the existing harbor and to general criteria for operational acceptability. A physical model study is recommended as a final phase of developing harbor modification plans.

14. SUBJECT TERMS
Harbor resonance
Kahului Harbor
Numerical modeling
Prototype wave data
Wind waves and swell

15. NUMBER OF PAGES
224

16. PRICE CODE

17. SECURITY CLASSIFICATION OF REPORT UNCLASSIFIED	18. SECURITY CLASSIFICATION OF THIS PAGE UNCLASSIFIED	19. SECURITY CLASSIFICATION OF ABSTRACT	20. LIMITATION OF ABSTRACT